MATHEMATICAL MODELLING TECHNIQUES FOR THE COMPUTER SIMULATION OF VEHICLE DYNAMIC PERFORMANCE AND RESPONSE

by

M.P. RENUCCI B.Sc., M.Sc.

Submitted

for

The Degree of Doctor of Philosophy

in the

Department of Mechanical Engineering

University of Glasgow

1984

UNIVERSITY OF GLASGOW

DEPARTMENT OF MECHANICAL ENGINEERING

ABSTRACT

MATHEMATICAL MODELLING TECHNIQUES FOR THE COMPUTER SIMULATION OF VEHICLE DYNAMIC PERFORMANCE AND RESPONSE

by

Michael P. Renucci

Computer based mathematical modelling techniques are developed for the prediction of:-

* Vehicle dynamic performance characteristics.

* Vehicle dynamic response to specific road surface excitation.

The simulation technique addresses response mainly in the 0-30 Hz frequency range and thus covers primary ride, secondary ride and the lower body and chassis structural vibrations.

The simulation techniques are applied to the two main classifications of Road Vehicles, i.e.

* Passenger cars with semi-rigid body structures.

* Trucks with flexible structures including both articulated and non-articulated types.

To simulate vehicle dynamic performance it has been necessary to develop:-

1] Mathematical models with sufficient degrees of freedom to represent the dynamic elements of these vehicles and their complex interaction with acceptable accuracy.

2] Approaches to the acquisition of individual component performance data, e.g. tyres, suspension elements etc. to ensure that their performance is adequately defined. [It will be shown that in certain cases this is far from a simple task and requires the development of special measurement and analysis procedures].

3] Computer analysis software for the solution of the mathematical models to simulate the total vehicle dynamic characteristics.

The simulation of vehicle <u>dynamic response</u> has further required:-

4] Methods of exciting the vehicle models with representations of road surface excitations to predict the vehicle response.

All of the above simulation techniques have been developed for a range of vehicle configurations.

The objectives of the work have been to provide analytical techniques for the prediction and optimisation of vehicle vibration and ride quality.

In addition the techniques developed also permit realistic laboratory simulations of component and sub-assembly loading with the use of electro-hydraulics hardware which can be driven by specific outputs from these mathematical models.

Various applications of the above techniques are presented to highlight the potential breadth of application.

ACKNOWLEDGEMENTS

The research work reported in this thesis was undertaken by the author at the National Engineering Laboratory, East Kilbride while registered for research at the Department of Mechanical Engineering, University of Glasgow.

As a full time employee of the National Engineering Laboratory during the research period the author gratefully acknowledges both the computer and experimental facilities made available for the period. In particular the liaison with the UK Motor Industry which was active at that time afforded the author several opportunities to apply the techniques being developed to specific, current problems within their Industries.

The author is especially indebted to Leyland Truck & Bus [now Leyland Vehicles], to BL Cars [now the Austin Rover Group], and to the Ford Motor Company.

The author also gratefully acknowledges the supervision of Professor J.D. Robson as Academic Supervisor for the research period.

CONTENTS

LIST OF SYMBOLS

V	Vehicle Road Velocity
I[δ]	Road Profile [Vertical Displacement]
δ	Road Profile [Horizontal Displacement]
M, C, K	Vehicle Mass, Damping Rate and Spring Rate with Appropriate Subscript
h[τ]	Weighting Function
H[if]	Complex Frequency Response Function
f	Frequency [Hz]
fn	Resonance Frequency [Hz]
X[t], X[f]	Time Varying Function X[t] and Fourier Transformation X[f]
S_X[f]	Power Spectral Density [PSD] Function of Time History X[t]
ξ	Damping Ratio
S_D[f], S_X[f]	Direct and Cross Spectral Densities between Parallel Tracks of a Road Surface
I[t]	Time Varying Random Excitation
J	Moment of Inertia
θ	Rotation Variable
ω	Circular Frequency
λ	Eigenvalues
TFD, TFX	Compound Transfer Functions
X_R[δ]	Right Hand Road Profile
X_L[δ]	Left Hand Road Profile
ϕ	Functional Variable

$I_1(t)$	Time Varying Road Profile Input Excitation Subscripts 1-4 Denote Wheel Position
$I_2(t)$	
$I_3(t)$	
$I_4(t)$	
a	Vehicle Wheelbase
V	Vehicle Velocity
τ	Time Delay = a/v
$\gamma(f)$	Coherence Function
Re	Real Part
Im	Imaginary Part
RMS	Root Mean Square Value
SE	Strain Energy
EI	Flexural Rigidity
$\frac{\partial w}{\partial x}$	First Derivative W with Respect to X
$\frac{\partial^2 w}{\partial x^2}$	Second Derivative
KE	Kinetic Energy
qi	Generalised Co-ordinates
ω	Transverse Displacement
ψ	Transverse Slope
M	Bending Moment
V	Shear Force
Δ	Increment

REVIEW OF PREVIOUS WORK

The dynamic response of road vehicles - both passenger cars and trucks - has interested many researchers over a considerable period.

A major element of this interest has been the analytical prediction of Ride Quality. Ride Quality is simply defined as the vibration performance of the vehicle which is excited by road surface roughness, generally as the vehicle moves at specific constant velocities over the road profile without manoeuvres.

The behaviour of road vehicles under driver and environmentally induced manoeuvres such as cornering is generally dealt with under the context of vehicle handling and in these studies the road surface profile is rarely considered; only road surface inputs of a very severe nature are likely to have a significant effect upon vehicle handling.

A degree of commonality does exist between the analytical techniques used for both types of study in respect of the mathematical models which represent the vehicle dynamics: however, the vehicle excitation used in each case is clearly quite different, i.e. road surface profiles for ride quality studies and driver induced inputs [steering wheel rotation etc.] for vehicle handling analyses.

The content of this thesis addresses the analytical prediction of the ride quality of road vehicles when traversing road surfaces at constant speeds.

In order to predict vehicle dynamic characteristics, it is necessary to develop a mathematical model which adequately represents the major dynamic elements of the vehicle to include proper representation of the performance of the vehicle components, e.g. springs, dampers, elastomeric mounts etc..

To predict ride quality it is necessary in addition to have an adequate description of the road surface excitation as seen by the vehicle as it moves over that surface profile.

Interest in the prediction of vehicle ride in response to road surface inputs began to be reported in the literature around the mid-fifties although interest in the dynamics of vehicle systems had been investigated as early as 1938 by Haley [1]. In 1955 the SAE Riding Comfort Research Committee began to impact upon the analysis of the ride quality of tractor-trailer road vehicles. Janeway [a sub-committee Chairman] reported in 1958 [2] on aspects of truck dynamics which were inherent problems with the truck dynamic configuration and suggested practical methods for their alleviation.

Clark [3] reported in 1962 on the results of an investigation into the dynamic behaviour of vehicles on highways although the main objective was to study the loads induced at the tyre-road interface, the motivation for the work having originated from the Bureau of Public Roads.

Clark used a two-dimensional four degree of freedom mathematical model of a truck which was analysed by an analogue computer. The road profile excitation was represented by sine wave displacements of varying amplitude and frequency which were applied individually to the wheel input positions on the vehicle model, the rear wheel input being identical to the front wheel input but with the appropriate time delay. Frequency response functions were discussed and although some basic conclusions were drawn based upon the very simplified vehicle and road surface models, the key elements for subsequent development by other researchers had been established.

In 1967 Van Deusen [4] concluded that the excitation of mathematical models with simple deterministic inputs, such as sine waves, was of little help in the optimisation of vehicle design or with the study of the behaviour of

vehicles on real roads, since the input definition was not representative of typical road excitation. He introduced results on random road profile measurement from other authors which showed that the spatial frequency content of single tracks of typical road surfaces could be defined by:-

$$P[\Omega] = C\Omega^{-N}$$

where $P[\Omega]$ is the Power Spectral Density [PSD], Ω^{-1} is wavelength and C,N are constants.

He suggested that as a first approximation N be chosen to be 2, such that:-

$$P[\Omega] = C\Omega^{-2}$$

This relationship implied that the amplitude of a road surface undulation was directly proportional to its wavelength and that the surface slope [or velocity] spectrum was white.

Van Deusen also developed equations which catered for the situation where more than one input was imposed upon a linear system such as a vehicle model.

In the case of a vehicle with four inputs he showed that single wheel input frequency response functions [i.e. between the wheel input and any response position on the vehicle] could be combined mathematically with the road surface PSD function, $P[\Omega]$, to predict the response PSD at selected positions on the vehicle model due to the road input. He assumed that the relationship between parallel tracks on the road surface exhibited no correlation such that the Cross Spectral Density function could be assumed to be zero and used a simple model to evaluate the technique. [Later work showed this assumption to be invalid].

More authors subsequently tackled the problem of vehicle response prediction, many considering random road surface roughness, and the simulations were achieved with simplified vehicle models. See for example Walther et. al. 1969 [5] and Healey 1977 [6].

A detailed literature survey at the outset of the work programme reported in this thesis showed that in the case of automobiles the complexity of the description of the road surface excitation was becoming much greater and out of step with the complexity of the models used to represent the automobile. Two dimensional models were commonplace and where three dimensional models were used to benefit from the improved road surface description their degrees of freedom were restricted in number usually to a maximum of seven. Power train dynamics, for example, were rarely included.

In the case of truck simulation two dimensional models were inevitably used but sometimes with as many as 22 degrees of freedom [see Kojima 1969 [7]] but the interest in road profile excitation as seen in the automobile applications was not apparent. This was no doubt due to the increased effort needed to model the truck dynamic system particularly with respect to the increased structural flexibility of truck chassis frames.

It was also noticeable from the literature that very little effort had been expended in the measurement of vehicle component performance: only relatively simple models had been used by most authors and it was probably not considered worthwhile expending significant effort in the characterisation of, say, automobile dampers and in general only nominal values were used.

In the early sixties a new development gave considerable impetus to both road surface description and its application to vehicle dynamics response prediction. This was the rapid growth in laboratory based testing within the automotive industry with the use of servo-hydraulics.

There was particular interest in Road Simulators which allowed vertical inputs to be applied simultaneously to each of the wheels of a prototype vehicle. This highlighted a need for the accurate description of a wide range of road and proving ground surfaces and also for a means of using this data to drive Road Simulators and effect good laboratory simulation of vehicle road or proving ground response.

Work by the Motor Industry Research Association [8] and by Dodds and Robson [9] together with the increased motor industry interest in the subject led to the ISO Proposal ISO/TC/108/WG 9 [1972] - Generalised Terrain Dynamic Inputs to Vehicles. This document proposed a more detailed specification of the PSD content of single tracks of road surfaces and introduced some measurements of the relationship between parallel tracks on specific surfaces in the form of a coherence function - see Dodds and Robson [10].

In 1976 a technique was developed by Styles and Dodds [11] which, given PSD and Coherence data on a specific road surface, utilised inverse FFT methods to synthesise realisations of both tracks of the surface [of any length] in digital form. One application which stimulated this development was the use of these digital signals to drive Road Simulators.

Around the same time the National Engineering Laboratory had installed a Road Simulator and was developing techniques [in conjunction with Glasgow University] for the laboratory simulation of vehicle response to road surface inputs. This research was funded in part by an SRC grant.

The NEL Road Simulator was also used commercially to solve specific vibration problems for the automotive industry. There was clearly a need to develop analytical tools to assist with the solution of these problems and to provide in the longer term a means of avoiding these problems at the vehicle design stage by advanced computer simulation.

It had also been shown at that time by this author [12] that the response of a single degree of freedom model excited by a digital representation of a random white noise signal could be predicted in the time domain with good accuracy as well as in the frequency domain by frequency response analysis.

The objectives of the work reported in this thesis are to develop more accurate mathematical models of automobiles and trucks to take advantage of the increased accuracy of road surface description that was then available. In addition emphasis would be placed upon response simulation in the time domain since it was clear that the ability to cope with non-linearities would eventually be necessary to design and develop 'active' suspension systems even if not needed to realise the simulation accuracy desired at the outset of this research. The need to test not only complete vehicles but also components and sub-assemblies was also apparent: if mathematical models could be developed which predict vehicle response in the time domain with acceptable accuracy then component loading environments could be generated and used to drive servo-hydraulic actuators to permit laboratory testing of the relevant components.

It was also anticipated from the outset that increased sophistication of the vehicle models would require both more component performance data and also more accurate component data if the benefits of improved road surface description and the intended improvements in the mathematical model would yield better response simulation accuracy.

The availability of the Road Simulator at NEL would allow the comparison of predicted and experimental vehicle responses since it was the intention to excite the mathematical models with the same digitally synthesised data which was used to drive the Road Simulator.

The research work reported in this thesis was therefore instigated with the above aims, i.e. to develop computer simulation techniques for the prediction of the dynamic response of road vehicles (cars and trucks) to random road profile excitation with particular emphasis on time domain solutions.

1.0 INTRODUCTION

The Vehicle Industry has long been concerned with the task of producing passenger cars and trucks with competitive ride quality and vibrational characteristics.

Clearly the accepted standards in these aspects will be different for each class of vehicle, but, given this, the vehicle designer is faced with a similar type of problem in both instances.

All types of road vehicle are essentially complex dynamic systems. The constituent elements - e.g. tyres, suspension springs, dampers, engine mounts etc. - each have their individual dynamic characteristics. Assembled they form the complex vehicle dynamic system over which the vehicle designer has more or less full control.

If the vehicle is considered to be the dynamic system then the road surface is the major excitation and the resultant response defines the ride quality and vibrational behaviour of the system.

The simple input-output dynamic system in Figure 1 is helpful in conceptual terms but is clearly over simplified. Road vehicles when driven even at constant speed over a specific road surface are subject to a multiple input excitation.

A four wheeled passenger vehicle will be excited by four simultaneous discrete time varying inputs [although in the constant speed situation the rear wheel inputs will be identical to the front wheel inputs but time-delayed by a factor dependent upon the vehicle speed and its wheelbase dimension].

In the case of articulated commercial vehicles with several axles the road surface excitation is even more complex.

Definition of the road surface excitation is complicated still further in that road surfaces are in general non-deterministic. Road surface description leads us into the theory of random processes by virtue of their nature and specialised techniques are required for their adequate description.

The dynamic response of a vehicle on any specific road surface is therefore the response of a complex dynamic system to multiple input random excitation.

Road surfaces vary considerably in their profile severity and character, and vehicles must exhibit acceptable ride and vibration quality over a wide range of these surfaces.

It is clear that vehicle dynamicists are faced with a far from simple task and inevitably an element of engineering compromise is necessary.

Until fairly recent times vehicle ride optimisation was achieved largely by 'trial and error' or 'seat of the pants' prototype testing. This is no longer acceptable in today's competitive market and much emphasis is now being placed on computer simulation or Computer Aided Engineering (CAE) to achieve better designs in much shorter timescales.

In addition, the development of acceptable ride quality and vibrational performance is becoming increasingly more difficult in the case of passenger vehicles. This is as a result of the need to produce much lighter vehicles of similar load bearing capacity but with no loss in vibrational performance. Traditional 'truck ride problems' are now encroaching upon the territory of the passenger vehicle designer as a result of increasing laden-to-unladen weight ratios.

Analytical tools are therefore increasingly needed to help the vehicle designer predict and optimise the ride and vibration performance of his vehicles.

The prediction of ride and vibrational performance of road vehicles requires:-

* Mathematical representation of the dynamic characteristics of the vehicles including techniques for the definition of component performance.

* Description of road surface inputs compatible with the representation of the vehicle excitation format in the above.

* Simulation techniques (inevitably computer-based) for the prediction of vehicle dynamic response by the excitation of the vehicle models with mathematical representations of the road surface inputs.

and

* Application of the above to both passenger car and truck configurations.

The above requirements and their interrelation as part of the design optimisation procedure are shown schematically in Figure 2.

The work reported in this thesis addresses all of the above requirements.

It will be shown in the following Sections that there is no single mathematical model which, for a given vehicle type, will be appropriate at all instances; indeed it will be shown further that two analysis domains, i.e. time and frequency, are necessary and appropriate at different stages in the vehicle design analysis process.

Mathematical models of varying degrees of complexity will be developed each with a specific application and related analysis domain.

The thesis is divided into three parts:-

Part 1 Passenger Car Simulation

In Section 2 simplified vehicle models, typical of those used by other authors, are discussed, the differential equations representing their dynamics are developed and their individual limitations are set out.

The models are developed from the simplest single degree of freedom mass/spring/damper system through to the three-dimensional sixteen degree of freedom model. This model includes six degree of freedom power train dynamics and was developed to provide more accurate response simulation. The utility and application of each model is highlighted as well as its limitations.

Since both frequency and time domain simulations will be dealt with in this thesis, Section 3 is devoted to a description of the various methods of solution of the mathematical model equations.

Section 4 deals with road surface description and defines how the technique developed by Styles and Dodds [11] is used to excite the mathematical models described previously.

To conduct simulation runs with the various models and road excitations described up to this point it is necessary to supply component data representative of specific vehicles. Sections 5 and 6 deal with the problems of obtaining accurate component data. By far the greatest effort had to be expended with respect to the characterisation of vehicle dampers and this is dealt with in Section 6. It will be seen that a new approach to the performance measurement of these components had to be developed which gave much more representative data for the model simulations but also gave additional insight into the 'in-vehicle' dynamic behaviour of these components.

Section 7 reports on the use of the most complex model developed in Section 2 together with the road profile excitation described in Section 4 and component data collected using the techniques of Section 5 and 6 to assess how accurate the combined simulation technique had become with respect to the prediction of actual vehicle response. This was assessed by a comparison of the predicted responses of the vehicle model with the experimentally measured responses from the actual vehicle under road and also Road Simulator excitation.

Part of Section 7 is dedicated to a quantification of the loss of simulation accuracy when restricting models to two dimensions thereby compromising not only the model realism but also the more adequate representation of the road surface input which was then available.

Part II-Commercial Vehicle Simulation

Section 8 describes the development of commercial vehicle models and includes both articulated and non-articulated configurations.

The major difference from the models developed for passenger cars is the need to represent truck frame flexibility. Finite difference techniques are applied to model this flexibility and truck models of increased sophistication are introduced.

Both frequency and time domain solutions are considered and problems with the acquisition of accurate component data are also highlighted. The accuracy of simulation provided by the time domain truck models is assessed in a manner similar to that of the passenger car models in Section 7.

Part III - Motor Industry Applications

Part III describes three applications of the simulation techniques to specific projects within the vehicle industry which were active at the time of the research work. They will serve to indicate how the modelling techniques can be applied to a wide range of vehicle dynamic problems.

PART I

PASSENGER VEHICLE SIMULATION

2.0 MATHEMATICAL MODEL FORMULATION

2.1. Overview

In the design and development of competitive ride quality and vibration the vehicle dynamicist will be concerned with different parameters of vibration, each appropriate to a specific stage in the design and development process.

At the initial design stage when the basic dimensions, projected vehicle weights and payload capacities are under formulation the specification of the primary suspension spring rates and wheel travel will dictate the vehicle rigid body resonance frequencies, i.e. the vehicle bounce, roll and pitch.

At this stage the centres of percussion, which have a significant effect on primary ride, will need to be examined and optimised. The absolute values of the spring rates will dictate the resonance frequency values whereas the ratio of the front to rear rates will influence the locations of these centres of oscillation. This optimisation can be done effectively with a simple two degree of freedom model [Figure 3].

At an intermediate stage in the design process the engine and power train mounting positions must be specified after optimisation. Preliminary work in this area can be undertaken with a 6 degree of freedom model [Figure 4] to analyse the coupled modes of engine/gearbox vibration.

As the design and development progresses the stage will be reached where a more complete vehicle model will be needed, i.e. where all the dynamic elements are included so that the effects of their interaction can be studied. At this point the seat

dynamic system needs to be incorporated so that it can be 'tuned' to the vehicle and thereby optimise ride quality. Figure 5 shows a complete vehicle model which could be used at this stage.

The main concern at this time will be the dynamic response of the total vehicle to road surface inputs and other driver induced excitations such as 'power on-off'. Road surface inputs will generally be further subdivided into both 'transient' and 'steady state' categories. Examples of transient excitation are pot-holes, step inputs etc. and the steady state inputs will be the variety of road surface inputs to be considered appropriate to the vehicle type and covering the speed range of the vehicle.

It is clearly important to note that mathematical models of varying degrees of complexity are each appropriate to a different stage in the design process. It is just as incorrect and inappropriate to use a very complex mathematical model of the total vehicle - even if sufficient data was available - at early stages in the design process, as it is to use a very simple model at the final stages where more complete and accurate simulations are necessary for the final optimisation and validation of the dynamic behaviour of the vehicle.

It is good practice to adopt a policy where the appropriate mathematical model is the one which will dynamically represent the situation with the minimum number of degrees of freedom.

It should be stated though that it is not always possible to know in advance how many degrees of freedom are needed to adequately define the dynamic situation of interest. This is particularly so where mathematical models are used to analyse and remove specific vibration problems the cause of which is not necessarily known at the outset.

In the following sections a range of computer based mathematical passenger vehicle models will be developed together with analysis procedures to provide the vehicle dynamicist with analytical design tools for the optimisation of vehicle ride quality and vibration in the appropriate frequency range.

2.2. Single Degree of Freedom Model

It will be in the interest of simplicity if we restrict attention for the time being to simplified mathematical models of passenger vehicles with no structural flexibility in the frequency range considered.

The mathematical model in Figure 6 is the simplest possible representation of a road vehicle. It consists of a mass, M, representing the sprung mass of a vehicle supported by a suspension spring and damper K_f, C_f respectively. Let us assume the vehicle to move at constant velocity V over a road surface profile defined by $I[\delta]$ where δ is the spatial horizontal distance along the surface.

If we assume further that the point contact with the road surface does not separate from the profile we have, for a constant V:-

$$\delta = Vt \qquad 2.2.1.$$

$$I[\delta] = I[Vt] = VI[t] \qquad 2.2.2.$$

The dynamic input/output model is thus defined in the time domain by Figure 6.

The response of the mass M is defined to be X[t] and is given by:-

$$M\ddot{X}[t] + C_F[\dot{X}[t] - \dot{I}[t]] + K_F[X[t] - I[t]] = 0 \qquad 2.2.3.$$

$$\Rightarrow M\ddot{X} + C_F\dot{X} + K_F X = C_F\dot{I} + K_F I \qquad 2.2.4.$$

dropping the independent variable for convenience.

This model represents the classic linear single input - single output dynamic system with constant parameters. Such a system can be defined by:-

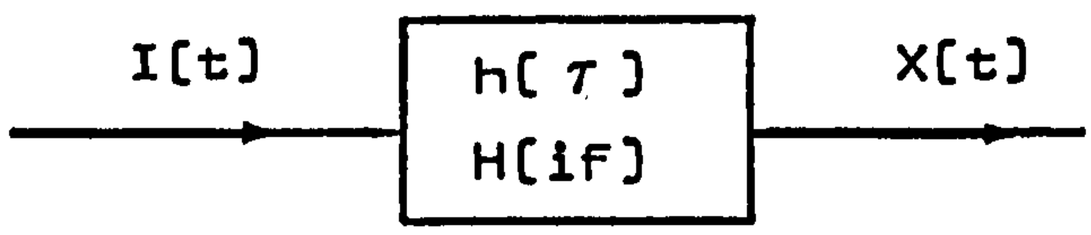

where h[τ] is the weighing function, H[if] is the complex frequency response and their relationship is defined by:-

$$H[if] = \int_{-\infty}^{+\infty} h[\tau] e^{-i\,2\pi f \tau}\, d\tau \qquad 2.2.5.$$

If I[t] is assumed to be a realisation of a stationary random process then X[t] will be also.

The convolution integral can thus be defined:-

$$X[t] = \int_{-\infty}^{+\infty} h[\tau] I[t - \tau] d\tau \qquad 2.2.6.$$

If we apply Fourier Transformations to both sides of equation 2.2.6. we obtain:-

$$X[f] = H[if]\ I[f] \qquad 2.2.7.$$

where X[f] in the Fourier Transformation of X[t] and I[f] is the Fourier Transformation of I[t].

Note that H[if] is a complex function and defines the <u>frequency response</u> of the system.

Suppose we take the spectral density of the input I[t] and of the output X[t] and denote these functions $S_I[f]$ and $S_X[f]$ respectively. The relationship between input and output is given by:-

$$S_X[f] = \left|H[if]\right|^2 S_I[f] \qquad 2.2.8.$$

where $\left|H[if]\right|$ denotes the modulus of the complex function.

For the simple dynamic system in Figure 6 it can be shown that:-

$$H[iF] = \frac{1 + 2i\xi\left(\frac{F}{Fn}\right)}{1 - \left(\frac{F}{Fn}\right)^2 + i2\xi\left(\frac{F}{Fn}\right)} \qquad 2.2.9.$$

where f_n = system resonance frequency = $\frac{1}{2\pi}\sqrt{\frac{K}{M}}$

ξ = damping ratio = $C[2\sqrt{MK}]^{-1}$

It is apparent that, for the model in Figure 6, prediction of the dynamic response to a stationary random input I[t] with spectral density $S_I[f]$ is easily accomplished either:-

1] In the frequency domain by equation 2.2.8.

or

2] In the time domain by equation 2.2.4 using numerical techniques such as that described in Reference [12] and assuming I[t] is defined as a time varying function.

It should also be noted that with certain restrictions, e.g. linearity, stationarity, it is possible to change from the time to frequency domain with such a simple model. The model in Figure 6 is however of little real use in the simulation of vehicle dynamics or response in view of its simplicity.

2.3. Two Degree of Freedom Vehicle Model (Single Input)

The model shown in Figure 7 is partially representative of one corner of a vehicle and includes the unsprung mass, M_1, and associated tyre spring and damping factor as well as the sprung parameters used in the previous single degree of freedom model.

In representing the total vehicle system it has several deficiencies:-

1] Vehicle body inertias are not included and so the pitch and roll modes of the body structure cannot be represented.

2] Power train dynamics are excluded.

3] Road inputs are represented by a single input only.

Nevertheless, the two degree of freedom model can be useful for basic studies although it falls far short of full vehicle simulation.

The dynamic equations of motion for this model are given below:-

i] Sprung Mass

$$M_2\ddot{x}_2 + K_F[x_2-x_1] + C_F[\dot{x}_2-\dot{x}_1] = 0 \qquad 2.3.1.$$

ii] Unsprung Mass

$$M_1\ddot{x}_1 - K_F[x_2-x_1] - C_F[\dot{x}_2-\dot{x}_1] +$$

$$K_T[x_1-I_1] + C_T[\dot{x}_1-\dot{I}_1] = 0 \qquad 2.3.2.$$

It will be convenient to rearrange the above equation into matrix format:-

$$\begin{bmatrix} M_1 & 0 \\ 0 & M_2 \end{bmatrix} \begin{bmatrix} \ddot{x}_1 \\ \ddot{x}_2 \end{bmatrix} + \begin{bmatrix} C_F+C_T & -C_F \\ -C_F & C_F \end{bmatrix} \begin{bmatrix} \dot{x}_1 \\ \dot{x}_2 \end{bmatrix} +$$

$$\begin{bmatrix} K_F+K_T & -K_F \\ -K_F & K_F \end{bmatrix} \begin{bmatrix} x_1 \\ x_2 \end{bmatrix} = \begin{bmatrix} K_T I_1 + C_T \dot{I}_1 \\ 0 \end{bmatrix} \qquad 2.3.3.$$

This system will have two natural frequencies and two associated mode shapes (or eigenvalues and eigenvectors).

The above two degree of freedom model is an example of the generalised 'stacked' system as shown in Figure 8.

The general equation of the nth mass of such a system can be shown to be given by:-

$$M_n\ddot{x}_n + (K_{n-1,n}+K_{n,n+1})x_n +$$

$$(C_{n-1,n}+C_{n,n+1})\dot{x}_n - K_{n-1,n}x_{n-1} \qquad 2.3.4.$$

$$-C_{n-1,n}\dot{x}_{n-1} - k_{n,n+1}x_{n+1} - C_{n,n+1}\dot{x}_{n+1} = 0$$

(Noting that $K_{n',n+1}$ and $C_{n',n+1}$ may be 0, i.e. at the end point).

The generalised Matrix equation of such a system with n masses is given by:-

$$[M][\ddot{X}_i]+[C][\dot{X}_i]+[K][X_i]=[E] \qquad 2.3.5.$$

where [M] is given by $\begin{bmatrix} M_1 & 0 & 0 & .. \\ 0 & M_2 & 0 & .. \\ 0 & 0 & M_3 & .. \\ & & & \\ \multicolumn{4}{c}{\ldots\ldots\ldots\ldots M_n} \end{bmatrix}$ (n x n diagonal)

[C] is given by

$$\begin{bmatrix} C_{01}+C_{12}, -C_{12}, 0, 0, 0 \ldots \\ -C_{12}, C_{12}+C_{23}, -C_{23}, 0, 0 \ldots \\ 0, -C_{23}, C_{23}+C_{34}, -C_{34}, 0 \cdot \\ \cdot \quad \cdot \quad \cdot \quad \cdot \quad \cdot \quad \cdot \\ \cdot \quad \cdot \quad \cdot \quad \cdot \quad \cdot \quad \cdot \\ -C_{m-1,m}, [C_{m-1,m}+C_{m,m+1}], -C_{m,m+1}, \ldots \\ \cdot \quad \cdot \quad \cdot \\ \cdot \quad \cdot \quad \cdot \\ -C_{n,n-1}, C_{n-1,n} \end{bmatrix} \quad (n \times n)$$

[K] is similar to [C] but with [K] terms in place of [C] terms.

[E] is given by $\begin{bmatrix} K_{01}X_0 + C_{01}X_{01} \\ 0 \\ 0 \\ \cdot \\ \cdot \\ \cdot \\ 0 \end{bmatrix}$ and (n x 1)

$$[X] = \begin{bmatrix} X_1 \\ X_2 \\ X_3 \\ \cdot \\ \cdot \\ X_n \end{bmatrix} \quad (n \times 1)$$

2.4. Simple Two Degree of Freedom Primary Ride Frequency Model

Refer back to Figure 3 which illustrates the simplest two input vehicle model. It comprises a rigid representation of the vehicle body, with mass M and pitch inertia J. Its motion is defined by the displacement of, and rotation about the centre of gravity x, θ respectively.

This model does not include the unsprung masses but is nevertheless very useful in studies of the bounce and pitch modes of vehicles and leads to analysis of vehicle centres of oscillation. This model was used extensively in the development of the principles of centres of oscillation and their basic effect on vehicle dynamics which are discussed in Part II.

Provided we are concerned with primary suspension modes only this model is surprisingly useful, despite its simplicity, for frequency and mode shape analysis of vehicle rigid body modes.

It is worthwhile, therefore, listing the relevant dynamic equations of motion.

Equations of Motion

i) Vertical Displacement

$$M\ddot{x} + [K_1 + K_2]x + [K_2\ell_2 - K_1\ell_1]\theta = 0 \qquad 2.4.1.$$

ii) Rotational Motion

$$J\ddot{\theta} + [K_2\ell_2 - K_1\ell_1]x + [K_1\ell_1^2 + K_2\ell_2^2]\theta = 0 \qquad 2.4.2.$$

Clearly the above equations will be uncoupled when $K_1\ell_1 = K_2\ell_2$ and the terms involving $[K_2\ell_2 - K_1\ell_1]$ equate to zero. Equation 2.4.1. will then involve x only and equation 2.4.2. will involve θ only.

2.5. Four Input Rigid Vehicle Model

Figure 9 shows the basic 4 input vehicle model. The vehicle body is represented by a 3 degree of freedom rigid mass to which are attached the suspension springs and damper at appropriate locations. Four degrees of freedom are included to represent the unsprung masses noting that where a vehicle has coupled rear suspension, e.g. for a beam axle, the two vertical degrees of freedom are replaced by:-

i) the axle centre of gravity vertical motion,

and

ii) the roll about this centre of gravity position.

Vertical displacements at the wheel positions are then obtained from a simple geometric combination of i) and ii) above.

The 7 degree of freedom model is useful for the analysis of rigid body dynamics and represents bounce, pitch and roll. It is important to include the power train mass and inertias in the specification of the 'body' inertias since these have a significant effect.

The coupling of axle shake to body response can also be studied with this model but care is needed since it is not uncommon to find axle and body interaction significantly affected by power train shake dynamics.

The dynamic equations of motion of this model will not be reproduced here since they are in effect a subset of the dynamic equations of the 13/16 degree of freedom high level simulation model described below.

2.6. 13/16 Degree of Freedom Ride Simulation Model

The mathematical vehicle model developed to provide high level simulation of vehicle dynamics and response has been shown schematically in Figure 5.

It represents considerably more realism and therefore complexity than any of the earlier models and has the following additional features:-

1) Model is 3 dimensional and caters for 4 inputs.

2) Power train dynamics are included [with upto 6 degrees of freedom].

3) For detailed ride studies seat dynamics can be incorporated with upto six degree of freedom complexity.

4) Suspension geometry effects can be easily incorporated.

5) Features such as anti-roll bars are easily incorporated.

6) 'Beam axle' or completely independent suspension systems are catered for.

The dynamic equations of this mathematical model are inevitably complex but are represented in their simplest form, i.e. with a 3 degree of freedom engine model and no driveshaft coupling or anti-roll bar in Appendix A. The model variables are also listed in Appendix A.

The dynamic equations of such a model can be developed in a variety of ways, e.g. Lagrange, force balance at each mass etc. The force balance method was chosen in this case however, in order that forces at each mass centre could be easilly identified within the differential equations in view of the application to laboratory component testing.

Figure 10 illustrates the use of the force balance method in developing the dynamic equilibrium of the nearside front unsprung mass (one of the simpler equations).

In order that the model be applicable to a wide range of vehicles, the spring and damping rates required are the effective vertical wheel rates and not necessarily those of the individual suspension components. This implies that where appropriate, the suspension geometry of the vehicle must be taken into account in the model input data. The front suspension of the test vehicle used to validate the model was of the wishbone type incorporating inclined spring-damper units and a geometric correction, as indicated by Figure 11, was applied to the component rates K, C, to give the effective wheel rates K_F, C_F.

The front axle responses produced by the model are therefore at the wheel position and responses at points on the lower suspension links, inboard of the wheel, can be simply calculated. This is often necessary in vehicle component testing to determine the displacement response of the lower mounting point of the front damper.

The model was extended in later stages by expanding the power train representation from 3 to a full 6 degrees of freedom.

A fuller description of this model is given in Reference (13).

3.0 METHODS OF SOLUTION

The formulation of the range of mathematical models developed in the preceding sections has provided us with sets of differential equations of motion which are representative of the vehicle or part vehicle dynamics.

Various methods of solution can be applied to these equations covering both the specification of dynamic performance and of dynamic response to specific external excitation.

Three principal approaches have been adopted in this work and are described below:-

1) Normal Mode Analysis

2) Frequency Response Function Analysis, and

3) Time Domain Response

In all of the above cases software packages have been developed - of general applicability - and the various mathematical model equations incorporated.

3.1. Analysis of Dynamic Performance

3.1.1. Eigenvalue/Eigenvector Analysis (Normal Mode Analysis

The object of mathematical simulation of dynamic systems is generally the prediction of the system response to particular excitations. However, this is the ultimate objective and requires definition of both the system properties and the excitations. The definition of the dynamic system properties can often be of use in itself.

In the case of both passenger and commercial vehicle systems the simplest dynamic properties are the natural frequencies and mode shapes. These define the basic dynamic character of the vehicle. Of interest to the vehicle designer are the rigid body modes, axle resonances, frame resonances and cab and engine resonances. The corresponding mode shapes also indicate the extent of coupling existing between the various components at the various resonance frequencies. There is, of course, no way of knowing directly from the natural frequency and mode shape information whether any ride or vibration problems will arise when the vehicle is subject to service excitation. However, if at the prototype evaluation stage, a ride problem does occur at a particular frequency, knowledge of the vehicle resonance frequencies may indicate the source of the problem. In addition the ability to predict natural frequencies will allow the designer to select the appropriate stiffnesses to achieve particular resonance frequencies.

Theory

A brief description is given here of the theoretical background to the prediction of the natural frequencies and corresponding mode shapes of the vehicle systems as incorporated in the computer simulation software.

An undamped dynamic system can be represented by the following matrix equation.

$$[M][\ddot{X}] + [K][X] = [E] \qquad 3.1.1.$$

where $[M]$ is the mass matrix,
$[K]$ is the stiffness matrix, and
$[E]$ is the excitation matrix

In general the above matrices will be of order n where the dynamic system has n degrees of freedom.

Setting $[E] = 0$ we remove any external forces and equation 3.1.1. is representative of free vibration. Assuming simple harmonic natural frequencies of the form:-

$$X_j = A_j \cos \omega t$$

where ω is the circular frequency, it follows that:-

$$\ddot{X}_j = -A_j \omega^2 \cos \omega t = -\omega^2 X_j$$

Rewriting equation 3.1.1. we have:-

$$[K]\,[X] = \omega^2\,[M]\,[X]$$

and premultiplying by $[M]^{-1}$ gives:-

$$[M]^{-1}[K]\,[X] = \omega^2 [X]$$

or in canonical form:-

$$\{[A - \lambda I]\}\ [X] = 0 \qquad 3.1.2.$$

where $A = [M^{-1}]\,[K]$, I is the unity matrix and $\lambda = \omega^2$.

Since [A] and [I] are known, the solution to the above equation will give values of λ or ω^2 and hence the system natural frequencies ω. Substituting the various values of λ into equation 3.1.2. gives the corresponding mode shape or eigenvector, i.e. the ratios of the amplitudes of the remaining degree of freedom to any one degree of freedom [usually chosen to be unity]. At each natural frequency the system will vibrate with simple harmonic motion according to a definite shape defined by the eigenvector. For the n degree of

freedom system there will be n natural frequencies with n associated mode shapes.

A software package was developed to perform eigenvalue/eigenvector analysis on the range of mathematical models discussed in this work.

3.1.2. Frequency Response Function Analysis

This type of analysis is concerned with the prediction of the vehicle response to discrete sinusoidal inputs usually applied at the wheel positions. The results of this type of analysis lend themselves well to correlation with vehicle measurements on Electro-Hydraulic ride simulators (see e.g. Figure 12) where the model inputs can be physically reproduced. The predicted response at selected positions in the vehicle model can be measured at identical positions on the actual vehicle and the degree of correlation assessed.

Provided we restrict our mathematical models to have <u>linear</u> elements (or perhaps frequency dependent non-linearities) these single input responses can be combined in a certain way to enable complete vehicle response to be predicted in the frequency domain. Several authors (e.g. 3, 4, 5) have used this approach with simpler mathematical models and the techniques have been extended to more complex models in this work.

A brief description of the theory is given below as it applies to the mathematical models developed here.

In Section 2.2.1. the single degree of freedom dynamic system was stated to have a frequency response function H(if) which relates the system output to the system input by the equation:-

$$X[f] = H[if]\ I[f]$$

where I, X were the input and output respectively.

This was the simple case of a single input/single output system.

In the case of [say] a 4 wheeled road vehicle [or the corresponding 4 input vehicle system model] we need to develop equation 2.2.1. further.

We now have a choice of 4 input positions and any number of response positions on the vehicle but consider a four wheeled vehicle with three of its wheels at rest. A unit sinusoidal displacement of frequency f_o is imposed at the remaining wheel denoted i, say. The response at some point j on the vehicle is monitored. Since we are confining attention to <u>linear</u> systems the point j will also execute sinusoidal displacement but with different amplitude and phase with respect to the unit input at wheel i. The relationships between the gain and phase can be described by a complex number: this is the single wheel transfer function,

$$H_{ij}[if_o]$$

where $|H_{ij}|$ = the gain, and

$\arg [H_{ij}]$ = the phase relation

If f_o now varied over the whole frequency range we obtain the function $H_{ij}[if]$. If the input is now moved to each wheel in turn we obtain four such functions for the point j, i.e.

$$H_{1j}[if],\ H_{2J}[if],\ H_{3j}[if],\ H_{4j}[if] \qquad 3.1.3.$$

$$f_{min} \leq f \leq f_{max}$$

Since the above functions are linear they can be subjected to vector addition in the complex plane. For example the transfer function between the point j and the simultaneous input of sinusoids to the four wheels is equal to:-

$$\sum_{i=1}^{4} H_{ij}[if]$$

It is also a simple matter to incorporate a phase lag between the inputs to the front wheels and those to the rear - this is representative of a moving vehicle where the rear wheels encounter the same displacements from the road as do the front wheels, but after a time increment proportional to the vehicle speed.

3.2. Analysis of Dynamic Response

3.2.1. Method of Combined Transfer Functions

Extending the theory of the previous section it can be shown that the following relationship exists between the road spectra, $S_D[f]$ and $S_X[f]$ and the spectrum of the point j can be obtained with some algebraic manipulation.

$$S_j[f] = \sum_{\ell=1}^{4} \sum_{m=1}^{4} H_{j\ell}[if]H^{*}_{jm}[if]S_{\ell m}[f] \qquad 3.2.1.$$

$$= \left[TFD\right]S_D[f] + \left[TFX\right]S_x[f]$$

where * denotes the complex conjugate,

$S_{\ell m}[f]$ = direct spectral terms, $\ell = m$,

= cross spectral terms, $\ell \neq m$, and

TFD,TFX are functions of both frequency and vehicle speed.

In effect then the PSD of a point on the vehicle is composed of [TFD] times the direct spectrum of the road plus [TFX] times the cross spectrum of the road. The relationships between TFD, TFX and the single wheel input transfer functions are somewhat complex and are discussed in some detail in Reference 6 .

Clearly then, for any linear model, the response spectrum can be obtained from a combination of the single wheel transfer functions $H_{ij}[f]$. It should be noted that the above arguments are not applicable, in general, where the model is non-linear.

The above theory is utilised in a software package developed to cater for all the models discussed here and the computer programme can output plots of the following transfer functions for any degree of freedom j:-

1) $\left|H_{1j}[if]\right|, \left|H_{2j}[if]\right|, \left|H_{3j}[if]\right|, \left|H_{4j}[if]\right|$, i.e. the moduli of the single wheel transfer functions.

2) $\left|\sum_{i=1}^{4} H_{ij}[if]\right|$, i.e. the 'all-four-wheels-in-phase' transfer function

3) $\left|TFD[f]\right|^2, \left|TFX[f]\right|^2$, i.e. the compound transfer function as defined above.

3.2.2. Time Domain Solution Method

Time domain response is the most general. It places no restriction on either:-

i] the type of input excitation provided it can be represented digitally, e.g. non-stationary excitation can be accommodated.

or

ii] the linearity of the mathematical models.

It is also a simple matter to convert computed time domain responses into the frequency domain by, for example, spectral analysis. It is much more difficult to convert in the reverse direction.

The techniques are extremely powerful in that by simulating the time domain response of a vehicle where each part vibrates with the correct amplitude and place relationships, drive signals for a wide range of component and sub-assembly tests can be synthesised relatively easily. As will be shown later, component vibration and durability tests can be conducted in this way by using the output from time domain models to drive electro-hydraulic rigs directly.

Inevitably the 'trade off' against all of the above listed benefits is that time domain response simulation is the most complex and the most computer processor intensive of all the methods of simulation. For high level simulation however, it provides the most effective technique.

A brief description of the techniques developed will be appropriate here.

The mathematical vehicle models described above provide sets of dynamic differential equations representative of the vehicle motion, when subjected to tyre excitation, in the form:-

$$\ddot{x}_j = \phi^j[x_j, \dot{x}_j, I_k, \dot{I}_k] \qquad 3.2.2.$$

where j = 1,n

k = 1,p

n is the number of degrees of freedom, and

p is the number of inputs.

The accelerations $\ddot{X}_j$ are defined therefore as functions of the velocities, $\dot{X}_j$, the displacements, X_j, and of the input displacements and velocities, I_k, $\dot{I}_k$.

It was shown by the author [12] that with the use of a commercially available numerical integration package, the response of a single degree of freedom model subject to a white noise input could be predicted with acceptable accuracy.

The integration method used was a fourth order Runge Kutta algorithm. [At this point the reader is referred to Reference [12] Section 3.2 which gives a brief overview of the theory of integration methods in the context of the existing problem].

It was found necessary during the course of this work to develop a dedicated software package for the solution of the various time domain simulations since the commercially available packages do not give sufficient flexibility particularly with respect to the definition of multiple input random excitation data and with respect to error analysis.

<u>The Software Operates as Follows</u>;

The input displacement excitation is defined by a series of digital samples. In general these displacements are representative of the road surface displacements as applied to the vehicle tyres.

Note that the surfaces represented digitally can be either:-

i) deterministic, e.g. sine wave, steps, ramps etc.

or

ii) random, e.g. road profiles.

The displacement profile of the surface of itself is insufficient however to specify the input to the vehicle. Before the vehicle excitation can be fully defined it is necessary to compute the input velocities which are necessary for the computation of the tyre damping forces. Figure 6 illustrates the situation for the simple case of the single degree of freedom system.

The velocities are computed digitally with a digital differentiator. Clearly it was necessary to determine the accuracy of this subroutine before proceeding with the development of high level simulation models since errors at the input definition stage would merely be reflected throughout the entire simulation.

Reference should now be made to Appendix B which gives an analysis of the accuracy of the digital differentiator.

At the start of the simulation process therefore we have a series of digital values representing the wheel input displacement and velocities, i.e.

$$\begin{matrix} I[n\delta] \\ I[n\delta] \end{matrix} \qquad n = o,N$$

where δ = time interval between samples.

N = total number of digital values

i.e. $N\delta = T$ where T is total simulation time.

At time t = o the vehicle system is assumed at rest, i.e. all elements of the system differential equation:-

$$\ddot{x}_j = \phi[\dot{x}_j, x_j, \dot{I}_j, I_j] \text{ are zero}$$

The first road inputs $I_j, \dot{I}_j$ are then applied and values of $\ddot{x}_i$ can be calculated from equations [3.2.2.]. These values of acceleration are then integrated numerically to give the corresponding velocities and displacements. These updated values of x_i and $\dot{x}_i$ together with the next values of the road excitation are then input to the right-hand side of equations 3.2.2. resulting in new values of acceleration for time $t = \delta$, where δ is the integration step size. This procedure is repeated at each time increment throughout the duration of the simulation. At each time interval then, we have the displacements, velocities and accelerations of each degree of freedom.

This highlights one of the benefits of time domain simulations. Since the complete vehicle model motions are predicted at each time interval we can generate quite complex component and sub-assembly test signals directly from the models by outputting any number of responses in any combination. For example the relative displacements of the ends of the suspension dampers may be output as a time history for damper testing. Alternatively engine mounts and bracket loads can be selected.

More complex test environments can be selected. Suppose we need to durability test a front subframe which carries the engine mounts and to which the suspension assembly is attached. The simultaneous output of the engine and suspension loads can be achieved easily and this would provide a multi-channel test drive signal set with all channels having the correct individual and cross correlation properties.

Examples of the use of the outputs from specific models in the component test environment are given in Part III.

4.0 DEFINITION OF ROAD SURFACE EXCITATION

The representation of the road surface excitation is clearly of crucial importance in the mathematical simulation of vehicle response. In the previous sections techniques have been developed for:-

i) the representation of vehicle dynamic characteristics by mathematical models of varying degrees of complexity.

ii) the solution of the above models in either the time or frequency domains assuming adequate definition of the vehicle excitation properties where appropriate.

This section will therefore address the techniques which have been developed to obtain adequate descriptions of road surface inputs and how these inputs are interfaced with the mathematical modelling software to provide the model excitation.

4.1. Road Surface Description

Road surfaces are random in nature. If we neglect discrete discontinuities in the surface profile, such as pot-holes etc., we are justified in assuming that road profiles are examples of stationary random processes [8,10,14-18]. It is, in addition, reasonable to assume that their amplitude distribution is Gaussian [or at least clipped Gaussian].

Road surfaces are physically static. An appropriate definition of a single longitudinal profile of such a surface would be by the function [see Figure 13].

$$x[\delta]$$

where X is the surface height, and

δ is distance along the surface from some convenient reference position.

To define the surface completely we would require specification of not only $X[\delta]$ but all $X_i[\delta]$, each $X_i[\delta]$ being representative of adjacent longitudinal profiles.

Such a complete definition is not necessary however.

Consider a four wheeled vehicle moving at <u>constant speed</u> over two parallel road surface tracks $X_R[\delta]$, $X_L[\delta]$, where R and L denote right and left respectively. [δ is distance measured longitudinally along the surface]. If the vehicle speed is denoted by V then $\delta = Vt$ and hence a description of the road surface profiles in the spatial domain provides the excitation displacement-time history applied to the wheels of the vehicle, i.e.

$$X_R[\delta] = X_R[Vt] \Rightarrow I_1[t] = I_3[t + \tau] \qquad 4.1.1.$$

$$X_L[\delta] = X_L[Vt] \Rightarrow I_2[t] = I_4[t + \tau]$$

where $\tau = a/v$, a = wheelbase and I_1-I_4 are the mathematical model inputs as defined previously.

It has been assumed in the above equations that the rear wheels of the vehicle follow the same profile as the front wheels but with a time delay τ dependent upon the speed of the vehicle and its wheelbase.

Two main types of road survey have been used to define the road surface environment in either the spatial or the frequency domain. The earliest road surveys were undertaken manually by measuring the point-by-point heights of two parallel road surface tracks at some predetermined intervals. These spatial domain descriptions consisted therefore of thousands

of digital samples of the surface heights which were subsequently transferred and stored in a digital computer. While this technique gives an adequate description of the road surface it is laborious to undertake and it is clearly not feasible to classify a wide range of road surface types by such methods. More rapid single track surveys have been conducted from moving vehicles where the velocity spectrum of the surface was measured by a small trailing wheel following the road profile [8]. With knowledge of the survey vehicle speed it is then a simple matter to obtain the surface profile displacement spectrum $S_D[n]$ as a function of wave number n, which is measured typically in cycles/metre. $S_D[n]$ is thus a measure of the wave content of the surface. This spectrum can be converted to the displacement frequency spectrum as seen by the wheels of a vehicle moving at velocity v by the relationship:-

$$f = vn$$

$$\longrightarrow S_D[f] = \frac{1}{v} S_D[n] \qquad 4.1.2.$$

A wide range of road surfaces has been surveyed in this manner and the spectra of single track profiles of these roads have been classified [8].

If the main interest is in linear models and frequency response functions then spectral descriptions of road surfaces are sufficient. However, since one of the principal objectives of the present work is time domain response simulation including the generation of inputs for multi-channel component testing it will be necessary to work to define road surface inputs in the time domain.

This need to model vehicle response in the time domain is in conflict with the current trend towards a frequency domain description of road excitations. The conflict is, however, conveniently resolved by a

technique [11] which uses inverse Fourier transform methods to generate realisations of both track profiles of any road surface given information on its surface properties. The information required is the spectral density, $S_D[n]$, of the individual profiles together with the coherency and phase relationships between the tracks. The coherency γ [n] and phase $\phi[n]$ are defined by:-

$$\gamma[n] = \frac{\left|S_X[n]\right|}{S_D[n]} \text{ and } \phi[n] = \tan^{-1}\left[\frac{Im\{S_X[n]\}}{Re\{S_X[n]\}}\right] \quad 4.1.3.$$

where $\left|S_X[n]\right|$ is the modulus of the complex valued cross spectral density of the two track profiles and Re, Im denote the real and imaginary part, respectively.

The realisations provided by the above technique take the form of any selected number of digital samples representing the surface heights of each track. They do not represent any particular stretch of the road surface but exhibit the statistical properties of the surface. That is, they are realisations of a specific random process which defines the surface properties.

In summary then, the road surface excitation of the vehicle models requires a spectral description of the road profile for frequency domain simulations, i.e.

$$S_D[f],\ S_X[f]$$

the spectral density of each profile and the cross spectral density between profiles.

For time domain simulations the point-by-point road profiles are required in the form of digital representations of both the right and left hand tracks.

These digital samples can be obtained for either:-

i. Point-by-point surveys of specific road surfaces.

ii. Computer synthesized digital samples from previously measured spectral information.

or,

iii. Digital representations of specific road features, e.g. ramps, potholes etc.

5.0 MEASUREMENT OF VEHICLE COMPONENT PERFORMANCE

In the previous Sections mathematical equations which define vehicle dynamics have been developed together with methods of analysis. Section 4 also developed techniques for the integration of road surface inputs with these mathematical models.

Consideration will now be given to aspects of vehicle and component data. The task involved in the collection of accurate and representative vehicle data - such as that listed in Appendix A which relates to the 13 degree of freedom model - must not be underestimated.

Simulation accuracy is just as dependent upon representative vehicle data as it is on the inclusion of a sufficient number of degrees of freedom in the mathematical model to define the vehicle dynamic characteristics.

In the following Sections some aspects of vehicle component data are discussed.

5.1. Masses and Inertias

These are the least problematical items in the data list. Vehicle body mass, engine and gearbox mass are simple to obtain accurately. Corresponding inertias are a little more difficult but can be calculated or measured experimentally with acceptable accuracy. Masses of suspension elements including wheels and tyres are again simple to measure. However, calculation of the relevant unsprung masses requires some care if accurate simulations are to be achieved. Those items - such as wheel and tyre - which are totally unsprung present no problems. Items such as suspension springs, links from axle to body/subframe etc. must have

their masses apportioned between sprung and unsprung mass.

The most effective method to obtain the unsprung masses for a specific vehicle is to excite the vehicle on a Road Simulator (Figure 12), measure the axle resonance and calculate the effective unsprung mass M from the relationship:-

$$M_u = \frac{(K\ tyre + K_S)}{4\pi^2 fu^2}$$

where K tyre = tyre stiffness

K_S = suspension stiffness

(generally $K_S << K\ tyre$) and fu is the measured unsprung mass resonance frequency.

Experience with specific suspension types will generally lead to the establishment of effective guidelines so that relationships between total axle and suspension mass and the corresponding effective unsprung mass can be established. (It should be noted that the above experimental measurement is best done with the vehicle suspension dampers disconnected although care is obviously needed in the excitation of the undamped vehicle).

5.2. Suspension Spring Stiffness

Passenger car suspension springs are generally free from significant levels of friction and stiction and are in many cases linear across the typical working range. Figure 14 shows the load v deflection curves for the front and rear suspension springs of a typical passenger car. It can be seen that the front spring is almost ideally linear across the entire operating range.

The rear suspension spring however, is more non-linear. This is not untypical of rear suspensions and the rising spring rate with increased deflection (compression) is intended to help maintain consistent sprung frequencies with increased payload. It will generally be found, however, that the rate about any given mean position is reasonably linear for all but the most severe inputs; nevertheless, each simulation must be taken on its own merits and the measured rates examined with respect to:-

a) static position

and

b) likely spring travel for type of input under consideration to determine the optimum effective rate for modelling purposes.

The springs represented in Figure 14 were of the Helical Coil type which are generally free from stiction/friction. In certain variants of passenger vehicle, e.g. estate cars and particularly van versions there is a tendency in the Industry to use leaf springs which do exhibit increased levels of non-linearity and these must be the object of more careful consideration and in fact fall more correctly into the 'truck spring' category dealt with in Section 8.3.2.

6.0 THE MEASUREMENT & REPRESENTATION OF DAMPER PERFORMANCE

No apology is made for the dedication of an entire Section to the measurement and characterisation of the dynamic performance of the automobile hydraulic damper.

It is the author's opinion that these components represent the single greatest obstacle to the high level simulation of vehicle dynamic response.

6.1. Overview

The hydraulic suspension damper of the modern vehicle is a simple enough device in its construction. Its performance characteristics are however not equally simple. The operation of vehicle dampers, being based on fluid flow, is necessarily complex. It is further complicated by the inclusion of various internal valves (blow-off etc.) all of which conspire to make these devices perhaps the least understood components of the modern vehicle in relation to their effect on ride quality and vibration.

In the main, final damper settings for new models are determined from subjective assessments of the ride quality they provide when installed in the prototype vehicle: once accepted their performance - as measured with standard sine wave inputs - is defined as being that which provides the best ride quality.

There appears to be little attempt made to relate the measured performance of the damper itself to the ride quality it is likely to induce in the vehicle.

Since the object of the present task is to use the damper performance to predict and optimise vehicle ride and vibration it is clear that any description of the damper characteristics input to the mathematical models must be a complete and accurate definition of the installed performance of the damper.

In the early simulations using the vehicle models the traditional methods of defining damper performance - i.e. with sine wave inputs - were used. It was found that characterisation of damper performance by these methods led to unacceptably poor simulation accuracy with respect to the use of the technique as an analytical design tool for ride quality and vibration. Indeed a totally new approach to the measurement and characterisation of damper performance had to be developed, the results of which give very significant improvements in response simulation accuracy and in themselves gave additional insight into the behaviour of the dampers themselves. The results of this aspect of the simulation technique development are discussed below.

6.2. Damper Testing Under Random Loading

It is clear from the previous Section that discrete sine wave test procedures do not lend themselves to an adequate characterisation of the 'in vehicle' performance of dampers. As a result it was necessary to investigate more realistic testing methods.

It was considered that the ideal testing procedure would be to measure damper behaviour while the damper was being excited with realistic service inputs.

The service environments of vehicle dampers are always random, being the relative displacement of the two ends of the damper. Since the top of the damper is connected to the vehicle body and the bottom to the unsprung mass (axle) it is clear that the relative displacement of the two ends will reflect both body and axle responses. It is also apparent that the damper motion will be different for varying road surface types. In addition damper performance is likely to be affected by overall input level - particularly at very low and very high levels - as well as by input frequency distribution.

The ability to reproduce typical service loadings on vehicle dampers is offered by Servo-Hydraulics. The relative displacement time histories of vehicle dampers can be measured on the road or in the laboratory with a Road Simulator and recorded onto magnetic tape. Several road surface inputs can be used. These recorded signals can then be used to drive a purpose built servo-hydraulic test rig and reproduce the service environment of the damper.

When such a rig is driven by the relative displacement signals measured on the vehicle, the damper will be subject to the same vibration environment as it experienced in the vehicle for any particular road input. While it is being excited in this manner any performance measurements which are taken must be totally valid and representative of the dampers installed performance.

Accordingly random data analysis procedures were in need of development in order to analyse the results of any such tests.

6.2.1. Test Method

The devised test method is illustrated in Figure 15. However, since initially no damper relative displace-

ment data was immediately available the 13 degree of freedom mathematical model was used, with the best estimates of damper coefficients, to produce the relative displacement time histories of the front and rear dampers of both vehicles A and B in time domain digital form when subjected to various road inputs.

Using this digital data and a digital-to-analogue facility relative displacement time histories were produced and used to drive a Servo-Hydraulic test machine such as that shown in Figure 16 noting that for increased realism the dampers were tested complete with their end bushes.

Figure 17 shows one of the relative damper displacement PSD plots for one of the vehicles on a simulated 'A' road surface as output by the time domain model. As expected the low frequency body motions have the higest amplitudes (around 1-2 Hz) but there is also evidence of the axle motion at around 8-10 Hz.

The corresponding damper velocity PSD is shown in Figure 18.

The signal time history $-x_3(t)$ in Figure 15 - corresponding to the displacement PSD in Figure 17 - was fed into the damper and the transmitted load F(t) was recorded simultaneously with the input feedback displacement. The PSD of this load history is given in Figure 19.

6.2.2. Analysis of Random Test Data

Two functions which were used to characterise the performance of the damper were computed from the input displacement and transmitted load time histories.

These are:-

i) The modulus of the Frequency Response Function [*] between the transmitted load and input velocity histories which gives the variation in damping level across the frequency range of interest. See Figure 20 for example, noting that the Y-axis units are N/m/s [i.e. units of damping].

ii) The Coherency and Phase relationship between the load and input velocity which gives a measure of the 'linearity' of the damper. Note that an ideal linear damper - i.e. where the force transmitted is directly and constantly proportional to velocity - would have a Coherency of unity and Phase shift of 0^{o} between the force and velocity across the entire frequency range. Figure 21 shows the plot of these functions for a specific damper.

[*] The Frequency Response Function in i] is defined by:-

$$FR_{FV}[f] = \frac{S_{FV}[f]}{S_{F}[f]} \qquad 6.2.1.$$

The most interesting observations from Figures 20 and 21 are:-

1] The effective damping level for this particular damper is more or less constant from about 0.5 Hz upto about 12-15 Hz after which there is a gradual reduction in damping coefficient.

2] Over the same frequency interval the damper Coherence and Phase behaviour is almost that of and ideal damper, i.e.

$$F = CV$$

These results were surprising in view of the almost general acceptance that damper behaviour was non-linear as seen in the typical force-velocity plots. Testing of a range of different dampers showed the results above to be typical although clearly the overall level of damper coefficient was different in each case. In addition other factors such as the frequency at which fall off occurred and the rate of fall off also varied from damper to damper but some of these are discussed below.

Also of interest was the value of the effective damper coefficient obtained from the random tests when compared to the values obtained from the sinusoidal tests. A typical comparison is given in the Tables below.

[All numerical values are quoted in N/m/s]

Vehicle B	Com-pression	Extension	Equivalent[1] Linear Value	Effective Value From Random Test
Front Damper	780	2840	1810	2910
Rear Damper	705	1800	1253	2375

Vehicle A[2]	Average Value (12.5mm)	Average Value (25mm)	Effective Value From Random Test
Front Damper	310	730	1760

It is clear from the above that there is little correlation evident between the various sinusoidal

---

1 See Appendix C Figure C-2
2 See Appendix C Figure C-3

results and those from the random tests. Considerable effort was expended in an attempt to obtain a degree of correlation by considering various manipulations of the sinusoidal data, e.g. averages, peaks, equivalent damping rates, averages of equivalent damping rates etc. but no significant rules or correlation could be established which applied to more than one specific damper. Appendix C develops the formula used to calculate the 'equivalent damping rate' and gives the 'average damping value' plots for a particular damper.

Although results will not be presented here, attempts were also made with the time domain model to represent the damper performance with one of the force-velocity plots, i.e. the instantaneous damper force during the simulation was obtained by using the instantaneous relative velocity of the damper ends to obtain the instantaneous force from the stored list of force-velocity pairs as defined by the force-velocity plot.

This was also unsuccessful in obtaining high level simulation.

It was ultimately concluded that for high level simulation modelling it is necessary to obtain damper performance from random tests.

Figure 22 shows the marked improvement in simulation accuracy for vehicle A by using the random test results as compared with earlier attempts based upon the sinusoidal results.

Figure 23 also shows the level of simulation achieved with the random result for vehicle B.

At this stage some additional work was performed to investigate:-

i) An alternative analysis approach.

ii) The sensitivity of the results to the type of random excitation used.

iii) The effect of temperature on damper performance under random loading.

and

iv) The scatter of results when testing different dampers of the same type.

These are discussed briefly below.

6.2.3. Analysis by PSD Ratio

Recall that the damper coefficient plot in Figure 20 is in effect a plot of the modulus of the Frequency Response function between the velocity and force random signals as defined in equation 6.2.1. As a result when the coherence is less than unity the Frequency Response will be biased downwards by a factor dependent upon the deviation from unity of the coherence function.

Since the test performed is in effect single input/ single output with no significant extraneous noise present in either signal, the ratio of the PSD's was also examined, i.e.

$$C_{FV}(f) = \left[\frac{S_F(f)}{S_V(f)}\right]^{\frac{1}{2}}$$

The function $C_{FV}(f)$ so defined will in effect be the 'equivalent linear frequency response function' between the input and output.

To compute this the input <u>displacement</u> X(t) and the output force F(t) were recorded as time signals and $C_{FV}(f)$ computed via the relationship:-

$$C_{FV}[f] = \frac{1}{\omega} \left\{ \frac{S_F[f]}{S_X[f]} \right\}^{\frac{1}{2}}$$

where $\omega = 2\pi f$

The function $C_{FV}[f]$ will thus have units of damping, i.e. N/[m/s].

Figure 24 shows the comparison between the results obtained for a specific damper by the Frequency Response Function method and by the PSD ratio approach.

As would be expected the differences are small where the coherence values between input displacement and output force are close to unity and only become significant as the coherence values become significantly less than unity. Nevertheless the differences are marginal in the 0-15 Hz range where the dampers have their greatest effect upon the vehicle ride and vibration considered in this work.

6.2.4. Sensitivity of Results to Input Excitation

The object of this exercise was to establish whether the improvement in damper characterisation by the random input method was due to either:-

i) the fact that the input was random and not discrete sine wave.

or,

ii) the fact that the input was not only random but also representative of service vibration, i.e. with respect to both the level of and shape of the PSD plot.

To assess the above, two series of tests were conducted:-

1] Variation of frequency content of the input excitation by using a 'white noise' signal of identical RMS to the 'correct' input displacement.

and

2] Variation of the input level by factoring the 'correct' input by $\pm$50% and reanalysing the results.

The two inputs for test 1] are illustrated graphically in Figure 25 which shows the band-limited (0-15 Hz) white noise of equal RMS to the original input data. Figure 26 shows the results of both tests with respect to damper coefficient and Figure 27 gives the corresponding coherence and phase plots.

Very significant differences are apparent.

The damping level at low frequency (i.e. in the rigid body mode region) is greatly increased. This is as a result of this damper's sensitivity to low input level and is undoubtedly as a result of inherent stiction/friction. (The white noise signal effectively reduces the low frequency input and amplifies the higher frequency inputs when compared to the 'correct' input - Figure 25).

This information on damper sensitivity to low input levels is invaluable to vehicle designers since this phenomenon often causes ride problems on smooth roads, e.g. motorways where the low input levels cannot break the stiction in the dampers the effect of which is that the vehicle 'rides on its tyres'

with attendant increases in sprung mass frequencies and greatly reduced ride comfort.

At the higher frequencies the increased input level of the white noise input has caused a reduction in effective damping. This effect has been found to be true of all the dampers tested but it does need very significant increases in input level before the effect is noticeable.

The coherence and phase plots also confirm the stiction effect at the low frequency end which manifests itself with low coherence, i.e. increased non-linearity and with the phase between transmitted force and input displacement being much closer to 0^{o}.

To assess the effects of varying the levels of the 'correct' input analysis was performed on the results of tests with $\pm$ 50% factors applied. The results are tabulated below.

Damper Type / Excitation	'Correct'* Input N/m/s	Input +50% N/m/s	Input -50% N/m/s
Rear (Vehicle B)	1050	1000	1234

* RMS Displacement = 0.0131 m
RMS Velocity = .1831 m/s

The tendency for the effective damping rate to:-

i) Increase with reduced input level

ii) Reduce with increased input level

was found to be a general one but in each case a 'threshold' level had to be reached before the

changes become significant. It is clear from the above Table that the standard input is closer to the lower threshold than the upper.

6.2.5. The Effect of Temperature on Damper Performance Under Random Loading

The phenomenon of damper 'fade' is well known as the loss of damper control at elevated temperatures. A single qualitative test was established to ensure that this effect could be detected by this new measurement approach.

A specific damper was tested at normal laboratory ambient temperature with the -50% input and then again at high temperature (approximately 80^{o}C) and results compared.

Figure 28 gives the load spectra for both cases and the loss of transmitted load for the high temperature test is evident.

Figure 29 shows the corresponding damper coefficient plots and the loss in damper rate is quite apparent representing about a 50% loss of performance.

6.2.6. Scatter of Test Results on Samples of Specific Damper Designs

It was important to establish whether any significant scatter would be apparent if various dampers of the same type purchased from different sources were tested in sequence.

The results are tabulated below:-

Damper Type	Measured Coefficient			Max Scatter (Max-Min)/Min
	No.1	No.2	No.3	
Vehicle 'A' Front	2745	2910	3101	13%
Vehicle 'B' Rear	1020	1050	-	3%

Without batch testing a large number of dampers of different types which is clearly outside the scope of the work, it is difficult to generalise on scatter. The results obtained here are encouraging if they indicate the limit on scatter since the scatter on the total vehicle damping is likely to be less than the 13% level above.

7.0 PASSENGER VEHICLE MODEL VALIDATION

Considerable effort has been expended with the aim of increased realism in the simulation technique with respect to:-

- Mathematical Model complexity
- Realistic measurement of component performance

and

- Adequate descriptions of the road surface input.

This led to the development of the four-input three-dimensional model [as shown in Figure 5] for the high level simulation of passenger vehicle dynamics. The availability of such a model will allow us to quantify the loss of simulation accuracy when using less realistic models, e.g. two-dimensional or two input only etc. [This is important in that it will help us decide whether the increased complexity of higher level models is justified by their improved accuracy].

Using the three-dimensional model three conditions were considered and results were compared from each of the following:-

1] the complete four-input three-dimensional model with four properly correlated road surface inputs.

2] the corresponding 'half width' two-dimensional model using a single profile input.

and

3] the model as in 1] but with <u>independent</u> inputs to the right and left hand sides of the vehicle such as might be used where no information was available on cross track correlation.

The results of this exercise are given below.

7.1. Comparison of Two-Dimensional and Three-Dimensional Model Responses

A simple exercise was devised to quantify the loss of simulation accuracy sustained when restricting the mathematical model for example to two dimensions. Any three-dimensional model which is symmetrical about its longitudinal axis and which is excited by two identical road surface tracks will respond in a similar manner to the corresponding half width two-dimensional model excited by the single profile. Consequently if the three-dimensional model is excited with the correlated profiles and then again with either profile applied simultaneously to both sides, comparison of the resulting responses will quantify any loss of simulation accuracy for a two-dimensional model.

Two such results are given in Figures 30 and 31 using data from a typical passenger vehicle. Figure 30 shows the acceleration response spectra of a point on the front body of the vehicle predicted from both models. Considerable differences are apparent between the curves. Figure 31 gives corresponding results for the left hand end of the rear axle. The error induced by the two-dimensional simulation would have been more tolerable had it provided some bound on the true response. However, the error in the simulation as shown in Figure 30 reduces response around 8 Hz but increases it at higher frequencies. Little difference was observed between the spectra of the front unsprung masses for the two-dimensional and three-dimensional models; this is to be expected since the front suspension is independent and hence the motions of the axles will be largely uncoupled. However any response highly dependent on vehicle roll will be poorly represented by a two-dimensional model. Furthermore the test route did not induce much roll in the vehicle as would be expected on rougher

roads or proving grounds. Two-dimensional models in these instances would introduce more serious errors.

From the simulation results of the three-dimensional model with typical saloon car parameters, the following can be concluded:-

1) Serious errors result in response prediction when using a two-dimensional model. The error is not confined to roll parameters but also affects the bounce and pitch modes, in some cases by as much as 100% [in the spectrum] over a large part of the frequency range - usually for all f > 5 Hz.

2) For roll parameters the error is serious since two-dimensional models cannot incorporate roll and it is therefore effectively zero. In general therefore a two-dimensional model will:-

   i) Neglect roll

   ii) Overestimate pitch

   iii) Overestimate bounce - seriously at the centre of gravity position, rather less so at the nearside and offside body positions since the lack of roll response tends to cancel the overestimation of bounce.

A similar exercise was carried out using uncorrelated track profiles and some general conclusions can be shown.

Three-dimensional models utilising two independent random road profile inputs introduce the following errors:-

   i) Body bounce underestimation - the error reducing with increasing frequency.

   ii) Body pitch underestimation - errors as above.

iii) Roll overestimated around the component roll resonance frequencies - the magnitude of this error reducing with increasing frequency.

iv) Unsprung mass bounce overestimated - seriously upto approximately 2 Hz - the error decreasing with increasing frequency upto and beyond wheel hop. Wheel hop is relatively free from track correlation errors since at these frequencies the correlation of the tracks is in any case very small.

It was also concluded that the errors in simulation of a three-dimensional model using uncorrelated inputs are much less than with any two-dimensional model, especially at frequencies higher than the primary rigid body modes.

7.2. Experimental Validation of Mathematical Simulation

It was important to establish the quality of response simulation accuracy attainable with the high level simulation model. To do this a correlation exercise was devised which used data recorded on the actual vehicle [19] when driven over a specific, previously surveyed road surface.

The data obtained from the road survey was used to estimate the direct spectral density and the coherency and phase relationship of tracks corresponding to the track width of the test vehicle.

The road profile synthesis programme [discussed in Section 4.1] was then used to synthesize realisations of the surface heights of both track profiles to give

digital time domain excitations to the vehicle model as required by the differential equations.
(It might at first sight appear an overly complex method of defining the road surface heights since survey data was available: it was important however to assess the accuracy of the technique as a whole, i.e. to include any errors arising from the approximation errors in the synthesis programme as well as any limitations imposed by the modelling technique).

It can be seen from the vehicle model (Figure 5) that a point contact is employed to represent the tyre-road interface. A smoothing function (19) was therefore used to modify the generated road profiles to compensate for the filtering effect of the tyre contact patch. Figure 32 gives the spectral density of the single tracks after compensation for tyre enveloping effects. Figure 33 indicates the relationship between right and left synthesized profiles and shows the coherency and phase as functions of vehicle input frequency. These plots were the result of digital spectral analysis on the synthesized digital profiles.

The test vehicle had previously been instrumented and driven over the test route at a constant speed of 65 km/h. Acceleration was recorded at various points on the vehicle including front and rear axles, engine and several points on the body. The mathematical model of the test vehicle was then used in conjunction with the time domain simulation programme to predict the time domain acceleration responses at the accelerometer positions on the vehicle.

The acceleration spectra of the predicted and experimental responses are superimposed in Figures 34 to 38. It is apparent that a high degree of simulation has been achieved. No attempt was made to simulate the higher frequencies (>20 Hz) arising from engine, drive-train and other sources, and the loss

of simulation accuracy at these frequencies is evident, particularly in the engine response prediction. [The large peak at about 40 Hz on the engine and front axle responses was due to ignition interference with the instrumentation].

For the modelling technique to be applied to reproduce component environments in the laboratory it is necessary to simulate not only single responses, as in the above Figures, but also relative responses. A suspension spring for example is stressed by the relative displacement of its ends and provided inertia effects are neglected, the absolute motion of either end of the spring, taken by itself, gives no information on the loading of the spring. The quality of simulation of relative responses predicted by the model may be seen in Figure 39 which shows the spectra of the vertical acceleration of one of the front axles relative to the other, generated by the model and also as recorded on the test road. Included in Figure 39 is the relative axle response of the test vehicle on the Road Simulator with the same generated road profiles as were used in the model simulation imposed at the wheels. The Road Simulator provides an intermediate step to complete vehicle response simulation since it used the actual vehicle but applies synthesized road surface displacements to the wheels. Comparison between simulator and model responses gives an indication of the model's representation of the vehicle dynamics by removing the effects of any simulation errors which arise from differences in the generated and actual road surface properties. It is apparent from Figure 39 that the model response corresponds even more closely to the Simulator response. This suggested that improvements could still be made in the surface description for this particular road.

PART II

COMMERCIAL VEHICLE SIMULATION

8.0 COMMERCIAL VEHICLE SIMULATION

The other class of road vehicle dealt with in this work is that of the commercial vehicle. This class includes both articulated and non-articulated vehicles. Many of the techniques developed for passenger vehicles will be seen to read across directly to commercial vehicles but in the following Sections specialised techniques which had to be developed to cater for the significantly increased task of mathematically modelling this class of vehicle are described.

8.1. The Truck Ride Problem

The problem of improving commercial vehicle ride quality is of continuing concern to truck designers. It is a problem for which there is no easy solution since the factors which ultimately determine the ride quality in a commercial vehicle are numerous. The truck ride problem is largely a consequence of the geometry and operating conditions of this type of vehicle and is not solely attributable to the quality of road surfaces: passenger vehicles traverse similar surfaces at similar speeds, yet their ride qualities are notably better.

It is worth examining briefly the properties of commercial vehicles, particularly articulated vehicles, which hinder the design of good ride quality.

The most significant geometric difference from passenger vehicles is the high location of the truck operator in the vehicle cab. High vertical and fore-and-aft motions can occur at this position as a result of comparatively small angular pitching motions of the cab structure and can be particularly disturbing to the occupants.

These motions can arise by either:-

i) The rigid body pitching motions of the truck frame being reflected in the cab.

ii) The cab pitching on its own suspension relative to the frame.

iii) The frame imposing pitch motions on the cab where the frame motion is due to some other source, e.g. axles, engine, trailer etc.

or, more usually, by some combination of i) to iii).

The large laden-to-unladen weight ratios experienced during the commercial operation of these vehicles result in equally large variations in their mass and inertial properties.

The designer is thus faced with the task of optimising the vehicle ride characteristics where the dynamic properties of the vehicle vary greatly in service.

This makes suspension optimisation a much more complex task. For example, designing primary suspension to be adequate for the fully laden vehicle will result in increased sprung mass frequencies - and hence a tendency towards inferior ride - for lighter loads.

In addition the trailers of articulated vehicles will frequently impose their dynamics on the tractor unit through the fifth wheel coupling. Their effect will be apparent in the tractor frame which will, in turn, affect the cab response and the vehicle ride quality.

The frames of commercial vehicles differ significantly from the equivalent passenger vehicle body structure.

The flexibility of these structures is such that their dynamics appear in the ride frequency range to

a significant extent. This is especially true of articulated vehicle trailers in the fully laden condition.

The consequence of this is that the 'rigid body' assumption for passenger vehicles is never applicable to commercial vehicles and techniques for incorporating truck frame flexibility had to be developed. [It should be pointed out that very occasionally it is necessary to depart from the 'rigid body' assumption even for passenger vehicles but these occasions are clearly the exception].

8.2. Techniques for the Representation of Truck Frame Flexibility

Before attempting to develop complete truck models it was very necessary to first establish whether truck frames were amenable to relatively simple mathematical representation such as could be incorporated into the modelling approach adopted for the passenger vehicle simulation.

It was therefore necessary to establish:-

1] Whether truck frames could be modelled dynamically to a sufficiently good degree of accuracy without for example the complexity of the finite element approach.

2] Whether the models of the frames could be combined with the lumped parameter representations of the other dynamic elements of the vehicle such as axles, engine etc.

and

3] Whether the models so produced would provide adequate simulation quality.

8.2.1. Representation of Truck Frames by the Transfer Matrix Approach

An initial attempt was made to employ the method of Transfer Matrices [20] to mathematically model truck chassis structures. A generalised computer programme was developed [MATRIX] which is capable of predicting the natural frequences and mode shapes of idealised 'beam-type' structures supported on spring elements representative of the truck suspension springs.

The theory and use of Matrix is described in Appendix D.

Information was obtained on the sectional geometry of a particular truck tractor frame. The frame was divided into a series of discrete sections and the individual mass and flexural stiffness [EI] properties were calculated.

The truck primary suspension spring rates were obtained and incorporated into the idealised model and the data used in the MATRIX programme.

The truck suspension springs were of the 'taper leaf spring' type where each spring is attached at two spring hanger positions onto the chassis frame at two separate positions and to improve realism in the model it was necessary to model each spring by two half rate springs each of which was attached at the appropriate spring hanger position.

A 50 mass idealisation of the tractor unit [Figure 40] was used and the natural frequency and mode shapes plotted. Figures 41 show the plotted mode shapes for this tractor unit.

The primary vehicle bounce and pitch modes occur at 2.56 Hz and 4.7 Hz respectively with the tractor primary bending mode at 16.5 Hz.

Note the location of the centres of oscillation, particularly in the pitch mode, with pitch centre just beneath the centre of the cab position. This is the cause of disturbing fore-and-aft vibrations typically experienced in tractor units of articulated vehicles when separated from their trailers. Reference should be made to Appendix E which discusses the topic of centres of oscillation the results of which were derived by the use of the two degree of freedom rigid body model described in Section 2.4.

It soon becomes apparent however that the transfer matrix approach was not readily amenable to the expansion which would be necessary to incorporate unsprung masses, cab and engine dynamics as well as the addition of the trailer dynamics.

Nevertheless an attempt was made to model the effect of the trailer mass (but not inertia) on the primary modes of this tractor unit.

The static load applied to the tractor unit was added to the tractor mass distribution at the appropriate position and the primary tractor modes recomputed the results of which are given in Figures 42.

The effect of the trailer 'reaction mass' can be seen in that both modes have reduced frequencies and the centres of oscillation have both moved rearwards. Note also that frame bending is apparent in the 'laden' case for the lower mode as a result of the increased mass on the tractor frame. No significant bending is apparent in the second mode since the tractor trailer coupling is close to the centre of oscillation in this mode and thus the corresponding inertia loads are reduced.

The technique was also applied to the laden trailer by calculating the effective vertical spring rate of the tractor unit as the 'fifth wheel' position.

Figures 43 give the predicted first and second bending modes of the fully laden trailer at 6.5 Hz and 14.1 Hz respectively.

Although this approach was not deemed suitable for expansion to more complete representations of the coupled articulated vehicle it is seen to have application to the primary ride modes and also to the lower bending mode of both tractor and trailer frames.

8.2.2. The Finite Difference Approach

The finite difference technique was found to be more suitable for application to the dynamic modelling of articulated vehicles. For the present work a complete vehicle model was developed capable of predicting the natural frequencies and mode shapes of articulated vehicles relevant to the ride comfort range.

Both the mathematical model formulation and the application of the finite difference technique are discussed below.

1) Two-Dimensional 63 Degree of Freedom Articulated Vehicle Model

A two-dimensional 63 degree of freedom model of the articulated vehicle configuration was developed. A schematic of the model is given in Figure 44. A key to the variables used in the model is given in Appendix F with a list of the 63 degrees of freedom.

The model is two-dimensional and full width (i.e. the total mass of the vehicle is considered) with both tractor and trailer frame bending flexibility included. The tractor frame is idealised by 27 masses (25 main frame and 2 end masses) and for the specific vehicle being modelled in this exercise, the 19th mass on the tractor frame was coupled to the 3rd mass on the trailer frame. The trailer frame is also idealised by 27 masses including the coupled mass. The coupling between tractor and trailer frames reduces the 54 degrees of freedom to 53, the coupled mass being the sum of the tractor and trailer frame component masses. The rows in the matrix equation which would have corresponded to the 19th tractor and 3rd trailer masses are coalesced to effect the coupling. The corresponding row in the mass matrix contains the sum of the component masses. In total, the vehicle model has 63 degrees of freedom:-

53 for the frame idealisations - all vertical,

4 for the tractor and trailer axles - vertical,

3 for the cab - vertical, longitudinal and pitch, and

3 for the engine - vertical, longitudinal and pitch.

The longitudinal mount stiffnesses of the cab and engine were incorporated into the model since these stiffnesses can have a significant effect on the ride dynamics but are not shown in the model schematic.

The suspension springs of the tractor unit are modelled as two semi-springs (half rate) located

at the spring hanger positions, each semi-spring being attached to the appropriate mass element on the frame. This allows more representative deformations of the frame. The cab and engine mounts are attached to the appropriate frame mass elements in a similar manner. This refinement was not included in the trailer model as shown in Figure 44 since the ratio of frame length to spring-hanger separation is much greater in the case of the trailer.

2) Differential Equation of Model

The dynamic equations of a model of the complexity are difficult to present neatly and in a meaningful manner but, for completeness, the Fortran listing of the subroutine which fills the stiffness matrix of the model is listed also in Appendix F. This subroutine is part of the model solution computer programme which computes the undamped natural frequencies and mode shapes of the model from the matrix equation.

The algorithm for developing the equations of frame bending is given in the following section and was incorporated in the equations of motion of the total vehicle.

3) Derivation of Finite Difference Algorithm for Truck Frame Idealisations

Consider transverse vibration of a beam (Figure 45 a) neglecting rotary inertia and the effects of shear deformation. The strain and kinetic energies of the beam can be written:-

$$SE = \frac{1}{2}\int_0^{\ell} EI\left[\frac{\partial^2 w}{\partial x^2}\right]^2 dx \qquad 8.2.1.$$

where w is the transverse displacement,
x is the distance along beam, and
ℓ is the total beam length.

Note that for non-uniform beams (EI) will be a function of x, and

$$KE = \frac{1}{2}\int_0^{\ell} m\dot{w}^2 \, dx \qquad 8.2.2.$$

where m is the mass per unit length, and
$\dot{w}$ is the transverse velocity.

Dividing the beam into n equal segments each of length h, such that

$$nh = \ell$$

we can replace the integrals by discrete summation. Recall the trapezoidal rule for approximate integration:-

$$\int_{x_o}^{x_n} f(x)\,dx = \tfrac{1}{2}h(f_0 + 2f_1 + 2f \ldots + fn) \qquad 8.2.3.$$

where f(x) is the function,
h is the step length, and
x_o, x_n are the bounds on the integral.

Recall also the central difference formula (Appendix G):-

$$\left\{\frac{\partial^2 w}{\partial x^2}\right\}_j = \frac{1}{h^2}\left(w_{j-1} - 2w_j + w_{j+1}\right) \qquad 8.2.4.$$

Equations 8.2.1. and 8.2.2. can now be written:-

$$SE \doteq \frac{1}{2}\sum_{j=0}^{n} (EI)_j \frac{h}{2}\frac{1}{h^4}\alpha_j\left(w_{j-1} - 2w_j + w_{j+1}\right)^2$$

where $\alpha_j = \frac{1}{2}$ $\quad j = 0, n$

$= 1$ otherwise

$$\doteq \frac{1}{2} \sum_{j=0}^{n} [EI]_j \alpha_j [w_{j-1} - 2w_j + w_{j+1}]^2 / h^3 \qquad 8.2.5.$$

and

$$KE \doteq \frac{1}{2} \sum_{j=0}^{n} \alpha_j m_j \dot{w}_j^2 h \qquad 8.2.6.$$

In this form the equations define the beam vibration which can be solved by matrix manipulation or by numerical integration methods in the time domain.

The energies of the flexing beam are now defined as functions of the beam element motions. To modify them to the format required for dynamic differential equations we must use Lagrange.

$$\frac{d}{dt} \left\{ \frac{\partial [KE]}{\partial \dot{q}_i} \right\} + \left\{ \frac{\partial [SE]}{\partial q_i} \right\} = 0 \qquad 8.2.7.$$

where q_i are the generalised co-ordinates.

Applying Lagrange to the beam energies we have

for $q_i = w_o$

$$\frac{\partial [SE]}{\partial w_o} = \left\{ \left(\frac{EI}{h^3} \right)_o [2w_o - w_{-1} - w_1] + \left(\frac{EI}{h^3} \right)_1 [w_o - 2w_1 + w_2] \right\}$$

or replacing $[EI/h^3]_j$ by A_j

$$= A_o [2w_o - w_{-1} - w_1] + A_1 [w_o - 2w_1 + w_2] \qquad 8.2.8.$$

$$\frac{d}{dt}\left\{\frac{\partial[KE]}{\partial \dot{q}_i}\right\} = \frac{d}{dt}\left(\frac{h}{2} m_o \ddot{w}_o\right) \qquad 8.2.9.$$

In equation 8.2.8. the unknown displacement w_{-1} can be removed by considering the boundary conditions in this application:-

$$\left[\frac{\partial^2 w}{\partial x^2}\right]_{j=0} = 0$$

i.e. $w_{-1} - 2w_o + w_1 = 0$

or $w_{-1} = 2w_o - w_1$ from equation 8.2.4.

Substituting in equation 8.2.8.

$$\frac{\partial[SE]}{\partial w_o} = A_o[o] + A_1[w_o - 2w_1 + w_2]$$

Applying equation 8.2.7.

$$\frac{h}{2} m_o \ddot{w}_o + A_1[w_o - 2w_1 + w_2] = 0 \qquad 8.2.10.$$

This is the differential equation of motion of the end mass of the beam. In a similar manner the equations of the j-th mass of the beam can be given by:-

$$\ddot{w}_j = \{2[A_{j-1} + A_j]w_{j-1} + 2[A_j + A_{j+1}]w_{j+1} - A_{j-1}w_{j-2} - [A_{j-1} + 4A_j + A_{j+1}]w_j - A_{j+1}w_{j+2}\}/M_j$$

where M_j is the mass of the j-th element [$= m_j h$].

Where other components are attached to the above masses - for example suspension springs - the appropriate dynamic force is simply added to the relevant equation above.

Figure 45 b gives an example of a spring attachment at the j-th mass and indicates the adjustment to the differential equation of motion.

This type of analysis was applied to the matrix equation representing the dynamics of the articulated vehicle. The mathematical model provides the dynamic equations which are collected into matrix form and computer analysis yields the eigenvalues and eigenvectors. Since the model has 63 degrees of freedom there will be 63 natural frequencies and mode shapes. However only the lower frequency mode shapes will be of interest to us in the ride context. To aid interpretation of the various mode shapes [each will have 63 co-ordinates] computer graphics software was developed and interfaced with model eigenvector solution programme. This enabled the mode shapes to be displayed at a graphics terminal and greatly simplifies interpretation of the various modes.

8.2.4. Extension of Frame Flexibility to Include Torsion

It was shown in the previous Section how frame bending flexibility could be incorporated into the models by the techniques of finite differences.

The next stage in the development of the frame flexibility was to incorporate torsional flexibility.

The only frame torsional data which was available was an experimentally measured overall torsional stiffness of the particular tractor unit as measured between the front and rear spring mounting positions. No similar data was available for the corresponding trailer frame. Nevertheless it was important to proceed to determine the feasibility

of incorporating torsional stiffness into the model simulations and evaluate solutions in both the frequency and time domains.

A 34 degree of freedom model of the tractor unit was developed to include frame bending as before but with the addition of frame torsional flexibility. [This model was used for time domain response correlation and will be discussed later]. The frame was assumed to have uniform sectional torsional stiffness equivalent to the overall stiffness which was measured experimentally. Note that this is not a restriction imposed by the model but by the data available at the time since the idealisation, as shown in Figure 46, allows discrete torsional inertia and stiffness to be incorporated at each section of the frame idealisation. [This data would originate from either a finite element analysis of the frame structure of perhaps from more discrete measurements of the frame torsional flexibility].

The inclusion of rotational flexibility significantly increases the complexity of the differential equations representative of the vehicle dynamics.

8.3. Eigenvalue/Eigenvector Analysis with Frame Flexibility

Sample results are given here which are clearly vehicle specific but will be included to illustrate the output format and to indicate the degree of interpretation which can be obtained from such analysis. [The results recorded here are from runs of the 63 degree of freedom articulated vehicle model using data on a specific prototype supplied by the vehicle manufacturer, most of which originates from component dynamic tests.

8.3.1. Vehicle in Fully Laden Condition

Using the data supplied, the set of modes shown in Figure 47 was generated. The first two modes are the rigid body modes of the tractor unit and these are the spring modes, i.e. no friction is included in the spring stiffness. The trailer mode is seen to be a rigid body mode on the trailer tyres. The overall trailer stiffness supplied as a 'bounce on tyres' stiffness was taken as trailer tyre stiffness and the trailer springs were effectively locked. A brief description of each mode is given below.

Mode at:

a) 1.78 Hz. This is clearly the bounce mode of the tractor unit with the bounce centre outside the trailer frame to the rear. Notice in this mode that there is less motion at the tyres than on the frame and more motion at the front of the frame than at the rear.

b) 2.6 Hz. This is the tractor pitch mode with the pitch centre just ahead of the tractor centre of gravity. Again there is more motion at the frame than at the axles.

c) 3.24 Hz. The trailer can be seen to be bouncing on its tyres in this mode with no relative motion between trailer frame and axles. This is as expected since the suspension stiffness is much higher than the tyre stiffness and indeed no dampers were needed as a result of the friction levels. These are the body modes of the laden vehicle.

d) 6.22 Hz. This mode is predominantly first bending in the trailer. The rear of the tractor frame is moving in phase with the fore end of the trailer frame and this motion is not totally

absorbed by the rear tractor spring and significant motion of the rear axle is evident. Both the cab and engine are seen to respond to the tractor frame motion by moving in phase with it.

e] 7.79 Hz. This mode is predominantly longitudinal motion of the engine on its mounts but the cab can be seen to move in phase. The cab motion is mostly longitudinal/pitch.

f] 8.19 Hz. The most significant motion here is the cab on its rear mounts. There is noticeable bending of the tractor frame and motion of the engine on its rear mounts. Again the motion of the rear of the tractor frame is accompanied by in-phase motion of the rear axle on its tyres. This time the rear axle and cab are moving in anti-phase in contrast to the condition at 6.2 Hz.

g] 8.67 and 9.31 Hz. These modes are the front and rear tractor axle resonances. In the mode at 8.67 Hz the only other motion is an out of phase bounce of the cab and engine. At 9.3 Hz the rear axle moves in anti-phase with the rear tractor frame and again motion of the cab on its rear mounts is evident. A little bending of the tractor frame is present and the node is at the cab/engine position. This accounts for the different phase of motion of cab and engine since both rear mounts lie on portions of the frame which are on opposite sides of the node. Again it is apparent that significant cab motion accompanies significant rear axle motion. However it must be noted that the rear axle motion is in addition accompanied by significant frame motion.

h] 10.8 Hz. The significant motion here is the engine on its rear mounts accompanied by tractor

bending and cab vertical motion. The cab motion is bounce on the front mounts in phase with the front frame of the tractor. Again motion of the rear axle is evident and is greater than at the front axle.

i] 14.55 Hz. This is the engine pitch mode. In contrast to the previous mode the printout of the eigenvector indicates that the pitch/vertical motion ratio is much higher in this mode than in the previous mode but clearly the pitch/vertical coupling is high in both cases. There is significant cab motion in this mode both vertical, pitch and longitudinal. The second bending mode of the trailer is also in evidence.

j] Higher modes. The trailer second bending mode is seen to dominate at 15 Hz. At 18.5 Hz the cab pitch resonance mode occurs, i.e. where the cab pitch relative to the other cab motions is a maximum.

At 24 Hz the tractor frame has significant bending but the other tractor components have no significant motion. The deformed shape has a node at about the fifth wheel position and the maximum displacement occurs at about the cab rear mount position.

8.3.2. Effects of Suspension Friction/Stiction

The effects of friction in the suspension springs is given in this section. The tractor spring stiffnesses were increased by a nominal factor of three and the set of modes recomputed. The vehicle configuration is otherwise as before.

a] Rigid Body Modes

Figure 48 gives the rigid body modes with the stiffened tractor springs. The bounce mode has increased from 1.78 to 2.23 Hz and there is now more motion at the axles on the tyres. The trailer mode is unchanged as expected.

The tractor pitch mode is now apparent at 3.58 Hz with the pitch centre at more or less the same position as in the spring modes.

There is a significant change in the tractor rigid body modes due to the friction effect and a series of runs were undertaken varying the stiffness of the springs from the original values to effectively solid. The results indicated that the limits on the tractor mode frequencies are:-

Normal Mode	Nominal → Solid
Tractor Bounce	1.78 Hz - 2.6 Hz
Tractor Pitch	2.68 Hz - 5.9 Hz*

[*Trailer bending becoming involved]

In the 'solid' condition the tyres become the primary suspension of the tractor unit.

b] Higher Modes

The effects of nominal levels of spring friction are also apparent in some of the higher modes.

The cab/engine mode which occurred at 10.8 Hz for the original condition now occurs at a slightly lower frequency at 10.7 Hz but is

accompanied by much greater front and rear axle motion.

The front and rear axle resonances in the fully laden condition which occurred at 8.67 and 9.3 Hz respectively no longer occur at these frequencies. The front axle mode is now apparent at 11.3 Hz with considerably more cab and engine motion. The rear axle mode is seen at 12.66 Hz but with rather less cab motion and a little more engine motion. It is apparent therefore that due to the tyre and spring stiffnesses being of the same order nominal friction levels in the suspension springs affect not only the rigid body modes which are associated with these springs, but also affect the axle resonances.

The higher modes are affected only slightly, the general difference being increased levels of axle motion.

8.3.3. Vehicle in the Unladen Condition

Figure 49 gives the modes for the unladen tractor-trailer combination.

As expected the rigid body modes occur at higher frequencies. At 2.27 Hz the bounce mode of the tractor occurs with the bounce centre just inside the tractor frame at the rear. The pitch mode occurs at 3.93 Hz and the pitch centre has moved forward to below the cab and engine. This is as expected since the static deflection of the rear tractor spring is now much less than that of the front. The trailer bounce mode occurs at 5.4 Hz.

The engine fore-and-aft mode remains unchanged at 7.8 Hz as does the cab mode at 8.15 Hz.

At 9.3 Hz trailer bending, rear axle, cab and engine motions are evident. The rear axle/cab coupling is again apparent here.

Trailer bending appears again in the mode at 10.76 Hz accompanied by cab bounce, engine motion on the gearbox mounts and rear axle motion.

At 13.3 Hz the trailer bending mode occurs with little motion of the other vehicle components except the tractor frame which follows the trailer frame at the fifth wheel location.

The cab vertical-engine pitch mode appears at 14 Hz again with a measure of trailer bending.

8.3.4. Vehicle Tractor Only

The uncoupled tractor modes are obtained by setting all masses relating to the trailer to zero. The resultant modes will then refer to the tractor unit with no trailer interaction.

Figure 50 gives the tractor modes.

The tractor bounce mode occurs at 2.15 Hz. The pitch mode at 4.38 Hz is significantly higher than the laden pitch mode due to the large reduction in the rear static deflection on removing the fifth wheel load. As indicated in Appendix E the result of this is that the pitch centre moves far forward of the centre of gravity and can be seen to lie close to the centre line of the cab. In addition the rear axle displacement is about the same as that of the frame above it, indicating that insufficient mass exists above the rear spring to cause much deflection of the rear spring - in effect the tractor frame will bounce on the rear tyres with the spring

effectively locked. The result of the higher frequency and oscillation centre location of this pitch mode will be high fore-and-aft motions in the cab at a particular disturbing frequency.

The engine longitudinal mode at 7.78 remains unchanged except that there is now motion at the rear axle and the inertia forces are sufficient at this frequency to cause the rear springs to operate since there is no corresponding motion on the frame above the axle.

The front axle resonance occurs at 8.5 Hz accompanied by some rear axle motion and more cab and engine pitch than in the laden case.

The rear axle resonance occurs at 8.6 Hz with considerable frame motion and associated cab and engine pitch. The frame motion is out of phase with the axle.

The mode at 11 Hz is predominantly the cab on its rear mounts with appreciable rear frame motion and rear engine motion.

The engine mode at 12 Hz has similarities to the previous mode except the engine moves on its rear mounts instead of the cab.

At 17.25 Hz there is significant cab and engine motion and considerable bending of the front portion of the frame. The cab has considerable vertical bounce and the engine motion is predominantly pitch with more motion at the front mounts than at the rear.

Tractor frame bending with no component motion is increased to about 28 Hz and the node has moved rearwards.

8.4. Response Correlation in the Time Domain

An attempt was made to simulate the response of a new prototype articulated vehicle to a specific road surface input.

It was the object of this part of the work to develop models of the total vehicle, both tractor alone and tractor with trailer, capable of predicting the vehicle response to road surface inputs. The model simulations were to be conducted in the time domain and would allow computation of the response spectral densities at various locations on the vehicle.

The models of the vehicle were to be excited with digitisations of the inputs to the Road Simulator used during the vehicle rig test programme. The hydraulic rig responses would also provide the means of checking the model responses.

The exercise was conducted in three parts:-

1. Tractor Simulation (Rigid Frame)
2. Tractor Simulation (Flexible Frame)
3. Tractor Trailer Simulation

These will be discussed in turn below.

8.4.1. Tractor Simulation - Rigid Frame

Using original data supplied by the manufacturer a 19 degree of freedom model of the tractor unit was used to measure the degree of correlation with the actual tractor unit on the Road Simulator using identical inputs.

Figure 51 gives a schematic of tractor time domain model (enclosed with dashed lines). The tractor

model is a complete representation of the tractor dynamics with the exception of frame flexibility and only the rigid frame modes are modelled.

Both the cab and engine have 6 degrees of freedom and the tractor frame has 3 degrees of freedom, bounce, pitch and roll defined about the centre of gravity of the frame assembly.

The front and rear suspension geometries are catered for by the spring and damper 'suspension ratios' which must be specified as input data. These ratios basically compensate for the various inboard locations of the suspension springs and dampers and are used in the computation of the roll responses of the vehicle axles and frame. The various suspension ratios are defined in Figure 51 and are a measure of the relative effectiveness of the components in the axle roll responses compared with their potential effectiveness if positioned at the tyre location.

Front and rear anti-roll bars are included in the tractor model and the appropriate stiffnesses are required in units of Nm/rad of relative frame-axle rotation.

The correlation results at six positions on the tractor unit are shown in Figures 52 and 57.

Axle Responses

Figures 52 and 53 give the front and rear axle responses for the model and the actual vehicle.

For the front axle response comparison it can be seen that while the overall shapes of the predicted and experimental responses are similar, the resonance peaks are at different frequencies, 8.5 Hz in the model and at about 11 Hz on the vehicle. This

implied that the supplied values of the front suspension tyre and possibly suspension spring rate were incorrect. Additional computer runs were conducted with varying spring rates (both tyre and suspension spring). The results of this exercise showed that whilst the predicted frequency could be increased to that of the experimental responses both the slope of the curve and its level at resonance did not match those of the experimental response. The situation remained unsolved until much later in the development of the vehicle where more accurate data was supplied by the manufacturer which was obtained from random testing - this will be discussed later.

In contrast to the above, the rear axle correlation was very good at axle resonance as in Figure 53 although there was clearly some error in the predicted response at the spring mass frequencies around 3/4 Hz.

Frame Responses

Unfortunately the errors in the front axle response simulation will have effects on the simulation of the other vehicle responses, particularly at the front of the vehicle.

The front frame simulation (Figure 54) is quite good up to about 6 Hz when the response of model can be seen to fall off fairly rapidly and to rise steeply at front axle resonance frequency. The experimental response is also seen to fall sharply and rise again before rig axle resonance at 11 Hz although the effect is less marked. The greater response on the rig from about 12-20 Hz can be partially explained as a consequence of lower axle response of the model in this range and improving the axle simulation would have beneficial effects here. But,

as can be seen, not a very good overall frame response simulation.

Figure 55 gives the predicted and experimental rear frame responses. The first peak at the frame pitch frequency is higher in the model response than in the rig response as was the case for the rear axle responses. While the general downward trend of the experimental plot for increasing frequency is reproduced in the model there is a more or less constant separation between the model and experimental responses, the experimental being higher. Since the rear tractor spring data was based on a static rather than a dynamic test it was reasonable to assume some error in the quoted value.

The rear frame response was re-computed with the rear spring rate doubled. The resulting PSD is also given in Figure 55.

The increase in rear spring rate has had practically no effect below 10 Hz but thereafter it produces a much higher response on the rear frame and is much closer to the experimental response.

Cab Responses

Figures 56 and 57 give the predicted and experimental DSV (driver seat vertical) and DSL (driver seat longitudinal) responses. As in the front frame responses the DSV responses compare well upto about 6 Hz; thereafter the differences in the DSV responses are similar to the differences in the front frame responses. The sharp dip in the PSD before axle resonance was again observed in both predicted and experimental responses.

The DSL responses compared quite well. What was encouraging about these plots is that the relation-

ship between the predicted DSV and DSL responses was very similar to that between the experimental DSV and DSL responses: the DSL response at tractor bounce frequency is higher than the DSL response but is lower at tractor pitch frequency in both the model and experimental PSD's. Furthermore the DSL responses are high where the corresponding DSV responses dip sharply before the appropriate axle resonance frequencies in both cases.

Overall however, it was concluded that while the predicted responses were encouragingly representative of the experimental responses it was clear that simulation errors were being introduced by either:-

i) model inadequacies

or

ii) unrepresentative component data or perhaps by some combination of both.

A request was made to the manufacturer to reassess the supplied component data and to obtain performance data for suspension springs, dampers and cab and engine mounts from random tests. In addition the tractor model was extended to include frame bending and torsional flexibility (as with the previous vehicle).

The results from the simulation using the final data set and the updated model are discussed in the following Section.

8.4.2. Tractor Simulation - Flexible Frame/Final Data Set

The final data supplied by the manufacturer was considerably different to that originally supplied. This highlights once again the very great importance of the need to measure component performance under random test conditions. This was shown to be the case for passenger vehicles with respect to suspension dampers. However, in the case of commercial vehicles it is equally applicable to suspension springs - particularly multi-leaf springs - which are in common use. The stiction/friction characteristics of these springs together with the great variation in their static loading make it essential to test these springs with their effective static preload applied and a representative random service input applied. This implies that the effective stiffness rate of, say, the rear tractor suspension spring will be very different for the unladen tractor unit than for the fully laden tractor-trailer combination.

The Table below highlights the different results obtained for some of the tractor component rates when measured under three test conditions:-

1] Static

2] Dynamic - with sinusoidal loading

and

3] Dynamic - with random service loading

Component	Static Rate (N/m)	Dynamic Rate		Error Ratio Random/ Static
		Sinusoidal	Random	
Front Tractor Suspension Spring	2.11×10^5	4.0×10^5	6.4×10^5	2.03:1
Rear Tractor Suspension Spring	4.81×10^5	1.0×10^6	1.6×10^6	3.33:1
Front Cab Mount (Vertical Rate)	6.92×10^6	-	6.6×10^6	0.95:1
Rear Cab Mount (Vertical Rate)	1.575×10^6	-	1.4×10^6	0.88:1
Engine Mount (Vertical Rate)	2.335×10^6	-	2.51×10^6	1.075:1
Gearbox Mount (Vertical Rate)	0.54×10^6	-	$2.15 \times 10^{6*}$	2.98:1

*Error in original data

It is clear from a consideration of these figures that high level simulation exercises should not be attempted without representative component data which must originate from random tests in the main.

In addition to the above stiffness data the results from random testing of the tractor dampers were considerably different to the equivalent linear damping values used for the initial simulation which was based on the supplied sinusoidal test data. The comparisons are illustrated below:-

Component	Equivalent Linear Damping N/m/s	Random Test Result	Ratio of Values
Tractor Front Damper	7960	19800	2.49:1
Tractor Rear Damper	7600	24500	3.22:1

Correlation Results

The time domain response was predicted with the tractor model subjected to typical road surface excitation. A period of 64 seconds was simulated and required about 6 minutes of cpu time on a UNIVAC 1108 mainframe computer.

Figure 58 give equivalent two second time frame displacement plots as in the following Table:-

Figure	Input/Response Position
58(a)	Input displacement applied to nearside front wheel
58(b)	Response of front axle centre (vertical)
58(c)	Response of tractor frame at centre of gravity position (vertical)
58(d)	Response of cab centre of gravity (vertical)
58(e)	Roll response of trailer frame centre of gravity

It is interesting to observe the gradually increased filtering effect of the vehicle as the response position is moved from initial road surface input to the vehicle axle, vehicle frame and cab positions. The most significant reduction in bandwidth is, as would be expected, observed in the tractor frame roll response.

This demonstrates the usefulness of such time domain simulations particularly with respect to the generation of laboratory test drive signals in that over the simulation time period the vibration time histories at all positions on the vehicle are computed.

The correlation results with the improved data and the inclusion of frame flexibility within the model are given in Figures 59 to 64.

The results show very significant improvements in correlation accuracy. The difficulties in improving the front axle responses by changes to the spring rates were in fact due to the need to alter both spring and damper rates of the front suspension as indicated by the Tables above.

8.4.3. Tractor-Trailer Correlation

A similar correlation exercise was conducted for the fully laden tractor-trailer combination.

No dynamic data was available for the trailer rear suspension which consisted of multi-leaf springs with high friction/stiction levels such that no hydraulic dampers were necessary. It was clear that the static rates supplied would be unrepresentative of the true rates.

The bending sectional stiffnesses were calculated for the finite difference representation of the trailer frame.

No torsional flexibility data was available and no attempt was made to model this. Instead the trailer was modelled as a frame rigid in all respects except in bending.

The model of tractor unit described above was connected to the trailer model as in Figure 51 and the response simulation conducted. (This was done initially with the rigid frame tractor model and original component data but little mention of these results will be made here).

The correlation results are given in Figures 65 to 70.

Figure 65 also shows the predicted front axle response when using the rigid tractor model with the originally supplied data.

The final model simulation can be seen to be very representative of the vehicle dynamics and is capable of being used to develop the vehicle dynamics analytically.

The correlation of the trailer response is poor above 10 Hz as a result of the inadequate component data and no doubt contributes to some of the errors in the other plots at these frequencies.

It was not possible in the time available to have the trailer suspension data measured with random inputs.

9.0 CONCLUSIONS

Mathematical modelling techniques have been applied to the prediction of the dynamic response of road vehicles to road surface roughness in the frequency range which determines ride quality.

It has been demonstrated that a much higher degree of simulation accuracy is achievable provided that:-

1) More sophisticated three dimensional models are developed and used.

2) More accurate vehicle component data is obtained representative of 'in-vehicle' performance.

and

3) A fuller description of the road surface excitation is employed for the model excitations.

The mathematical vehicle models needed to achieve higher simulation accuracy must include <u>all</u> the major dynamic components, appropriate to the vehicle type, which affect ride quality. These have been included in the more complex models developed for both passenger cars and trucks as described in the thesis.

The accurate measurement of vehicle component performance is essential if advantage is to be taken of increased model sophistication: <u>this cannot be stressed too highly</u>. For example, traditional methods of damper performance specification were found to be inadequate with respect to the representation of the installed performance of dampers. It was found to be necessary to develop a new approach to damper characterisation by means of tests using typical random service inputs.

These techniques in addition to providing more representative model data, gave a greater insight into damper

behaviour in general. A similar approach to the performance measurement of truck suspension springs and elastomer mounts was also necessary to achieve increased simulation accuracy for this application.

It is recommended that these techniques be applied to the measurement of all vehicle components exhibiting stiffness and/or damping characteristics whether for mathematical simulations or for other purposes. This is especially so for those components whose performance is known to be non-linear under variable sinusoidal loading.

A further major contribution to the improved accuracy of simulation has undoubtedly been the combination of the random descriptions of road profile excitation with the more complex three-dimensional models. It is recommended for all high level response simulation that the technique adopted in this work is used.

The task of simulating the time domain response of a complex road vehicle to multiple input random road surface excitation to an acceptably high degree of accuracy has been achieved. Further increases in accuracy, should they be required, will be attained by the use of even more complex models, but total accuracy will be limited at the higher frequencies by those factors not included in this type of model such as engine vibration excitation. Nonetheless this does significantly impact upon the prediction and development of ride quality.

The software packages developed in this work to provide solutions to the model equations in both time and frequency domains are sufficiently flexible to allow model changes to be easily incorporated.

The time domain solution method will also allow non-linearities to be included in the definition of component performance: this feature will greatly enhance the future development of the so-called 'active' suspension elements whose performance is by design non-linear. The future

trend in automobile suspension design lies in this area now that the automobile industry has accepted the concept of 'on-board' computer control together with the ever increasing standards of ride quality and the generally conflicting requirements for reduced vehicle weight.

Finally, the time domain solution method has demonstrated its potential in the area of laboratory component testing. The dynamic loading environments of vehicle components can be predicted using the mathematical models and the digital time domain responses generated by the software can be used to drive multi-channel servo-hydraulic tests.

10.0 FUTURE WORK

Two main aspects of the work reported in this thesis are vital for immediate future development.

Firstly, it was shown in Section 6 how the characterisation of automobile dampers by a frequency response function approach not only gives more representative performance data on these components for the mathematical simulations, but also gives additional insight into their behaviour under realistic service loading conditions. In particular the performance of dampers as a function of frequency when subjected to service inputs is a novel approach to the optimisation of ride quality as it relates to damper performance. This should be examined.

The function of an automobile damper is to damp out undesirable oscillations at two main vehicle resonance conditions;

1) the vehicle sprung mass resonances - bounce, pitch, roll - on its primary suspension springs and,

2) the resonance of the axles on the tyre springs (noting that in this situation the tyre damping assists the suspension damper).

It is likely that different degrees of damping will be required to optimise 1) and 2) above respectively, and yet it has been seen that for the dampers tested the effective damping rate is approximately constant in the range of frequencies covering the two resonances described above.

This approach should be extended such that the 'theoretically ideal' damper frequency response function can be predicted for specific vehicle installation - possibly by using the models developed in this thesis - the end product being a damper which can exhibit these ideal characteristics. The performance of such experimental dampers

can of course be measured by using the technique developed in this work.

Further extending the theme, it is strongly felt that the time domain modelling approach where response to representative road surface inputs is predicted in the time domain lends itself to the analysis of 'active' suspension systems.

An 'active' suspension system, be it a simple or complex example, is a suspension system whose characteristics can be made to vary according to the type of road input to which the vehicle is being subjected. For example, the ideal suspension characteristics for high speed motorway cruising are very different to those required for rapid travel on twisting, undulating 'B' class roads. Current passive suspension systems are inevitably a compromise between a range of ideal characteristics suited to each type of road input. Active suspension will allow the vehicle to 'sense' the road conditions and adjust the suspension characteristics to match, either on a 'stepped' or on a continuous basis. The time domain approach will allow particular control strategies to be studied and the likely response of the vehicle to be predicted under a variety of road surface inputs to develop the optimum control strategy.

PART III

VEHICLE INDUSTRY APPLICATIONS

1) The Generation of Drive Signals for the Testing of a Bodyshell Structure using Servo-Hydraulic Actuators.

2) Estimation of Dynamic Forces Transmitted to a Supporting Seismic Block during Hydraulic Road Simulator Testing of an Articulated Vehicle.

3) Optimisation of Commercial Vehicle Cab Response by Computer Simulation of the Cab System Dynamics.

APPLICATION 1

The Generation of Drive Signals for the

Inertial Testing of a Bodyshell Structure

Using Servo Hydraulic Actuators

1.0 DURABILITY TESTING OF AUTOMOBILE BODYSHELLS

At the time of the current work a separate research programme was underway part of which was an investigation into the feasibility of durability testing on automobile bodyshell structure using four servo-hydraulic actuators to apply loadings at each of the four suspension input positions.

The object was to apply realistic loadings and motions to the bodyshell so that with the addition of appropriate mass elements to represent the power train etc. the corresponding inertial loadings would be applied and thus effect a realistic durability test.

The test simulation described here is a specific example which illustrates the capability of the time domain models in the generation of drive signals - single or multi-channel - for laboratory testing using servo-hydraulic actuators. The digital output data representative of response time histories can be output directly via digital-to-analogue converters to produce the required drive signal(s).

1.1. Required Outputs for Bodyshell Testing

The requirement for the bodyshell tests described above was for four drive signals. These were to be three body displacement signals, one at each of the three corners of the bodyshell at the suspension mounting positions, with the fourth signal being the corresponding load (i.e. spring plus damper load) at the remaining corner.

The 13 degree of freedom rigid body passenger car model was used to generate the above responses.

A brief explanation of the need for three displacement and one load signal will be appropriate here.

If the four actuators controlling the test were used to apply the four corner displacements to the vehicle bodyshell there would be a great danger of distorting the bodyshell should the inputs at any-time become significantly non-planar.

Although with the rigid body model used here these simulated outputs would be exactly planar there are still problems with the start up procedure which preclude this approach.

The possibility of applying four loads to the body-shell was not feasible because of inherent stability problems when attempting force control of a 'free-floating' structure.

The approach to be adopted was one in which three corners of the bodyshell would be controlled by displacement with the fourth in load control.

Clearly planar motion is guaranteed by the applica-tion of the three displacement signals. The fourth input would then be the programmed load applied at that particular corner and would provide the con-trolled torsional input. The overall dynamic motion of the bodyshell would, with appropriate ballasting induce the required inertial loads.

1.2. Mathematical Model Output

The generation of the four required time histories is simply accomplished with the 13 degree of free-dom model under time domain solution.

The road surface input required was used to excite the model of the vehicle and the following para-meters output:-

i) Displacement responses at two front and one rear corner of the vehicle at the suspension mounting locations, all these outputs being planar in view of the rigid body assumption in the model.

ii) The load at the remaining suspension mounting position composed of the vector summation of the spring force and the damper force at each discrete instant in time.

All four responses were output on a point by point basis onto the computer disc storage medium and later corrected onto four analogue drive signals via the D/A converters.

Figure 71 gives a particular two second time frame plot of the displacements at each of the four body/ suspension mounting positions.

Figure 72 gives the corresponding load time history at the offside rear suspension position.

The RMS and peak values of the applied load history which corresponded to a typical 'A' road surface input at the wheels of the vehicle were as below:-

Road Surface Input		Bodyshell Displacements [m]				Load Time History (KN)
		O/S/F	N/S/F	O/S/R	N/S/R	
'A' Road	RMS	.023	.0242	.0237	.0236	0.341
	PEAK	0.11 ($\pm$ 4.3 in)	0.115	0.1126	0.1121	$\pm$ 1.67 (= $\pm$ 375 lbf)

Figure 73 also shows the coherence and phase relationships between the two front bodyshell input displacements and between one front and one rear input.

APPLICATION 2

Estimation of Dynamic Forces Transmitted to a Supporting Seismic Block during Hydraulic Road Simulator Testing of an Articulated Vehicle

2.0 ESTIMATION OF THE DYNAMIC FORCES TRANSMITTED TO THE SUPPORTING SEISMIC BLOCK DURING HYDRAULIC TESTING OF AN ARTICULATED VEHICLE

A commercial vehicle manufacturer was about to commission a new Electro-Hydraulic test facility part of which included a complete vehicle validation/durability Road Simulator. The Road Simulator was to be installed on a 1000 ton seismic mass which was to be supported on air springs in order to provide vibration isolation to the surrounding building structures.

At the commissioning stage it became apparent that the seismic block would have its 'mass on springs' resonance at around 2 Hz which is within the test excitation range. Concern was therefore expressed at the possibility of the block 'bottoming out' under certain Road Simulator test conditions with consequent potential structural damage.

The mathematical model of the tractor-trailer [in fully laden condition] was used to estimate the dynamic loads which would be applied to this seismic block under typically severe vibration and durability testing.

2.1. Objectives

The object of the investigation was to estimate the vertical dynamic forces occurring at the tyre/wheel pan interfaces during servo-hydraulic testing of a typical fully laden articulated vehicle. Since the forces applied to the vehicle tyres by the actuators must react against the supporting seismic block they can be considered to be the external force excitation to the block dynamic system.

Two separate vehicle input conditions were to be considered:-

i) A constant velocity 'sweep sine' input applied to the tyres at discrete frequencies over the 0-15 Hz range.

ii) A typically severe pave input such as might be used in assessing the fatigue life of the vehicle.

For i) a plot of peak force v frequency for the front and rear wheels of the tractor was required and for ii) computer plots of the force time histories (about 1 minute duration each) were requested.

2.2. Method of Load Prediction

Estimates of dynamic interface forces were obtained from the mathematical model of the fully laden articulated vehicle described in Section 8.4.3.

The vehicle excitations were applied vertically at the tyres as time histories for both the sine-wave and pave inputs and the vehicle response computed in the time domain. The outputs from the model were selected to correspond to the forces at the tyre/wheelpan interfaces for the four tractor wheels. No inputs were applied to the trailer tyres as this would be the experimental testing format on the Road Simulator.

2.3. Input Formats and Results

2.3.1. Constant Velocity Sine Waves

The sine wave inputs to the vehicle model were as follows:-

i) inputs applied simultaneously to all four tractor wheels <u>in phase</u> with no input at trailer wheels.

ii) all discrete sine waves of constant (peak) velocity with reference wave $\pm$ 1 in. at 1 Hz.

iii) discrete sine sweep from 1 to 15 Hz in 0.25-0.5 Hz increments.

The input reference wave $\pm$ 1 ins. at 1 Hz was chosen to be very severe bearing in mind the 'all four wheels in phase' input configuration and a check on the front spring motion at resonance frequency (1.75 Hz) showed it to be of the order of $\pm$ 5 in. It should be noted however that the computed peak forces can be scaled in proportion to the input displacement, e.g.,

for $\pm$ 1 in. at 1 Hz peak force = 4 tonf, say
for $\pm$ ½ in. at 1 Hz peak force = 2 tonf etc.

Figure 74 gives the plots of peak force v frequency for one front and one rear (double) tractor tyre/ wheelpan interface.

2.3.2. Pave Input

Estimates of the dynamic forces at the wheelpans during accelerated durability testing were required. A severe pave input was chosen, the details of which are given in Figure 75. The vehicle speed was taken to be just below 20 mph. Note that again the pave input was applied to the tractor wheels only. The pave chosen is very severe in overall level and also has a low value of W_2 which implies large high frequency input levels. The rms of this pave is 3.76 cm giving peak displacement of $\pm$ 6 in.

It is unlikely that an artic could be restrained on a hydraulic rig at these input levels but the computed forces should provide an upper bound. In any case the computed forces can be scaled in proportion to the rms level as with the sine wave inputs.

The computed forces at each of the tractor wheels were plotted as time histories [tons force v time]. Vector summation of all four dynamic forces as a function of time indicated that the maximum instantaneous downward force on the block would be about 200 KN [approximately 20 tonf].

Figures 76 and 77 gives the PSD's of one front and one rear tyre force and the vertical axis units are $tonf^2/Hz$.

2.4. Discussion on Results

2.4.1. Sine Wave

Various peaks are evident in both plots of peak force v frequency in Figure 74. For the front tyre the first peak occurs at about 1.75 Hz and corresponds to the front spring resonance. The rear tyre forces are also high at this frequency. At about 2.25 Hz the rear spring resonance is evident in the rear tyre plot. [It should be remembered that these plots are not transfer functions in the usual sense since the input levels reduced with increasing frequency].

The only other significant peak occurs at about 6-7 Hz in the rear tyre plot - this corresponds to the first bending mode of the laden trailer and is accompanied by significant spring/tyre motion which results in the large force requirement.

There is also slight evidence of both unsprung mass resonances in the plots at around 10 Hz.

2.4.2. Pave

It was apparent from both the load time histories and the corresponding PSD's that the rear tyre loads are higher than the front tyre loads. The rms load levels on the tyres are:-

Front wheel load rms = 2.5 tonf
Rear wheel load rms = 5.47 tonf.

Both these rms levels are based on the pave input with rms = 3.76 cms.

2.5. Conclusions

Computer predictions of the dynamic tyre wheelpan forces were obtained for various vehicle inputs. Plots of peak force v frequency for sweep sine (constant velocity) inputs were established which were amenable to scaling for different input levels.

Force-time histories for each of the tractor wheel loads were plotted with the vehicle model subjected to a severe pave input and the corresponding load spectra plotted. These loads can again be scaled to suit other rms input levels assuming the input waveforms do not change.

This information allowed the manufacturer to combine the dynamic information on the block suspension with the various loadings calculated above to be assured of the safety of testing on the block.

The block in question has been in use for several years without problems.

APPLICATION 3

Optimisation of Vehicle Cab Response by

Computer Simulation of the Cab System Dynamics

NOTE: This particular application will be reported in the form of a technical paper which will involve a little repetition of what has been described previously. This will, however, maintain the integrity of the technical paper format.

(Figures refered to in the text appear at the end of this paper and not in the main List of Figures).

COMPUTER SIMULATION OF CAB SYSTEM DYNAMIC PERFORMANCE FOR IMPROVED RIDE QUALITY

M.P. RENUCCI
CHIEF ENGINEER
ADVANCED ENGINEERING TECHNOLOGY
AUSTIN ROVER GROUP

Key Words:- Ride quality, vehicle dynamics, computer simulation, mathematical modelling, suspension design, truck ride, dynamic characteristics, vehicle response, random vibration

ABSTRACT

A computer simulation technique is presented which aims to provide the commercial vehicle designer with a means of rapidly assessing the effectiveness of various cab isolation systems at very low cost.

The cabs and their suspension systems are dynamically represented by a coupled six degree of freedom mathematical model.

The model can be excited by representations of the cab service excitations. These are defined by the vibrations measured on the vehicle frame at the cab mount locations. Time domain predictions of the cab response when subjected to these excitations can then be obtained by numerical methods.

The technique was used in the prototype development phase of a new articulated vehicle to achieve very significant improvements in the vehicle ride quality.

1.0 INTRODUCTION

The problem of improving commercial vehicle ride quality is of continuing concern to truck designers. It is a problem for which there is no easy solution since the factors which ultimately determine the ride quality in a commercial vehicle are numerous.

The truck ride problem is largely a consequence of the geometry and operating conditions of this type of vehicle and is not solely attributable to the quality of road surfaces: passenger vehicles traverse similar surfaces at similar speeds, yet their ride qualities are notably better and they present much less of a problem to their designers in this area.

Clearly the road surface is important since it provides the primary excitation to vehicles but there is little the vehicle dynamicist can do to reduce the road undulations - his approach in this area can only be to quantify the road surface undulations thereby defining the vehicle excitation.

Careful design of the dynamic characteristics of the vehicle components is the key to improved ride quality.

1.1. The Truck Ride Problem

It is worth examining briefly the properties of commercial vehicles, particularly articulated vehicles, which hinder the design of good ride quality.

The most significant geometric difference from passenger vehicles is the high location of the truck operator in the vehicle cab. High vertical and fore-and-aft motions can occur at this position as a result of comparatively small angular

pitching motions of the cab structure and can be particularly disturbing to the occupants. These motions can arise by either:-

i] The rigid body pitch motions of the truck frame being reflected in the cab.

ii] The cab pitching on its own suspension relative to the frame.

iii] The frame imposing pitch motions on the cab where the frame motion is due to some other source, e.g. axles, engine, trailer etc.

or, more usually, by some combination of i] to iii].

The large laden to unladen weight ratios experienced during the commercial operation of these vehicles result in equally large variations in their mass and inertial properties. The designer is thus faced with the task of optimising the vehicle ride characteristics where the dynamic properties of the vehicle vary greatly in service.

This makes suspension optimisation a much more complex task. For example, designing primary suspension to be adequate for the fully laden vehicle will result in increased sprung mass frequencies - and hence a tendency towards inferior ride - for lighter loads.

The trailers of articulated vehicles will frequently impose their dynamics on the tractor unit through the fifth wheel coupling. Their effect will be apparent in the tractor frame which will, in turn, affect the cab response and the vehicle ride quality.

It is not unusual to find two articulated vehicles of similar configuration with comparable tractor frame vibrations levels and yet with very different

ride qualities: the variation in frame vibrations does seem to be much less than the corresponding variation in cab response levels.

To state that truck ride quality is solely determined by the effectiveness of the cab isolation system would be incorrect. It is undoubtedly true however, that good ride quality can be attained or lost as a consequence of the cab isolator design.

It is the author's opinion that, apart from introducing radical changes to existing truck primary suspension configurations, the only viable means of achieving significant improvements in ride quality is by careful attention to the design of the cab suspension system.

1.2. Computer Simulation

A computer simulation technique is presented in this paper which aims to provide the vehicle designer with a means of rapidly assessing the effectiveness of various cab isolation systems at very low cost.

The cabs and their suspension systems are dynamically represented by a coupled six degree of freedom mathematical model.

The model can be excited by time domain representations of a range of measured service excitations defined by the vibrations of the vehicle frame at the cab mount locations.

Time domain predictions of the cab response to these vibrations can then be obtained by numerical methods.

The computer simulation procedure has been packaged to the state where the whole process is 'user

friendly'. This enables vehicle designers to concern themselves with the optimisation of their cab systems without the overhead of significant computer interaction.

The technique was used in the prototype development phase of the production of a new articulated vehicle to achieve significant improvements in the vehicle ride quality in a very short timescale.

2.0 SIMULATION PHILOSOPHY

2.1. Simulation Procedure

The cab suspension design procedure is illustrated schematically in Figure 1. It is used where a road-going prototype is available and thus the vehicle designer will have access to preliminary service vibration data.

The following steps will serve to define the procedure:-

1) Record acceleration data from the vehicle frame at the cab mounting positions where the vehicle is driven under a representative range of operating conditions e.g. Motorway, 'A' Road, fully laden, unladen etc. Tri-axial accelerations should be recorded at each position. Also record simultaneously the acceleration responses at positions of interest in the vehicle cab for the model validation and for the baseline of ride quality.

2) Digitize, integrate and double integrate the frame acceleration data to derive displacement and velocity excitations with which to drive the cab model. Also digitize the cab responses and compute the Power Spectral Densities (PSD) for each position for later use.

3) Acquire accurate physical data on the cab and its suspension system (i.e. mass, inertias, stiffness and damping) as required by the cab model.

4) Drive the cab model with the frame excitations to give the predicted time domain response of the existing cab system. Analyse the simulated

responses at the cab positions monitored in 1] to give the PSD's.

5] Compare the predicted and measured response PSD's to quantify the simulation accuracy. If satisfactory proceed to 6].

6] Reset the cab suspension parameters within the model and simulate the cab response for the range of service inputs. Repeat until the required improvement in cab response is predicted.

7] Translate the 'theoretically optimised' suspension system to hardware and road test the vehicle. [Alternatively exercise a complete vehicle model to verify improvement in response and follow with a road test].

A number of simulation runs will inevitably be necessary to achieve significant improvements in the predicted ride quality. The cost of each simulation run is however very small when compared with related costs in the areas of vehicle test and development.

2.2. Limitations

The simulation procedure we have adopted essentially separates the design of the cab suspension dynamics from the remainder of the vehicle.

We must be cautious of this approach in general: in separating part of an integral dynamic system for adjustment potential changes in the dynamic coupling between the separated part and the remainder of the system cannot be accounted for.

The present cab response simulation technique therefore is aimed at improving the effectiveness of the cab isolation system when the cab is subjected to a range of 'service inputs' as defined previously. The simulation process is not an attempt to predict the cab response when the vehicle is subjected to specific road surface inputs: to do so would clearly require a complete vehicle model.

It is not always possible or convenient to conduct repeated response simulations with a complete vehicle model. The cost of doing so can be prohibitive and accurate data on all the vehicle parameters is rarely available especially at early stages in the vehicle development process.

It is worth defining, however, the theoretical limitations of the present cab simulation process in its ability to predict exact cab response when the cab suspension parameters are altered.

It will simplify the illustration if we consider the truck dynamic system to be a simple two degree of freedom linear system as shown in Figure 2.

The mass M_V and its associated suspension system K_V, C_V, will serve to represent the truck frame and suspension: the mass M_C and suspension system K_C, C_C, will model the cab dynamic system.

Let the road excitation be represented by x(t), the frame response (or the cab 'input') by y(t) and the cab response by z(t). The responses z and y can be expressed by:-

$$z(f) = H_{zy}(f)\, y(f) \qquad (1)$$

$$y(f) = H_{yx}(f)\, x(f)$$

where H_{ij} denotes the frequency response function between i and j (and noting the change of independent variable from time to frequency).

It follows that:-

$$z = H_{zy} H_{yx} x \qquad (2)$$

(dropping the independent variable for convenience).

In the cab simulation process we record y(t) for a range of road surfaces with an initial cab suspension configuration. We subsequently use these y(t) to excite the cab model with alternative suspension configurations to assess the corresponding new cab responses - z'(t), say. In terms of the two degree of freedom analogue we therefore:-

i) Change the cab system receptance H_{zy} to H'_{zy} say (via a change of suspension parameters).

ii) Excite the new cab system with the original y(t) to predict the new z'(t).

$$\therefore \quad z' = H'_{zy} y = H'_{zy} H_{yx} x \qquad (3)$$

In the real situation the true cab response z''(t) would be given by:-

$$z'' = H'_{zy} H'_{yx} x \qquad (4)$$

since H_{yx} will in general change with H_{zy} to H'_{yx}, say.

The ratio of the true and the predicted responses is therefore given by:-

$$\frac{z''}{z'} = \frac{(H'_{zy} H'_{yx} x)}{(H'_{zy} H_{yx} x)} = \frac{H'_{yx}}{H_{yx}} \qquad (5)$$

Where the ratio H'_{yx}/H_{yx} departs from unity we will have an error in the predicted response.

The extent to which H_{yx} will change for a given change in H_{zy} will depend on the particular vehicle parameters and it is impossible to generalise.

It is debatable whether the optimisation of cab response is simply a case of the 'dynamic tuning' of the cab to the rest of the vehicle. The wide variations in truck operating conditions mean that the cab forms part of a dynamic system which varies greatly in vehicle service.

It is felt that the optimisation of the cab suspension system on the basis of the present strategy, i.e. when the cab model is subjected to a range of typical frame vibrations - has just as much likelihood of success as an optimisation procedure based on repeated complete vehicle model simulations where a range of road surface inputs and vehicle loading conditions must be used. In addition, the present approach is of course much less costly in its execution.

In any case the results obtained from optimising the cab response via the cab simulation process must of course be validated by using the prototype vehicle with the 'mathematically optimised' suspension parameters translated into hardware.

3.0 CAB SYSTEM DYNAMICS

Some general observations can be made regarding cab isolator design which will be useful to bear in mind when applying the cab simulation technique.

3.1. The Cab as a Vibration Isolator

The design of cab suspensions has its analogy in the design of vibration isolators.

A simple mass-spring-damper system will isolate disturbance frequencies which are greater than $\sqrt{2}$ times the system resonance frequency, the higher frequency being referred to as the 'isolation frequency'.

Cab systems behave in a similar manner but are obviously much more complex than the single degree of freedom system since their rigid body vibrations are capable of six individual component modes of vibration [generally heavily coupled] which for convenience can be defined relative to the cab centre of gravity - three translation, i.e. vertical, longitudinal and lateral motions and three in rotation, i.e. pitch, roll and yaw.

Although the concept of the cab system dynamics can be simplified by considering these six component modes of vibration it is of little use in the design of cab suspensions.

The designer is unable to alter the characteristics of these modes individually since the configuration of cab mounting systems does not allow him to alter say, the stiffness associated with a particular mode without simultaneously affecting the stiffnesses associated with the remaining modes.

The design of effective cab isolation systems is therefore not a simple task.

3.2. The Role of Damping in Cab Suspensions

The influence of the damping levels in cab systems is important and worthy of examination.

The degree of isolation offered by the simple mass-spring-damper system above increases as the damping is reduced for frequencies greater than its isolation frequency. Below the isolation frequency however the reverse is true: the system will in fact amplify the input disturbance the amplification increasing as the damping is reduced - see Figure 3.

There can therefore be no simple rule governing the effect that changes in cab suspension damping will have on cab response and hence on ride quality - it would require prior knowledge of which mode was predominant and on which side of its isolation frequency it was being excited. Note that it is seldom apparent which mode is involved due to the extent of coupling which exists between them.

Present day cab isolator systems can be classified into two main types.

The more traditional type is the all-elastomer suspension cab. Many of the modern designs however incorporate steel springing and hydraulic damping. These offer more suspension movement and a higher level of damping than is normally available with elastomer mounts.

The traditional low damped elastomer suspended cab system was designed to emulate the good vibration isolation properties of the low damped vibration absorber.

Vibration absorbers are however only effective if the service excitation frequency range is maintained well above the system isolation frequency.

In the truck operating environment this condition is seldom, if ever, met: the variations in the vehicle dynamic characteristics experienced during service are frequently the cause of poor ride quality.

Severe ride problems often occur when lightly damped cab systems are excited at frequencies below isolation and system gains of greater than an order of magnitude are not uncommon as a consequence of the inadequate level of damping.

There is thus a real probability that cabs suspended by low hysteresis rubber will be excited into resonance by particular vehicle loading configurations to the severe detriment of ride quality - all that could be done from the design viewpoint would be to ensure that these cab resonances occurred at frequencies corresponding to low driver sensitivity. [It is generally accepted that the critical frequency band is around 4-8 Hz].

However, this would mean either:-

i) Increasing the cab system resonances above the critical frequency band by using very stiff mounts.

or,

ii) Reducing the cab system resonances similarly by using very soft mounts.

Approach i) is not really a viable proposition since the cab ride would then be excessively 'harsh' due to a lack of isolation from the higher frequency frame vibrations.

Neither is approach ii) feasible since it would result in large relative displacements between the cab and frame as a result of the vehicle rigid body motions. In addition problems of excessive static deflection for increased cab loads would be encountered.

The more satisfactory solution is to provide a higher level of damping in the isolation system by using high hysteresis rubber or, more preferably, by using hydraulic dampers.

We can still 'design-in' isolation frequencies as before but without the fear of excessive gains being experienced when the resonance in the cab are excited.

Some reduction in isolation may be experienced above the isolation frequencies as a result of the higher damping levels. However the large reductions in gain at resonance will more than compensate for this, providing better overall system performance.

Higher potential ride quality is thus available with increased damping but it is not automatically so. The increased damping must be incorporated during the design analysis since merely increasing the damping levels on a particular cab system may degrade the ride quality for the aforementioned reasons.

4.0 CAB MODEL SIMULATION

4.1. Cab Model Description

Figure 4 shows the essential features of the mathematical model used to represent the cab dynamic system.

The model has six degrees of freedom, three in translation and three in rotation.

A four point suspension system is incorporated with each point having flexibility and associated damping in the three mutually perpendicular directions. The structure of the cab is assumed to be effectively rigid when compared with the cab suspension stiffness.

The mountings can be located at any position relative to the cab centre of gravity, which acts as the origin of the cab geometry, by appropriate choice of the dimensional variables.

The dynamic equations of motion which define the cab vibration are based on the six component motions related to the centre of gravity. These component motions with their direction conventions can also be seen in Figure 4.

The excitations to the cab model can be applied simultaneously to each of the four mounts in all three perpendicular directions giving a maximum of twelve inputs.

For the design exercise reported in this paper however, only the vertical excitations at the four mounts were considered, the other non-vertical inputs being set to zero. Time schedule restrictions did not allow for the inclusion of the non-

vertical inputs but it is felt that the horizontal inputs to the cab arising from frame flexibility should be considered and included in the model excitation if found to be significant in the frequency range of interest. The horizontal inputs can become significant at higher frequencies. See for example, Figure 5 which gives the vertical and corresponding fore-and-aft acceleration levels measured on a vehicle frame at the rear cab mount position during typical service conditions.

Note that above 10 Hz the two vibration levels are of the same order but that at lower frequencies the vertical vibration is dominant.

4.2. Dynamic Equations of the Model

Forced vibration response of multi-degree of freedom dynamic systems can be defined by sets of second order differential equations and represented by the matrix equation:-

$$[M][\ddot{X}] + [C][\dot{X}] + [K][X] = [E] \qquad [6]$$

where [M], [C] and [K] are the mass (inertia), damping and stiffness matrices and [E] is the excitation matrix.

For an n-degree of freedom system the matrices in equation [6] will be of order n.

The cab model dynamics are defined by the sixth degree matrix equation given in Table 1.

A description of the model variables is given in Table 2.

The motion at any selected position in the cab under excitation can be defined by the appropriate vector summation of the six degrees of freedom.

It is useful, however, to have the facility to examine the individual component responses particularly the angular responses (e.g. pitch), since these motions are more difficult to measure in practice.

4.3. Cab Physical Data

Crucial to the success of any simulation exercise is the accuracy of the representation of the system being modelled. This applies not only to the inclusion of sufficient degrees of freedom to represent the system dynamics adequately but also to the accurate representation of the physical properties of the system.

The mass and inertial properties of the cab are comparatively simple to obtain accurately.

The dynamic stiffness and damping properties of the cab mounts are more difficult to establish.

The simplest approach for elastomer mounts is to measure the static stiffness (with the appropriate preload) and assume a value for the damping, usually a function of the type of rubber used.

This approach was adoped for the initial validation of the cab simulation process.

More realistic measurements of dynamic stiffness and damping were subsequently obtained by preloading the rubber mounts and subjecting them to sinusoidal compression - extension at frequencies around 6-8 Hz which was the frequency band where the ride problem in the prototype vehicle was identified as being most severe.

The most satisfactory approach however, is to measure the dynamic properties of the mounts when subjected to service excitations. This method has been used successfully in previous modelling exercises [Renucci 1976] in obtaining more realistic damper characteristics.

4.4. Cab Model Excitations

Accelerometer recordings were taken from the prototype vehicle frame at the four cab mount positions in the vertical direction. It was necessary to record these accelerations simultaneously to maintain their correct coherence and phase relationship.

All four frame accelerations will in general differ in amplitude level, frequency content and phase. Figure 6 shows PSD plots of the frame accelerations at one front and one rear cab mount position for a particular service condition. Figure 7 gives the phase relationship between the two as a function of frequency. The complex relationship between all four mount positions must be maintained if the cab 'input' is to be adequately represented.

Each recording was then digitized at 64 Hz and 4096 samples per channel were obtained corresponding to about 1 minute of service data in each case.

The digitized acceleration values were then digitally integrated and double integrated to give the four vertical displacement and corresponding velocity inputs used subsequently to excite the cab model.

The record-digitize-integrate process was repeated for a range of operating conditions - e.g. Motorway, Rough Road etc. and for each condition two computer

disc files were set up containing in total 8 x 4096 digital values to represent the cab excitation.

4.5. Cab Response Solution Method

A computer software package was developed which incorporated the differential equations of the cab model and which, for given excitations and cab physical data, would simulate the dynamic response of the cab. The cab response in the time domain was predicted by numerical integration techniques.

The time domain approach was adopted since it allows non-linearities in the cab suspension system to be incorporated. It also enables the cab response to be predicted when the frame vibrations are non-stationary, e.g. when the vehicle encounters road discontinuities etc.

A brief description of the simulation procedure is appropriate here.

The matrix equation in the form of equation [6] is not amenable to solution by numerical methods.

For time domain solutions equations [6] must be re-arranged in the form:-

$$\ddot{x}_i = \emptyset^i\{\dot{x}_i, x_i, \dot{I}_j, I_j\} \qquad [7]$$

$i = 1,6$, $j = 1,12$ for triaxial inputs,

$j = 1,4$ for vertical inputs only

x_i denotes the ith degree of freedom and $\dot{x}_i$, $\ddot{x}_i$ are the first and second time derivatives. I_j, $\dot{I}_j$ are the displacement and velocity excitations. The

real time response of the cab is simulated for 64 seconds in each computer run.

The computer disc files containing the cab excitations are recalled as input to the package.

All the relevant cab physical properties must be supplied in a disc data file by the user.

The excitations are read into the programme sequentially and the cab responses, defined by the variables x_i, $\dot{x}_i$, and $\ddot{x}_i$, are computed at time intervals corresponding to those of the excitations.

It was found convenient to store the digital output of all the degrees of freedom by default and to use a post-processor programme to combine them to give specific responses such as the acceleration levels in the cab at the driver seat position. Other positions could be examined later if required by a re-run of the post-processor only.

For this design exercise attention was focused on the acceleration responses on the cab structure at the driver position in the vertical, longitudinal, and to a lesser extent, the lateral directions.

An example of a section of output from the package is given in Figure 8 which shows a 256 point data frame of simulated cab acceleration at the driver seat position in the vertical direction.

A digital spectral analysis package was interfaced with the post processor so that the user selected digital responses could be input directly for spectral analysis.

The Power Spectral Densities of the cab accelerations at the above positions were used as the ride quality indicators.

5.0 MODEL VALIDATION

Cab responses at the driver position were recorded on the prototype vehicle at the same time as the cab inputs. The predicted driver position responses obtained by exciting the cab model with these cab inputs were compared with the measured responses to validate the model.

Comparison of the predicted and experimental responses gives an indication of the accuracy of the overall simulation process; this is because we are not only testing the adequacy of the model itself but also the accuracy of the cab physical data.

Figures 9, 10 and 11 show the predicted and measured cab response PSD's. The response positions were on the cab structure at the driver seat position in the vertical, longitudinal and lateral directions.

On the basis of these plots the quality of the simulation was considered sufficiently accurate to be capable of indicating the relative merits of alternative suspensions configurations.

6.0 RESULTS

It is not the object of this paper to describe in detail the design process which was carried out, using the technique, to arrive at the final cab suspension design for the prototype vehicle. Instead a selection of initial, intermediate and final results are presented which highlight some milestones on the route to the final improved cab suspension design. Most of the conclusions drawn during the simulation optimisation process are clearly vehicle-specific, but some are applicable to vehicle cab suspension design in the wider sense.

6.1. Initial Cab Response

The original cab responses shown as the measured responses in Figures 9 to 11 highlight the ride problem which was evident at the prototype evaluation stage.

The longitudinal response in Figure 10 shows the main ride problem to be in the 6-10 Hz frequency band. This manifest itself as a pronounced fore-and-aft shake which was apparent over a range of road surfaces. The vertical cab responses were considered acceptable in this frequency band but not so in the 10-15 Hz band as shown by Figure 9.

The object of the modelling exercise was to significantly improve the cab response in both these directions by adjustments to the cab suspension system only.

The inevitable motor industry constraints of limited budgets and restricted time scales were prevalent in this exercise and little more than one month was available in which to specify the revised cab suspension parameters.

In addition, limited dynamic stiffness and damping data were available on the existing mount design with which to validate the model.

A nominal damping factor of 5% was assumed for the rubber mounts of the existing cab system and the simulation results using these values gave a sufficiently good correlation with the measured responses to enable the cab suspension optimisation process to proceed.

6.2. Early Simulation Results

Many different mount stiffness combinations were tried, e.g. 'soft front-stiff rear', 'stiff front-soft rear', 'stiff front-stiff rear' etc.

It was soon apparent that no combination of mounts with the 5% nominal rubber compund damping would give the desired improvement in cab response in both the vertical and longitudinal directions although either one of these directions could be optimised at the expense of the other. Attention was then brought to bear on the damping levels in the cab suspension system and simulations were conducted with gradually increased damping levels.

6.3. Final Results

As a result of more simulation runs it became evident that to achieve the desired reduction in cab response levels in both the vertical and longitudinal directions it was necessary to:-

i) Achieve higher damping levels in the mounts than was possible with elastomers, this being especially true of the cab rear suspension.

ii) Reduce the rear cab mount stiffness considerably in the vertical direction.

iii) Arrange for more suspension travel at the rear cab mount positions.

Figures 13 and 14 show the original and final cab response simulation results, with the optimised features i) to iii) above incorporated, in both the vertical and longitudinal direction. The very significant improvements in predicted vibration levels are readily apparent.

6.4. Experimental Validation

At this stage the theoretical suspension system was translated into actual hardware. To physically achieve the features listed in i) to iii) above it was necessary to change the rear cab suspension components from elastomers to steel springs and hydraulic dampers. A cab suspension with properties as close as possible to the 'theoretically optimised' system was fitted and the vehicle then road tested. Very significant improvements in ride quality were experienced which were in line with the mathematical prediction.

7.0 CONCLUSIONS

A cab simulation technique aimed at both predicting and optimising the dynamic response of cab systems to a range of measured frame excitations has been developed. It was used to achieve significant improvements in the ride quality of a prototype articulated vehicle in a very short timescale and at low cost.

Used at the prototype evaluation stage of the development of vehicles which feature cab systems, the technique will enable the optimisation of ride quality to be achieved much more quickly than with traditional testing methods.

ACKNOWLEDGEMENTS

The work reported here was undertaken by the author at the National Engineering Laboratory, East Kilbride, Scotland under contract with Leyland Vehicles, Preston.

The author gratefully acknowledges the role of both organisations in the successful development and application of the technique. The assistance of Professor J.D. Robson of the Department of Mechanical Engineering, University of Glasgow is also acknowledged.

REFERENCE

RENUCCI, M.P. [1976] 'A New Appraoch to Vehicle Component Testing by Computer Simulation of the Vehicle Response', International Symposium on Automotive Technology and Automation 'ISATA 1976]. Conference Proceedings, Volume I paper number 6.

LIST OF FIGURES

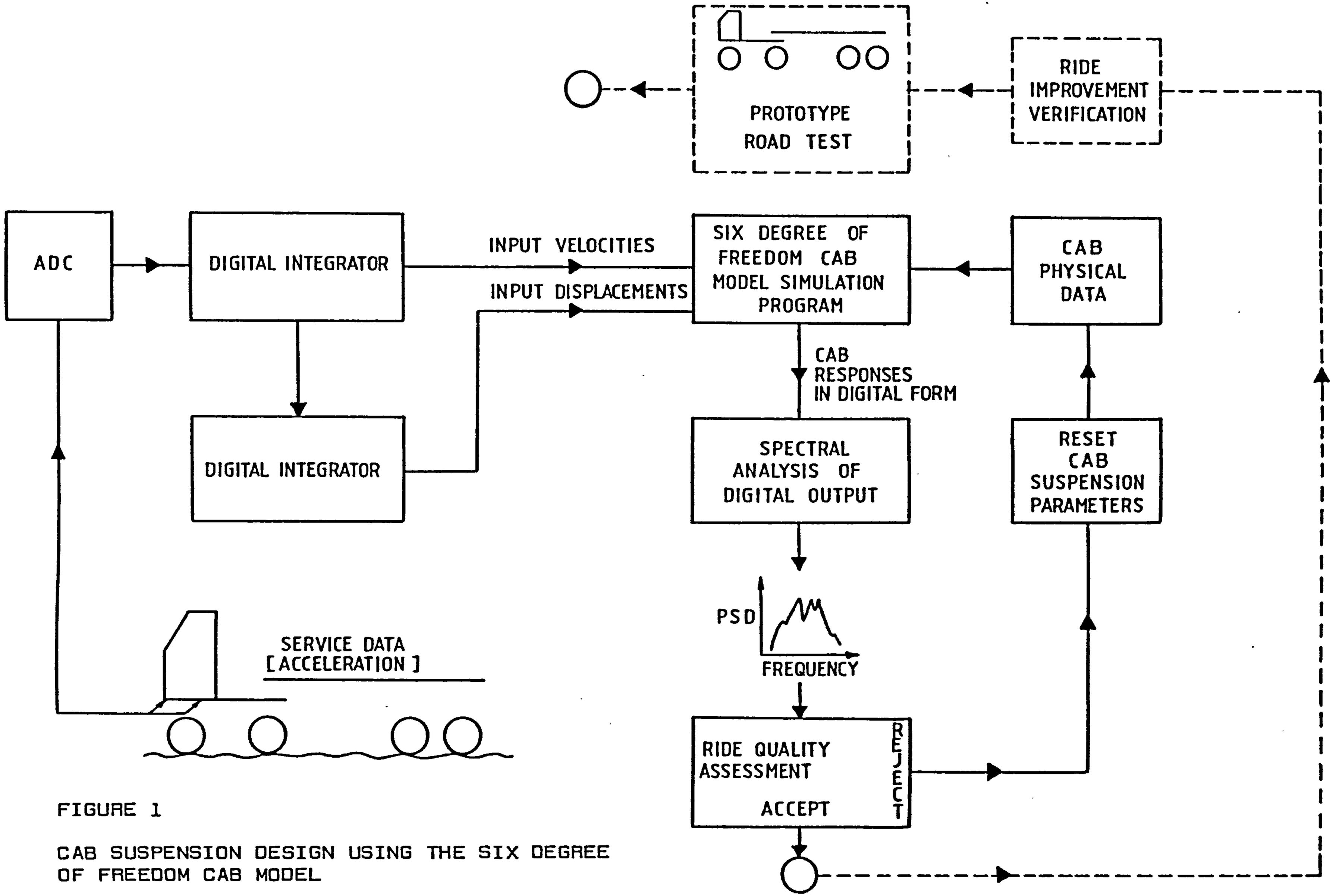

FIGURE 1

CAB SUSPENSION DESIGN USING THE SIX DEGREE OF FREEDOM CAB MODEL

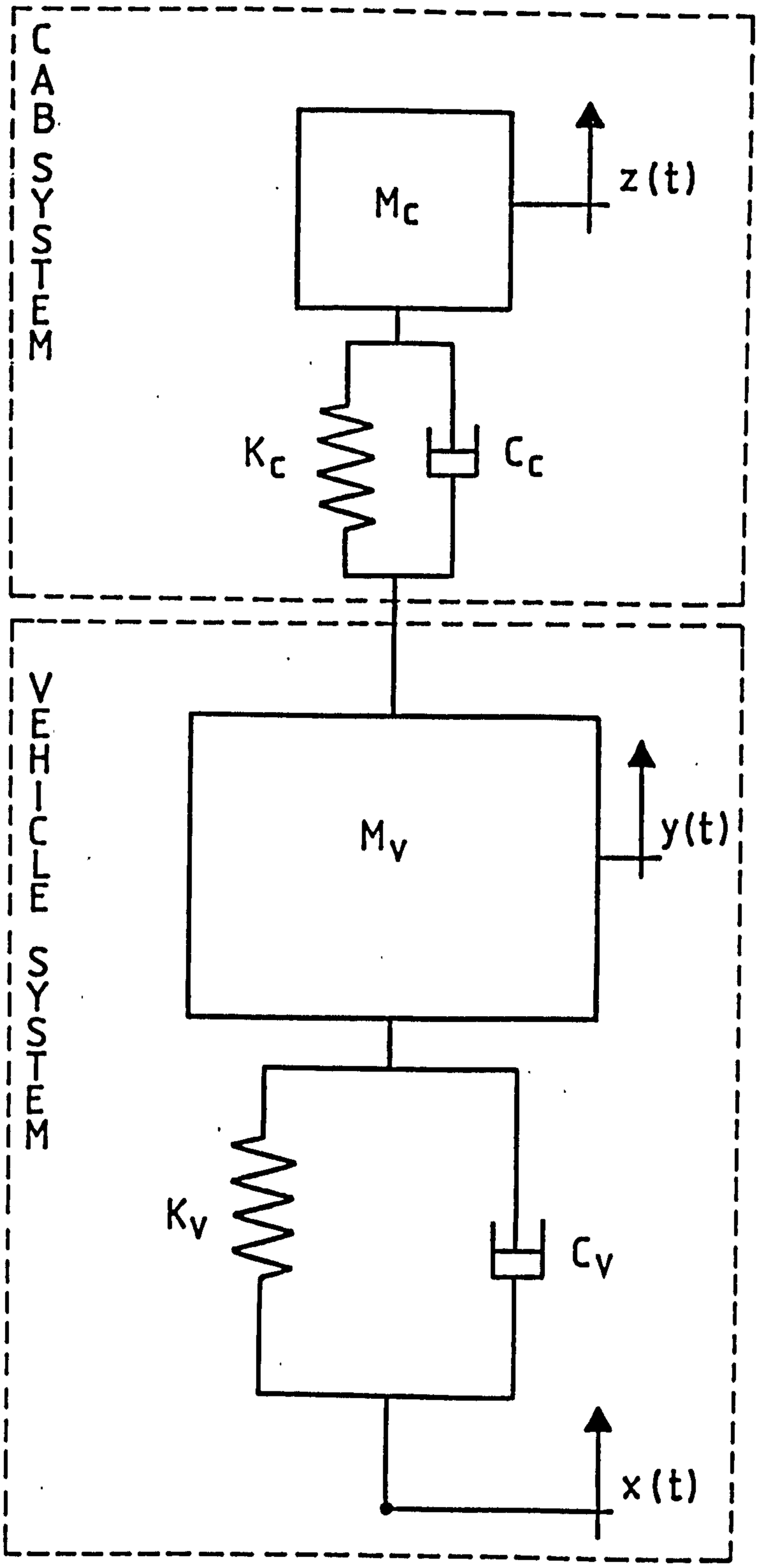

FIGURE 2

TWO DEGREE OF FREEDOM ANALOGUE OF THE CAB AND VEHICLE SYSTEMS

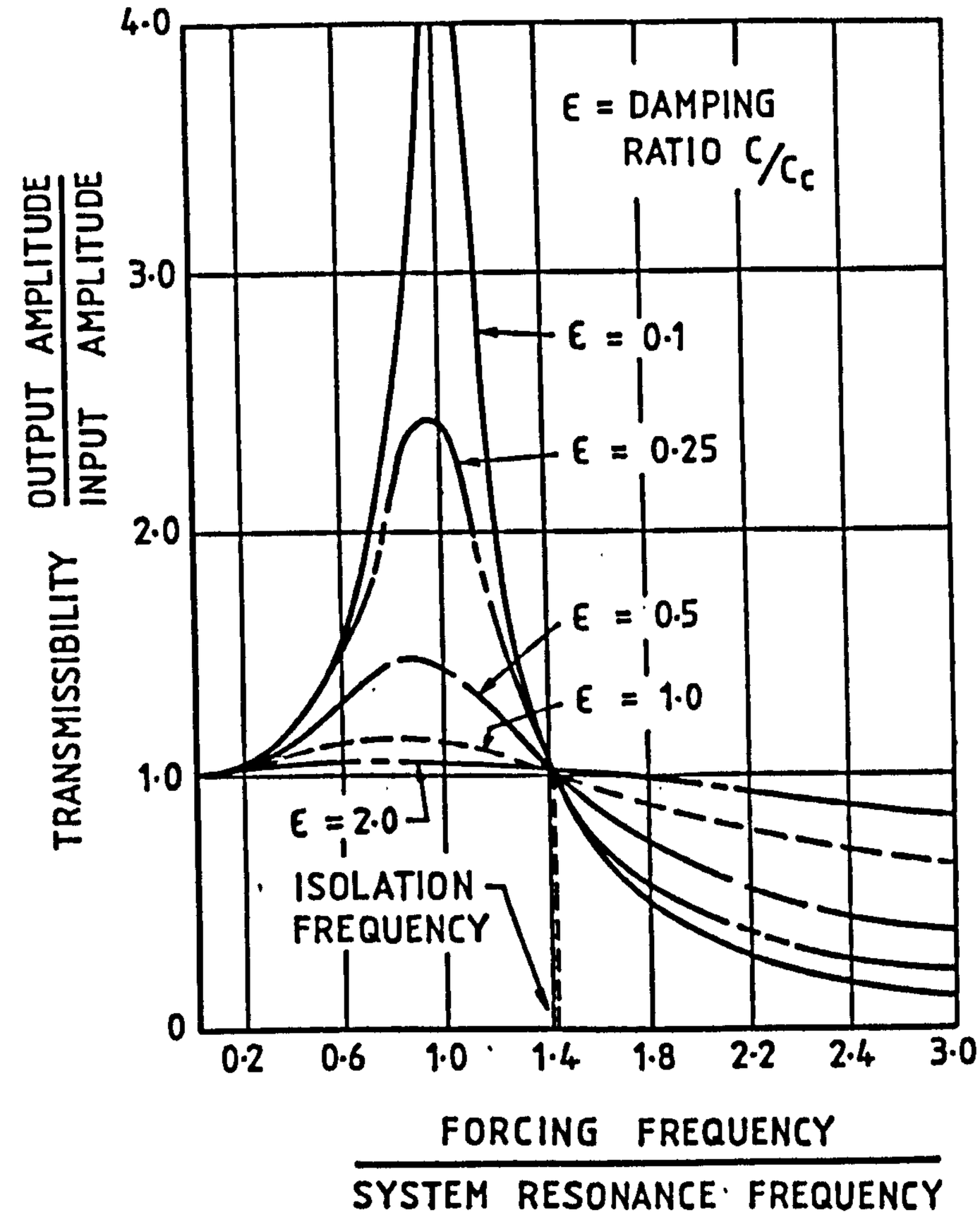

FIGURE 3

THE EFFECT OF DAMPING IN SINGLE DEGREE OF FREEDOM ISOLATION SYSTEMS

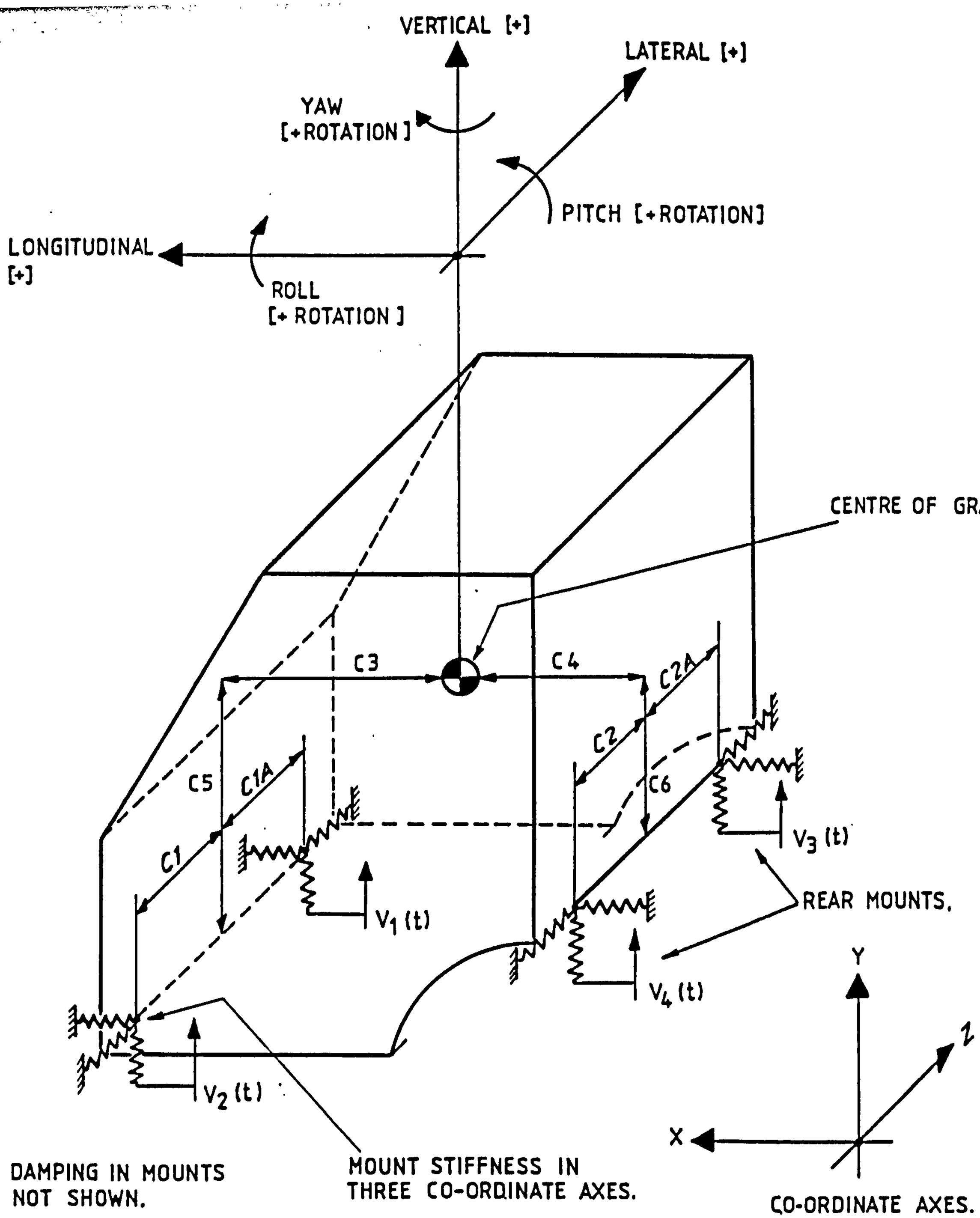

FIGURE 4

SIX DEGREE OF FREEDOM CAB MODEL SCHEMATIC

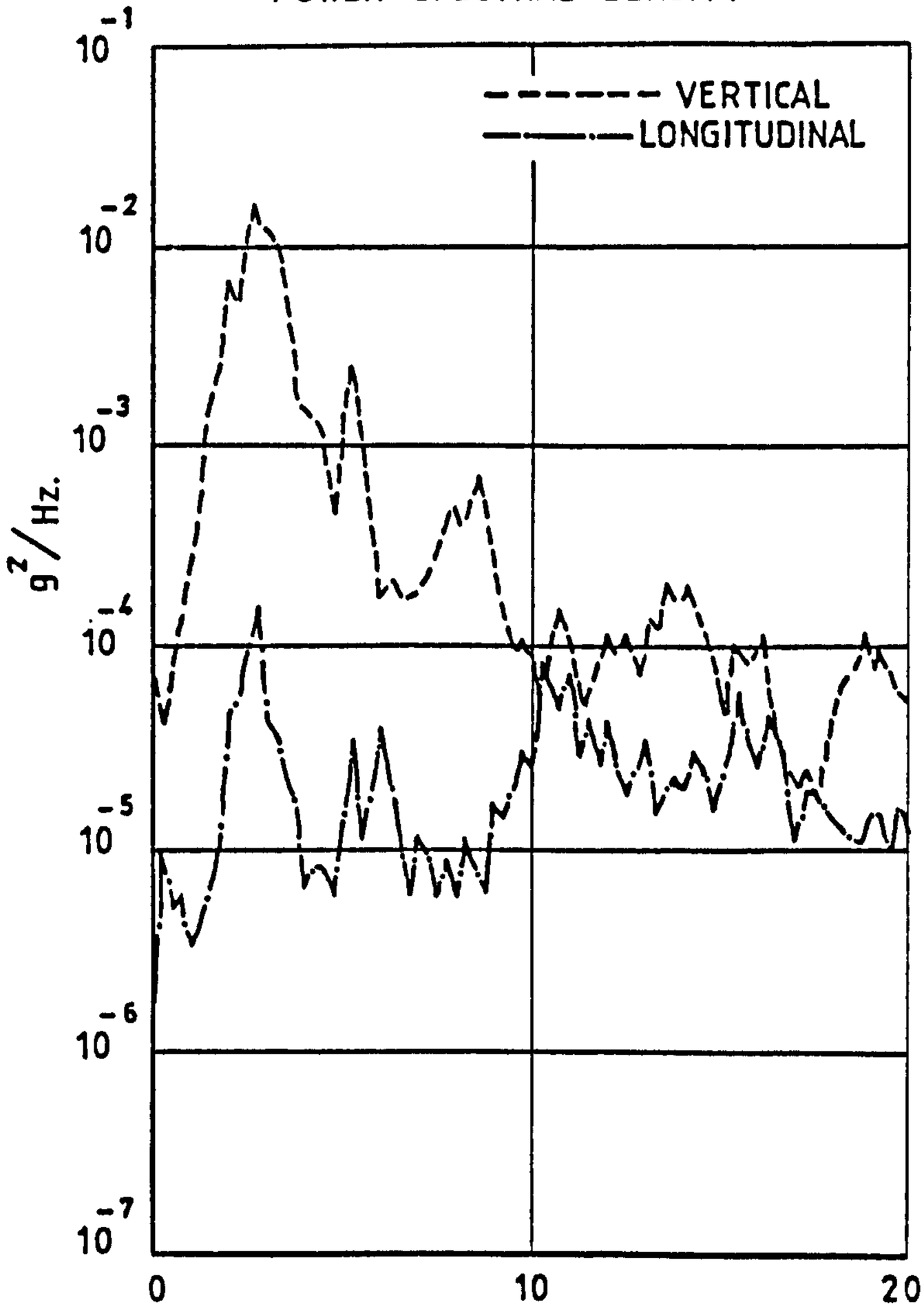

FIGURE 5

COMPARISON OF TYPICAL VERTICAL AND
LONGITUDINAL ACCELERATIONS ON A TRUCK FRAME

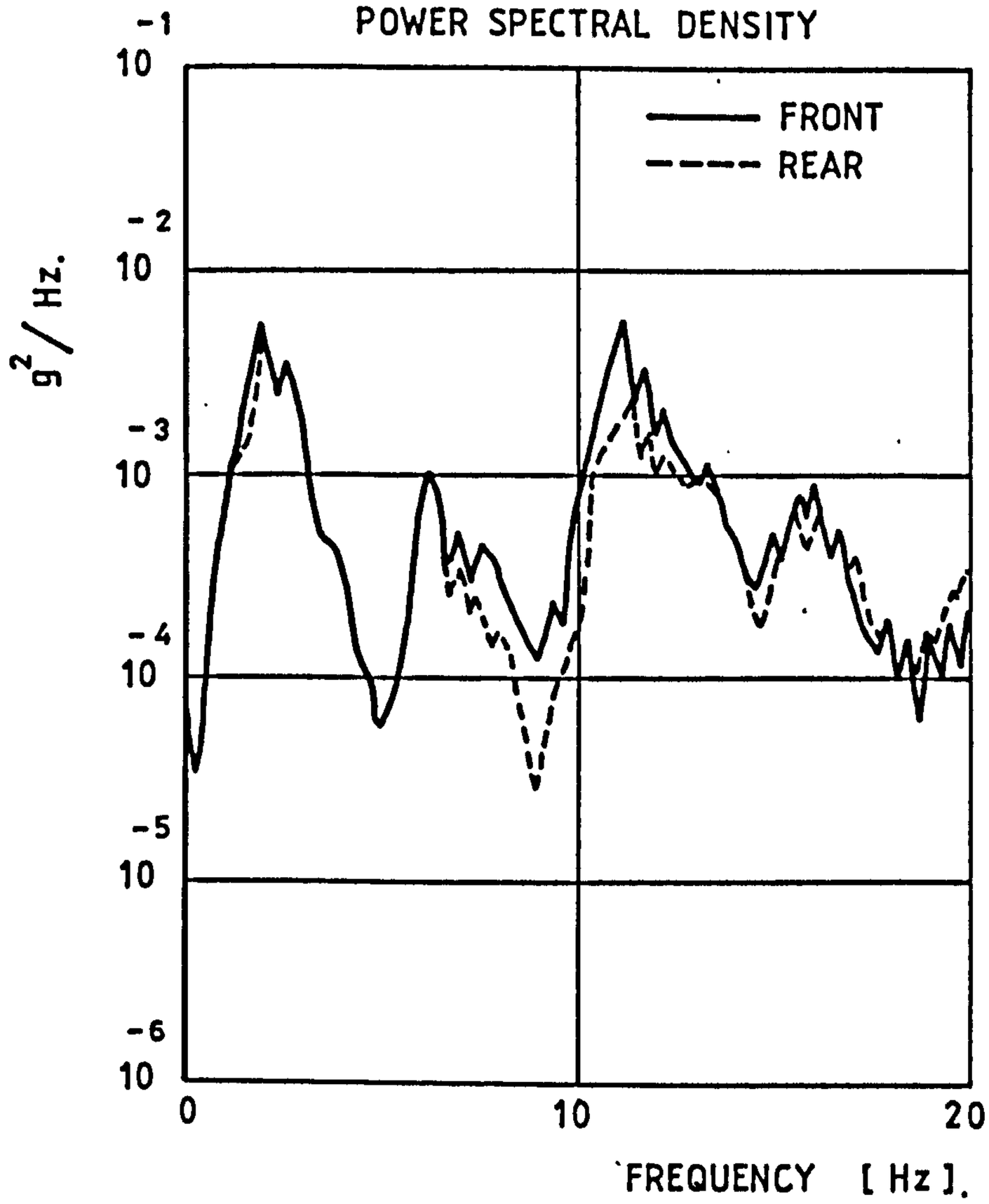

FIGURE 6

VERTICAL ACCELERATIONS ON THE TRUCK FRAME
AT ONE FRONT AND ONE REAR CAB MOUNT POSITION

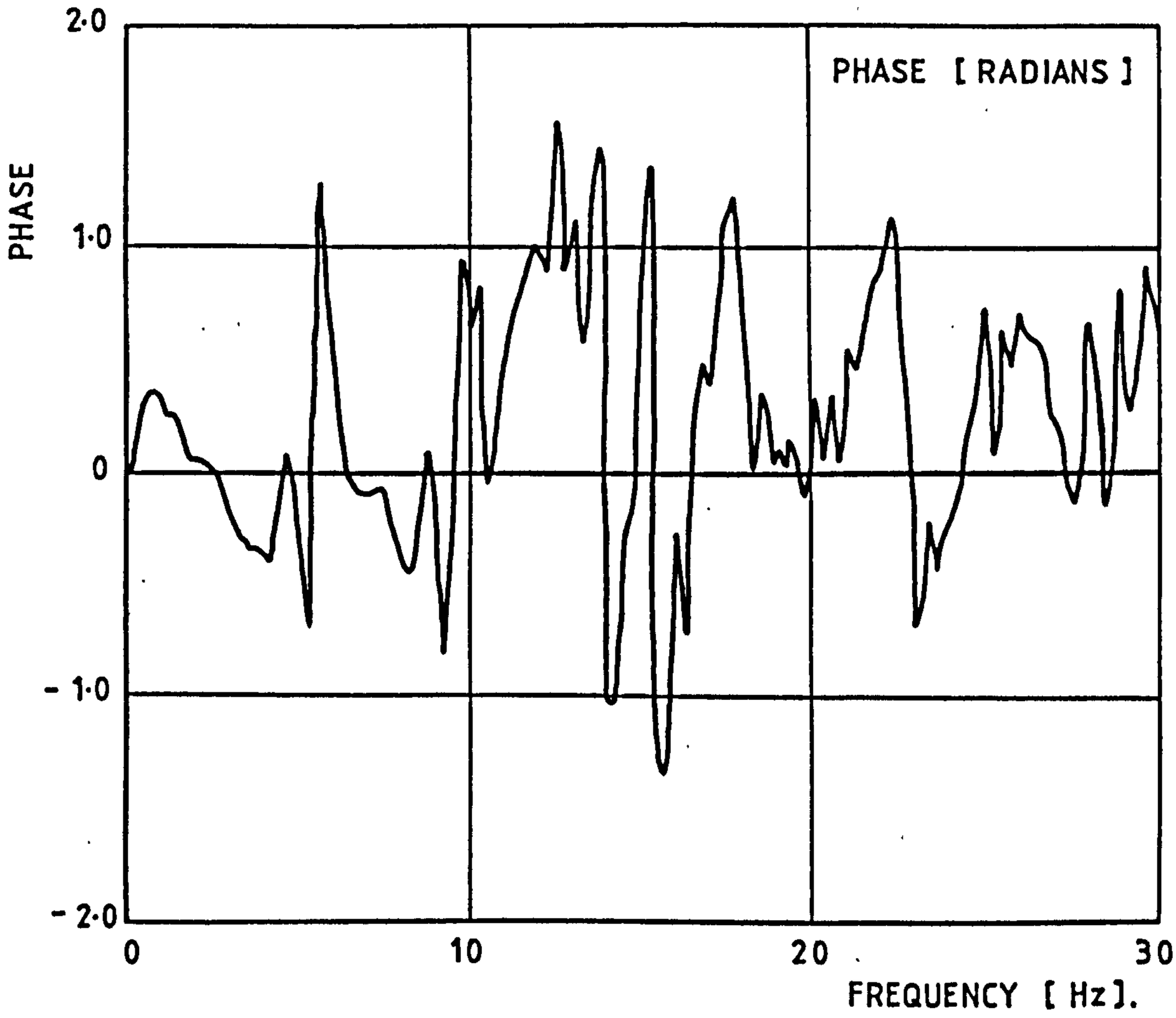

FIGURE 7

PHASE RELATIONSHIP BETWEEN ACCELERATIONS
SHOWN IN FIGURE 6

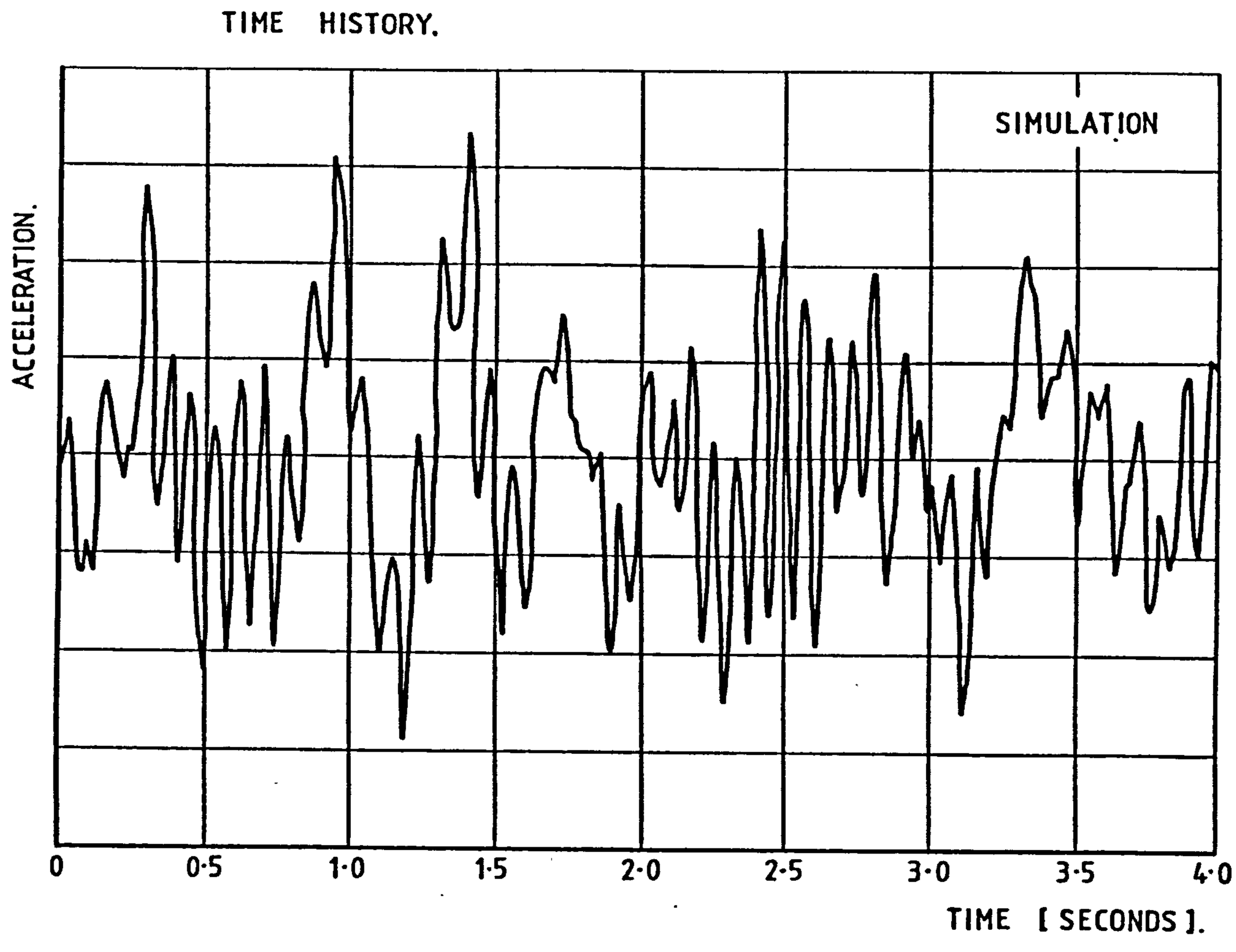

FIGURE 8

SAMPLE OF CAB ACCELERATION TIME HISTORY RESPONSE AT DRIVER POSITION IN THE VERTICAL DIRECTION (256 POINT DATA FRAME)

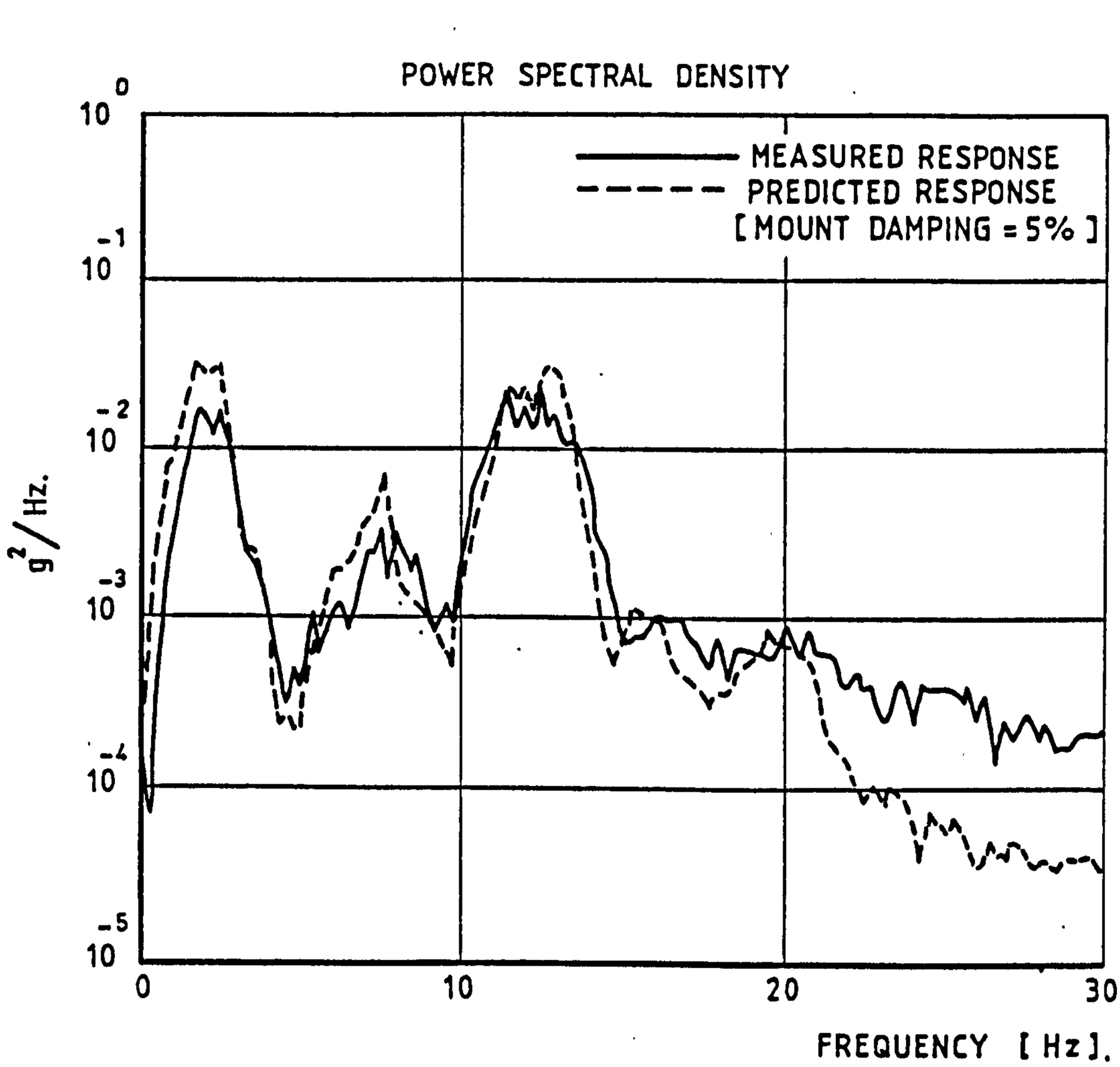

FIGURE 9

COMPARISON OF PREDICTED AND MEASURED RESPONSE IN THE CAB AT THE DRIVER POSITION (VERTICAL DIRECTION)

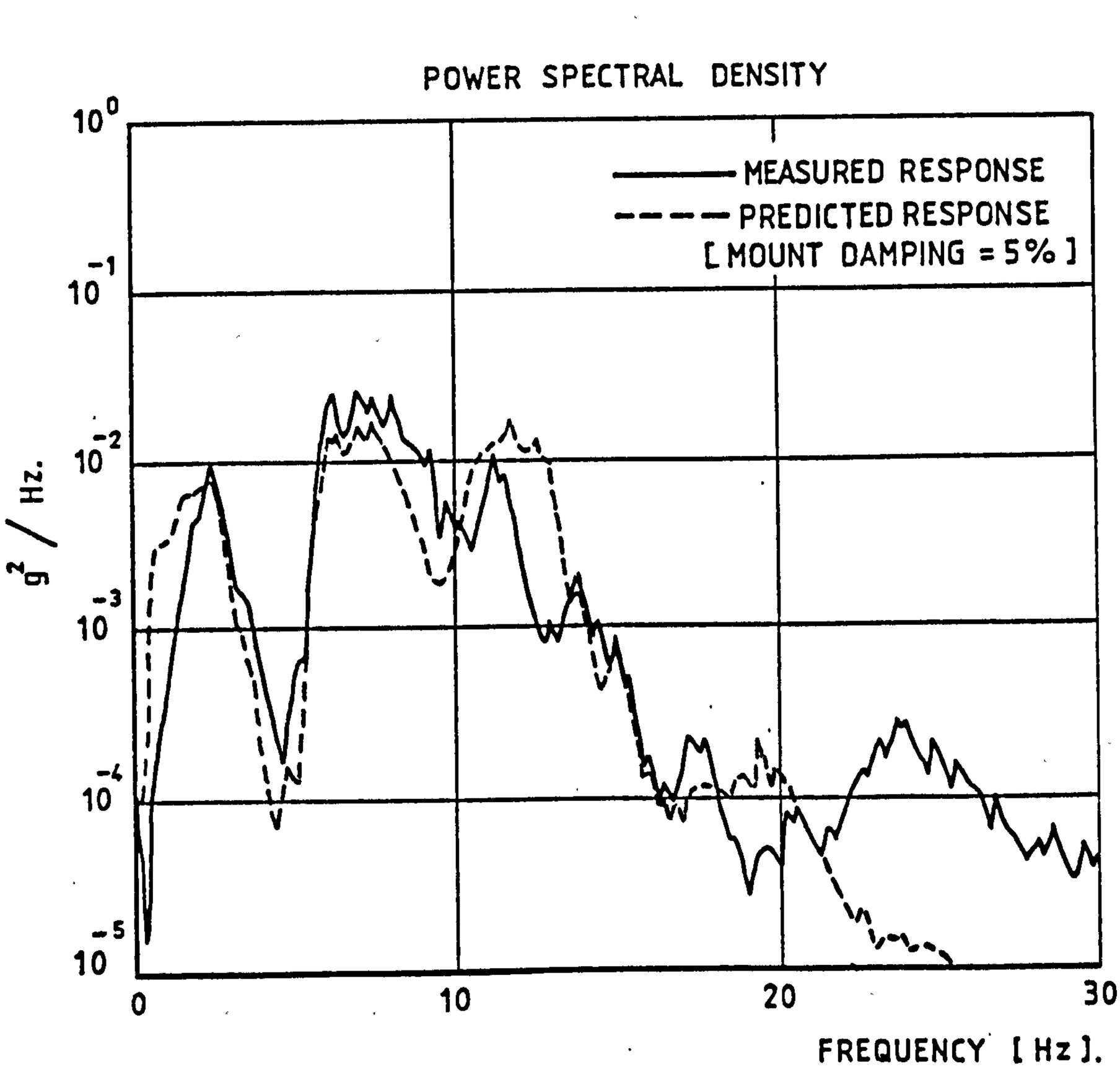

FIGURE 10

COMPARISON OF PREDICTED AND MEASURED RESPONSE IN THE CAB AT THE DRIVER POSITION (LONGITUDINAL DIRECTION)

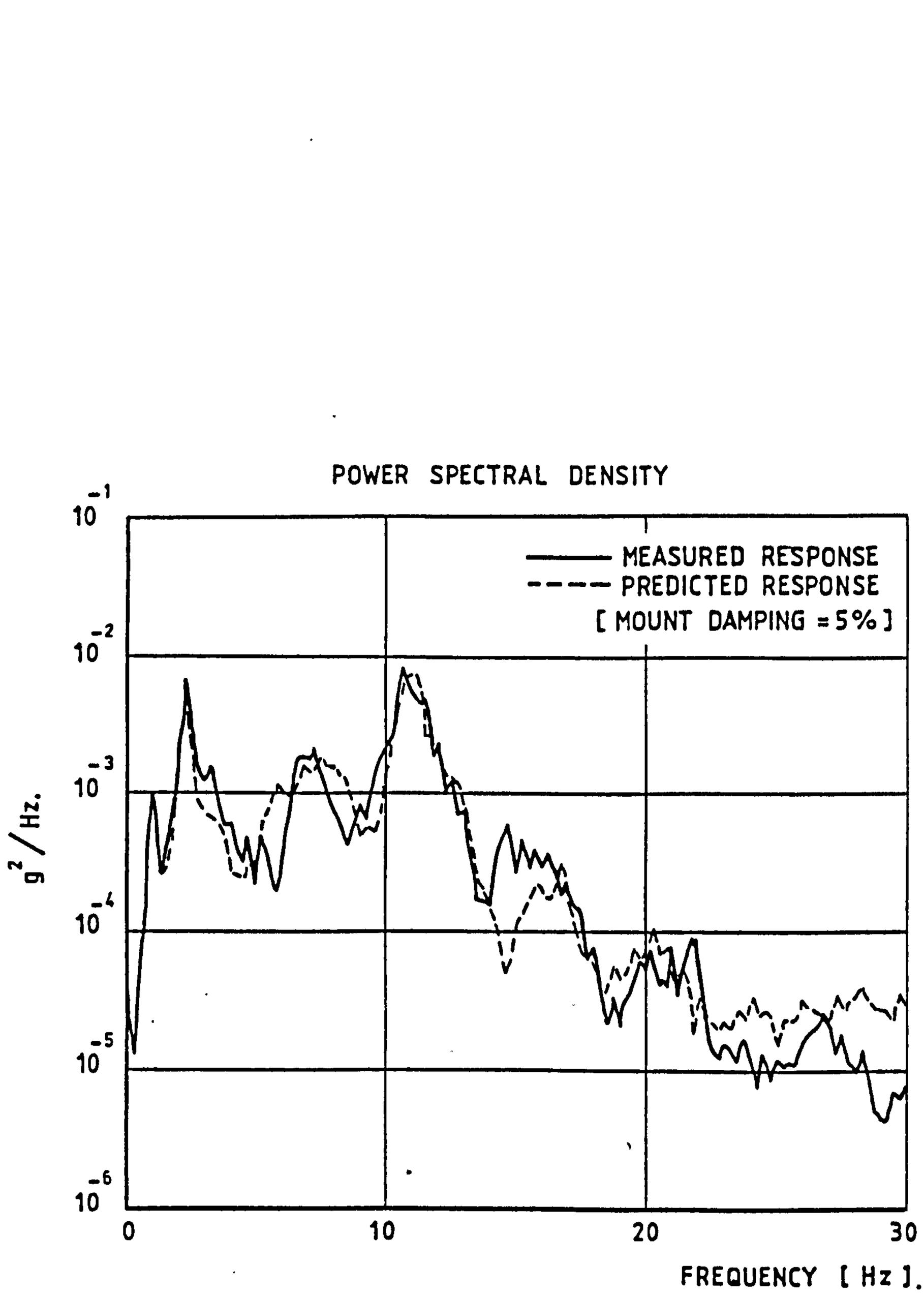

FIGURE 11

COMPARISON OF PREDICTED AND MEASURED
RESPONSE IN THE CAB AT THE DRIVER POSITION
(LATERAL DIRECTION)

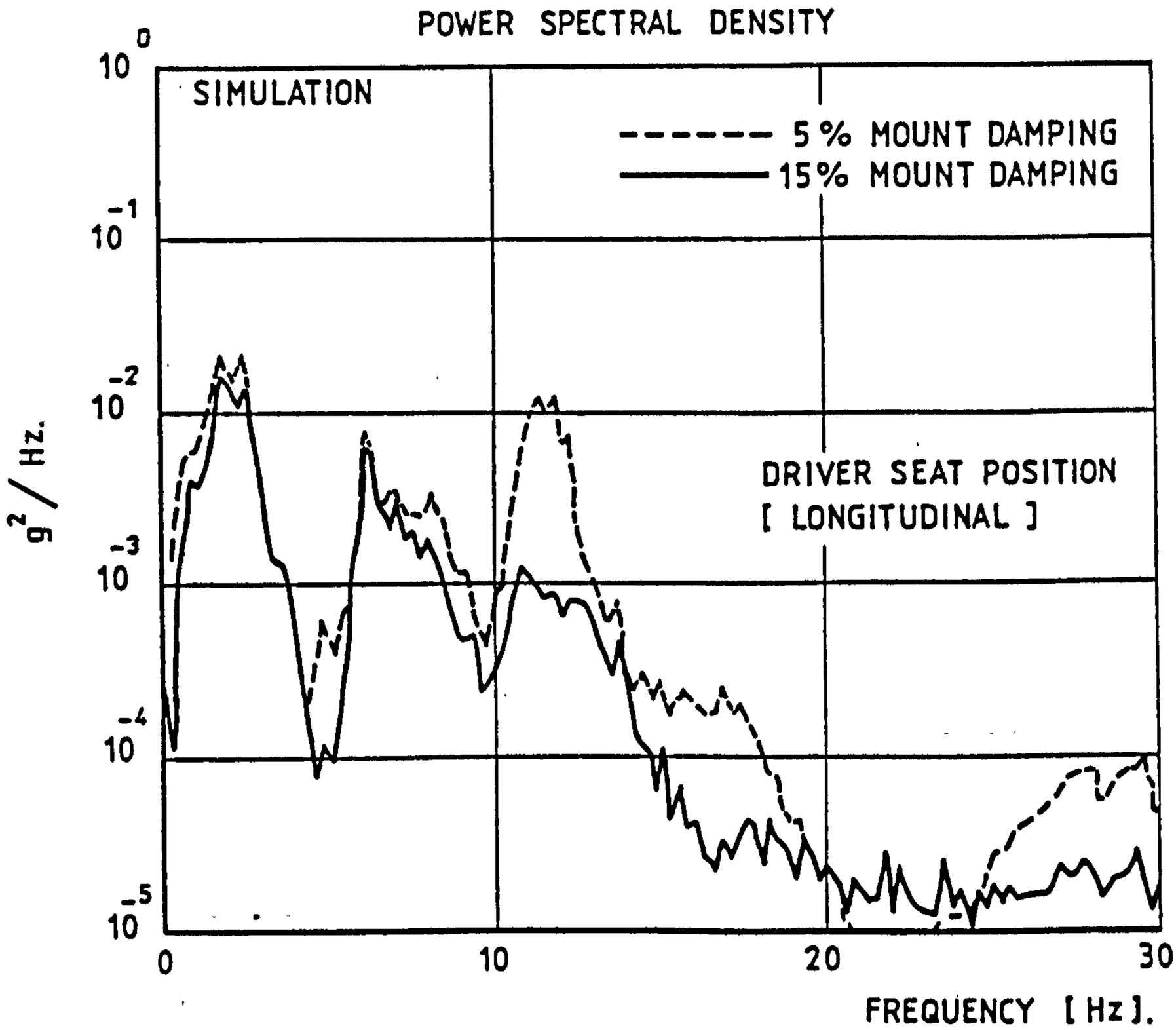

FIGURE 12

ILLUSTRATION OF THE EFFECT OF INCREASED MOUNT DAMPING LEVELS ON CAB RESPONSE

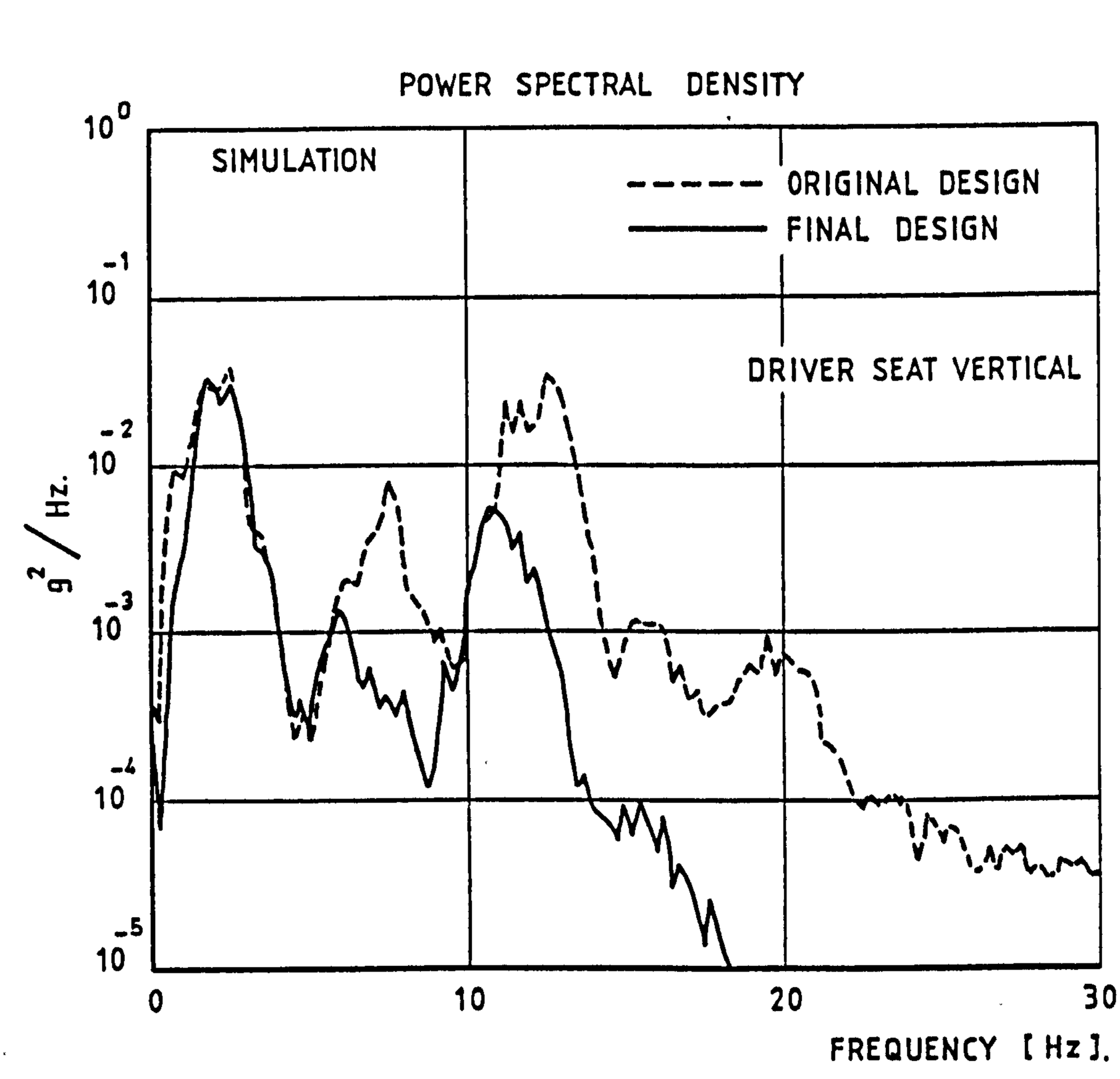

FIGURE 13

PREDICTED CAB RESPONSE FOR THE ORIGINAL
AND FINAL SUSPENSION DESIGN (VERTICAL DIRECTION)

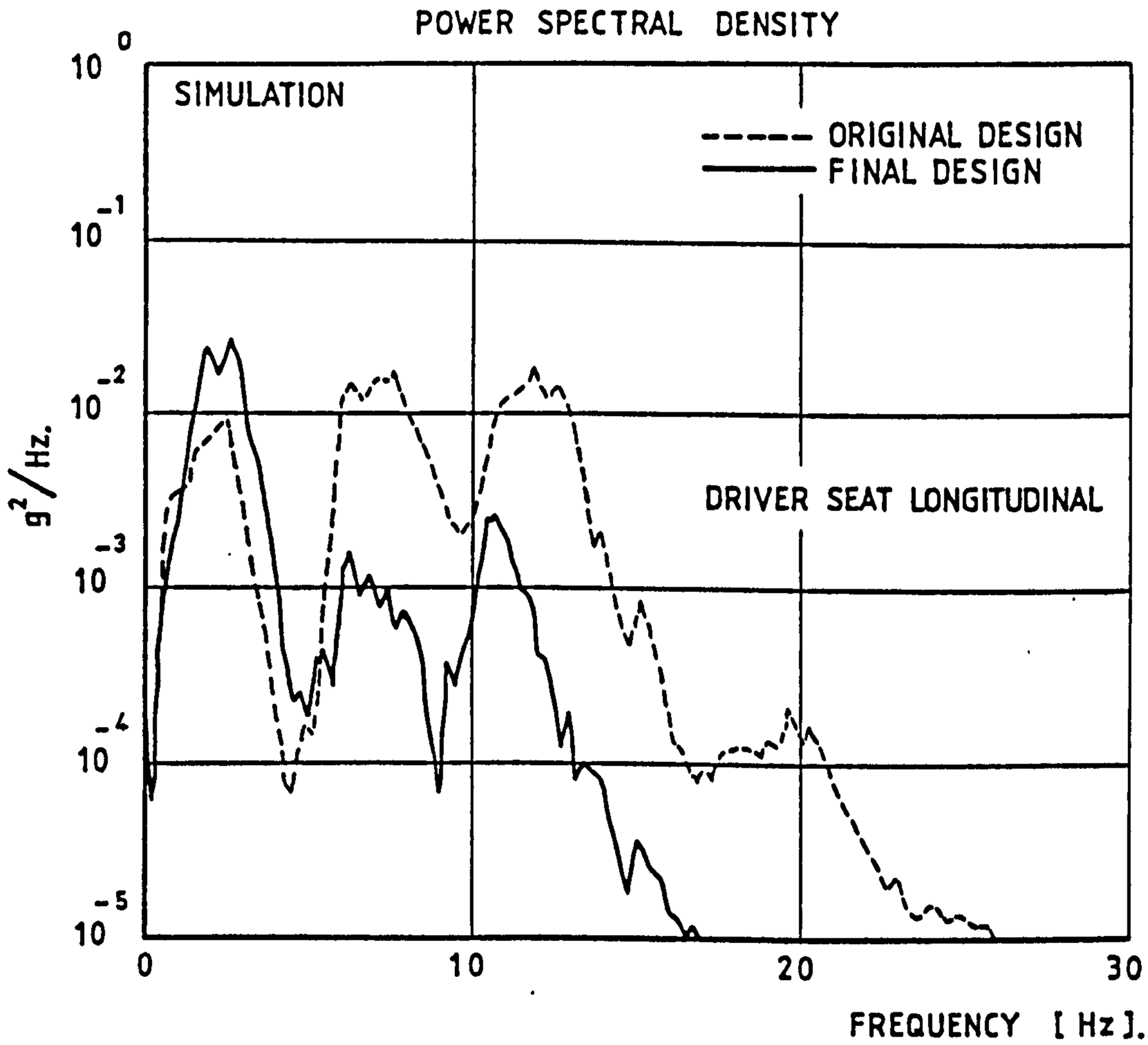

FIGURE 14

PREDICTED CAB RESPONSE FOR THE ORIGINAL AND
FINAL SUSPENSION DESIGN (LONGITUDINAL DIRECTION)

REFERENCES

REFERENCES

1] HALEY, H.P. 'Vibrational Characteristics of Automotive Suspensions' Mass. Inst. Tech. Doctoral Thesis 1938

2] JANEWAY, R.N. 'A Better Truck Ride for Driver and Cargo - Problems and Practical Solutions' SP-154 Society of Automotive Engineers New York 1958

3] CLARK, D.C. 'A Preliminary Investigation into the Dynamic Behaviour of Vehicles and Highways' SAE Trans., Vol 70, 1962 pp 447-455

4] VAN DEUSEN, B.D. 'Analytical Techniques for Designing Ride Quality into Automotive Vehicles' Society of Automotive Engineers Paper 670021 [1967]

5] WALTHER, W.D. et.al. 'Truck Ride - A Mathematical and Emperical Study' Society of Automotive Engineers, Paper 690099, 1969

6] HEALEY, A.J. 'An Analytical and Experimental Study of Automobile Dynamics with Random Roadway Inputs' Journal of Dynamic Systems, Measurement and Control, ASME 1977

7] KOJIMA, I. 'Analysis and Control of Shake of Trucks' Journal of Society of Automotive Engineers of Japan, 1969

8] LABARRE, R.P. et.al. 'The Measurement and Analysis of Road Surface Roughness' MIRA Report No. 1970/5

9] DODDS, C.J. & ROBSON, J.D. 'The Response of Vehicle Components to Road Surface Roughness' Proc. 13th F.I.S.I.T.A. Congress, Brussels (1970)

10] DODDS, C.J. & ROBSON, J.D. 'The Description of Road Surface Roughness' Journal of Sound and Vibration November 1973

11] STYLES, D.D. & DODDS, C.J. 'Simulation of Random Environments for Structural Dynamics Testing' S.E.S.A. Spring Meeting, Chicago 1976

12] RENUCCI, M.P. 'Response of Linear Systems to Non Gaussian Excitation' M.Sc. Thesis, University of Glasgow 1974

13] RENUCCI, M.P. 'A New Approach to Vehicle Component Testing by Computer Simulation of the Vehicle Response' Proceedings of I.S.A.T.A. 1976

14] MACAULAY, M.A. 'Measurement of Road Surfaces - Advances in Automobile Engineering' Cranfield International Symposium Series 4 pp 93-112 (1963)

15] PARKHILOVSKI, I.G. 'Investigation of the Probability Characteristics of the Surfaces of Distributed Types of Roads' Autom Prom 8 pp 18-22 (1968)

16] PEUZNER, Ya M. TIKHONOV A.A. 'An Investigation into the Statistical Properties of the Microprofile of the Main Types of Motor Road' Autom. Prom. 30 (1) pp 15-18 (1964)

17] WALLIS, J.H. et.al. 'Some Measurements of Power Spectra of Runway Roughness' N.A.C.A. T.N. 3305

18] WENDEBORN, J.O. 'Description of Road Profiles by Means of the Spectral Density of the Irregularities' A.T.Z. 69 No.5 (1967)

19] CRAIG, J.B. 'The Laboratory Simulation of Vehicle Response to Road Profile Excitation' NEL Symposium on Dynamic Analysis of Structures, 1975

20] PESTEL & LECKIE 'Matrix Methods in Elastomechanics' McGraw Hill Inc. 1963

APPENDICES

APPENDIX A — MATRIX REPRESENTATION OF DIFFERENTIAL EQUATIONS OF VEHICLE MODEL

APPENDIX B — ANALYSIS OF ACCURACY OF DIGITAL DIFFERENTIATOR

APPENDIX C — COMPUTATION OF EQUIVALENT LINEAR VISCOUS DAMPING RATES FOR SINUSOIDAL EXCITATION

APPENDIX D — DESCRIPTION OF PROGRAMME 'MATRIX'

APPENDIX E — CENTRES OF OSCILLATION

APPENDIX F — 63 DOF ARTICULATED VEHICLE MODEL PARAMETERS

APPENDIX G — CENTRAL DIFFERENCE FORMULAE

APPENDIX A

MATRIX REPRESENTATION OF DIFFERENTIAL EQUATIONS OF VEHICLE MODEL

A P P E N D I X A

MATRIX REPRESENTATION OF THE EQUATIONS OF MOTION OF THE VEHICLE

The matrix equation is given by

$$[M][\ddot{X}] + [K][X] + [C][\dot{X}] = [E]$$

ie

$$\begin{bmatrix} M_1 & & & & & & & & & & & \\ & M_2 & & & & & & & & & & \\ & & ME & & & & & & & & & \\ & & & I\theta E & & & & & & & & \\ & & & & I\psi E & & & & & & & \\ & & & & & MD & & & & & & \\ & & & & & & I\theta D & & & & & \\ & & & & & & & I\psi D & & & & \\ & & & & & & & & MC & & & \\ \text{All non-diagonal} & & & & & & & & & I\theta C & & \\ \text{terms zero} & & & & & & & & & & I\psi C & \\ & & & & & & & & & & & MA \\ & & & & & & & & & & & & I\theta A \end{bmatrix} \begin{bmatrix} \ddot{X}_1 \\ \ddot{X}_2 \\ \ddot{X}E \\ \ddot{\theta}E \\ \ddot{\psi}E \\ \ddot{X}D \\ \ddot{\theta}D \\ \ddot{\psi}D \\ \ddot{X}C \\ \ddot{\theta}C \\ \ddot{\psi}C \\ \ddot{X}A \\ \ddot{\theta}A \end{bmatrix} +$$

$$\begin{bmatrix} K1 & 0 & 0 & 0 & 0 & 0 & 0 & 0 & K2 & K3 & K4 & 0 & 0 \\ & K5 & 0 & 0 & 0 & 0 & 0 & 0 & K6 & 0 & K7 & 0 & 0 \\ & & K8 & 0 & K9 & 0 & 0 & 0 & K10 & 0 & K11 & 0 & 0 \\ & & & K12 & 0 & 0 & 0 & 0 & 0 & K13 & 0 & 0 & 0 \\ & & & & K14 & 0 & 0 & 0 & K15 & 0 & K16 & 0 & 0 \\ & & & & & K17 & 0 & K18 & K19 & K20 & K21 & 0 & 0 \\ & & & & & & K22 & 0 & 0 & K23 & 0 & 0 & 0 \\ \text{Matrix symmetrical} & & & & & & & K24 & K25 & K26 & K27 & 0 & 0 \\ \text{about diagonal} & & & & & & & & K28 & K29 & K30 & K31 & 0 \\ & & & & & & & & & K32 & K33 & 0 & K34 \\ & & & & & & & & & & K35 & K36 & 0 \\ & & & & & & & & & & & K37 & 0 \\ & & & & & & & & & & & & K38 \end{bmatrix} \begin{bmatrix} X1 \\ X2 \\ XE \\ \theta E \\ \psi E \\ XD \\ \theta D \\ \psi D \\ XC \\ \theta C \\ \psi C \\ XA \\ \theta A \end{bmatrix} +$$

$$\begin{bmatrix} & & & & & & & & & & & & \\ & & & & & & & & & & & & \\ & & & & & & & & & & & & \\ & & & & & & & & & & & & \\ & & & & & & & & & & & & \\ & & & & & & & & & & & & \\ & & & & & & & & & & & & \\ \text{Identical to stiffness} & & & & & & & & & & & & \\ \text{matrix with all K terms} & & & & & & & & & & & & \\ \text{replaced by C terms} & & & & & & & & & & & & \\ & & & & & & & & & & & & \\ & & & & & & & & & & & & \\ & & & & & & & & & & & & \\ & & & & & & & & & & & & \\ & & & & & & & & & & & & \end{bmatrix} \begin{bmatrix} \dot{X}1 \\ \dot{X}2 \\ \dot{X}E \\ \dot{\theta}E \\ \dot{\psi}E \\ \dot{X}D \\ \dot{\theta}D \\ \dot{\psi}D \\ \dot{X}C \\ \dot{\theta}C \\ \dot{\psi}C \\ \dot{X}A \\ \dot{\theta}A \end{bmatrix} = \begin{bmatrix} K_T I_1 + C_T \dot{I}_1 \\ K_T I_2 + C_T \dot{I}_2 \\ 0 \\ 0 \\ 0 \\ 0 \\ 0 \\ 0 \\ 0 \\ 0 \\ 0 \\ K_{TR}(I_3 + I_4) + C_{TR}(\dot{I}_3 + \dot{I}_4) \\ K_{TR}(I_4 - I_3) + C_{TR}(\dot{I}_4 - \dot{I}_3) \end{bmatrix}$$

where I is the wheel input displacement with subscript convention as in Fig.5.

The following substitutions have been made in the above matrices for ease of presentation.

$K1 = K_T + K_F$

$K2 = - K_F$

$K3 = bK_F$

$K4 = wK_F$

$K5 = K_T + K_F$

$K6 = - K_F$

$K7 = wK_F$

$K8 = 2K_E + K_G$

$K9 = fK_G - 2eK_E$

$K10 = 2K_E + K_G$

$K11 = 2vK_E + uK_G$

$K12 = 2t^2K_E$

$K13 = - 2t^2K_E$

$K14 = f^2K_G + 2e^2K_E$

$K15 = 2eK_E - fK_G$

$K16 = ufK_G - 2evK_E$

$K17 = 4K_D$

$K18 = 2(r - q)K_D$

$K19 = - 4K_D$

$K20 = 2(m + n)K_D$

$K21 = 2(h + j)K_D$

$K22 = 4p^2K_D$

$K23 = 2(n - m)pK_D$

$K24 = 2(r^2 + q^2)K_D$

$K25 = - 2(r - q)K_D$

$K26 = (m + n)(r - q)K_D$

$K27 = 2(rj - qh)K_D$

$K28 = 2K_E + K_G + 2(K_F + K_R) + 4K_D$

$K29 = - 2(m + n)K_D$

$K30 = - 2wK_F + 2(a - w)K_R - 2(h + j)K_D - 2vK_E - uK_G$

$K31 = - 2K_R$

$K32 = 2b^2K_F + 2b^2K_R + 2t^2K_E + +2(m^2 + n^2)K_D$

$K33 = (m + n)(h + j)K_D$

$K34 = - 2b^2K_R$

$K35 = 2K_R(a - w)^2 + 2w^2K_F + 2v^2K_E + +u^2K_G + 2(h^2 + j^2)K_D$

$K36 = - 2(a - w)K_R$

$K37 = 2K_{TR} + K_R$

$K38 = 2b^2(K_R + K_{TR})$

A P P E N D I X A (Continued)

DESCRIPTION OF TERMS USED IN 13 DEGREE OF FREEDOM MODEL

Degrees of Freedom

1	X1	Vertical displacement of offside front unsprung mass at wheel centre line
2	X2	Vertical displacement of nearside front unsprung mass at wheel centre line
3	XE	Vertical displacement of engine-gearbox assembly - centre of gravity
4	θE	Engine-gearbox roll about centre of gravity
5	ψE	Engine-gearbox pitch about centre of gravity
6	XD	Vertical displacement of driver-seat
7	θD	Driver-seat roll about centre of gravity
8	ψD	Driver-seat pitch about centre of gravity
9	XC	Vertical displacement of body-chassis centre of gravity
10	θC	Body-chassis roll about centre of gravity
11	ψC	Body-chassis pitch about centre of gravity
12	XA	Rear axle centre of gravity vertical displacement
13	θA	Rear axle roll about centre of gravity

Dimensions

a	Wheelbase
2b	Average of front and rear tracks
e	Distance from front engine mount to engine-gearbox centre of gravity
f	Distance from gearbox mount to engine-gearbox centre of gravity
g	Vertical distance from engine-gearbox centre of gravity to subframe mounting position
h	Distance from chassis centre of gravity to rear seat spring
j	Distance from chassis centre of gravity to front seat spring
l	Vertical distance from body-chassis centre of gravity to rear suspension heights
m	Distance from chassis centre of gravity to offside seat spring
n	Distance from chassis centre of gravity to nearside seat spring
p	Distance (offside-nearside) from seat centre of gravity to nearside and offside seat springs
q	Distance (front-rear) from seat centre of gravity to front seat spring
r	Distance from seat centre of gravity to rear seat spring
s	Vertical distance from seat centre of gravity to floor mounting points
t	Distance (nearside-offside) from body centre of gravity to front engine mounts
u	Distance (front-rear) from body centre of gravity to gearbox mounts
v	Distance (front-rear) from body centre of gravity to front engine mounts
w	Distance (front-rear) from body centre of gravity to front unsprung masses

Inertia Terms

M1	Offside front unsprung mass
M2	Nearside front unsprung mass
ME	Mass of engine-gearbox assembly
$I\theta_E$	Engine-gearbox assembly roll inertia about centre of gravity
$I\psi_E$	Engine-gearbox pitch inertia about centre of gravity
MD	Mass of driver and seat
$I\theta_D$	Driver-seat roll inertia about centre of gravity
$I\psi_D$	Driver-seat pitch inertia about centre of gravity
MC	Mass of body-chassis with design payload but excluding other masses
$I\theta_C$	Body-chassis roll inertia about centre of gravity
$I\psi_C$	Body-chassis pitch inertia about centre of gravity
MA	Mass of rear axle plus rear-unsprung masses
$I\theta_A$	Roll inertia of rear axle about centre of gravity

Spring Terms

K_D	Seat rate
K_E	Front engine mount rate
K_F	Effective vertical wheel spring rate of front suspension
K_G	Gearbox mount rate
K_R	Effective vertical wheel spring rate of rear suspension
K_T	Front tyre rate
K_{TR}	Rear tyre rate

Damping Terms

Same as spring terms with K replaced by C.

APPENDIX B

ANALYSIS OF ACCURACY OF DIGITAL DIFFERENTIATOR

APPENDIX B

The digital differentiator subroutine was applied to a typical road profile representation to assess its accuracy.

Two digital time histories - i.e. the road displacement digital signal and the computed velocity signal - were analysed to measure the digital error in the computation of the derivative.

Figures B1 and B2 give corresponding arbitary two second time history samples for the road profile displacement and computed velocities.

Figure B3 shows the phase relationship between the signals and is the argument of the complex frequency response function between the two signals as a function of frequency. It is clear that the theoretically ideal 90^{o} phase lag between the two signals is well simulated.

Figure B4 gives the modulus of the frequency response function between the two signals with the theoretical relationship superimposed.

Note that the road displacement signal is low pass filtered above 32 Hz which causes the frequency response function to drop off above this frequency.

The digital differentiator was therefore considered to be acceptably accurate over the frequency range of interest.

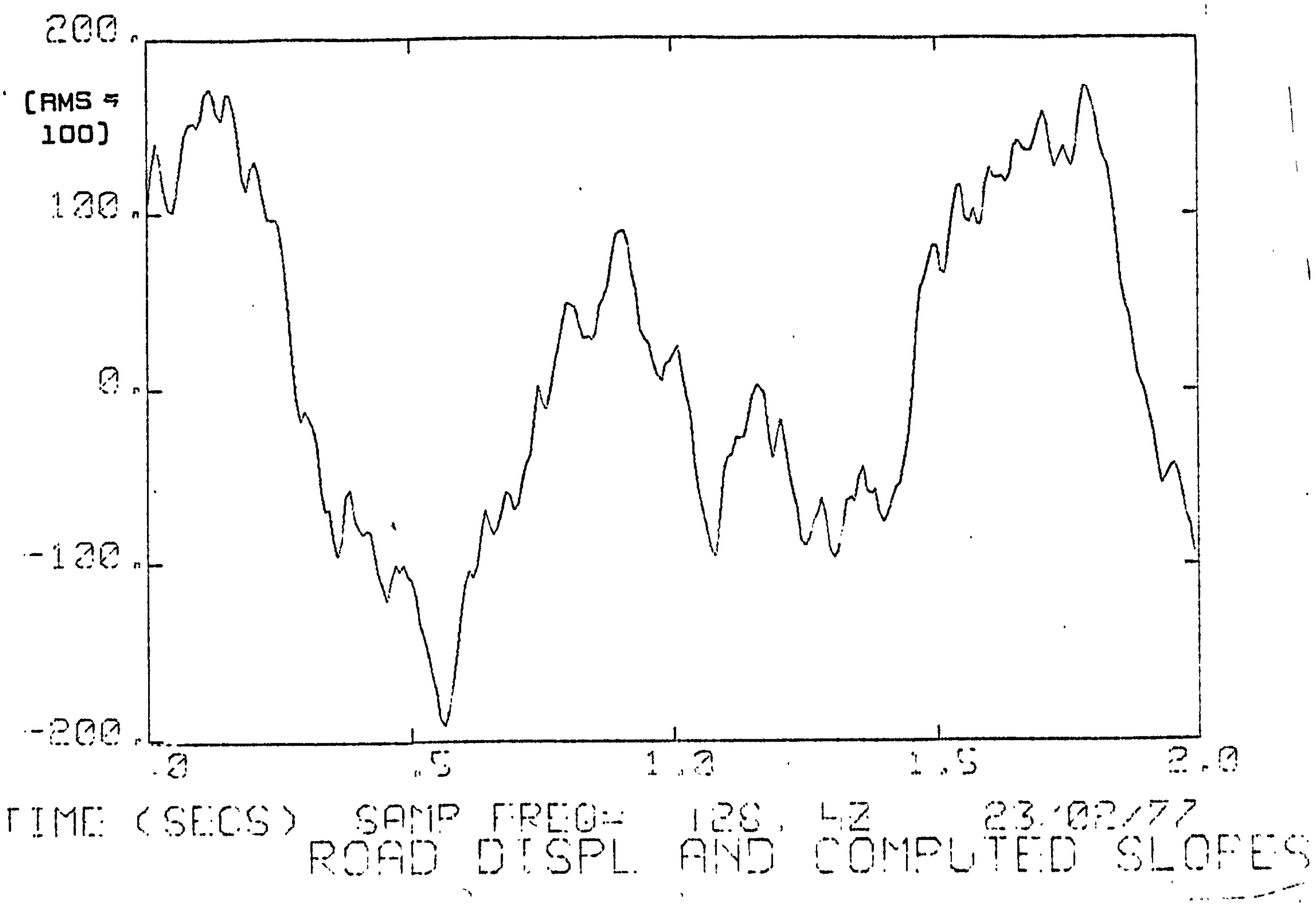

FIGURE B-1
TWO SECOND TIME FRAME ROAD PROFILE DISPLACEMENT

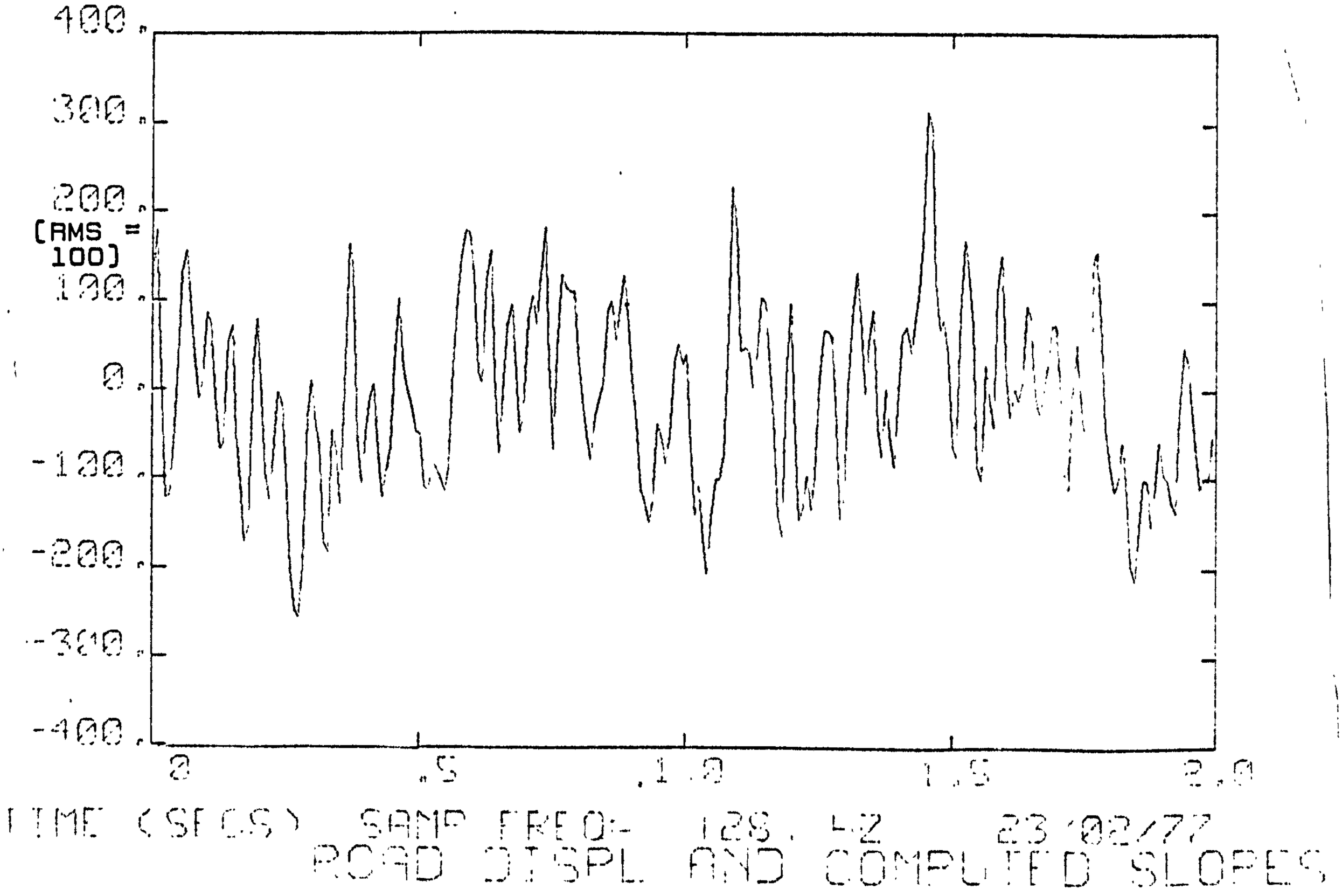

FIGURE B-2
CORRESPONDING COMPUTED DERIVATIVE (SLOPE/VELOCITY)

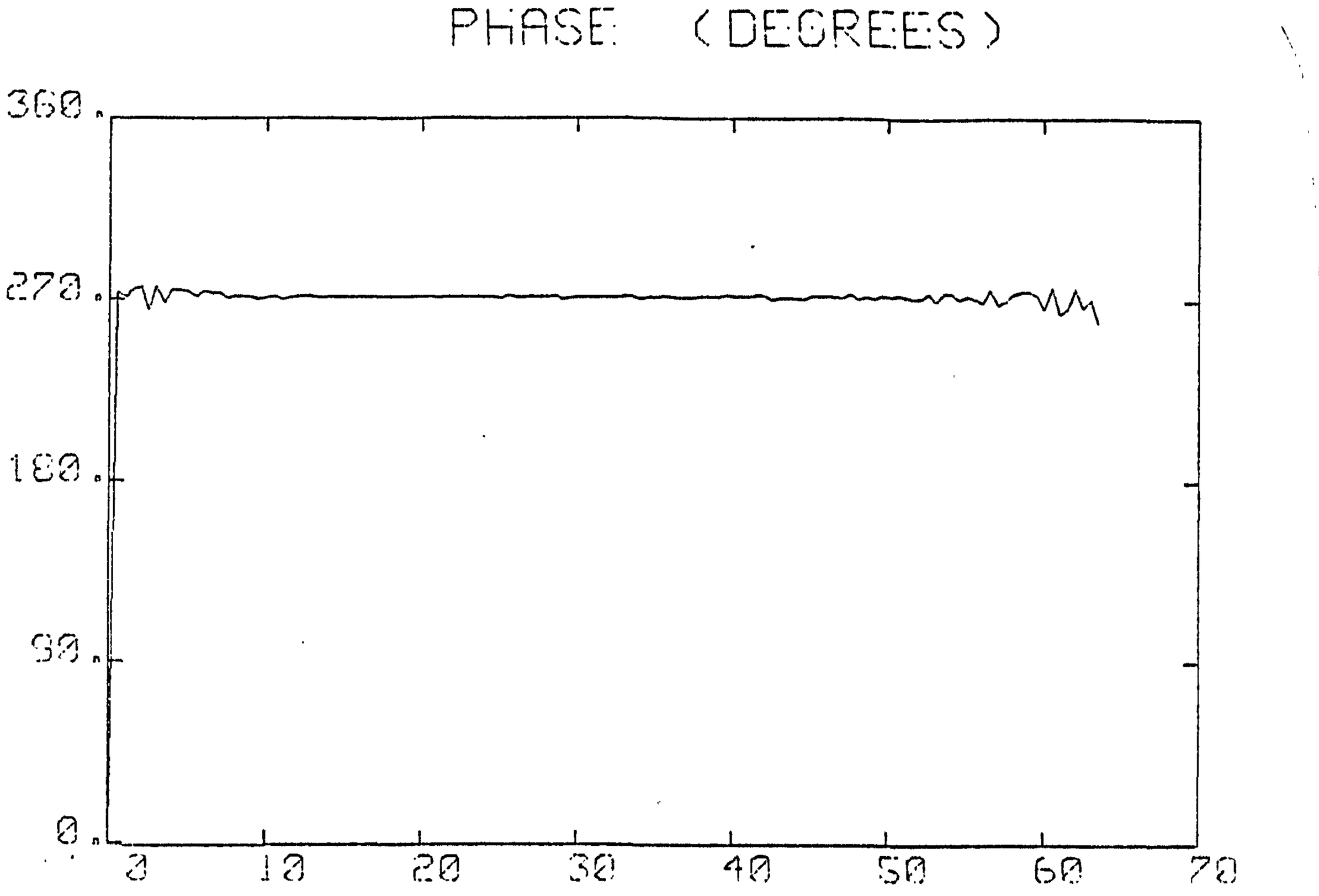

FIGURE B-3

PHASE RELATIONSHIP - DISPLACEMENT VS SLOPE

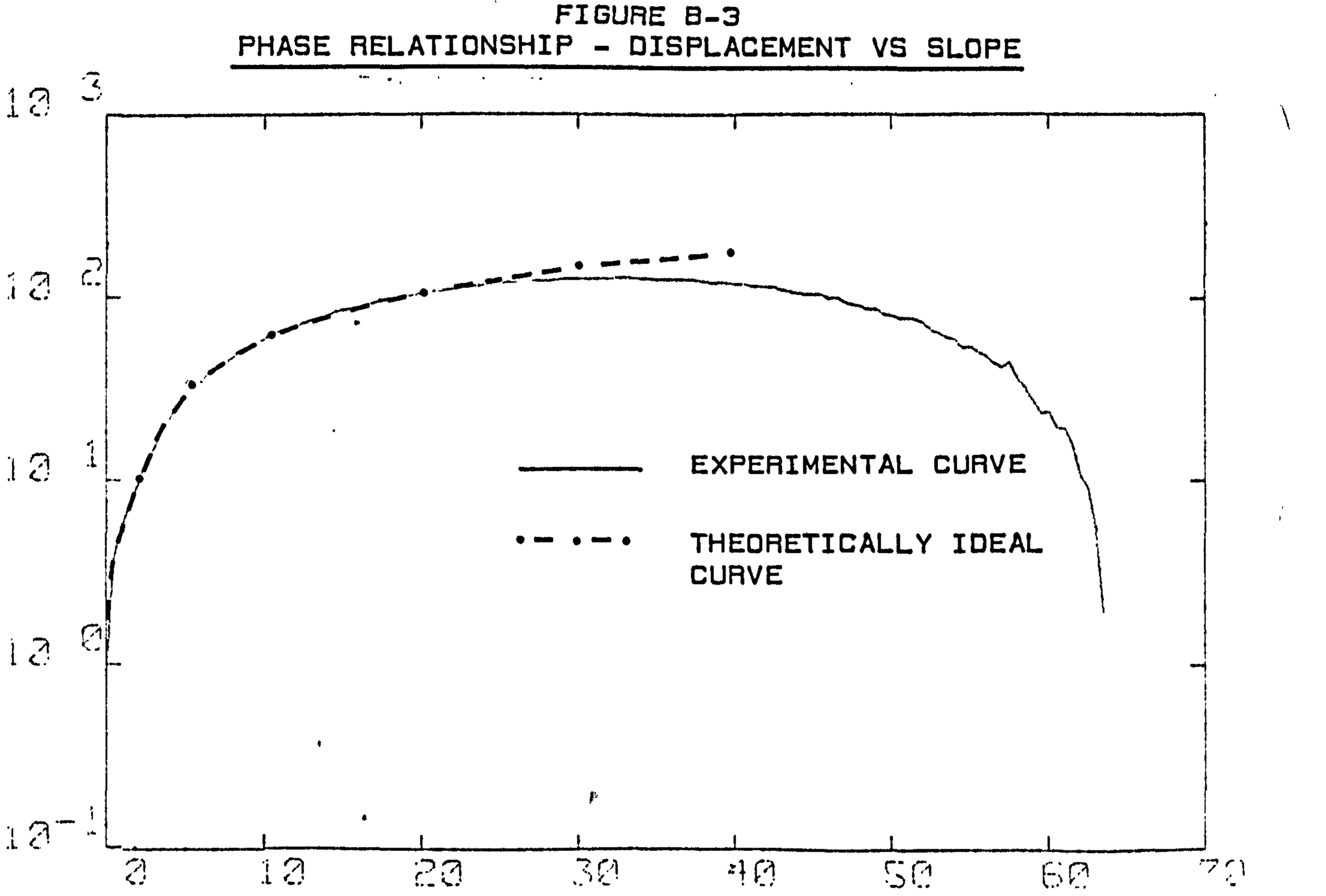

FIGURE B-4

FREQUENCY RESPONSE - DISPLACEMENT VS SLOPE

APPENDIX C

COMPUTATION OF EQUIVALENT LINEAR VISCOUS

DAMPING RATES FOR SINUSOIDAL EXCITATION

APPENDIX C

When vehicle dampers are subjected to discrete sinusoidal excitation their force velocity loops (see Figure C1 for example) can generally be represented by 4 separate linear portions as in plot 'A' of Figure C2. Four slopes C1-C4 which are each proportional to a damping factor (i.e. equivalent to F/V) and two 'blow-off' velocities V_C,V_R (in compression and rebound) characterise the plot.

It has been necessary to obtain an 'equivalent linear damping rate' for particular dampers from plots as above. This is conveniently done on the basis of equal energy dissipation per cycle. A linear damper will have a force velocity characteristic as in plot B of Figure C2 where the damping rate C_{EQ} is velocity <u>independent</u>. We therefore require a value C_{EQ} such that the energy disipated in cycling the damper through g-f-h-f-g is equal to that over the cycle c-b-a-d-e-d-a-b-c where V_{max} and V_{min} are maximum and minimum velocities attained in each case.

Computation of C_{EQ} may be obtained from C1, C2, C3, C4, V_C, V_R for a maximum velocity of V_{max} $(= -V_{min})$ as follows.

Consider one cycle of sinusoidal displacement as follows,

$$V = \frac{dx}{dt} = V_{max} \sin wt$$ where w is circular frequency

$$\Rightarrow dx = V_{max} \sin wt \, dt$$

Work done by the damper in time dt = Fdx

$$= FV_{max} \sin wt \, dt$$

where F is the damper force at time t.

For the <u>positive portion</u> of the cycle:-

$$t_1 = \frac{\sin^{-1}\frac{V_C}{V_M}}{w}$$

where t_1 is time at blow-off velocity since V_{max} $\sin wt_1 = V_C$

Force above blow-off $F[t] = C_1V_C + C_2[V-V_C]$

$= C_1V_M \sin wt_1 + C_2V_M [\sin wt - \sin wt_1]$

replacing V_{max} by V_M for convenience

Similarly, for the <u>negative portion</u>:-

$$t_2 = \frac{\sin^{-1}\frac{V_R}{V_M}}{w}$$

Force below blow-off $F[t] = C_3V_R + C_4[V-V_R]$

$= C_3V_M \sin wt_2 + V_MC_4 [\sin wt - \sin wt_2]$

Work done by damper in first half cycle is given by;

$$w_1 = 2\int_0^{t_1} C_1V_M^2 \sin^2 wt\, dt + 2\int_{t_1}^{\frac{\pi}{2w}} C_1V_M^2 \sin wt_1 \sin wt\, dt +$$

$$2\int_{t_1}^{\frac{\pi}{2w}} C_2V_M^2 \sin^2 wt\, dt - 2\int_{t_1}^{\frac{\pi}{2w}} C_2V_M^2 \sin wt_1 \sin wt\, dt$$

and in the second half cycle is given by;

$$w_2 = 2\int_0^{t_2} C_3 V_M^2 \sin^2 wt + 2\int_{t_2}^{\frac{\pi}{2w}} C_3 V_M^2 \sin wt_2 \sin wt\, dt +$$

$$2\int_{t_2}^{\frac{\pi}{2w}} C_4 V_M^2 \sin^2 wt\, dt - 2\int_{t_2}^{\frac{\pi}{2w}} C_4 V_M^2 \sin wt_2 \sin wt\, dt$$

It follows that;

$$w_1 = C_1 V_M^2 \left(t_1 + \frac{\sin^2 wt_1}{2w}\right) + C_2 V_M^2 \left(\frac{\pi}{2w} - t_1 - \frac{\sin 2\, wt_1}{2w}\right)$$

and $$w_2 = C_3 V_M^2 \left(t_2 + \frac{\sin 2\, wt_2}{2w}\right) + C_4 V_M^2 \left(\frac{\pi}{2w} - t_2 - \frac{\sin 2\, wt_2}{2w}\right)$$

Energy dissipated by linear damper $C_{EQ} = \dfrac{C_{EQ} V_M^2}{w}$

i.e. we require C_{EQ} such that

$$\frac{C_{EQ} V_M^2}{w} = w_1 + w_2$$

$$\text{i.e. } C_{EQ} = \frac{C_1}{\pi}\left[\sin^{-1}\left(\frac{VC}{VM}\right) + \frac{1}{2}\sin 2\left(\sin^{-1}\frac{VC}{VM}\right)\right] +$$

$$\frac{C_2}{\pi}\left[\frac{\pi}{2} - \sin^{-1}\left(\frac{VC}{VM}\right) - \frac{1}{2}\sin 2\left(\sin^{-1}\left(\frac{VC}{VM}\right)\right)\right] +$$

$$\frac{C_3}{\pi}\left[\sin^{-1}\left(\frac{VR}{VM}\right) + \frac{1}{2}\sin 2\left(\sin^{-1}\frac{VR}{VM}\right)\right] +$$

$$\frac{C_4}{\pi}\left[\frac{\pi}{2} - \sin^{-1}\left(\frac{VR}{VM}\right) - \frac{1}{2}\sin 2\left(\sin^{-1}\left(\frac{VR}{VM}\right)\right)\right]$$

Computer software which uses the above theory was developed to compute this equivalent damping. The programme requires C_1, C_2, C_3, C_4, V_C, V_R and the peak velocity V_M [or 2 x RMS] of the cycle. It will then output both the input data and the equivalent linear damping rate based on the peak velocity V_M.

Figure C-3 shows the peak force v peak velocity plots for a specific damper at two different strokes for sinusoidal excitation. This data was used on part of the exercise which attempted to relate the value of effective damping from the random testing with the sinusoidal results as discussed in Section 6.2.2.

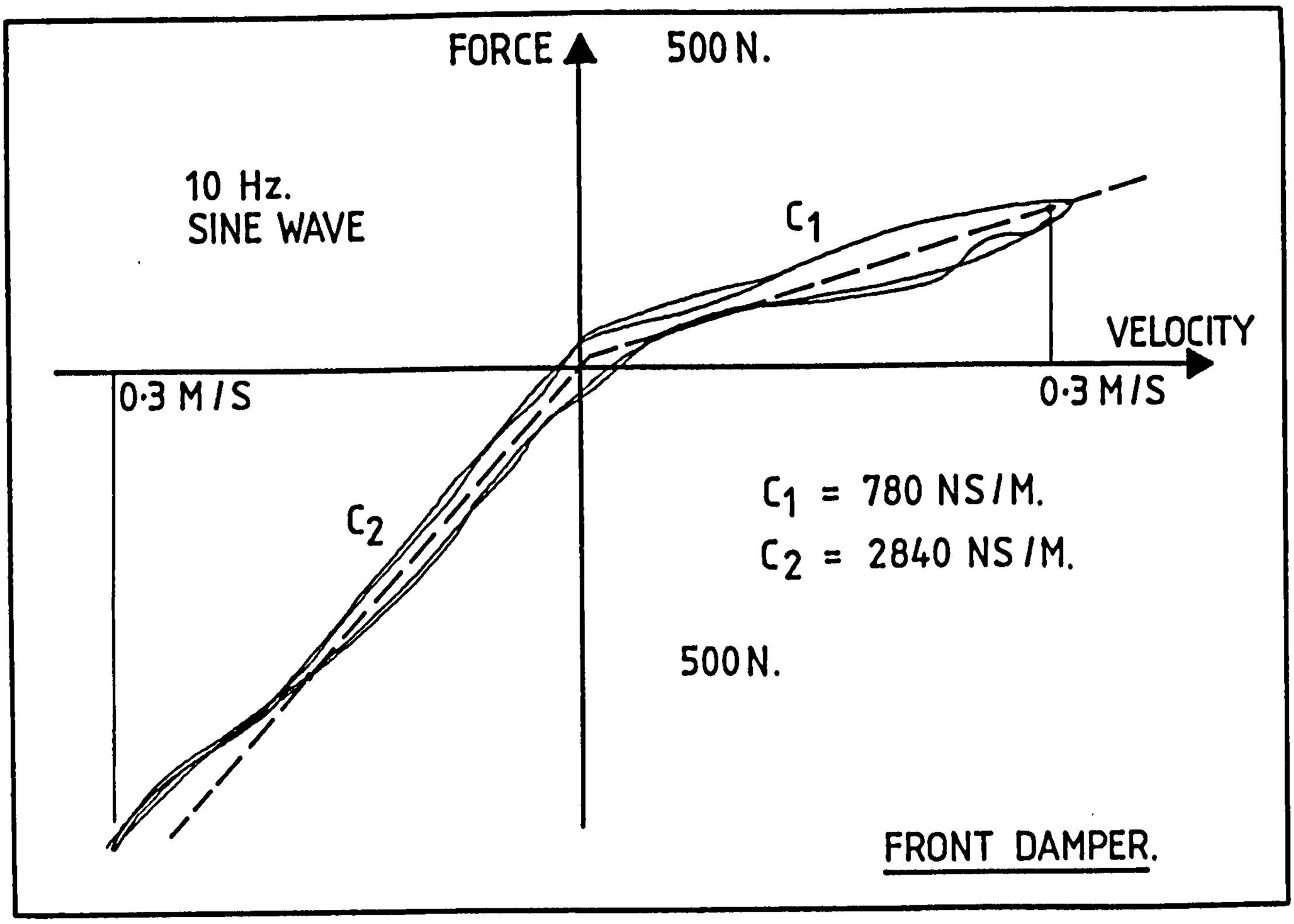

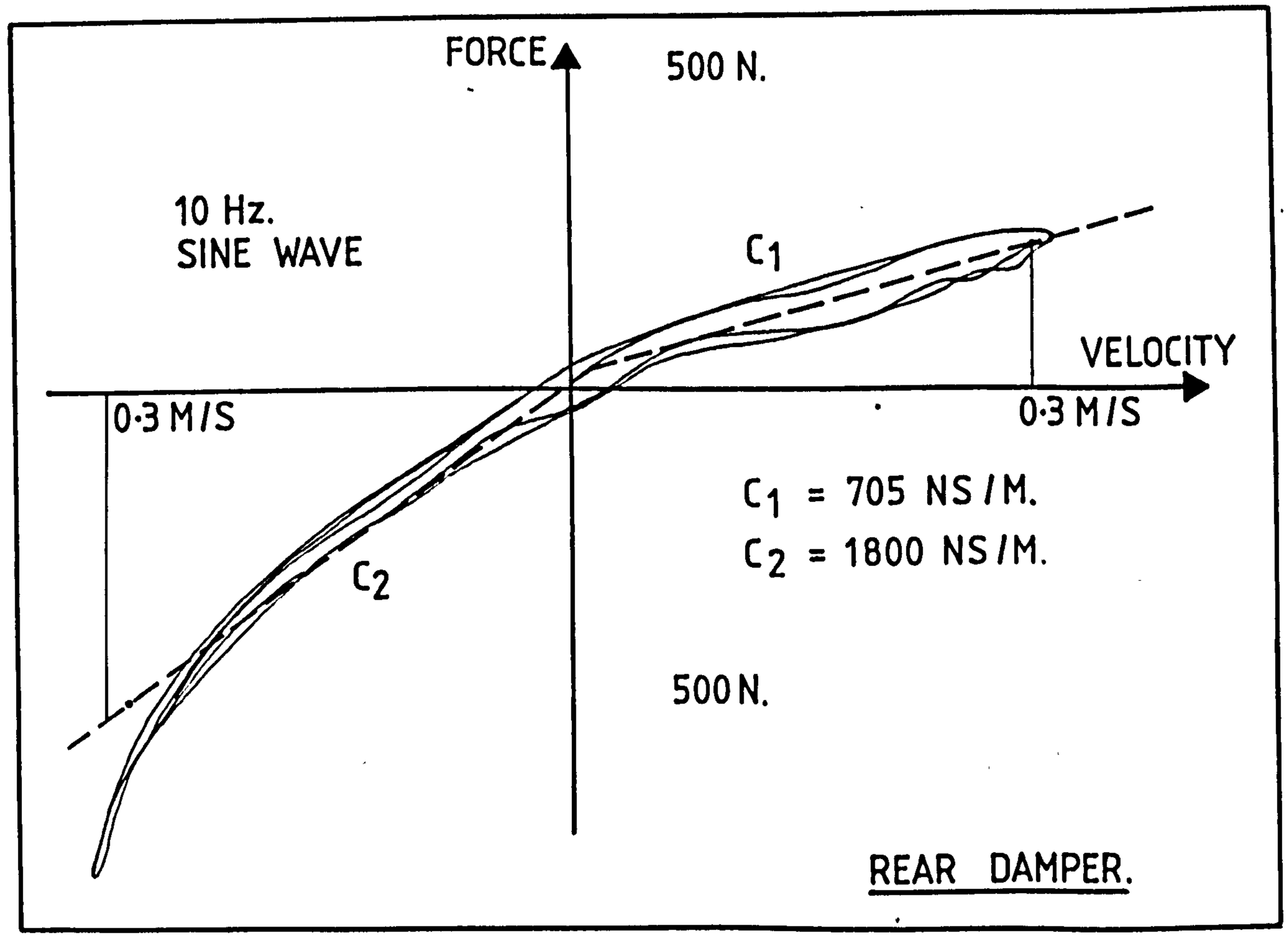

FIGURE C-1 MANUFACTURER – SUPPLIED FORCE – VELOCITY PLOTS. [VEHICLE 'B'].

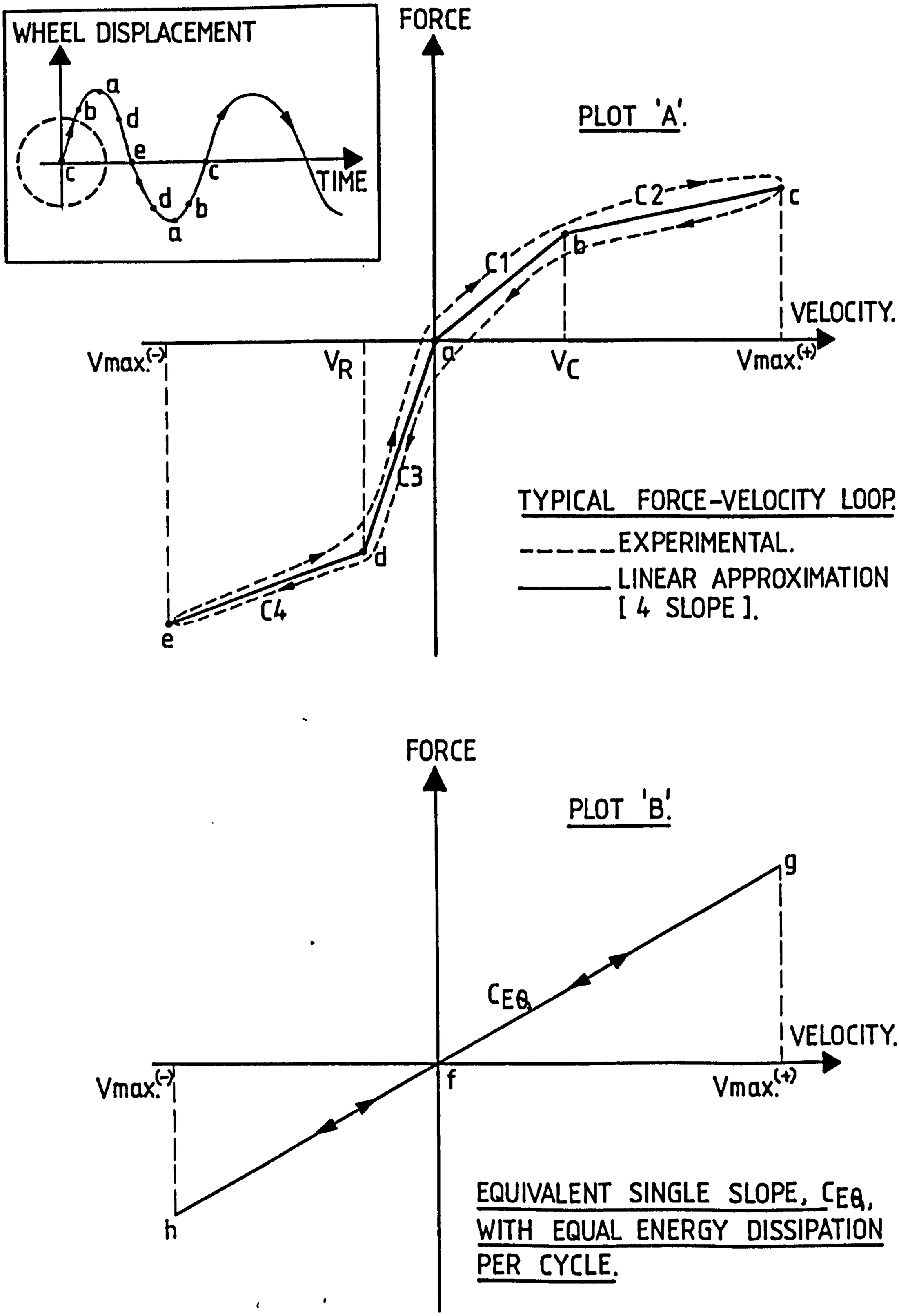

FIGURE C-2 SINUSOIDAL PERFORMANCE OF VEHICLE DAMPERS.

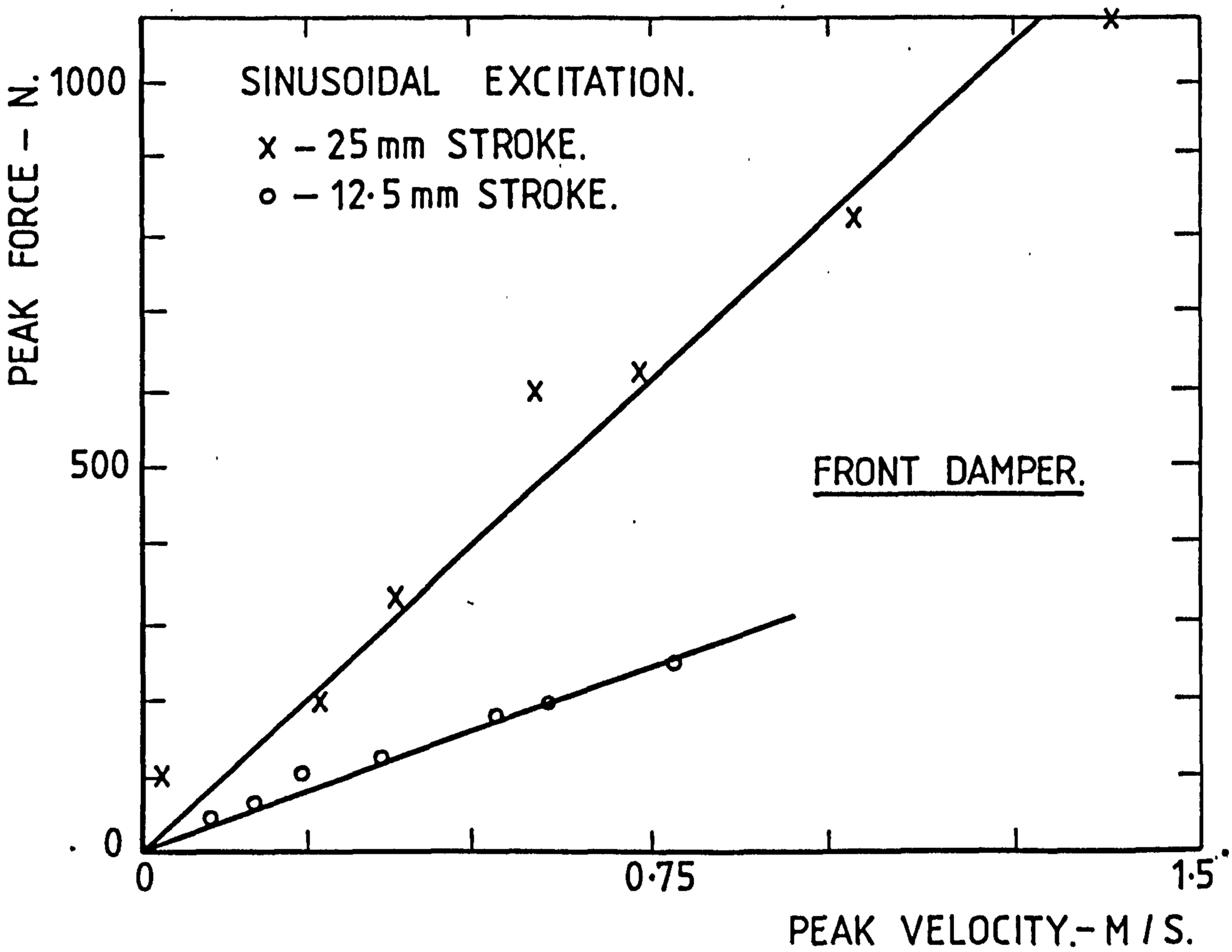

FIGURE C-3 DAMPER PEAK FORCE – VELOCITY DATA PLOTS [VEHICLE 'A'].

APPENDIX D

DESCRIPTION OF PROGRAMME 'MATRIX'

APPENDIX D

MATRIX - A PROGRAMME FOR CALCULATING RESONANCE FREQUENCIES AND MODE SHAPES OF FLEXURAL VIBRATIONS OF BEAM - TYPE STRUCTURES

The computer programme MATRIX exploys transfer matrix methods in the prediction of natural frequencies and corresponding mode shapes of beam - type structures. These structures can be supported in a variety of ways either by rigid supports or by a series of springs. The programme is specifically developed for truck chassis structures, although it may be extended to deal with a much wider range of structures. The following sections give a brief description of these matrix methods together with specific examples of known solution with which the programme was tested.

By considering a truck chassis to be a series of lumped masses connected by flexible beam elements and supported on springs representative of the truck suspension it will be possible to predict the various bending frequencies with the corresponding mode shapes. The information will enable the vehicle designer to avoid the problems which arise when frame bending frequencies coincide with those of the suspension or other components on the vehicle. One such problem which frequently arises is that of 'cab-nod'. It would seem that even a simple beam-on-springs analysis could help avoid these problems.

Very early in the development of new truck model such basic information as overall dimensions, chassis shape, engine type, etc. becomes available. It should be possible at this stage to predict the bending frequencies and mode shapes of the chassis enabling engine and cab mounts to be designed by indicating optimum stiffnesses and mounting positions thereby effectively 'tuning out' possible ride problems. By considering the chassis to be supported solely by the tire springs - i.e. with the suspension effectively locked - the frequently occurring motorway ride problems could be avoided.

Outline of the Theory of Matrix

For a detailed account of the theoretical background of transfer matrix methods reference should be made to [1]* but a brief description is given here for completeness.

The transfer matrix is a matrix which connects the STATE VECTORS at two points as a structure. Confining attention to beam structures the State Vector [Z] at a point is given by:-

$$[Z] = \begin{bmatrix} \omega \\ \psi \\ M \\ V \end{bmatrix} \quad \text{where} \quad \begin{aligned} \omega &= \text{transverse displacement} \\ \psi &= \text{transverse slope} \\ M &= \text{bending moment} \\ V &= \text{shear force} \end{aligned}$$

and thus defines the forces and displacements at the point. Consider the simple representation of a structure shown in Figure D1. The State Vectors $[z^0]$ and $[z^1]$ are related by a field matrix since points 0 and 1 are connected by a beam element. Field matrices are denoted [F]. The transfer matrix connecting the two ends of the mass M is known as a Point Matrix and referred to as $[P^M]$. The point matrix connecting the ends of the spring is denoted $[P^K]$. The vibration characteristics of the structure are defined by specification of the STATE EQUATION which relates the extreme ends of the structure in this case stations 0 and 2. It is simply written,

$$[z^2]_R = [P_2{}^K][F_2][P_2{}^M][F_1][z^0]_L$$

where R and L denote right and left.

Subroutines within MATRIX generate each transfer matrix given the system parameters - lengths, masses and stiffnesses. The state equation is input in numerical form by the user. Matrix recognises;

* Numbers in brackets indicate Appendix references.

$[F]$ by 1,
$[P^K]$ by 2, and
$[P^M]$ by 3

The above state equation is thus represented,

1,3,1,2

(i.e. starting with the lowest station number).

As a result of this convention the system parameters must be input in order, i.e. stiffness $(EI)_1$, mass M, stiffness $(EI)_2$ and spring stiffness k in this case. The state equation is now solved for a range of frequencies specified by the user. Specification of the boundary conditions is all that remains to complete the simulation. The programme computes a parameter DELTA (the determinant which on crossing zero is indicative a resonance frequence. This parameter is itself useful in determining whether or not a system has a natural frequency within some critical range. The values of circular frequency at which DELTA crosses zero are stored within the programme and the mode shapes which correspond to these frequencies are calculated. The programme outputs each resonance frequency and mode shape found within the user specified frequency interval.

Since for systems with a large number of elements the number of matrix multiplications is high, MATRIX has been written in double precision.

To illustrate the use of the programme, a simple test problem is given below.

2.3. Simple Beam Problems Solved by Matrix

Suppose it is required to predict the first bending mode of a simply supported continuous beam such as in Figure D2a. The exact solution is given by (2).

$$\omega_1 = 9.87\sqrt{\frac{EI}{M\ell^3}} \qquad (1)$$

where M, L, EI have the usual meaning.

The associated mode shape is a half sine wave. Consider the beam to be composed of 11 discrete masses each m, connected by beam elements of stiffness (EI) and length ℓ where

$$\sum m = M$$
$$\sum \ell = L$$

as in Figure D2b

Let m = 1, ℓ = 1 and EI = 1 for simplicity. It follows that M = 11, L = 12 and (EI) = 1 in equation (1).

The state equation for this beam is given by:-

$$[z^{12}] = F_{11}P_{10}{}^{M}F_{10}P_{10}{}^{M} \ldots P_{1}{}^{M}F_{1}[z^{0}]. \qquad (2)$$

The boundary conditions are again simply represented within MATRIX. In this case the conditions at stations 0 and 12 are ω = 0 and M = 0. i.e. the state vectors are:-

$$[z^{12}] = \begin{bmatrix} 0 \\ \psi \\ 0 \\ V \end{bmatrix}, \quad [z^{0}] = \begin{bmatrix} 0 \\ \psi \\ 0 \\ V \end{bmatrix}$$

The programme recognises these boundary conditions as 1,3,1,3 i.e. the zeros occur at positions (rows) 1 and 3 for stations 0 and 12 respectively. Had the beam been built in at the right-hand end the conditions would have been 1,3,1,2.

The input data (which must be in double precision where data is other than integer type) is as follows:-

Line 1 Title

2 12. Highest station number beginning with station 0

3 (EI)(J), L(J), J=1,12. System parameters in sequence

Line 4 0. Number of spring elements

5 -. Omitted if line 4 is 0. Parameters k_1, k_2

6 11. Number of masses

7 MASS[I], I=1,11. Masses in sequence

8 1.0, 3.0, 1.0, 3.0, ... etc. Representation of state equation

9 ω1, ω2, $\Delta\omega$ Minimum frequency, maximum frequency, interval.

10 Boundary conditions.

The output from MATRIX for the above case is given in Figure D3. The results for the built-in case (at both ends) where only the boundary conditions need to be altered are given in Figure D4.

Comparison of the predicted and exact values show good agreement (<5 per cent error) even for the small number of lumped masses considered. More accurate predictions may be made by merely increasing the number of masses.

It must be stressed that this simple test problem is not typical of the type of beam structure that can be analysed by MATRIX. The beams considered will in general be of variable mass distribution, variable stiffness along their length and be supported on springs of various stiffness.

REFERENCES

1 PESTEL AND LECKIE. Matrix methods in elastomechanics. McGraw Hill Inc. 1963.

2 BRUEL AND KJAER. Mechanical vibration and shock measurement. Bruel and Kjaer Technical Publication.

List of Figures

D 3 Matrix output - simply supported beam

D 4 Matrix output - built-in beam

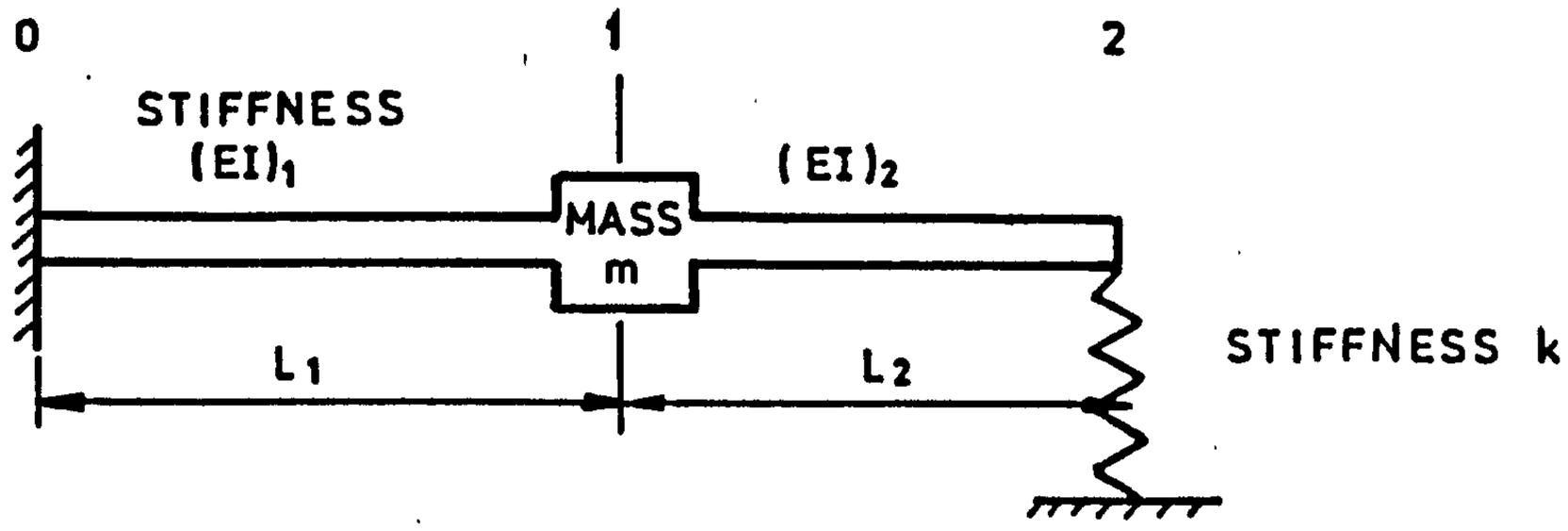

STATE EQUATION

$$[Z^2] = P_2^K F_2 P_1^M F_1 [Z^o]$$

STATE VECTOR AT STATION 0

$$[Z^o] = \begin{bmatrix} 0 \\ 0 \\ M \\ V \end{bmatrix}$$

STATE VECTOR AT STATION Z

$$[Z^2] = \begin{bmatrix} \omega \\ \psi \\ 0 \\ 0 \end{bmatrix}$$

FIGURE D-1

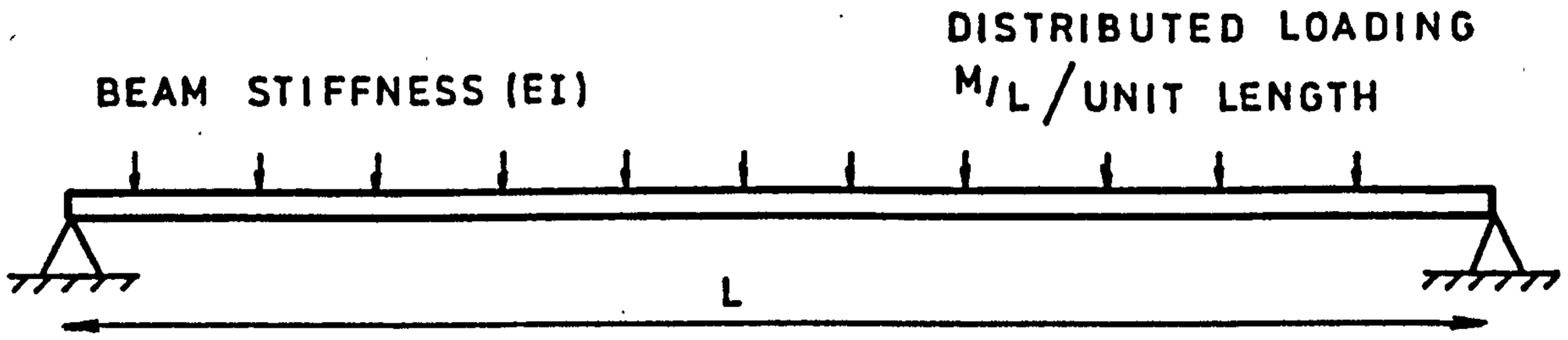

FIG 2a CONTINUOUS BEAM SIMPLY SUPPORTED

STATION NUMBER	0	1	2	3	4	5	6	7	8	9	10	11	12

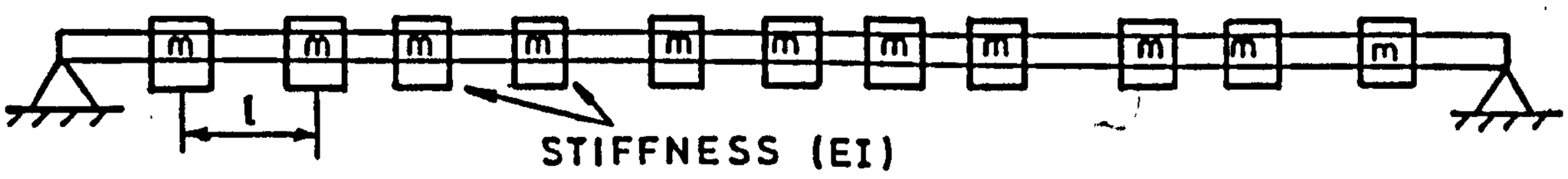

STATE EQUATION

$$[Z^{12}] = F_{11}\, P_{10}^{M}\, F_{10}\, P_{9}^{M} \text{ ----- } P_{1}^{M}\, F_{1}\, [Z^{0}]$$

STATE VECTOR AT STATION O

$$[Z^{0}] = \begin{bmatrix} 0 \\ \Psi \\ 0 \\ V \end{bmatrix}$$

STATE VECTOR AT STATION 12

$$[Z^{12}] = \begin{bmatrix} 0 \\ \Psi \\ 0 \\ V \end{bmatrix}$$

FIG 2b LUMPED 'MASS MODEL

FIGURE D 3

11 MASS REPRESENTN OF A SIMPLY SUPPORTED BEAM

IDENTIFICATION OF NATURAL FREQUENCIES AND MODE SHAPES
****

MODE SHAPE NUMBER 1

OCCURS AT A FREQUENCY OF .0636 RADIANS PER SEC.

EXACT SOLN = .072 RAD/SEC
ERROR = 4.7%

AMPLITUDE
1.4498+01
1.4498+01
2.8007+01
2.8007+01
3.9606+01
3.9606+01
4.8505+01
4.8505+01
5.4096+01
5.4096+01
5.5999+01
5.5999+01
5.4085+01
5.4085+01
4.8484+01
4.8484+01
3.9530+01
3.9530+01
2.7981+01
2.7981+01
1.4480+01
1.4480+01
-5.0873-09

NATURAL FREQUENCIES OCCUR WHEN DELTA CROSSES ZERO

EVALUATION OF DELTA FOR RANGE OF OMEGA

OMEGA	DELTA
.0630	-2.0750+00
.0631	-1.6906+00
.0632	-1.3059+00
.0633	-9.2076-01
.0634	-5.3526-01
.0635	-1.4940-01
.0636	2.3653-01
.0637	6.2343-01
.0638	1.0104+00
.0639	1.3977+00
.0640	1.7854+00

11 MASS REPRESENTN OF A BUILT IN BEAM

IDENTIFICATION OF NATURAL FREQUENCIES AND MODE SHAPES
****

MODE SHAPE NUMBER 1

OCCURS AT A FREQUENCY OF .1554 RADIANS PER SEC.

EXACT SOLN = .1624 RAD/SEC
ERROR = 4.3%

AMPLITUDE
1.1244+00
1.1244+00
3.8356+00
3.8356+00
7.1717+00
7.1717+00
1.0266+01
1.0266+01
1.2423+01
1.2423+01
1.3194+01
1.3194+01
1.2421+01
1.2421+01
1.0262+01
1.0262+01
7.1674+00
7.1674+00
3.8316+00
3.8316+00
1.1218+00
1.1218+00
-2.9008-06

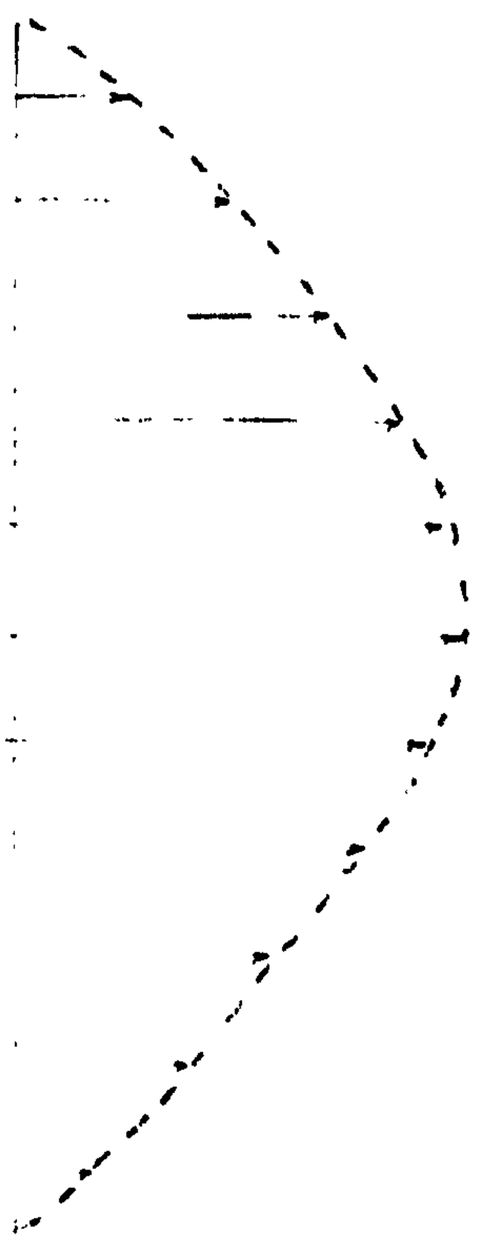

NATURAL FREQUENCIES OCCUR WHEN DELTA CROSSES ZERO

EVALUATION OF DELTA FOR RANGE OF OMEGA

OMEGA	DELTA
.1550	-6.6691+00
.1551	-4.8529+00
.1552	-3.0366+00
.1553	-1.2136+00
.1554	5.9624-01
.1555	2.4156+00
.1556	4.2339+00
.1557	6.0513+00
.1558	7.8691+00
.1559	9.6880+00
.1560	1.1506+01

FIGURE D 4

APPENDIX E

CENTRES OF OSCILLATION

APPENDIX E

CENTRES OF OSCILLATION

The rigid body modes of a passenger car or an articulated vehicle (neglecting the trailer mode) can be represented by a 2 degree of freedom system. Consider Figure E1 which illustrates the locations of the bounce and pitch centres for a particular spring configuration. Some general points are worth noting.

a) The bounce and pitch centres are always on opposite sides of the centre of gravity of the laden tractor.

b) The pitch centre is always on the same side of the centre of gravity as the spring with the greatest static deflection.

c) The longitudinal motion in the cab increases as the pitch centre moves forward of the centre of gravity.

d) It is desirable to have the largest static deflection at the front of the tractor so that the pitch centre is forward of the centre of gravity. The front deflection should not be much larger than the rear otherwise the pitch centre will be far forward of the centre of gravity and will result in longitudinal motions in the cab.

e) The result of having a greater static deflection at the rear of the tractor is that the pitch centre will then be behind the centre of gravity and the pitch frequency will increase markedly.

The importance of these centres of oscillation is shown in Figure E 2 where the effects of gradually increasing a very soft tractor front spring to the stage where it becomes much stiffer than the rear spring are illustrated.

Figure E 2[a]: Here the static deflection of the front spring is much greater than the rear. The bounce centre - associated with maximum deflection of the front spring - will lie close to the rear of the tractor frame and may be outside it. The pitch centre will be on the same side of the centre of gravity as the front spring and will be between the centre of gravity and the front spring.

Figure E 2[b]: As the front spring is progressively stiffened the bounce centre will move further to the rear of the tractor and the pitch centre will move rearwards towards the centre of gravity. When the static deflections are equal the bounce and pitch modes will be uncoupled i.e. the tractor will bounce with no associated pitch motion and vice versa. At this point the bounce centre will be at an infinite distance behind the tractor and the pitch centre will be at the centre of gravity.

At this point the bounce and pitch frequencies will be closest together.

Figure E 2[c]: Further increases in the front spring stiffness will result in the bounce centre moving instantaneously from an infinite distance behind the tractor to a corresponding position ahead of the tractor. With further increases in front spring stiffness the bounce centre centre will move rearwards from the centre of gravity.

Two factors will affect ride comfort levels in the vehicle cab:-

i) The frequency of oscillation

In the rigid body mode range it is generally true that the greater the frequency the greater the discomfort. It is desirable to keep the rigid body frequencies low.

ii) The oscillation centre location

Where the centre of oscillation is at a large distance from the vehicle cab, the cab motion will be mostly vertical. As the centre comes nearer the cab an increasing proportion of the cab motion will be longitudinal. Where the centre is directly below the cab centre of gravity the resulting cab motion will be almost totally longitudinal.

It is therefore important to be aware of the effects of any spring stiffness change on bounce and pitch centre location from the viewpoint of ride comfort.

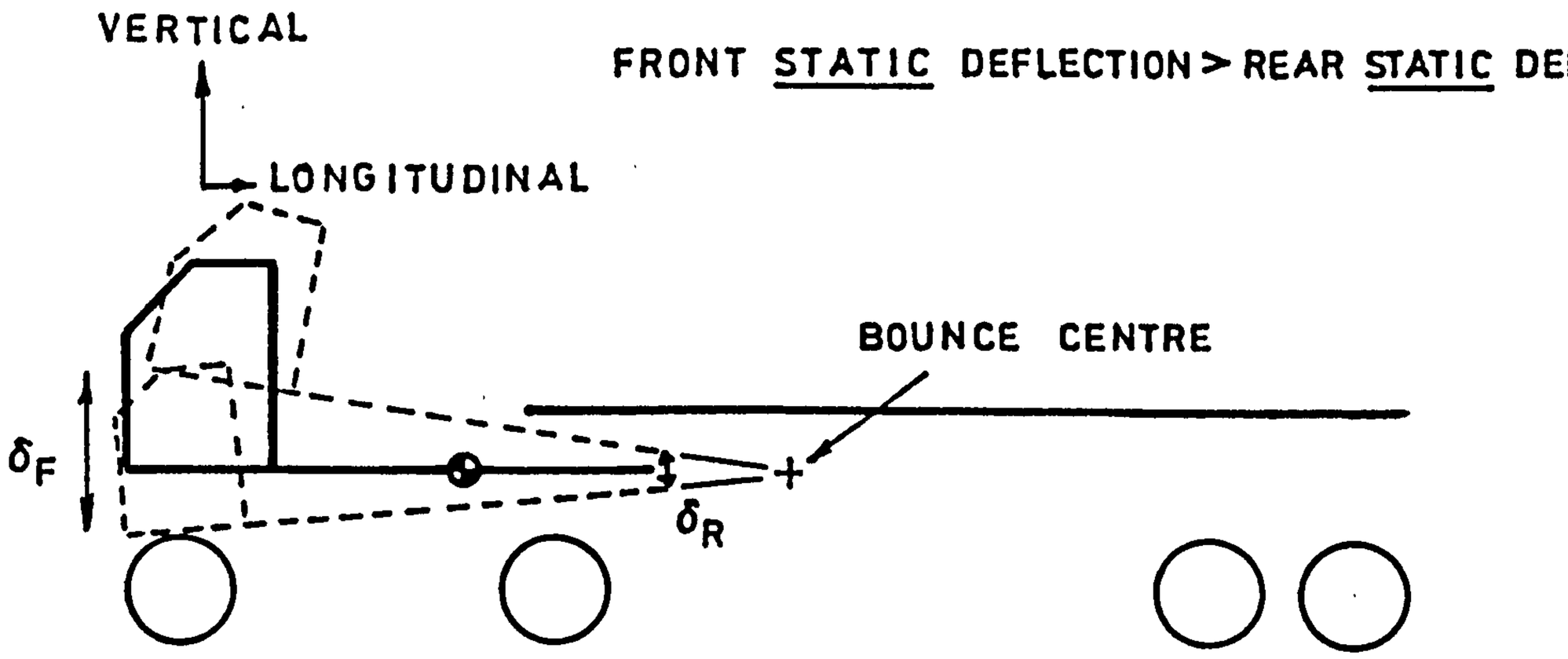

BOUNCE MODE

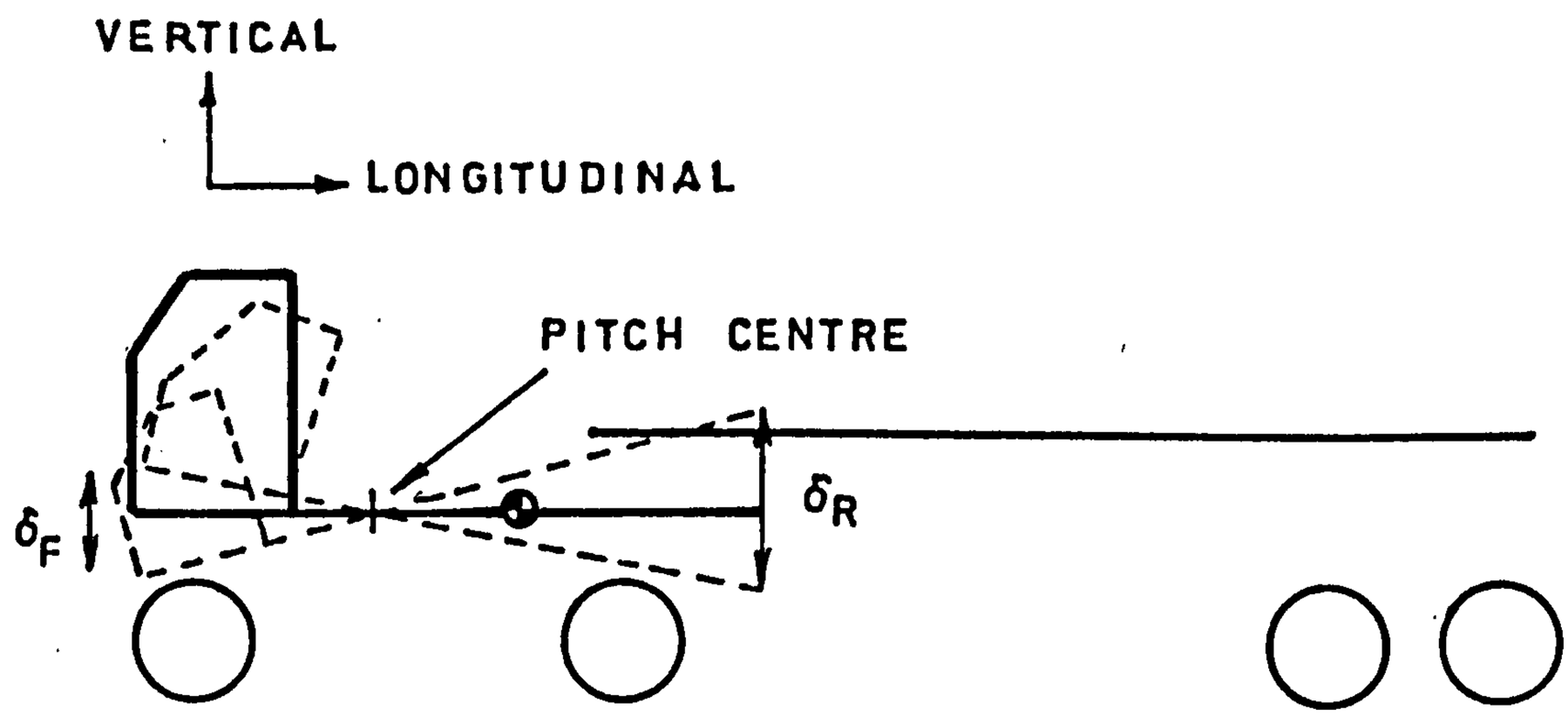

PITCH MODE

FIG E-1 ILLUSTRATION OF CENTRES OF OSCILLATION

(a) FRONT STATIC DEFLECTION > REAR

BOUNCE AND PITCH MOTIONS UNCOUPLED

(b) FRONT STATIC DEFLECTION = REAR

(c) FRONT STATIC DEFLECTION < REAR

FIG E.2 EFFECT OF VARIOUS STATIC DEFLECTION RATIOS ON BOUNCE AND PITCH CENTRE LOCATION

APPENDIX F

63 DOF ARTICULATED VEHICLE MODEL PARAMETERS

APPENDIX F

63 DOF ARTICULATED VEHICLE MODEL PARAMETERS

1 Degrees of freedom	
Number	Description
1-27	Tractor frame masses (19th mass includes trailer coupling mass for T45)
28-53	Trailer frame masses (3rd trailer mass excluded)
54	Tractor front axle vertical
55	Tractor rear axle vertical
56	Trailer front axle vertical
57	Trailer rear axle vertical
58, 59, 62	Cab centre of gravity vertical, pitch longitudinal
60, 61, 63	Engine centre of gravity vertical, pitch longitudinal

2 Masses and inertias	
Variable name	Description
Mass (1)-mass (63)	Masses and inertias numbered sequentially and relate to degree of freedom eg mass (61) = engine pitch inertia

3 Stiffness	
Flexural stiffness	Description
A (1)-A (25)	$(EI)/h^3$ values for tractor beam elements
AT (1)-AT (25)	$(EI)/h^3$ values for trailer beam elements
Spring stiffness	
KF, KR	Front and rear tractor suspension spring stiffness (per side)
KTF, KTR	Front and rear tractor tyre stiffness
KTA	Trailer spring stiffness (per side per axle)
KTTR	Trailer tyre stiffness
KFC, KLFC	Cab front mount vertical and longitudinal stiffness (each)
KRC, KLRC	Cab rear mount vertical and longitudinal stiffness
KFE, KLFE KRE, KLRE	As above for engine mounts

4 Dimensions	
Variable	Description
C1, C2	Cab centre of gravity to front and rear mounts respectively in longitudinal direction
D1, D2.	Cab cente of gravity to front and rear mounts in vertical direction
E1, E2	Engine centre of gravity to front and rear mounts in longitudinal direction
F1, F2	Engine centre of gravity to front and rear mounts in vertical direction
SPAC1, SPAC2	Tractor and trailer beam element lengths respectively

APPENDIX F [CONTD]

LISTING OF MATRIX FILL SUBROUTINE

```
C
C.....................................................
 C
C          THIS SUBROUTINE SETS UP THE STIFFNESS MATRIX OF A 2-D
C
C          63 DEGREE OF FREEDOM MODEL OF AN ARTICULATED VEHICLE.
C
C          BOTH TRACTOR AND TRAILER ARE INCLUDED.
C
C          THE MATRIX IS SYMMETRIC THE UPPER TRIANGLE BEING FIRST
C
C            FILLED AND THEN FOLDED.
C
C.....................................................
C
C
      SUBROUTINE FILL (D)
      DOUBLE PRECISION D(63,63)
      INCLUDE COM
C
C
C        START TRACTOR FRAME ELEMENT COMPUTATION
C
C        SET UP NON-ROUTINE TRACTOR FRAME ELEMENT ENTRIES
C
C        INCLUDING  COUPLING TERMS.
C
      D(1,1)=A(1)
      D(1,2)=-2.*A(1)
      D(1,2)=A(1)
      D(2,2)=4.*A(1)+A(2)+2.*KFC
      D(2,3)=-2.*(A(1)+A(2))
      D(2,4)=A(2)
      D(2,58)=-2.*KFC
      D(2,59)=2.*C1*KFC
      D(3,3)=A(1)+4.*A(2)+A(3)+KF
      D(3,4)=-2.*(A(2)+A(3))
      D(3,5)=A(3)
      D(3,54)=-KF
C
C
C          SET UP ROUTINE TRACTOR FRAME ELEMENT ENTRIES
C
C
C
      DO 10 I=4,25
      D(I,I)=A(I-2)+4.*A(I-1)+A(I)
      D(I,I+1)=-2.*(A(I-1)+A(I))
10    D(I,I+2)=A(I)
C
C
C          ADD COUPLING TERMS
```

```
C
      D(4,4)=D(4,4)+2.*KFE
      D(4,60)=-2.*KFE
      D(4,61)=2.*E1*KFE
      D(10,10)=D(10,10)+2.*KRC
      D(10,58)=-2.*KRC
      D(10,59)=-2.*C2*KRC
      D(11,11)=D(11,11)+2.*KRE
      D(11,60)=-2.*KRE
      D(11,61)=-2.*E2*KRE
      D(12,12)=D(12,12)+KF
      D(12,54)=-KF
      D(18,18)=D(18,18)+KR
      D(18,55)=-KR
C
C
C        ROW 19 CONTAINS TRACTOR - TRAILER COUPLING TERMS
C
C
      D(19,19)=D(19,19)+AT(1)+4.*AT(2)+AT(3)
      D(19,28)=AT(1)
      D(19,29)=-2.*(AT(1)+AT(2))
      D(19,30)=-2.*(AT(2)+AT(3))
      D(19,21)=AT(3)
      D(25,25)=D(25,25)+KR
      D(25,55)=-KR
      D(26,26)=A(24)+4.*A(25)
      D(26,27)=-2.*A(25)
      D(27,27)=A(25)
C
C
C        START TRAILER FRAME ELEMENT ENTRIES
C
C        SET UP NON-ROUTINE TRAILER FRAME ELEMENT ENTRIES
C
C
      D(28,28)=AT(1)
      D(28,29)=-2.*AT(1)
      D(29,29)=4.*AT(1)+AT(2)
      D(29,30)=AT(2)
C
C
C        SET UP ROUTINE TRAILER FRAME ELEMENT ENTRIES
C
C
      DO 20 J=30,51
      JJ=J-27
      D(J,J)=AT(JJ-1)+4.*AT(JJ)+AT(JJ+1)
      D(J,J+1)=-2.*(AT(JJ)+AT(JJ+1))
20    D(J,J+2)=AT(JJ+1)
C
C
C          ADD COUPLING TERMS
C
C
```

```
C
      D(45,45)=D(45,45)+2.*KTA
      D(45,56)=-2.*KTA
      D(49,49)=D(49,49)+2.*KTA
      D(49,57)=-2.*KTA
      D(52,52)=AT(24)+4.*AT(25)
      D(52,53)=-2.*AT(25)
      D(53,53)=AT(25)
      D(54,54)=2.*(KTF+KF)
      D(55,55)=2.*(KTR+KR)
      D(56,56)=2.*(KTTR+KTA)
      D(57,57)=2.*(KTTR+KTA)
      D(58,58)=2.*(KFC+KRC)
      D(58,59)=-2.*C1*KFC+2.*C2*KRC
      D(59,59)=2.*(C2**2*KRC+C1**2*KFC)+2.*(D1**2*KLFC+D2**2*KLRC)
      D(59,62)=-2.*(D1*KLFC+D2*KLRC)
      D(60,60)=2.*(KFE+KRE)
      D(60,61)=-2.*E1*KFE+2.*E2*KRE
      D(61,61)=2.*(E2**2*KRE
     +                    +E1**2*KFE)+2.*(F1**2*KLFE+F2**2*KLRE)
      D(61,63)=-2.*(F1*KLFE+F2*KLRE)
      D(62,62)=2.*(KLFC+KLRC)
      D(63,63)=2.*(KLFE+KLRE)
C
C
C        END FILL UPPER TRIANGLE OF MATRIX
C
C        FOLD UPPER TRIANGLE OF MATRIX
C
C
      DO 30 I=1,63
      DO 30 J=1,63
30    IF (J.LT.I) D(I,J)=D(J,I)
      RETURN
C
      END
```

APPENDIX G

CENTRAL DIFFERENCE FORMULAE

APPENDIX G

CENTRAL DIFFERENCE FORMULAE

Consider a function $Y = \phi[x]$ of which A, B and C are three points with co-ordinates:-

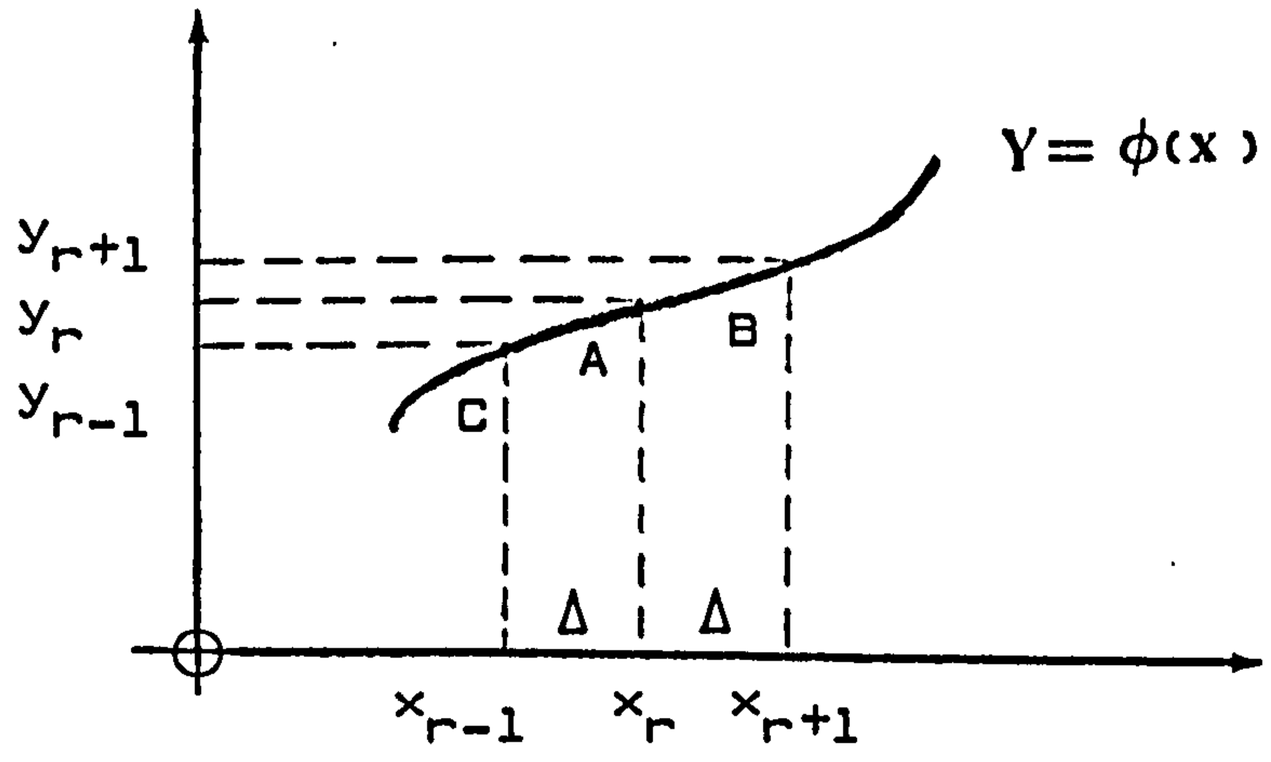

$A[x_r, y_r]$, $B[_{r+1}, y_{r+1}]$, $C[x_{r-1}, y_{r-1}]$

If the points A, B and C are sufficiently close together such that Δ is small relative to the shape of the curve $\phi[x]$ in this region, we can approximate:-

$$\left.\begin{aligned} \phi[x] &= \alpha x^2 + \beta x + \gamma \quad \alpha, \beta \text{ and } \gamma \text{ constants} \\ \Rightarrow y_{r-1} &= \alpha[x_r - \Delta]^2 + \beta[x_r - \Delta] + \gamma \\ \Rightarrow y_r &= \alpha x_r^2 + \beta x_r + \gamma \\ \Rightarrow y_{r+1} &= \alpha[x_r + \Delta]^2 + \beta[x_r + \Delta] + \gamma \end{aligned}\right] \quad [1]$$

Solving equation [A.1] yields:-

$$\alpha = \frac{1}{2\Delta^2}\,[y_{r-1} - 2y_r + y_{r+1}] \qquad [2]$$

$$\beta = \frac{1}{2\Delta^2}\{[\Delta - 2x_r]y_{r+1} + 4x_r y_r - [2x_r + \Delta]Y_{r-1}\}$$

for small Δ :-

$$\left[\frac{dy}{dx}\right]_r \doteqdot \left[\frac{d\,\phi[x]}{dx}\right]_r = \phi'[x]_r = 2\alpha x_r + \beta$$

and

$$\left[\frac{d^2y}{dx^2}\right]_r = \phi''(x)_r = 2\alpha$$

From equation (A.2)

$$\Rightarrow \left[\frac{dy}{dx}\right] \doteqdot \frac{1}{2\Delta}\,(Y_{r+1} - Y_{r-1}) \qquad (3)$$

$$\Rightarrow \left[\frac{d^2y}{dx^2}\right] = \frac{1}{\Delta^2}\,(Y_{r-1} - 2Y_r + Y_{r+1})$$

Equations (3) are the central difference approximations of the first two derivatives of $\phi(x)$.

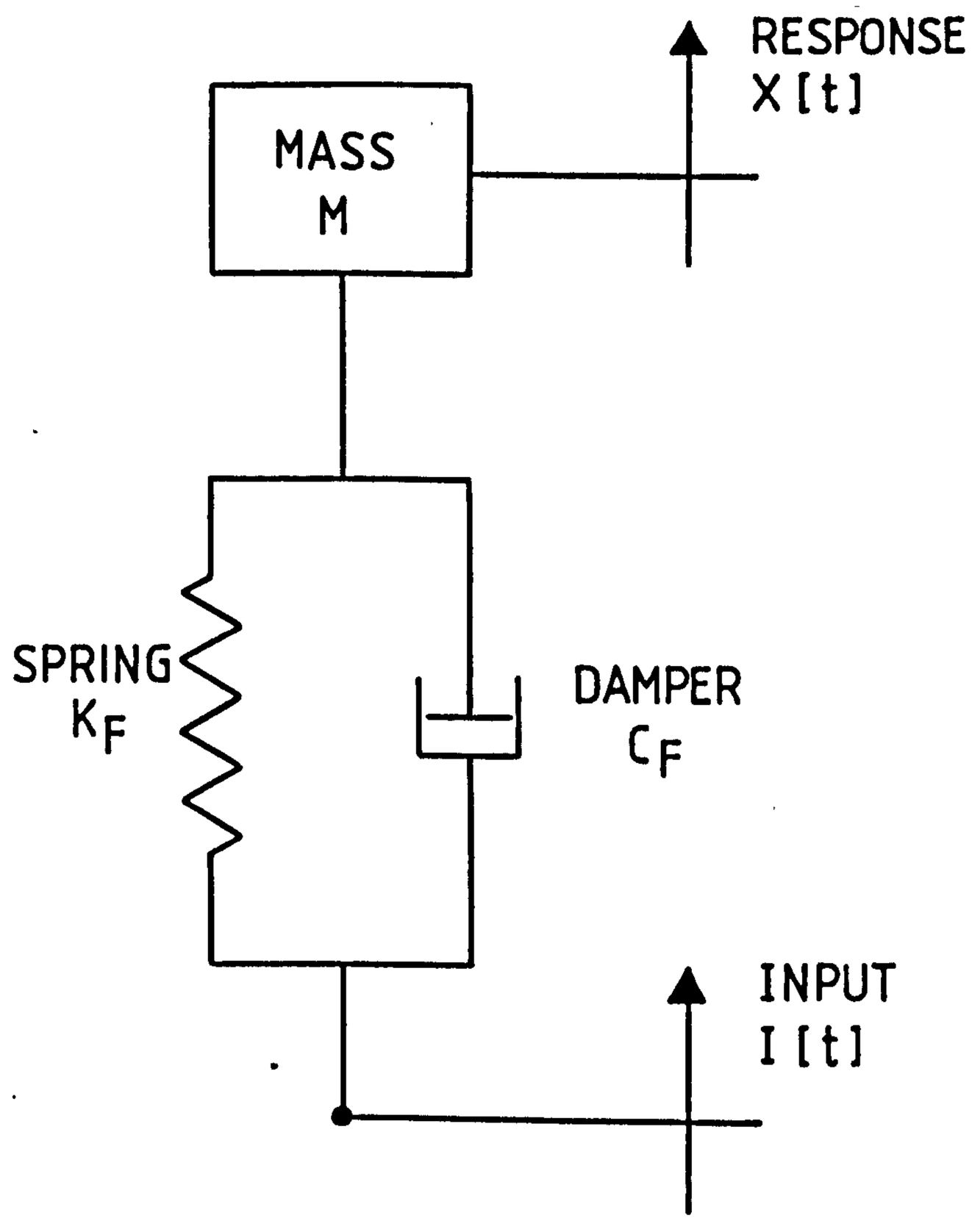

FIGURE 1. SIMPLIFIED VEHICLE MODEL.

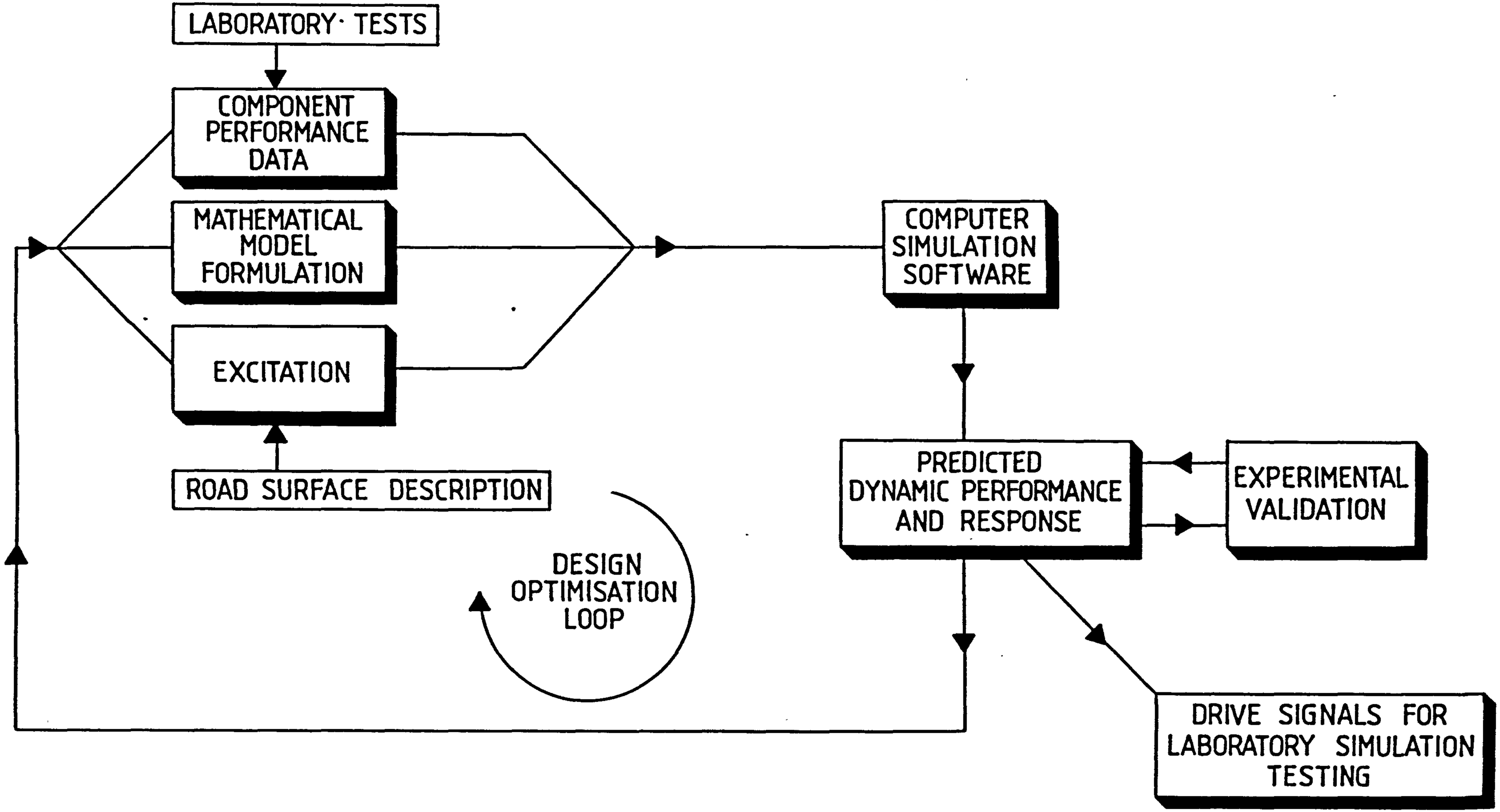

FIGURE 2. DESIGN OPTIMISATION FOR RIDE AND VIBRATION.

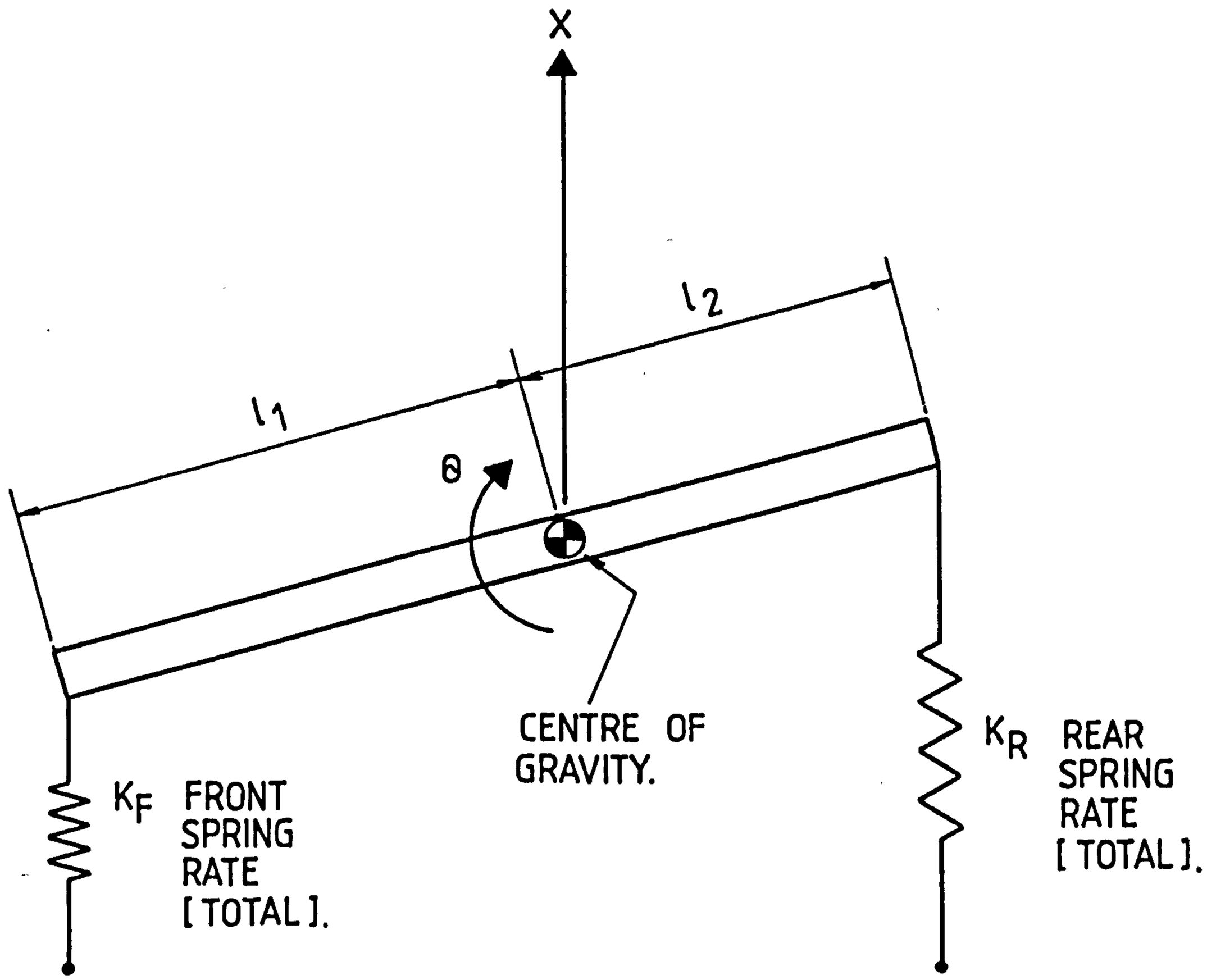

FIGURE 3. 2 DEGREE OF FREEDOM PRIMARY RIDE FREQUENCY MODEL.

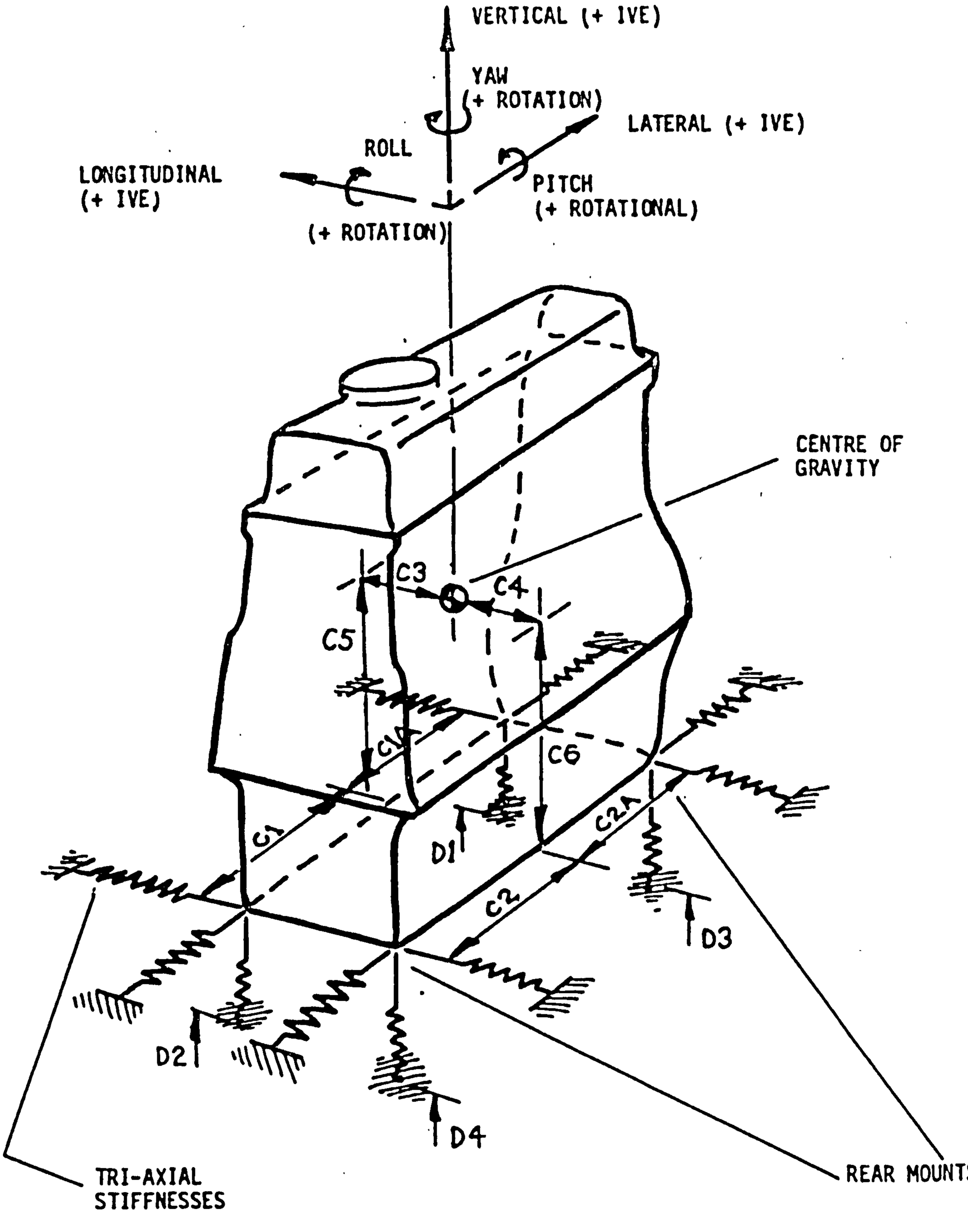

DAMPING IN MOUNTS NOT SHOWN

FIGURE 4

6 DEGREE OF FREEDOM ENGINE MODEL SCHEMATIC

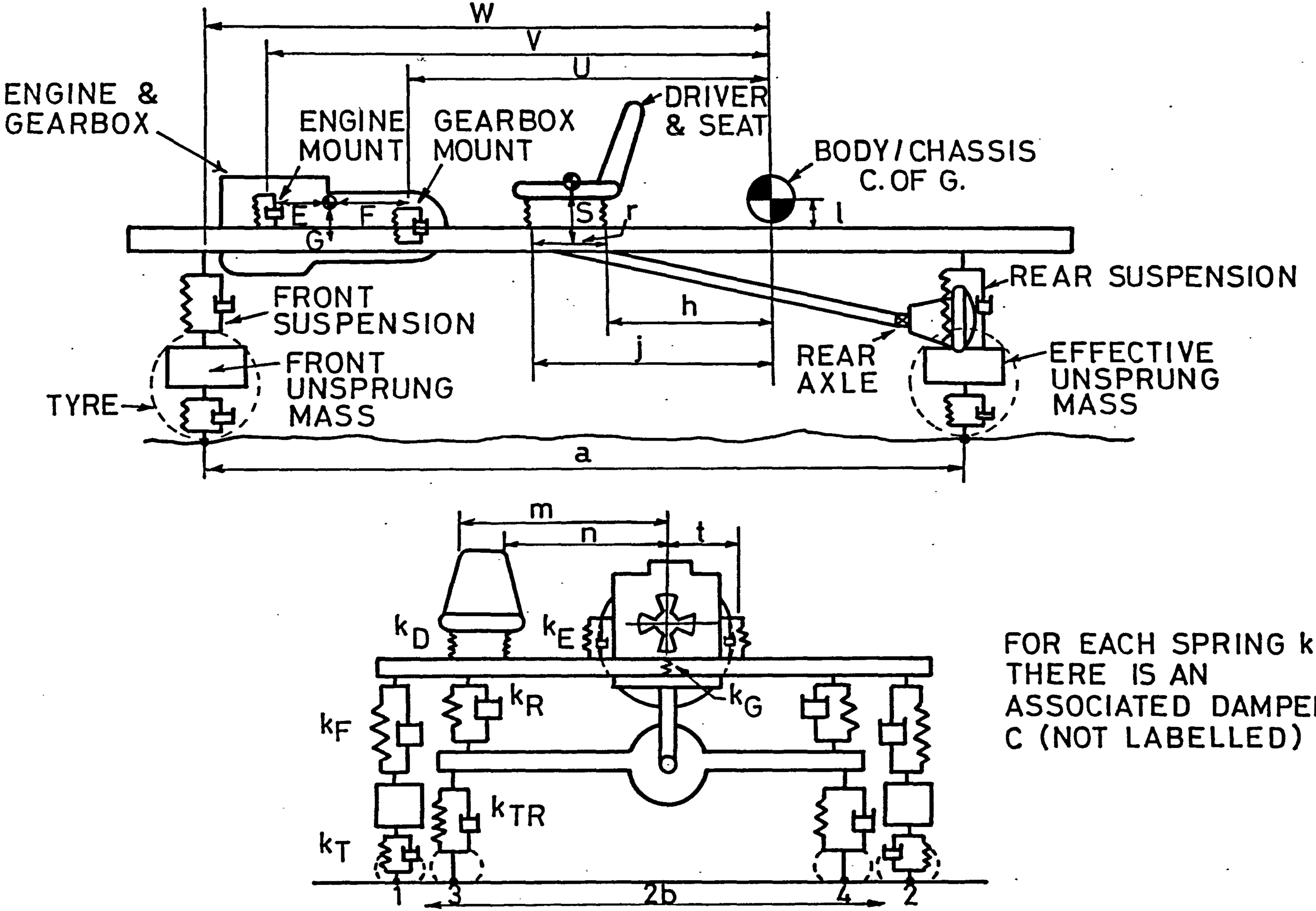

FOR EACH SPRING k
THERE IS AN
ASSOCIATED DAMPER
C (NOT LABELLED)

FIGURE 5. MULTI DEGREE OF FREEDOM RIDE MODEL.

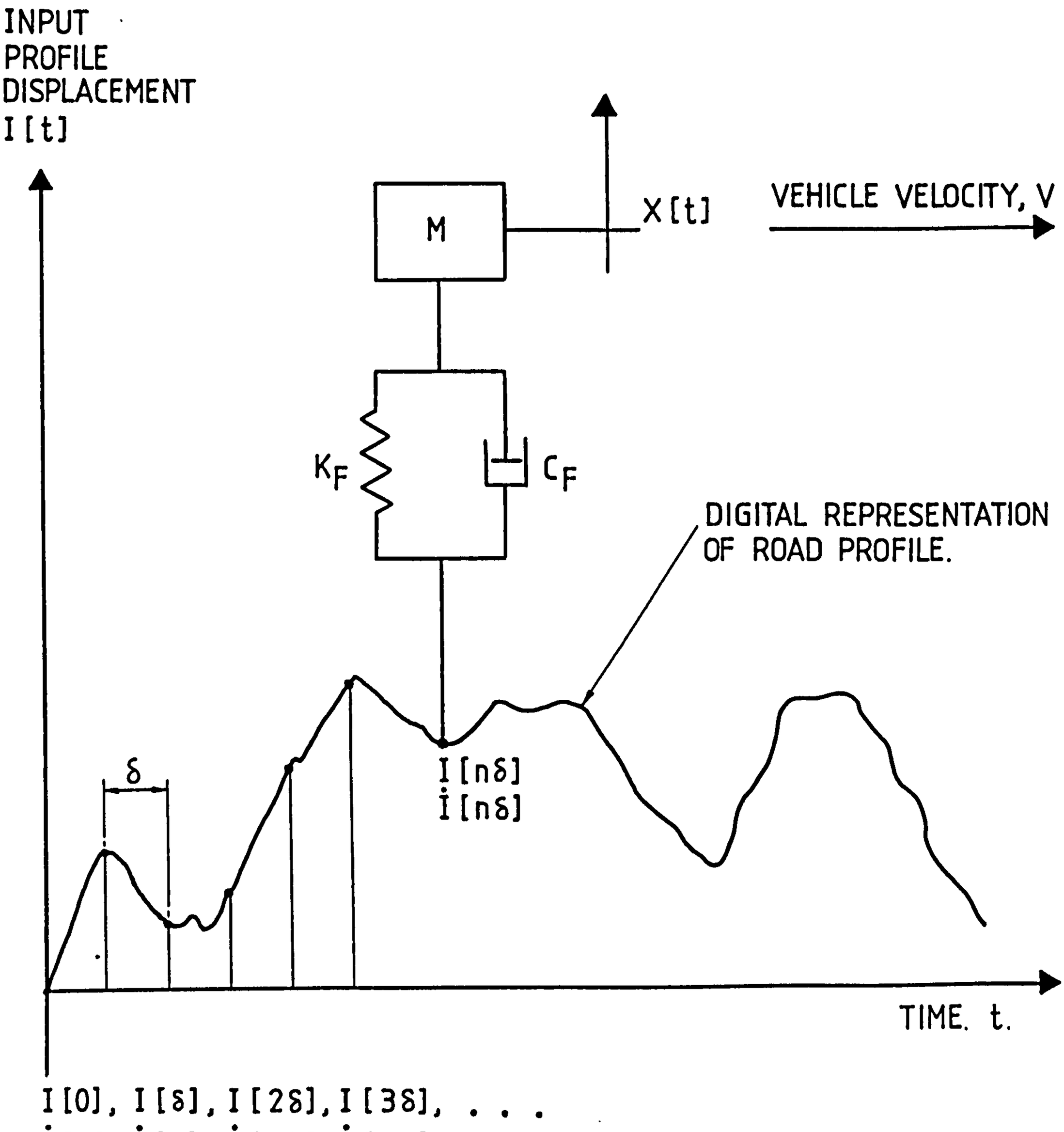

$$\delta = Vt$$

FIGURE 6. TIME DOMAIN RESPONSE.

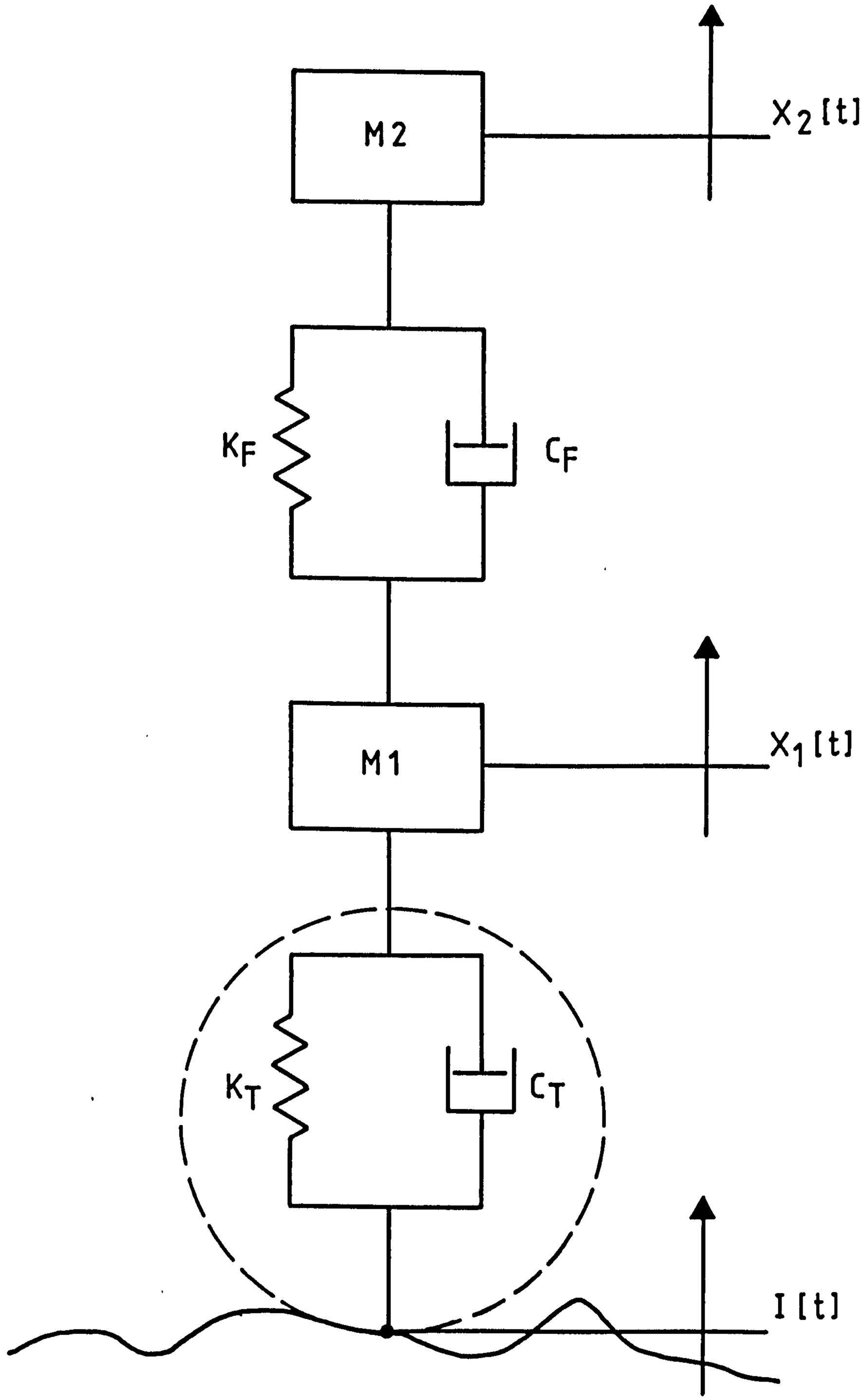

FIGURE 7. 2 DEGREE OF FREEDOM VEHICLE MODEL.

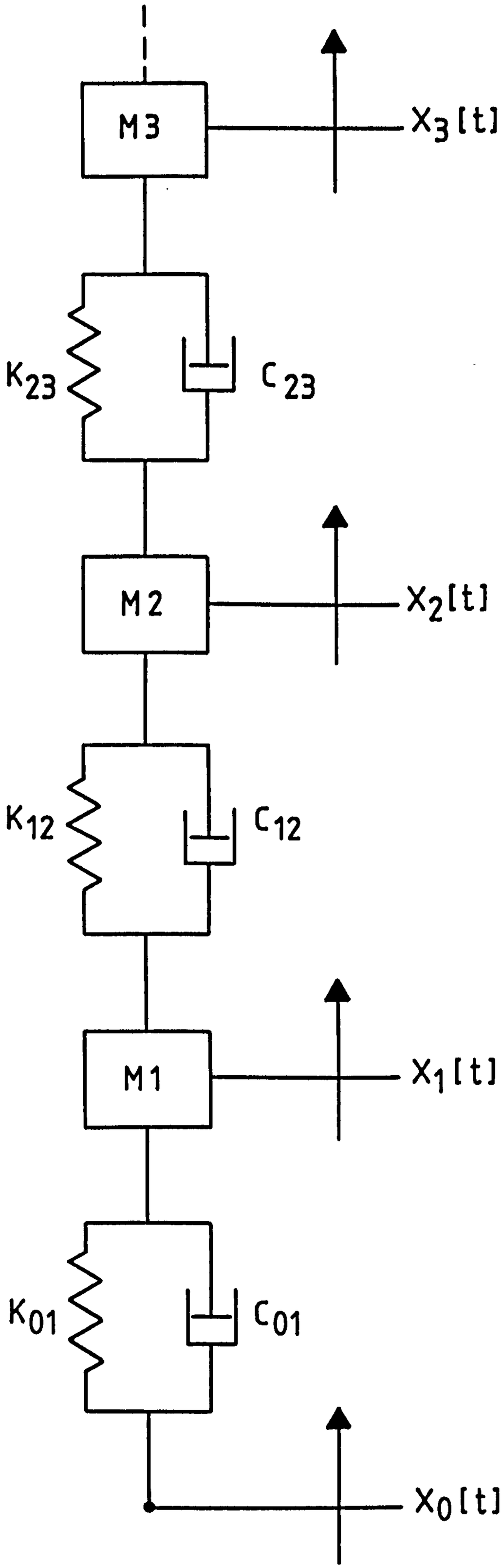

SYSTEM WITH 'n' MASSES.

FIGURE 8. GENERALISED 'STACKED' SYSTEM MODEL.

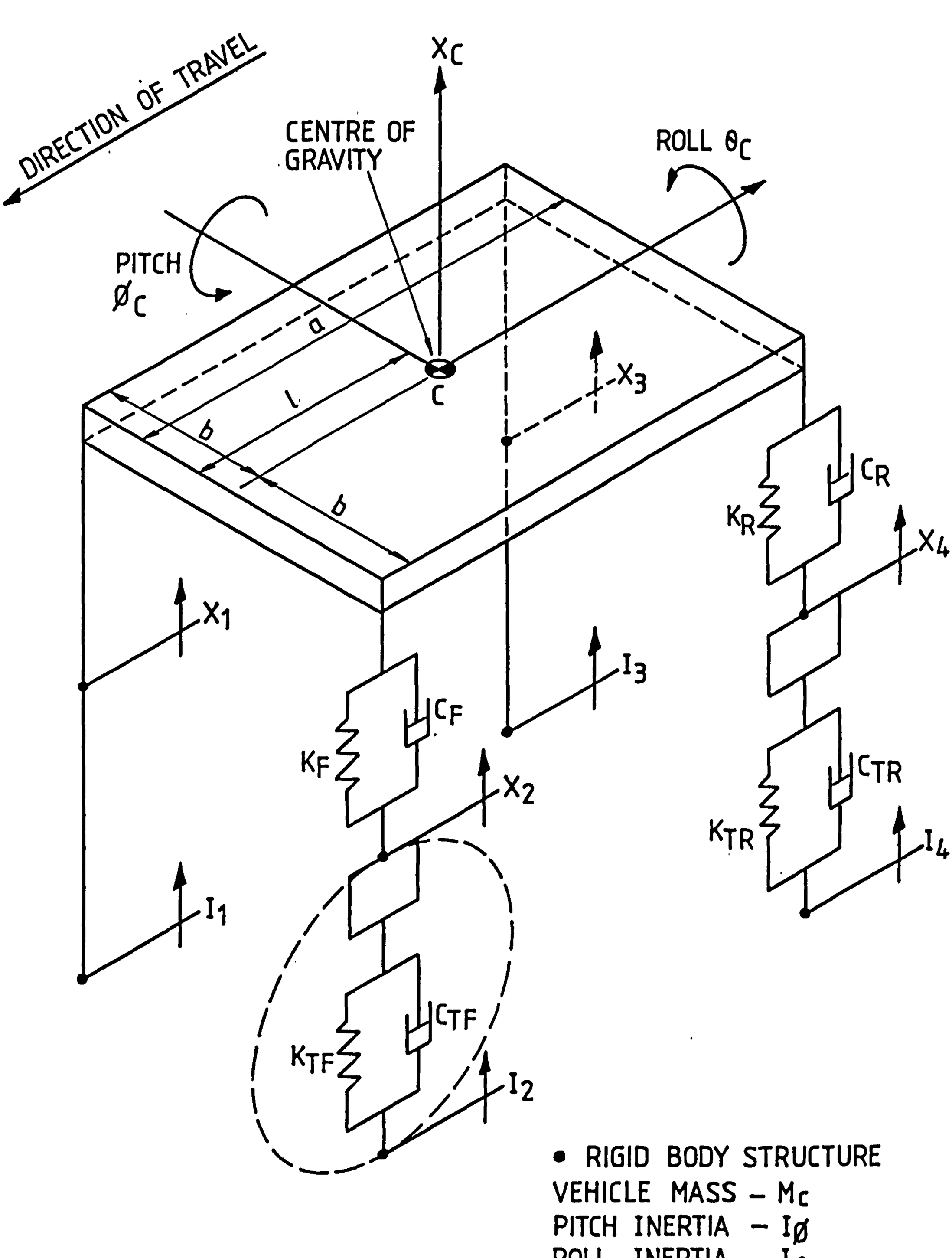

- RIGID BODY STRUCTURE

VEHICLE MASS – M_C
PITCH INERTIA – I_ϕ
ROLL INERTIA – I_θ

FIGURE 9. 7 DEGREE OF FREEDOM 3-D VEHICLE MODEL.

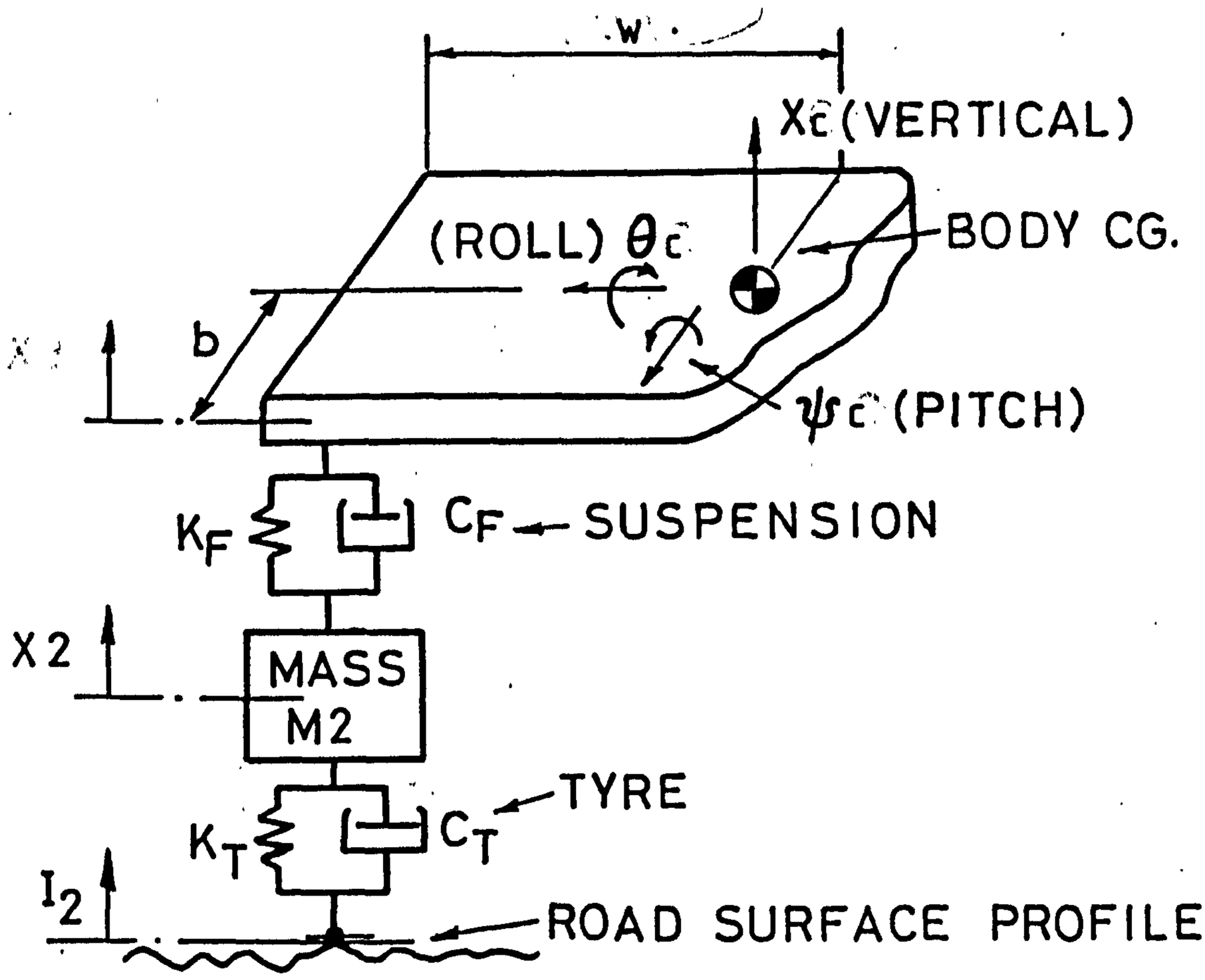

FORCE BALANCE
ON MASS

$$K_F(X_c + b\theta_c - w\psi_c - X2) + C_F(\dot{X}_c + b\dot{\theta}_c - w\dot{\psi}_c - \dot{X}2)$$

M2 $\ddot{X}2$

$$K_T(X2 - I_2) + C_T(\dot{X}2 - \dot{I}_2)$$

FIGURE 10. EQUILIBRIUM OF FRONT UNSPRUNG MASS.

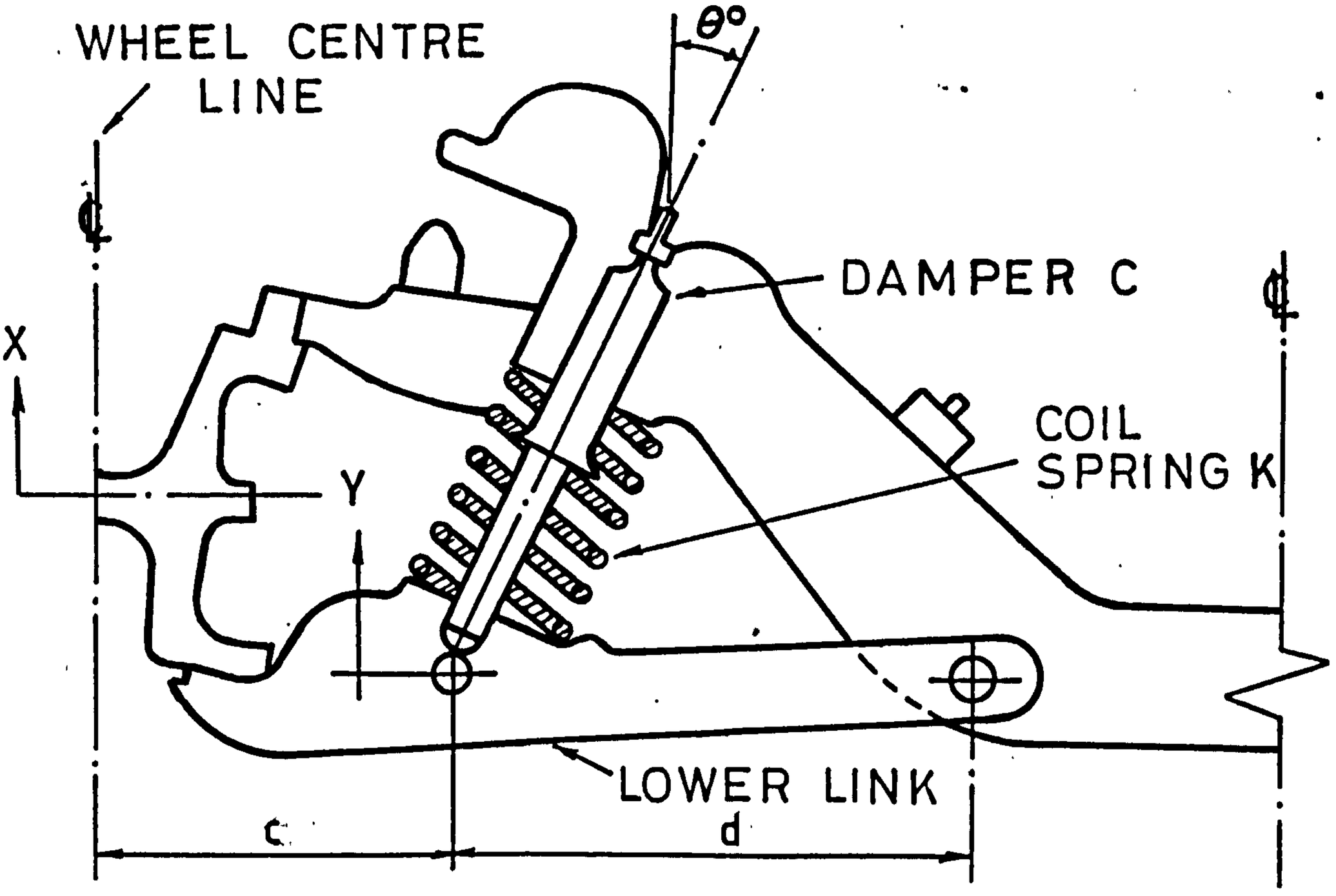

VEHICLE FRONT SUSPENSION CONFIGURATION.

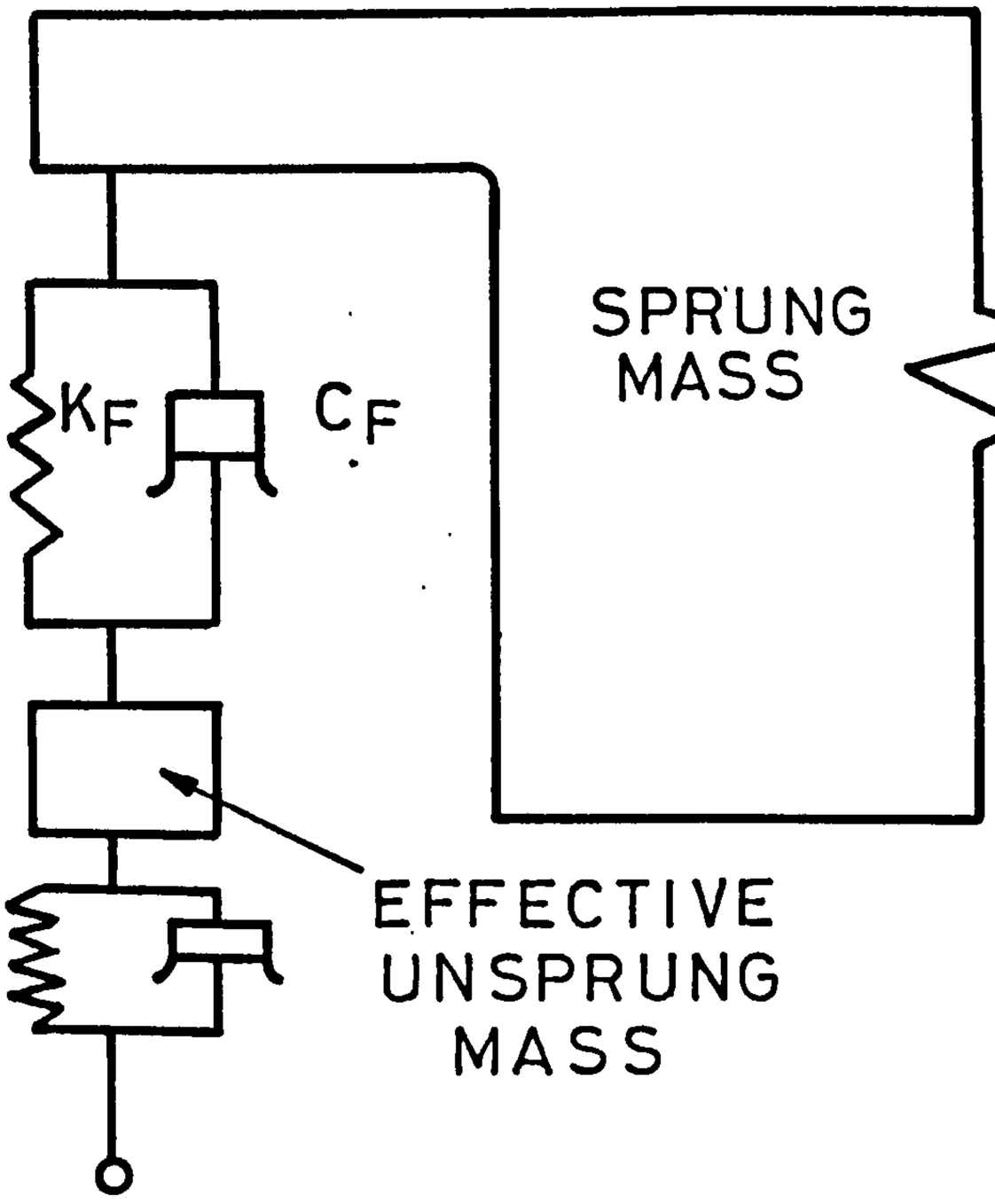

$$\frac{X}{Y} = \frac{(c+d)}{d}$$

$$\therefore K_F = \left[\frac{d}{(c+d)}\right] K \cos\theta^\circ = K \times R.$$

$$C_F = \left[\frac{d}{(c+d)}\right] C \cos\theta^\circ = C \times R$$

SUSPENSION RATIO = R
WHEEL VELOCITY = R x DAMPER VELOCITY
WHEEL LOAD = 1/R x DAMPER LOAD

MODEL EQUIVALENT.

FIGURE 11. COMPENSATION FOR FRONT SUSPENSION GEOMETRY.

FIGURE 12

TYPICAL ROAD SIMULATOR FACILITY

(REPRODUCED COURTESY OF THE
AUSTIN ROVER GROUP)

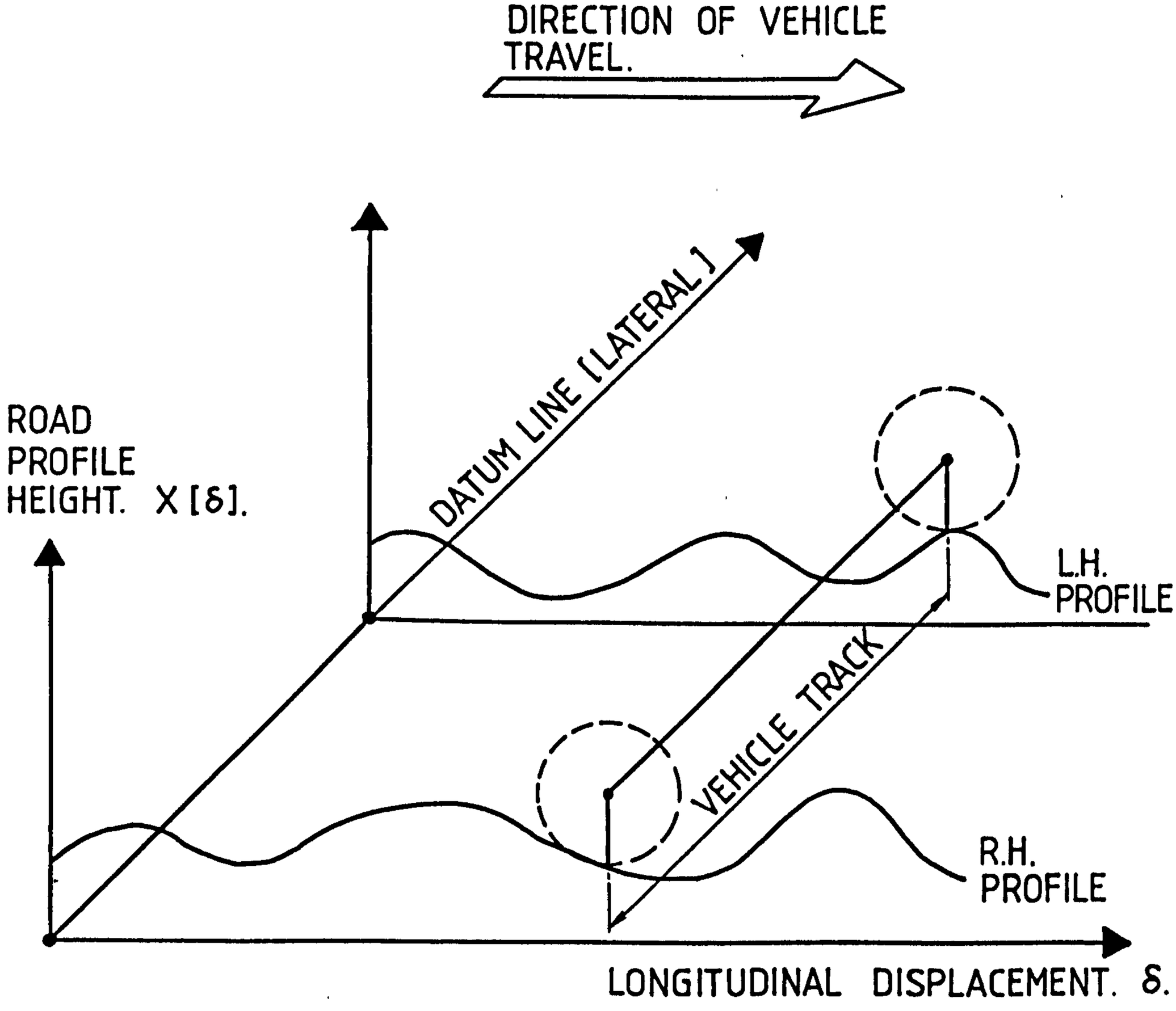

FIGURE 13. ROAD SURFACE PROFILES.

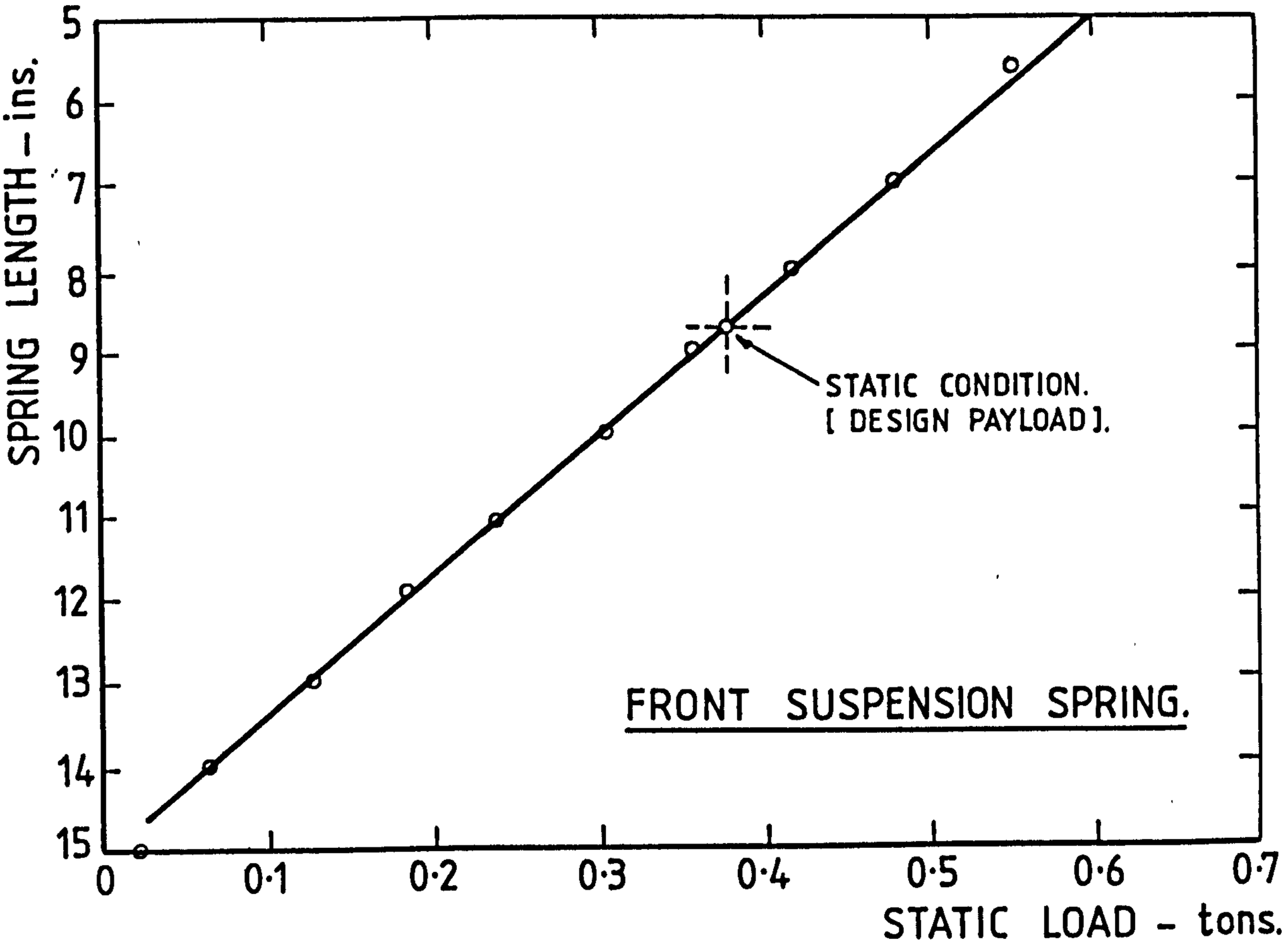

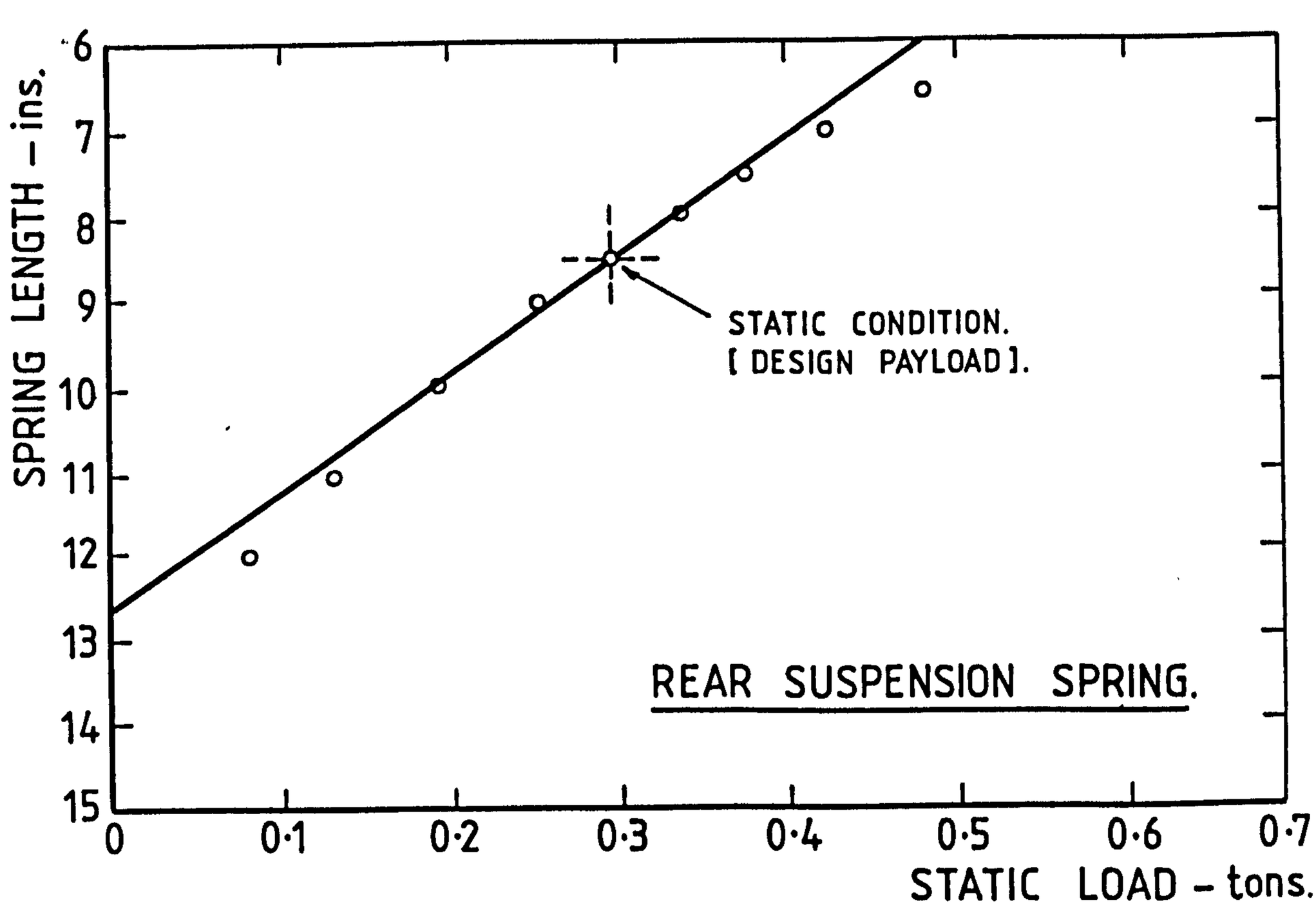

FIGURE 14. SPRING FORCE / DEFLECTION PLOTS. [VEHICLE 'A'].

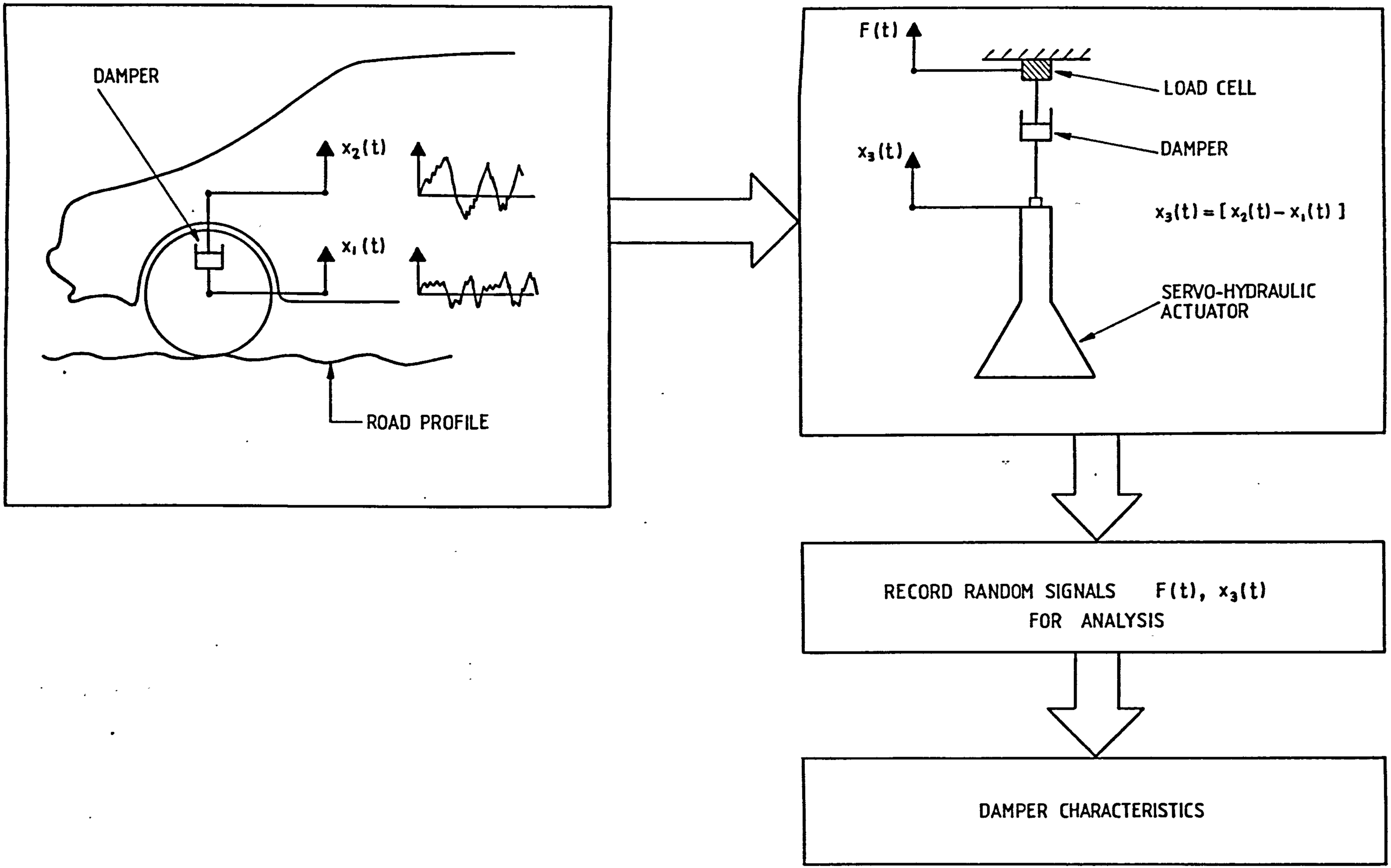

FIGURE 15. DAMPER TESTING USING SERVICE LOADING.

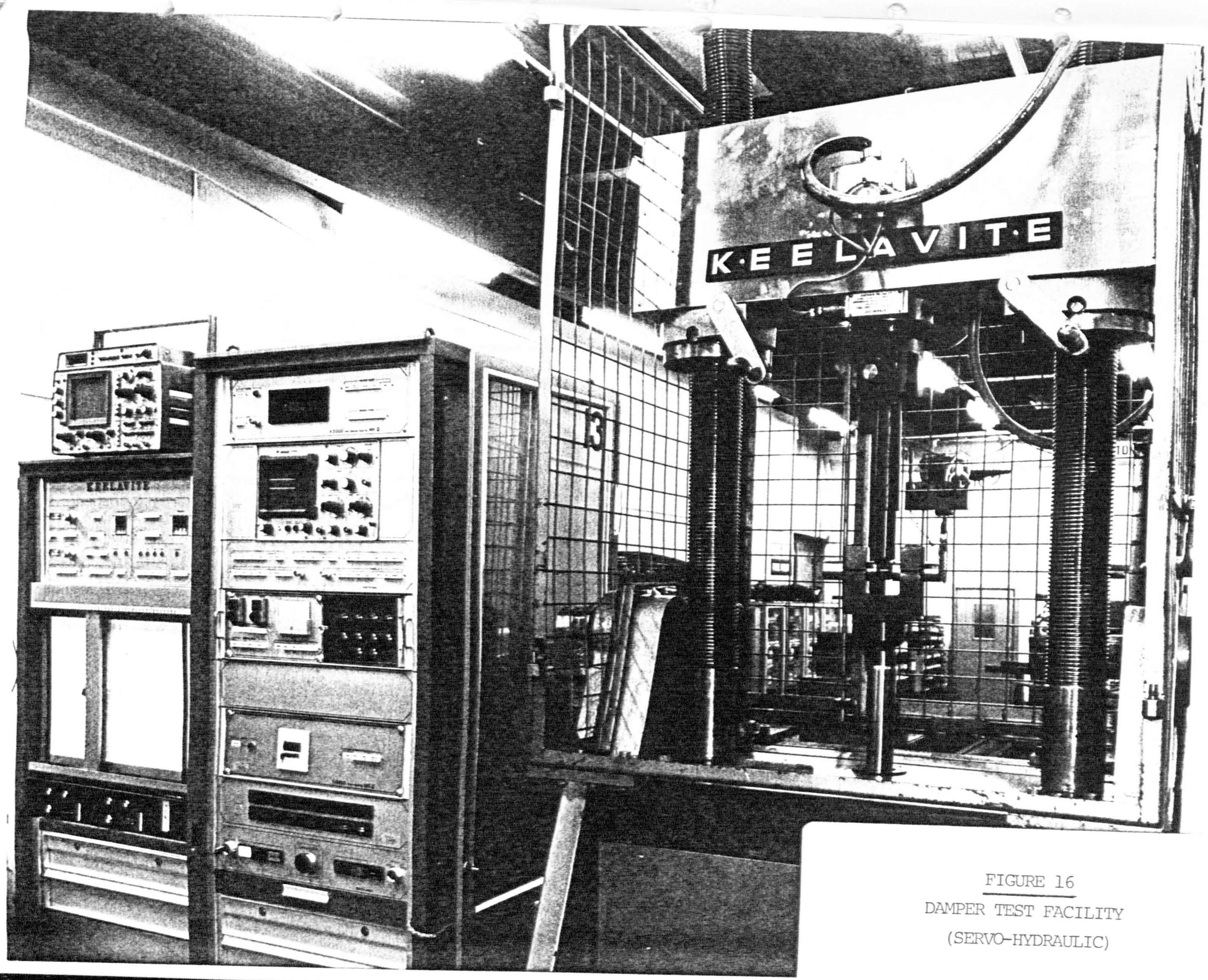

FIGURE 16

DAMPER TEST FACILITY

(SERVO-HYDRAULIC)

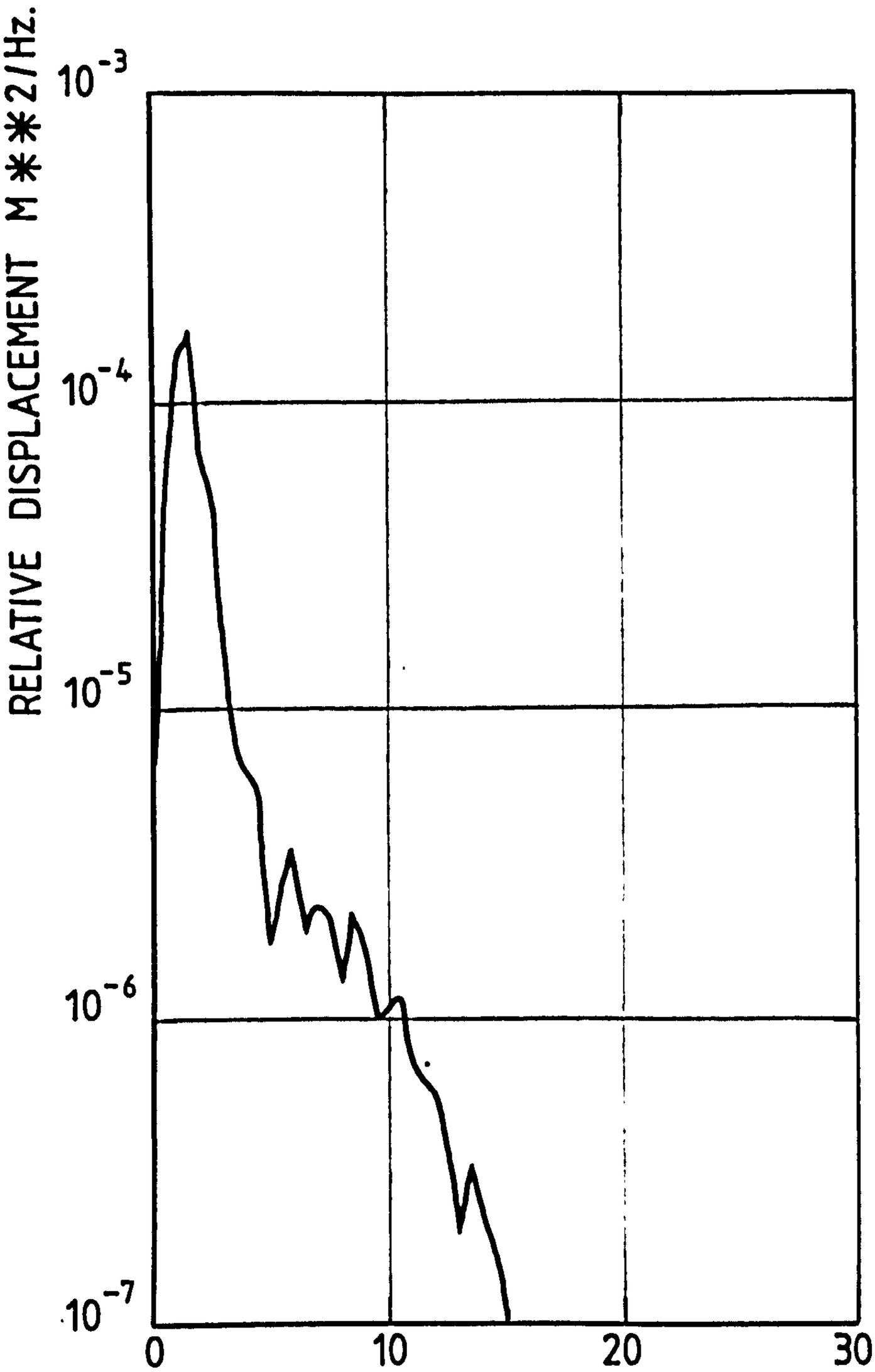

FIGURE 17. RELATIVE DISPLACEMENT PSD.

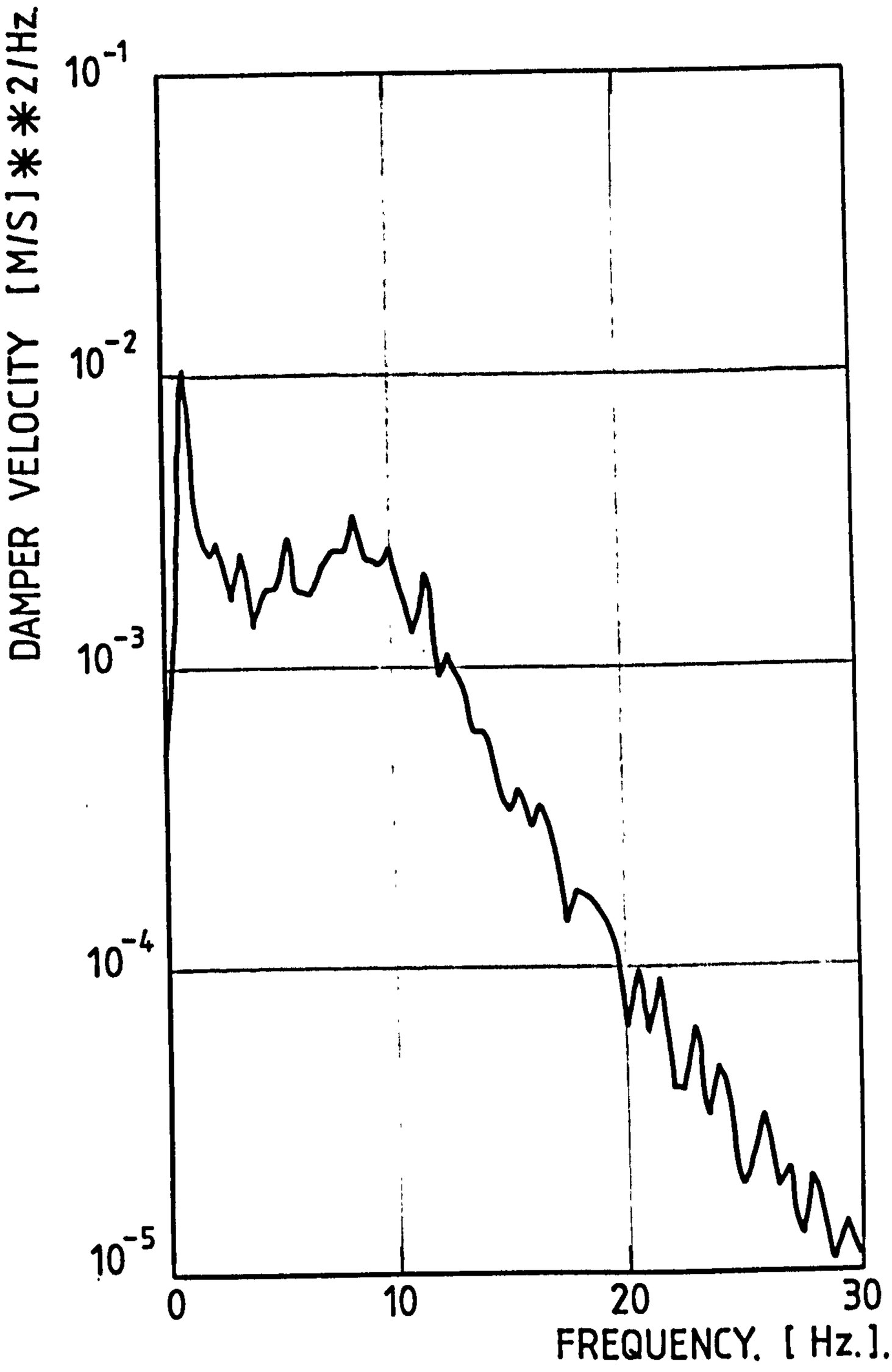

FIGURE 18. PSD OF DAMPER INPUT VELOCITY.

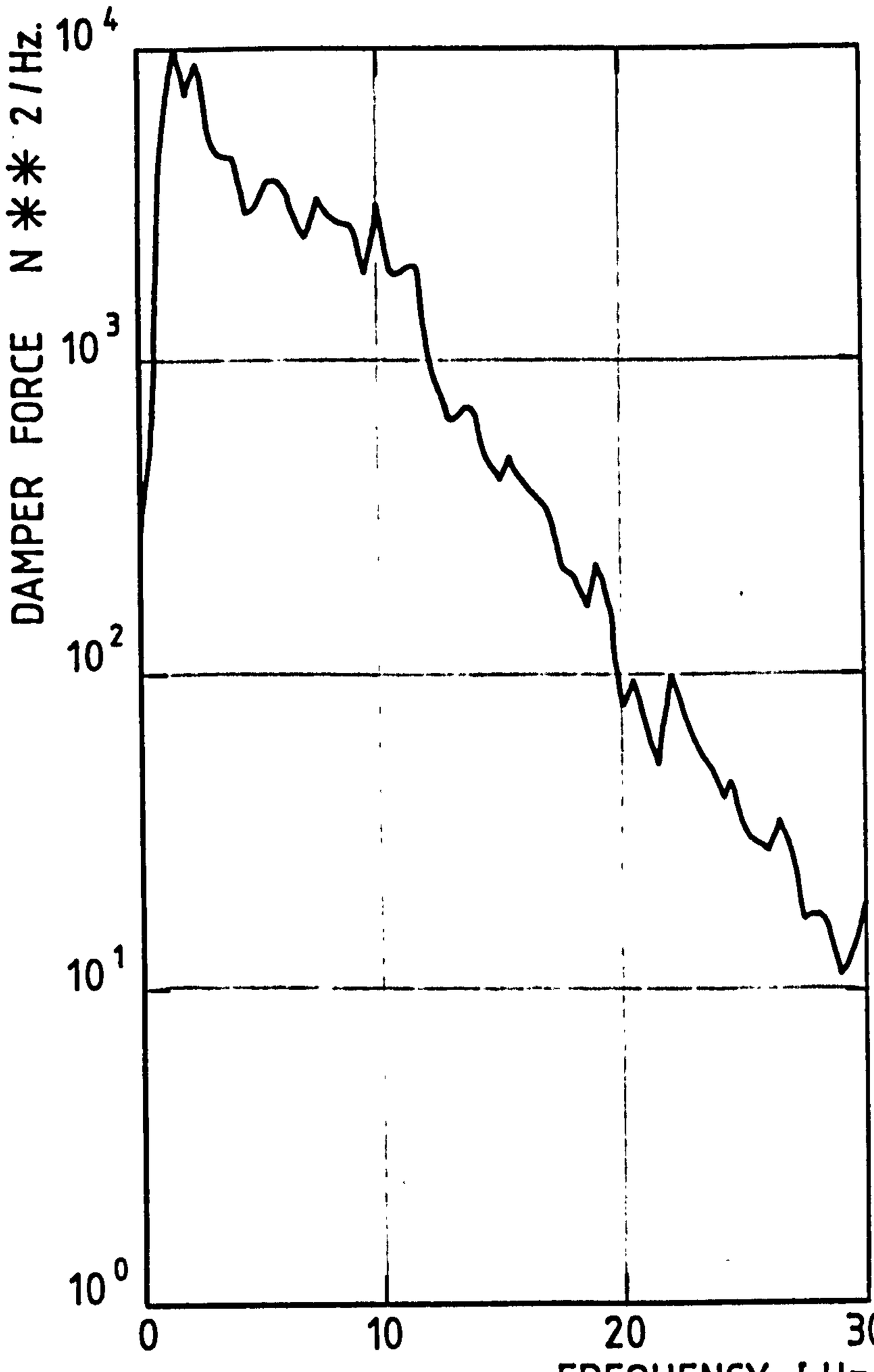

FIGURE 19. PSD OF TRANSMITTED DAMPER FORCE.

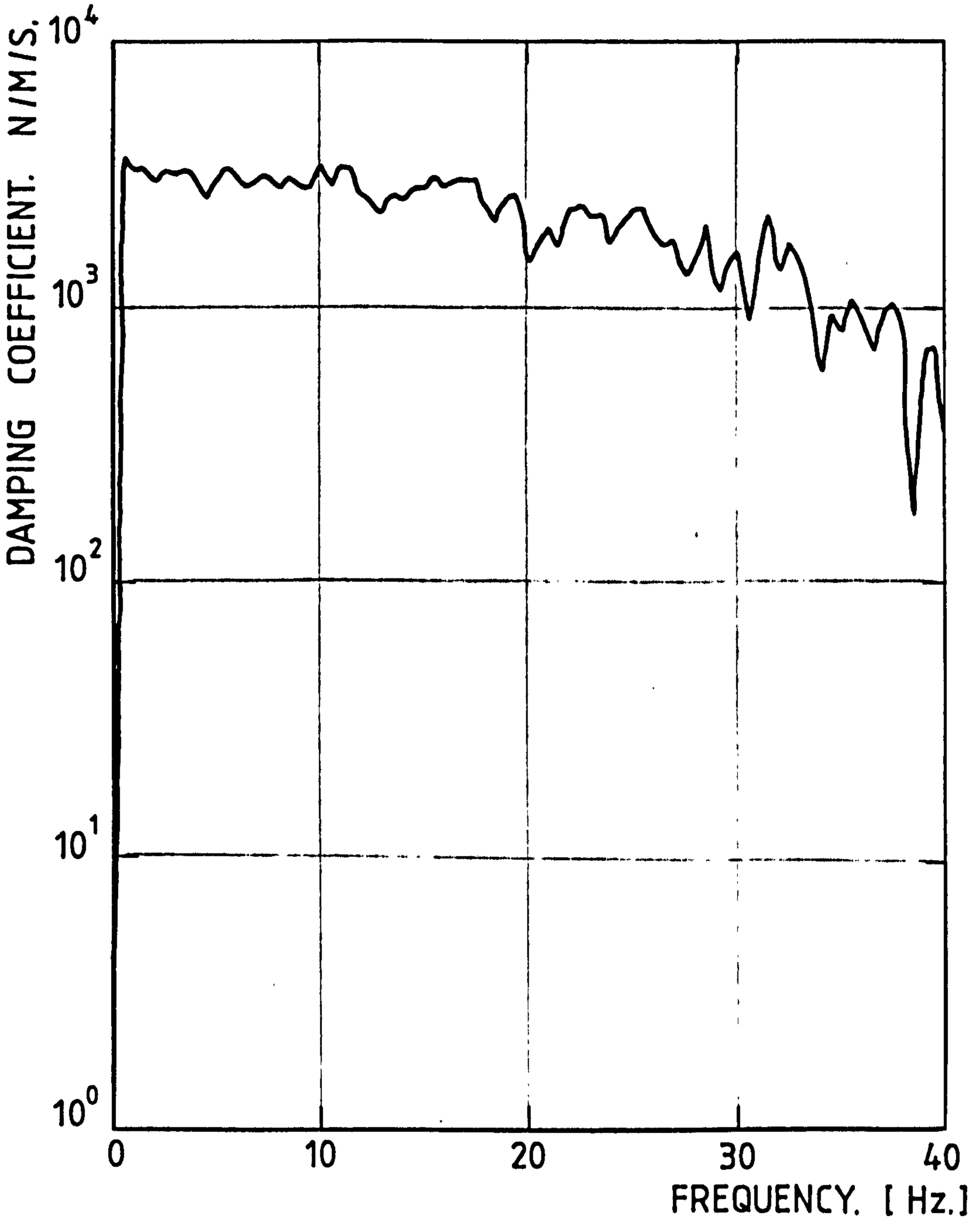

FIGURE 20. FREQUENCY RESPONSE FUNCTION
DAMPER FORCE TO DAMPER VELOCITY.

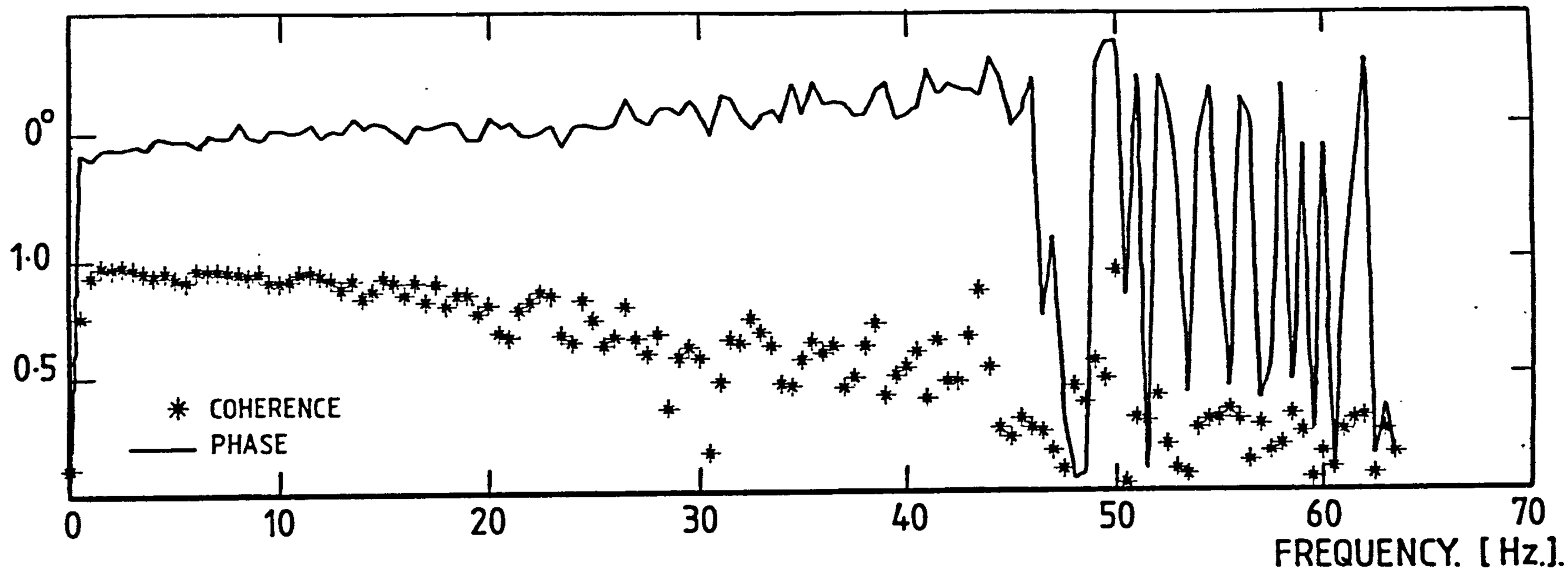

FIGURE 21. COHERENCE & PHASE PLOTS
DAMPER INPUT VELOCITY TO OUTPUT FORCE.

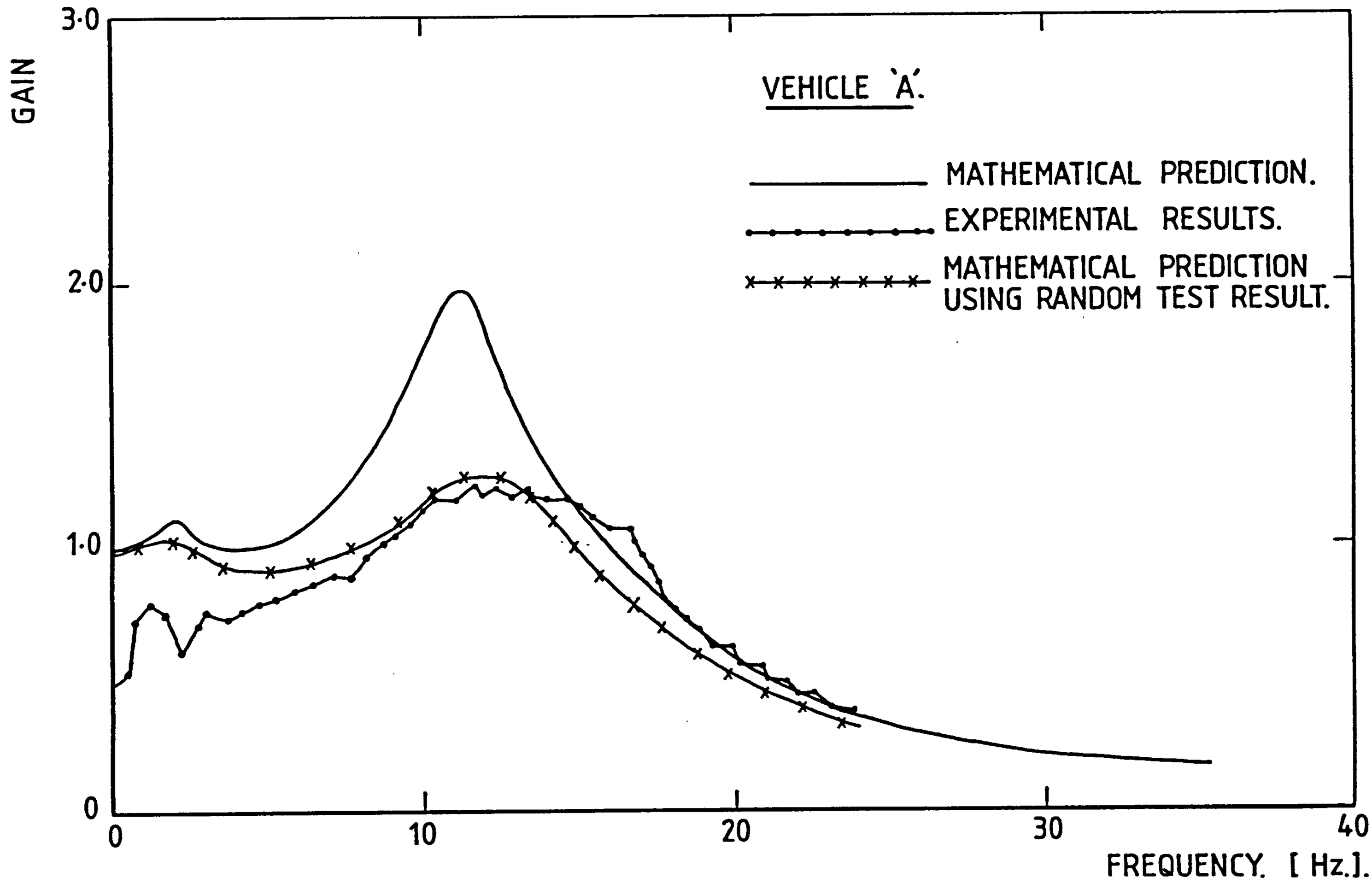

FIGURE 22. FREQUENCY RESPONSE FUNCTION O / S / R WHEELPAN TO RIGHT HAND REAR AXLE.

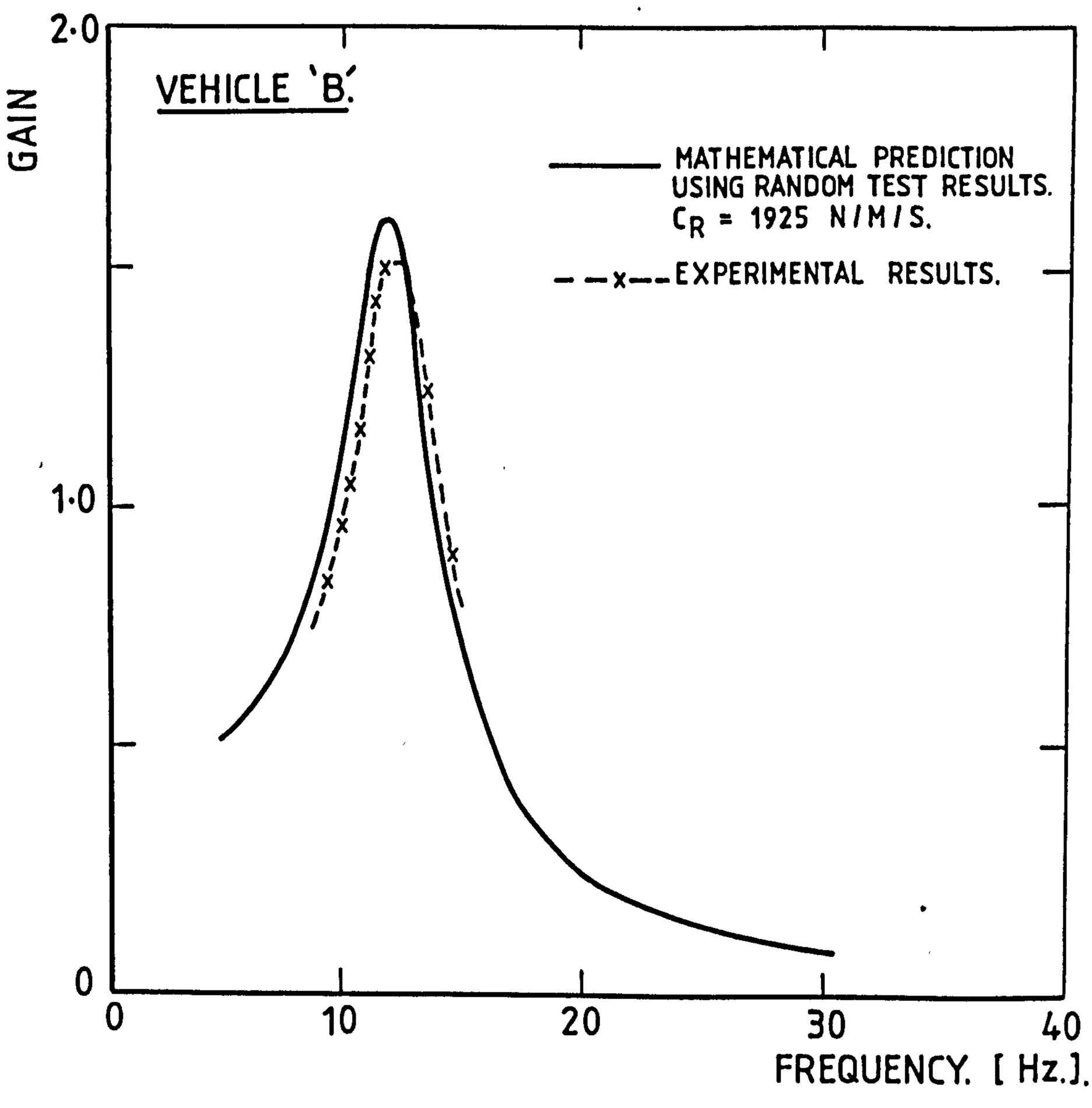

FIGURE 23. FREQUENCY RESPONSE O/S/R WHEELPAN TO REAR AXLE VERTICAL.

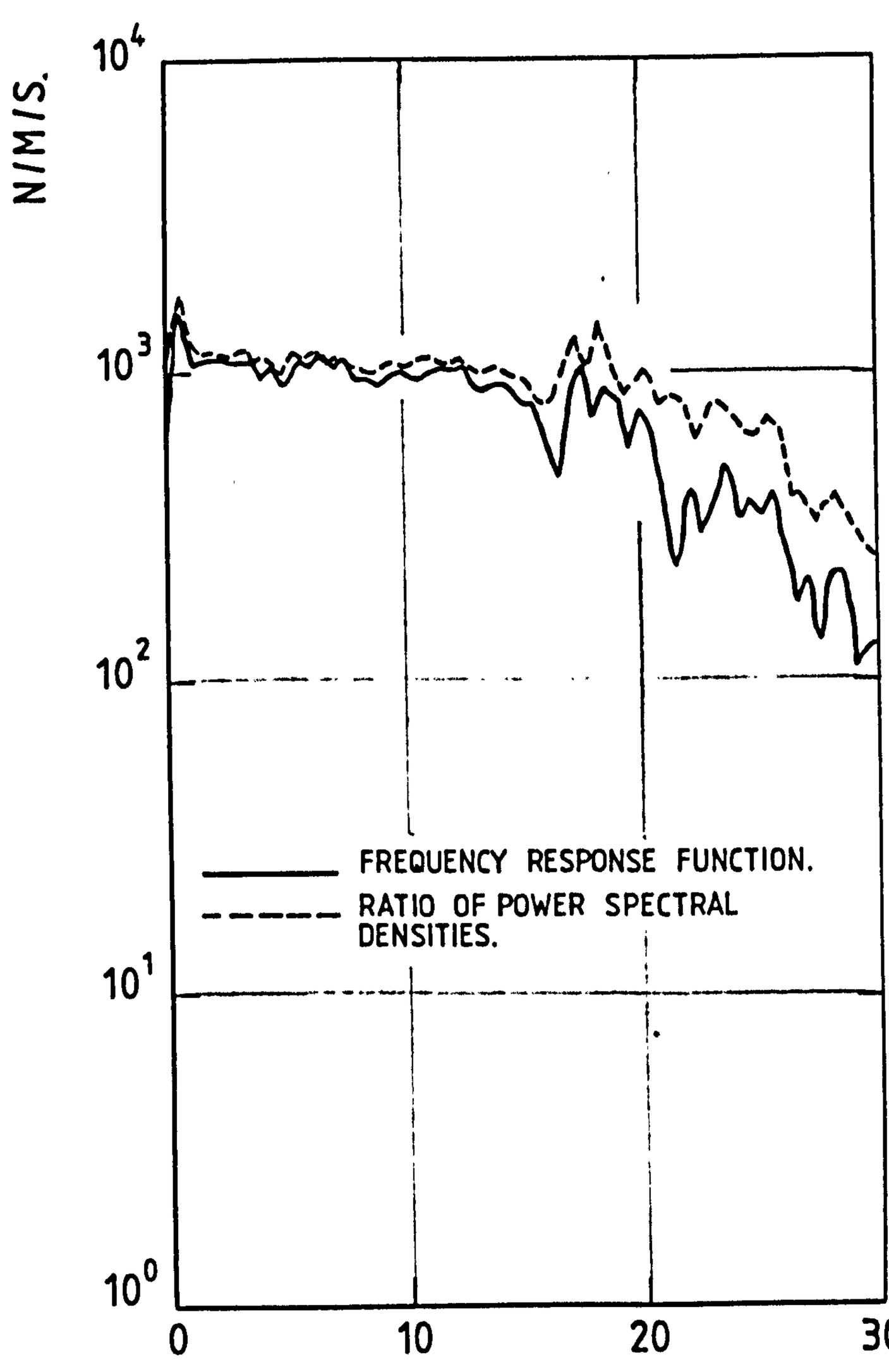

FIGURE 24. DAMPER COEFFICIENT PLOTS BY TWO ANALYSIS METHODS.

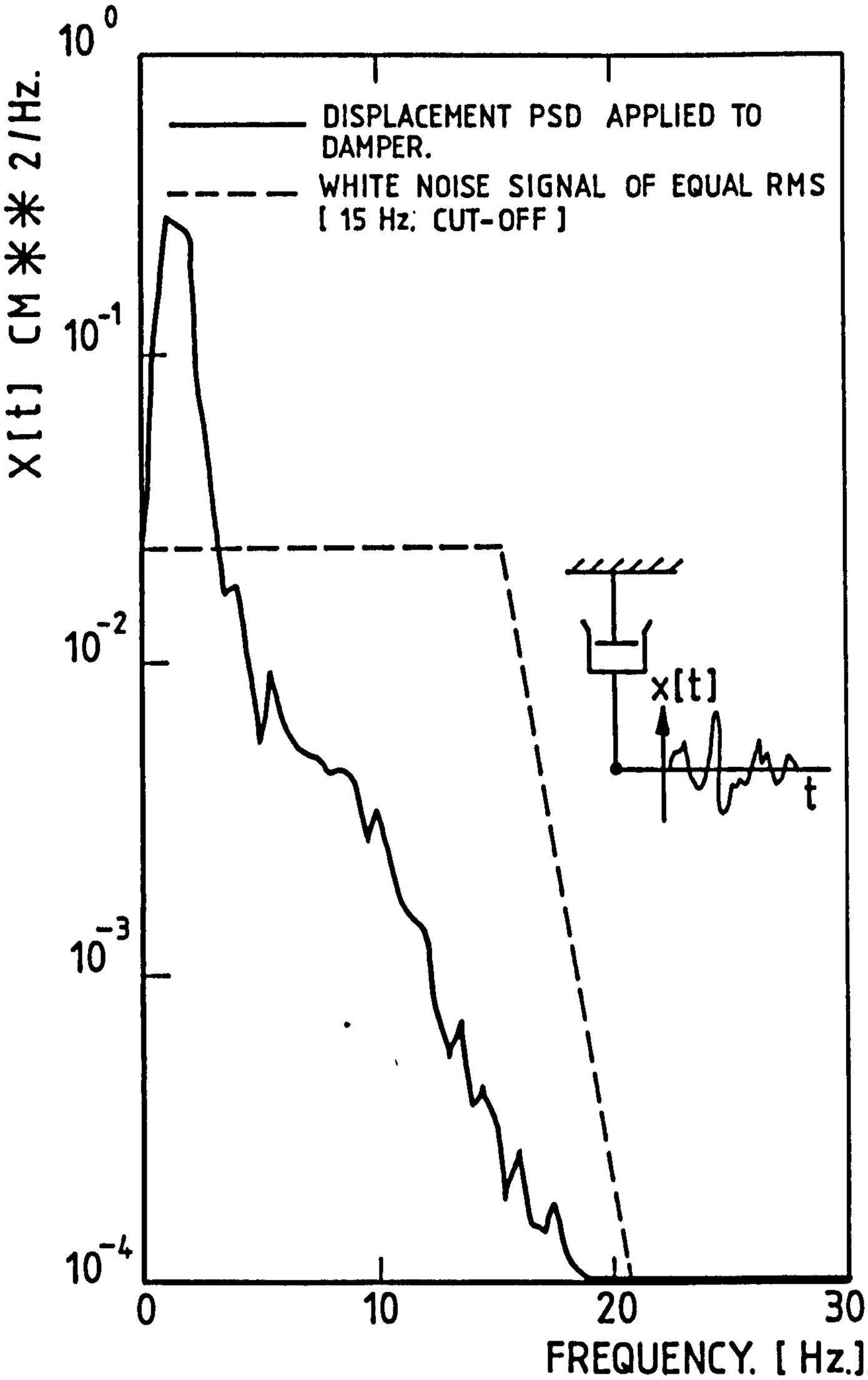

FIGURE 25. DAMPER DISPLACEMENT PSD AND WHITE NOISE PSD WITH EQUAL RMS.

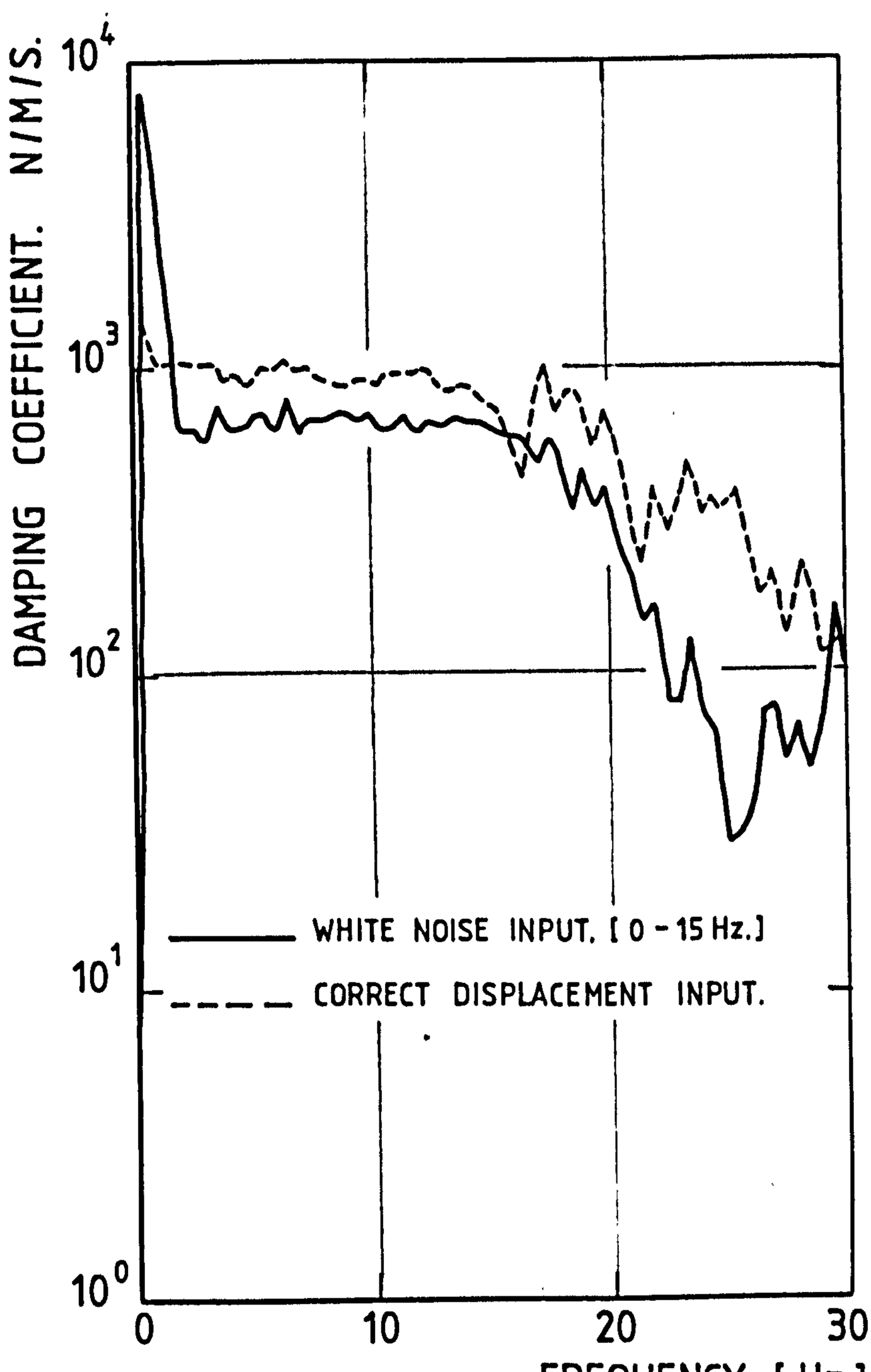

FIGURE 26. DAMPER COEFFICIENT RESULTS WITH DIFFERENT INPUT EXCITATION.

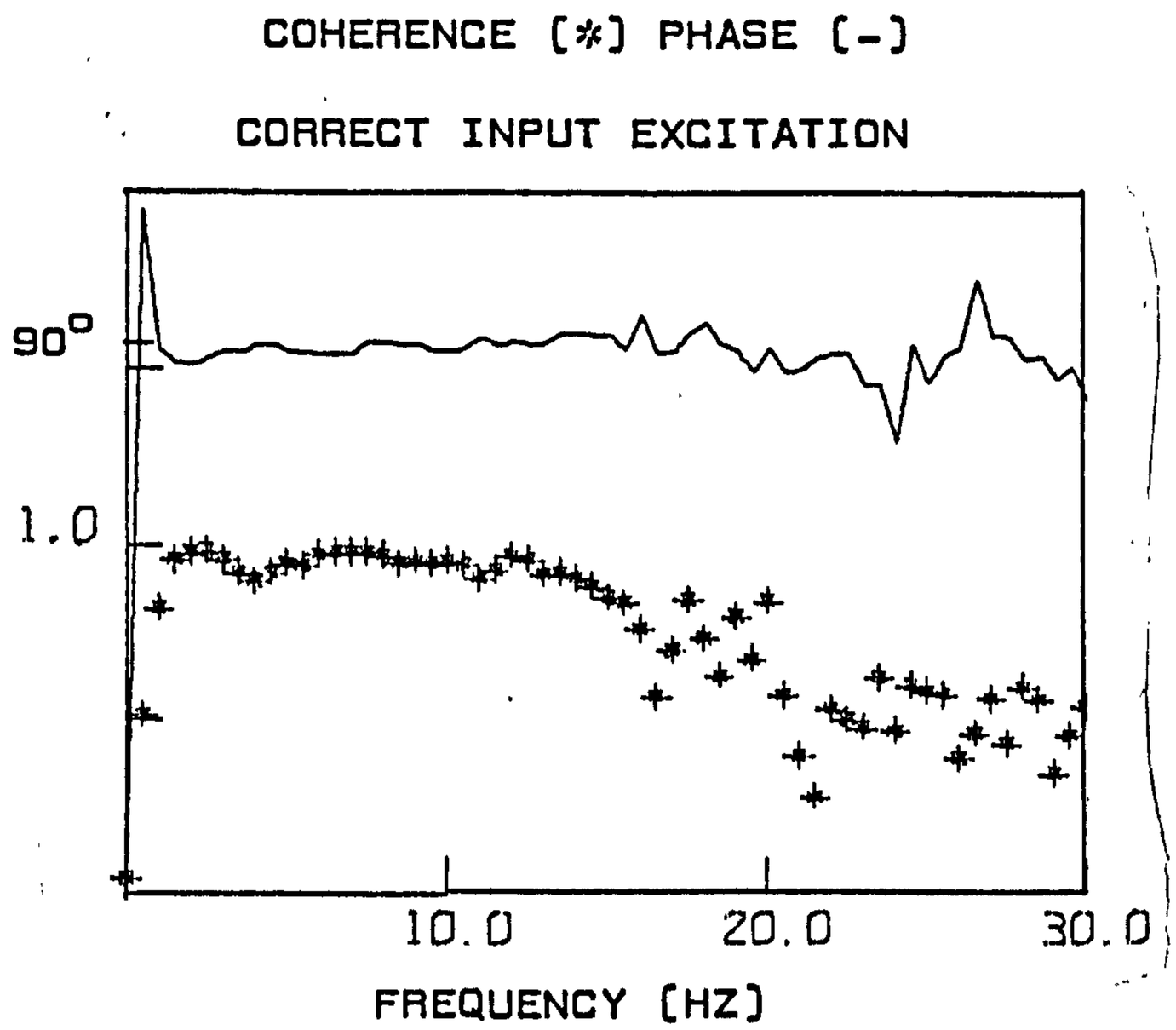

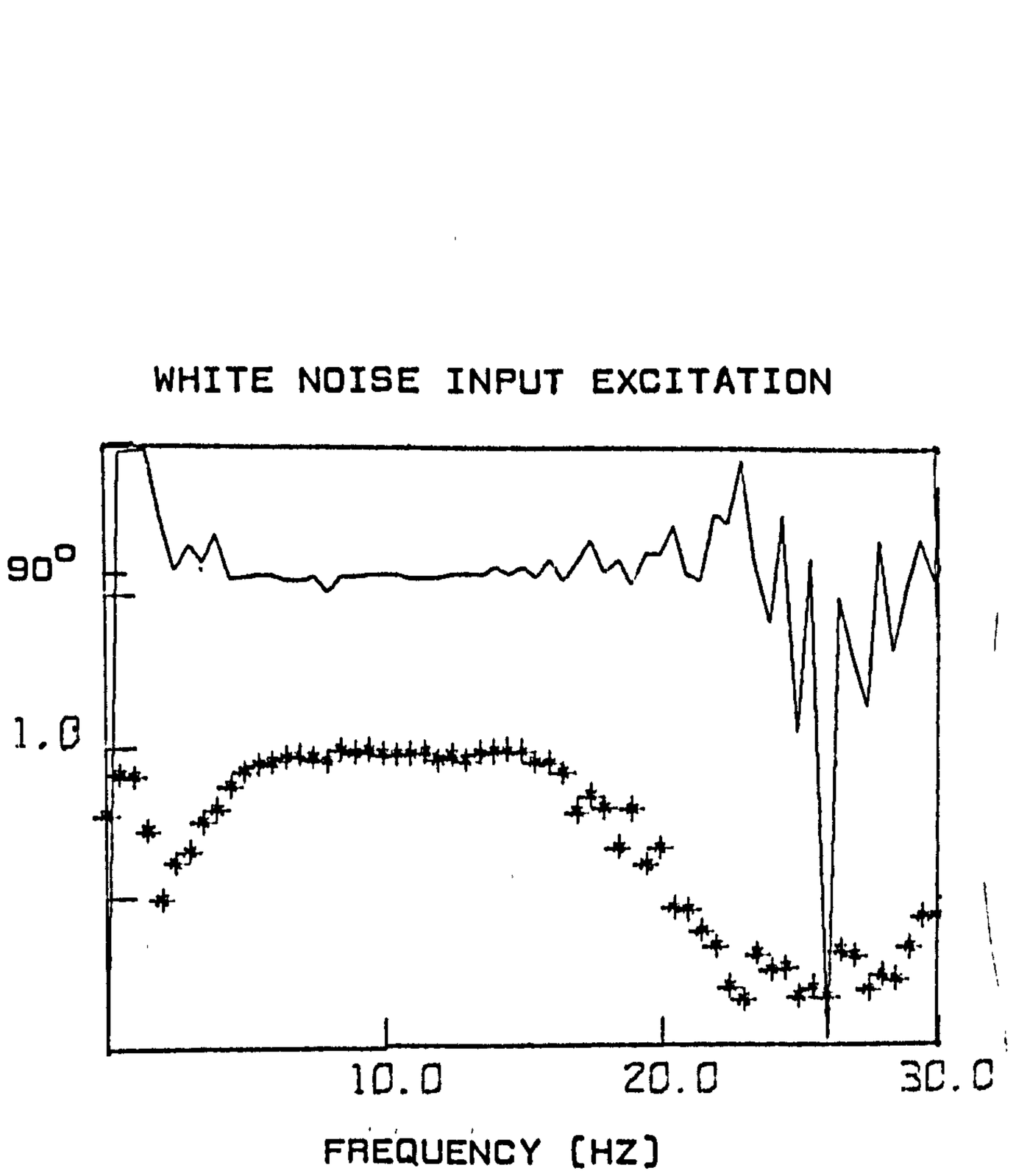

FIGURE 27

COHERENCE AND PHASE PLOTS FOR DAMPER

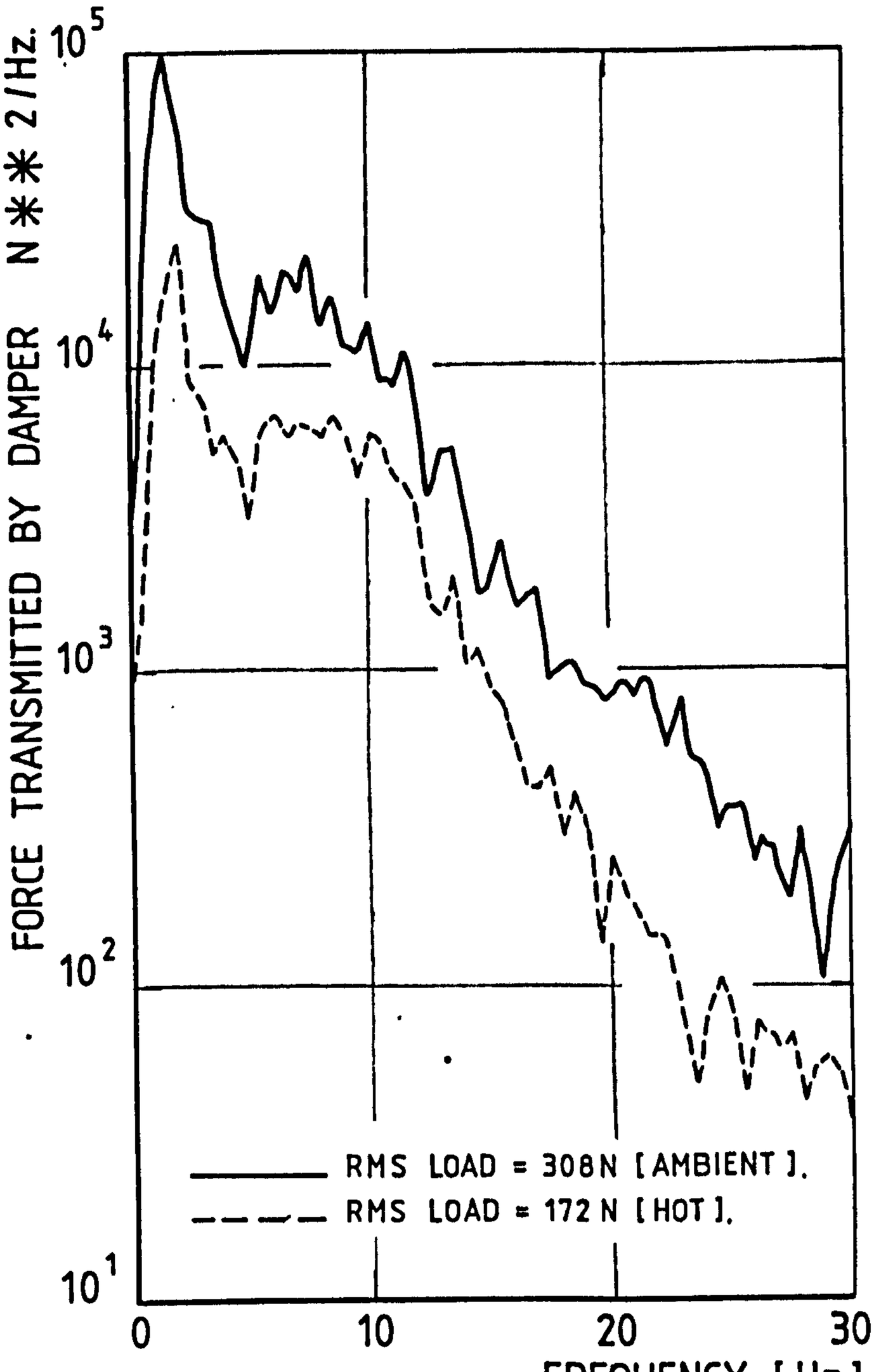

FIGURE 28. EFFECT OF TEMPERATURE ON LOADS TRANSMITTED BY DAMPER.

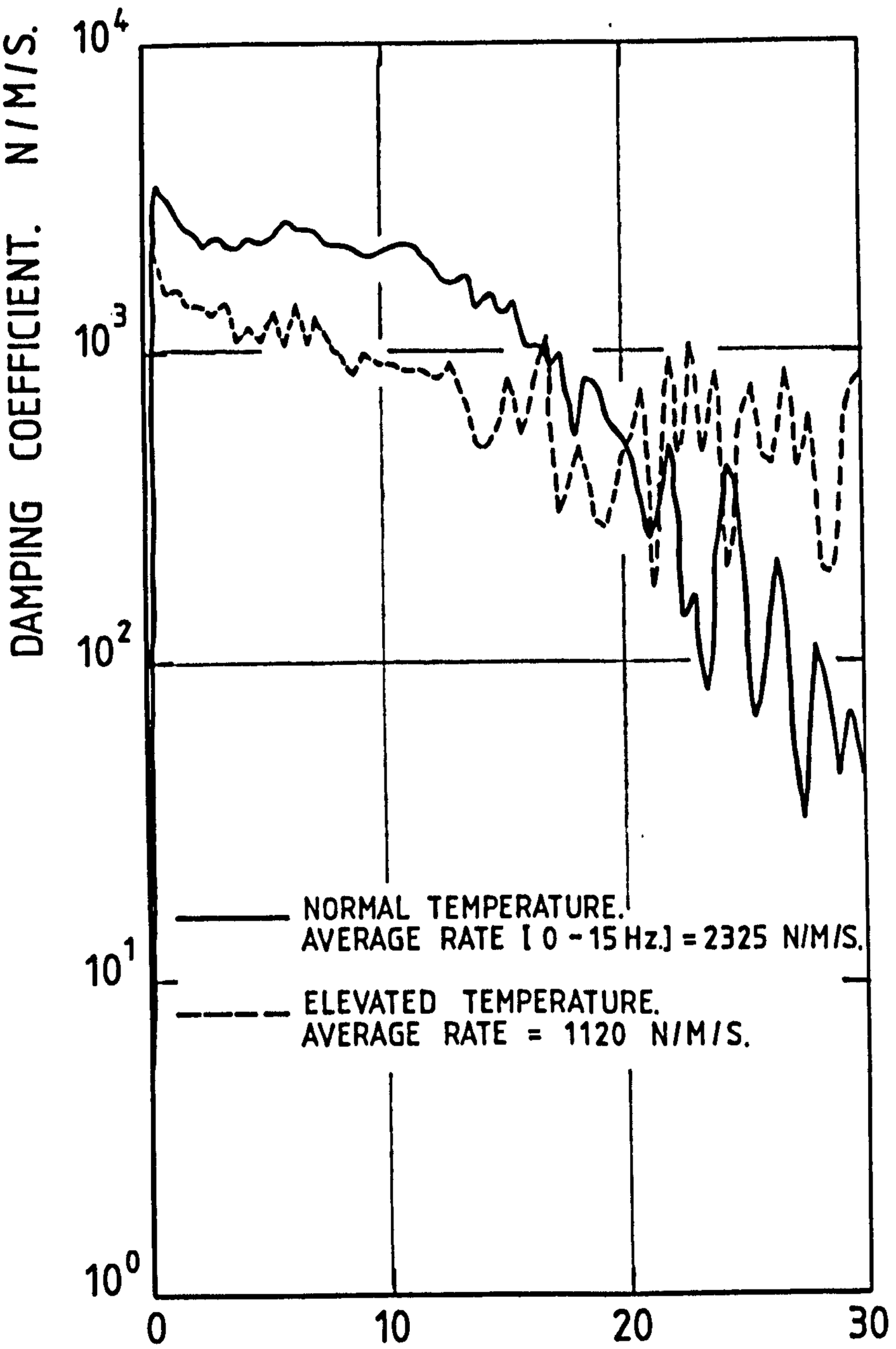

FIGURE 29. EFFECT OF TEMPERATURE ON DAMPER RATES.

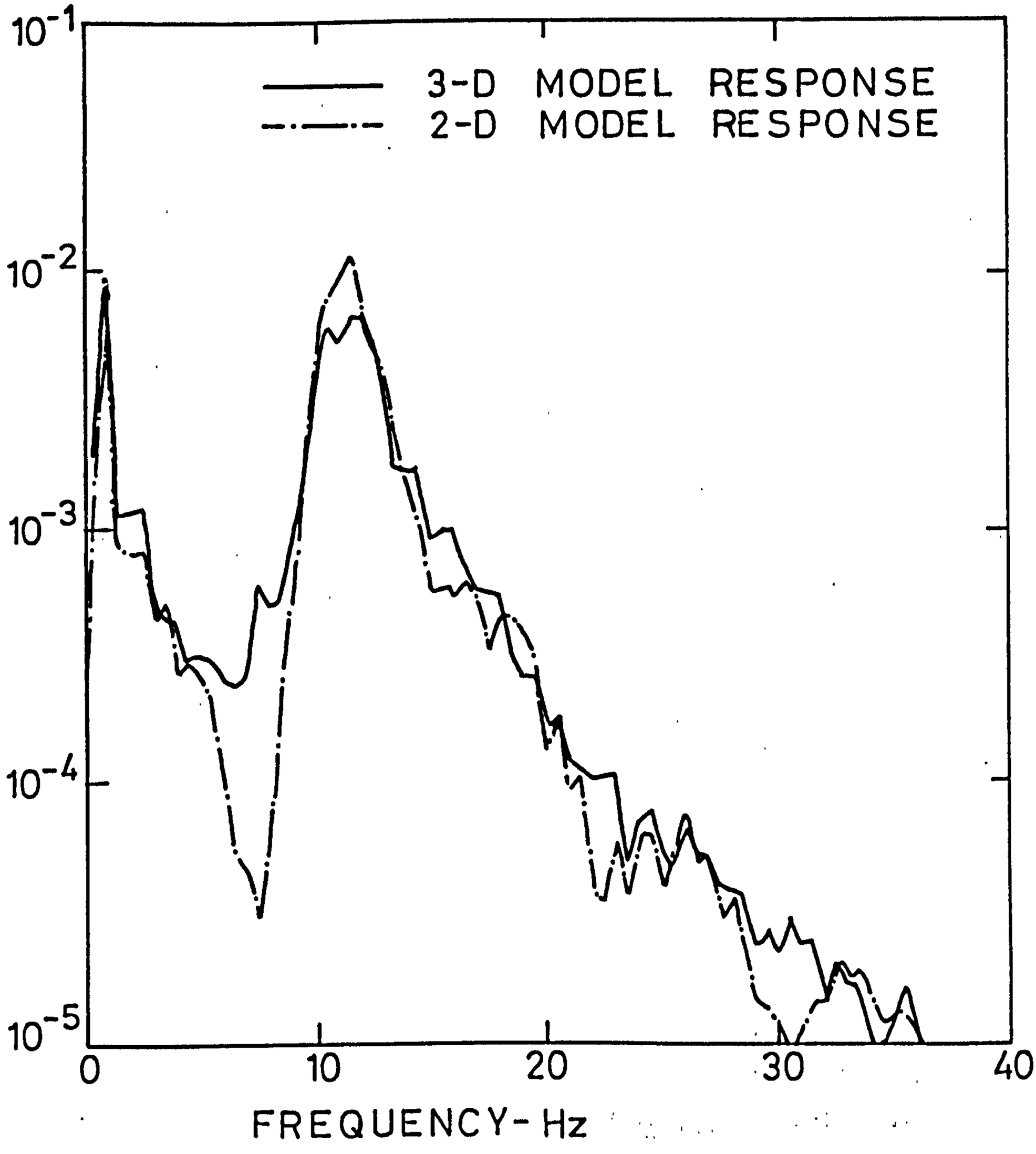

FIGURE 30. RESPONSE SPECTRA OF LEFT HAND FRONT BODY FOR 3-D & EQUIVALENT 2-D MODELS.

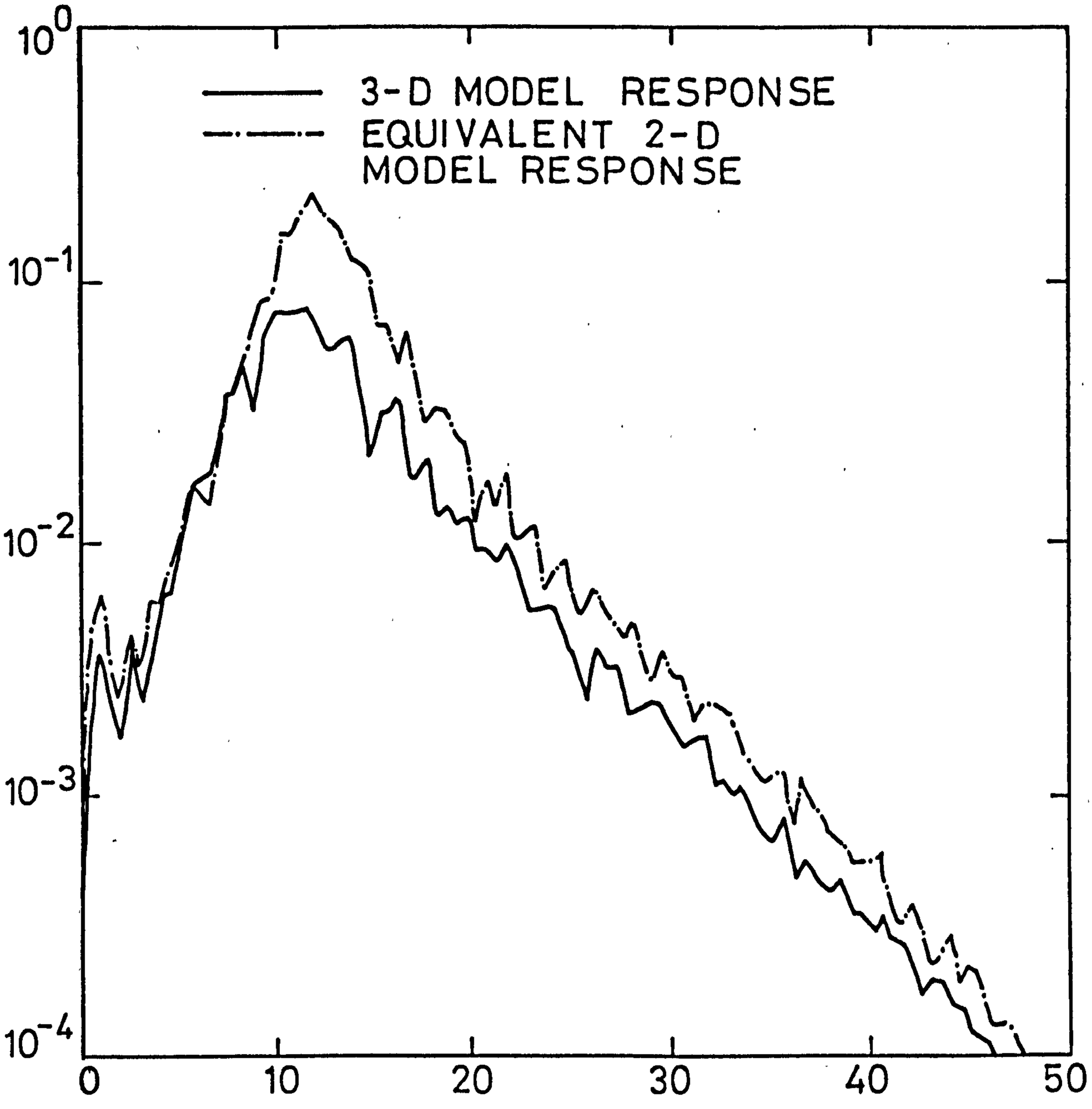

FIGURE 31. RESPONSE SPECTRA OF LEFT HAND REAR AXLE FOR 3-D AND 2-D MODELS.

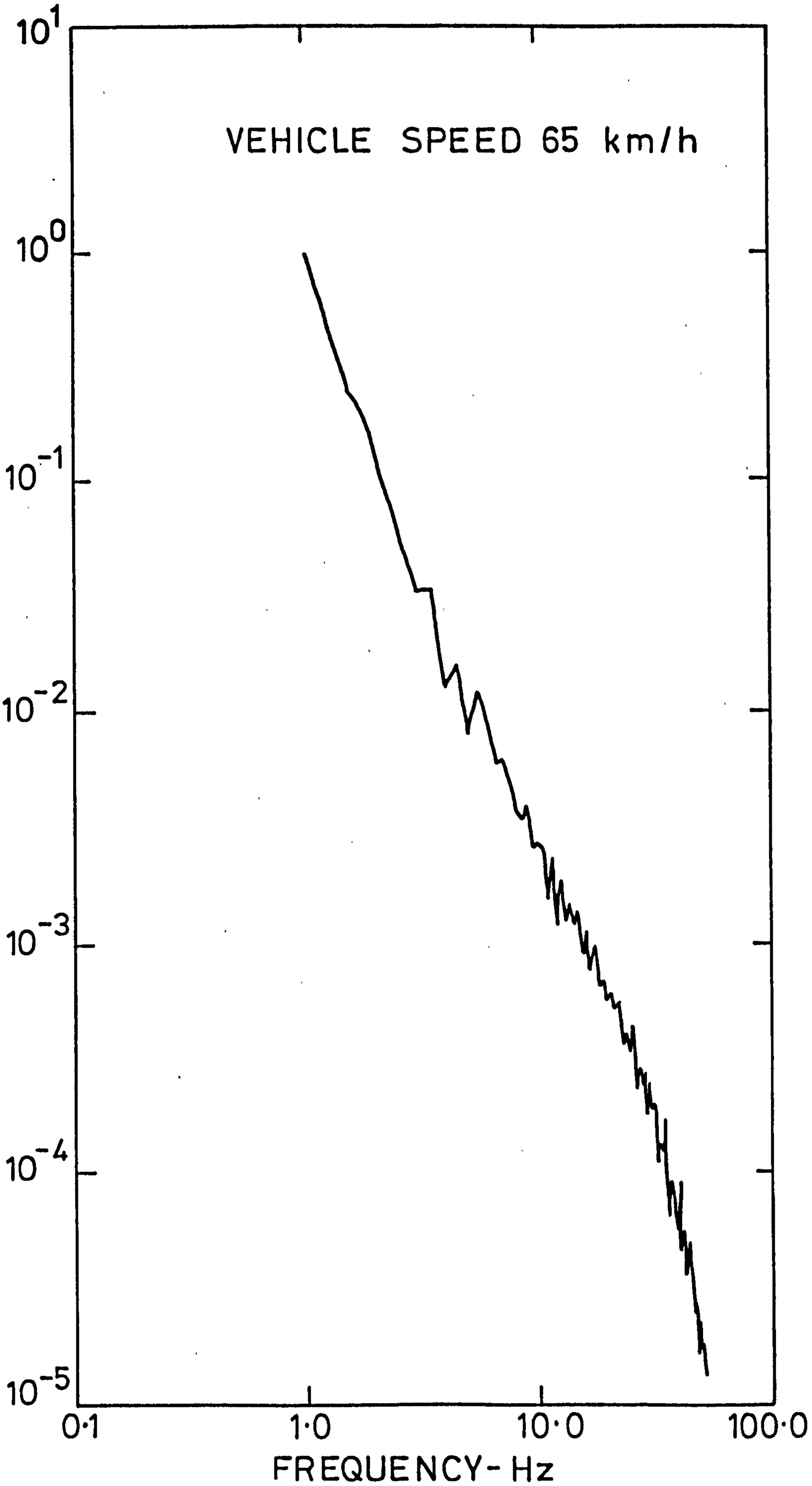

FIGURE 32. SYNTHESIZED ROAD PROFILE SPECTRUM. [COMPENSATED FOR TYRE ENVELOPING].

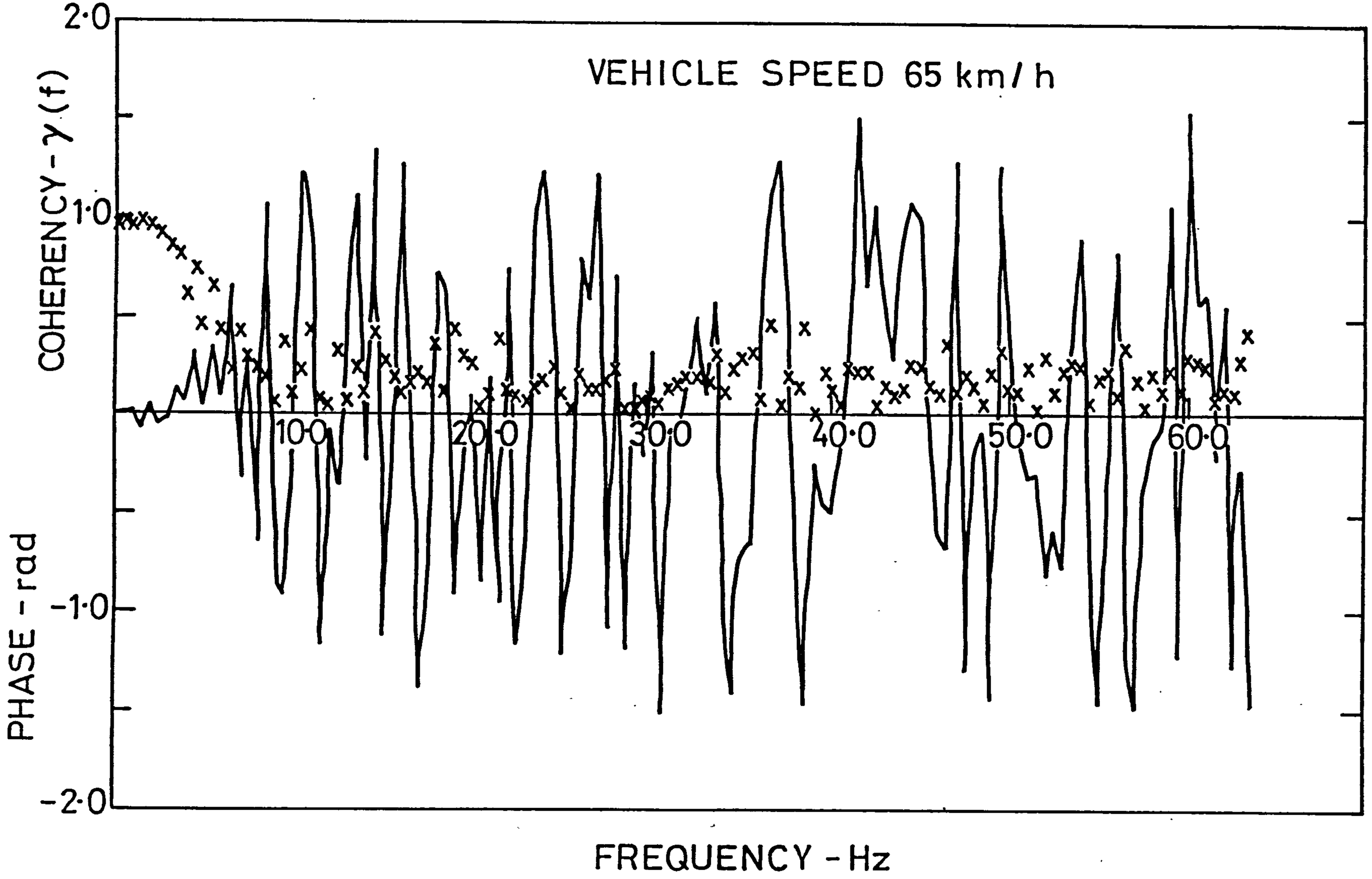

FIGURE 33. COHERENCY [x] & PHASE OF LEFT & RIGHT SYNTHESIZED PROFILES AS INPUT TO VEHICLE MODEL.

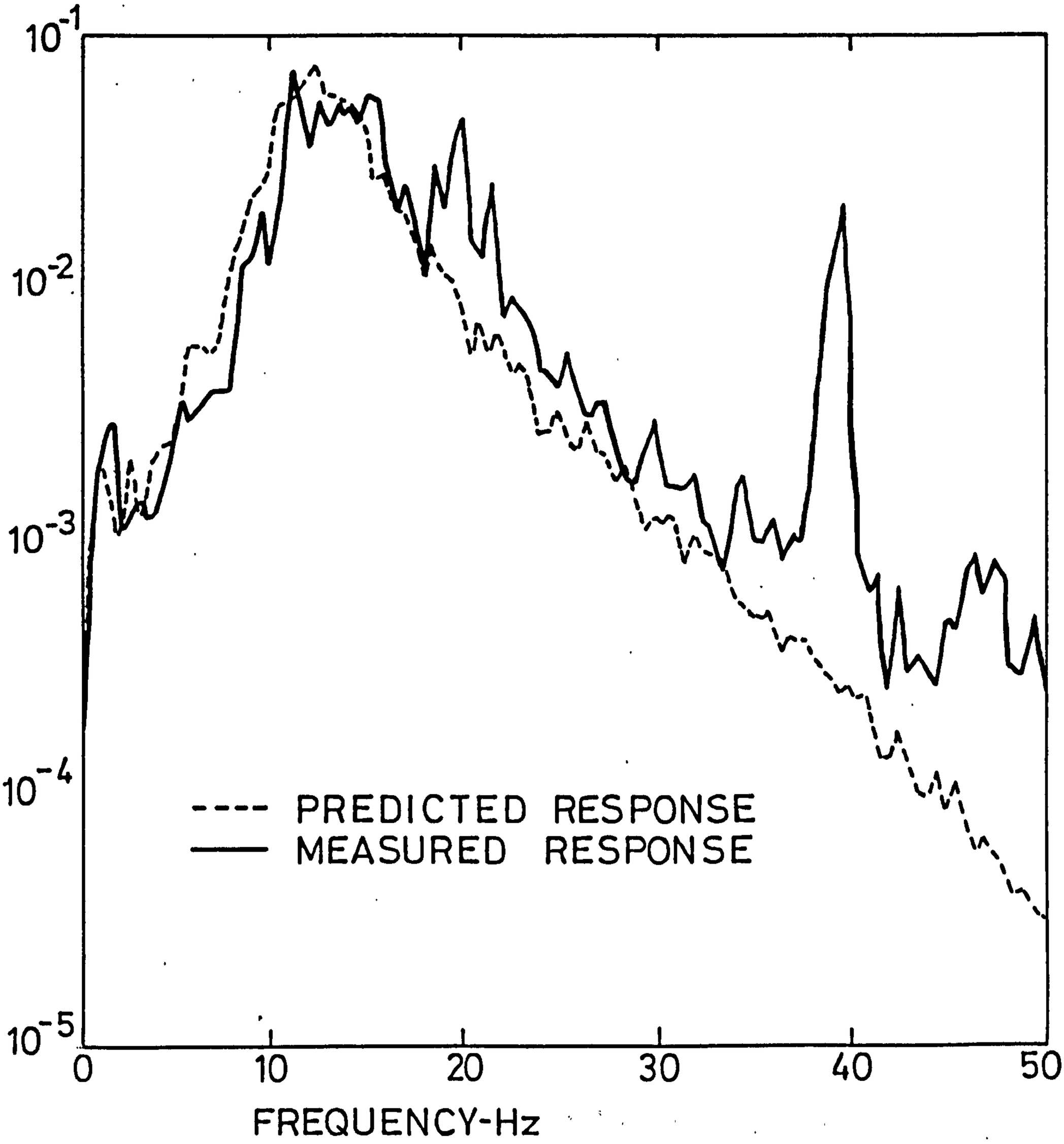

FIGURE 34. PREDICTED & MEASURED ACCELERATION SPECTRA FOR LEFT HAND FRONT AXLE.

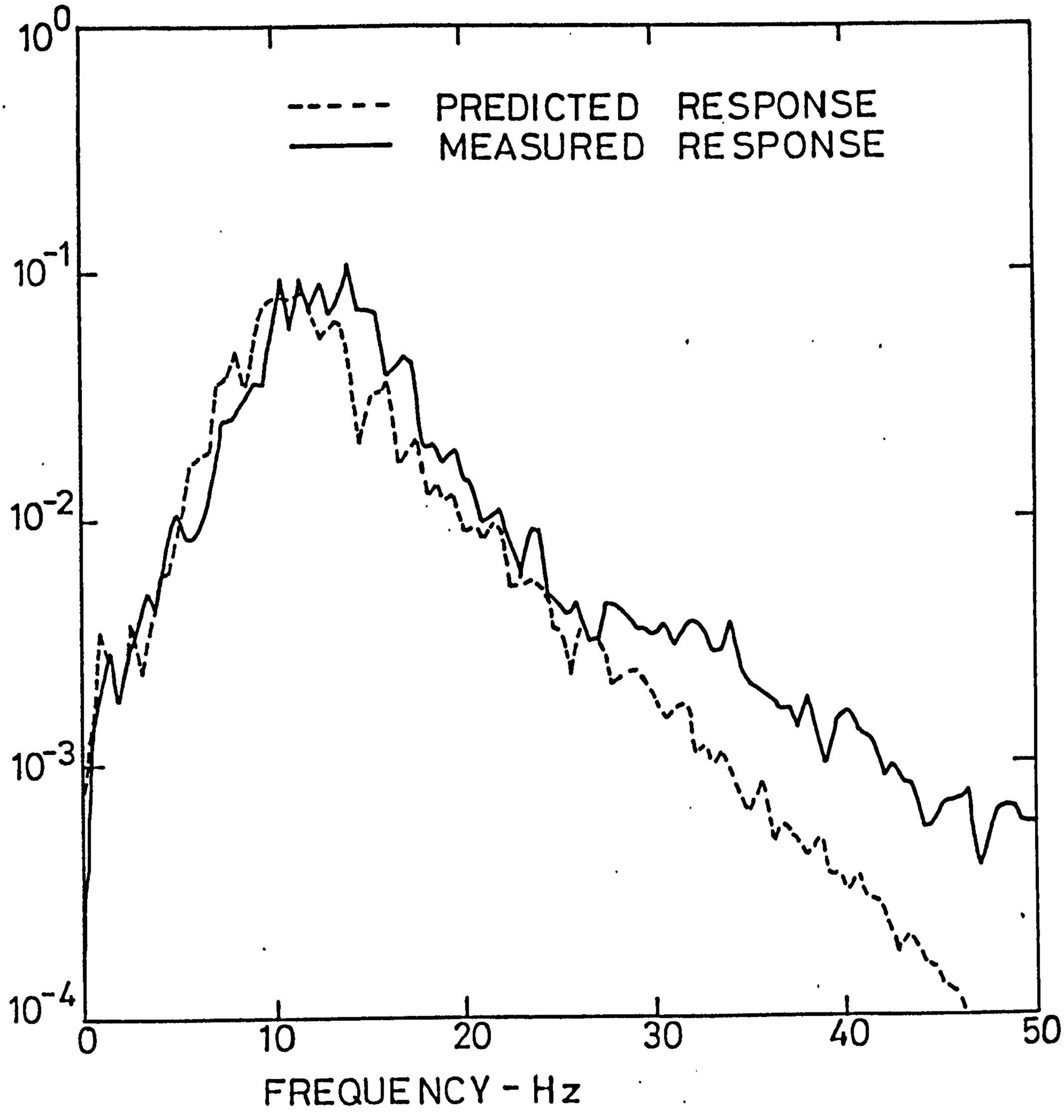

FIGURE 35. PREDICTED AND MEASURED RESPONSE SPECTRA OF RIGHT HAND REAR AXLE.

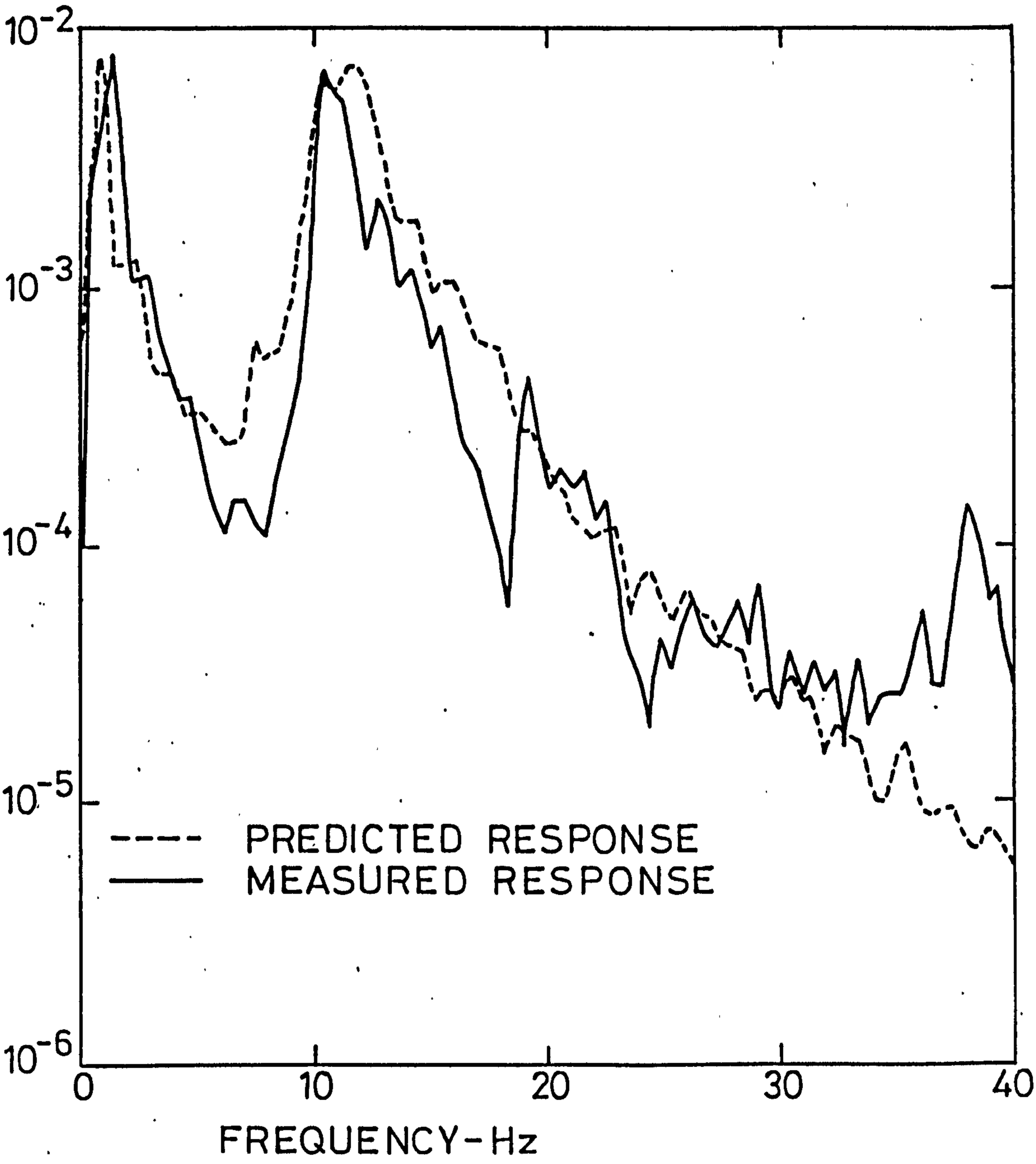

FIGURE 36. PREDICTED AND MEASURED RESPONSE SPECTRA OF RIGHT HAND FRONT BODY.

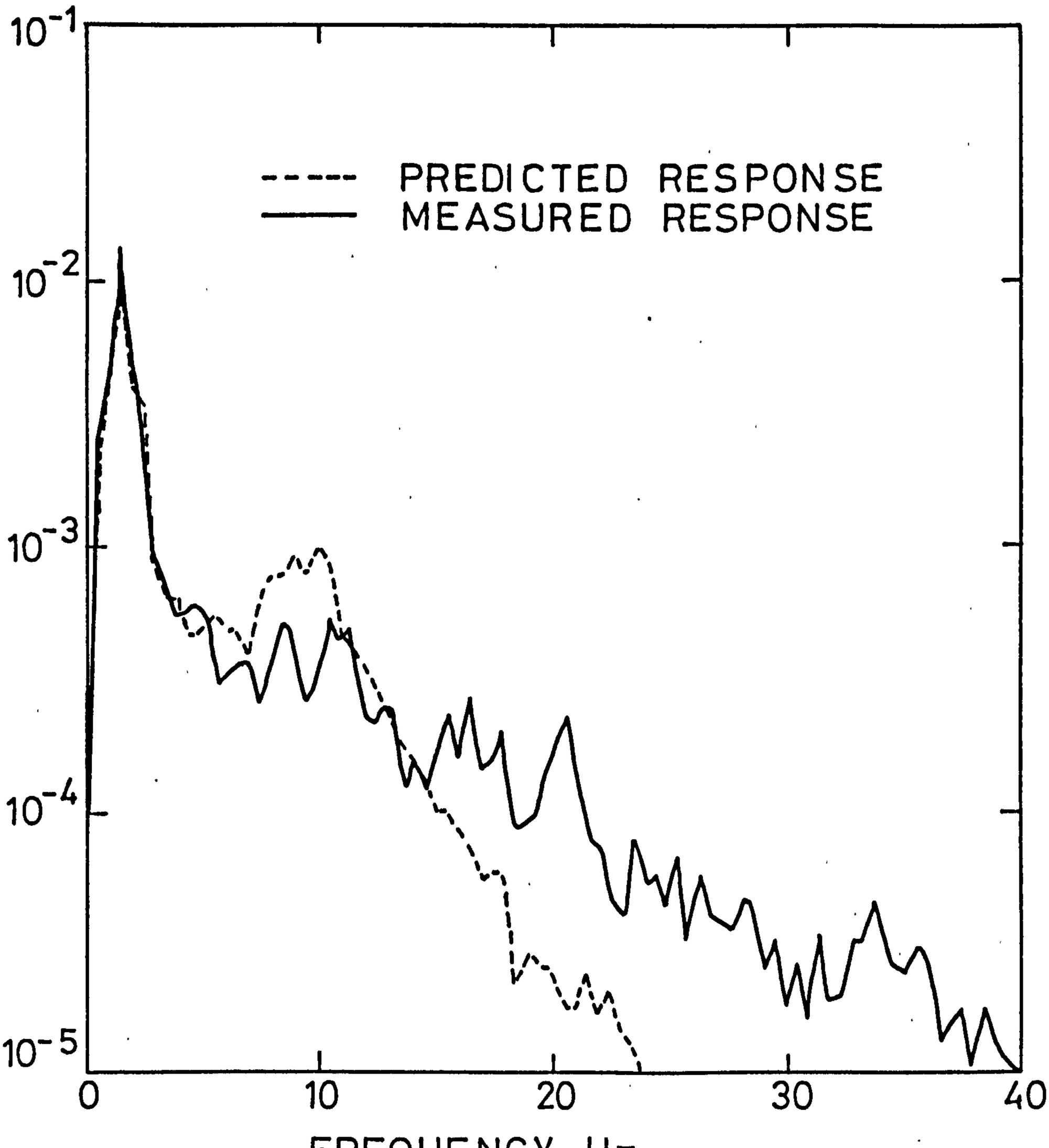

FIGURE 37. PREDICTED AND MEASURED RESPONSE SPECTRA OF LEFT HAND REAR BODY.

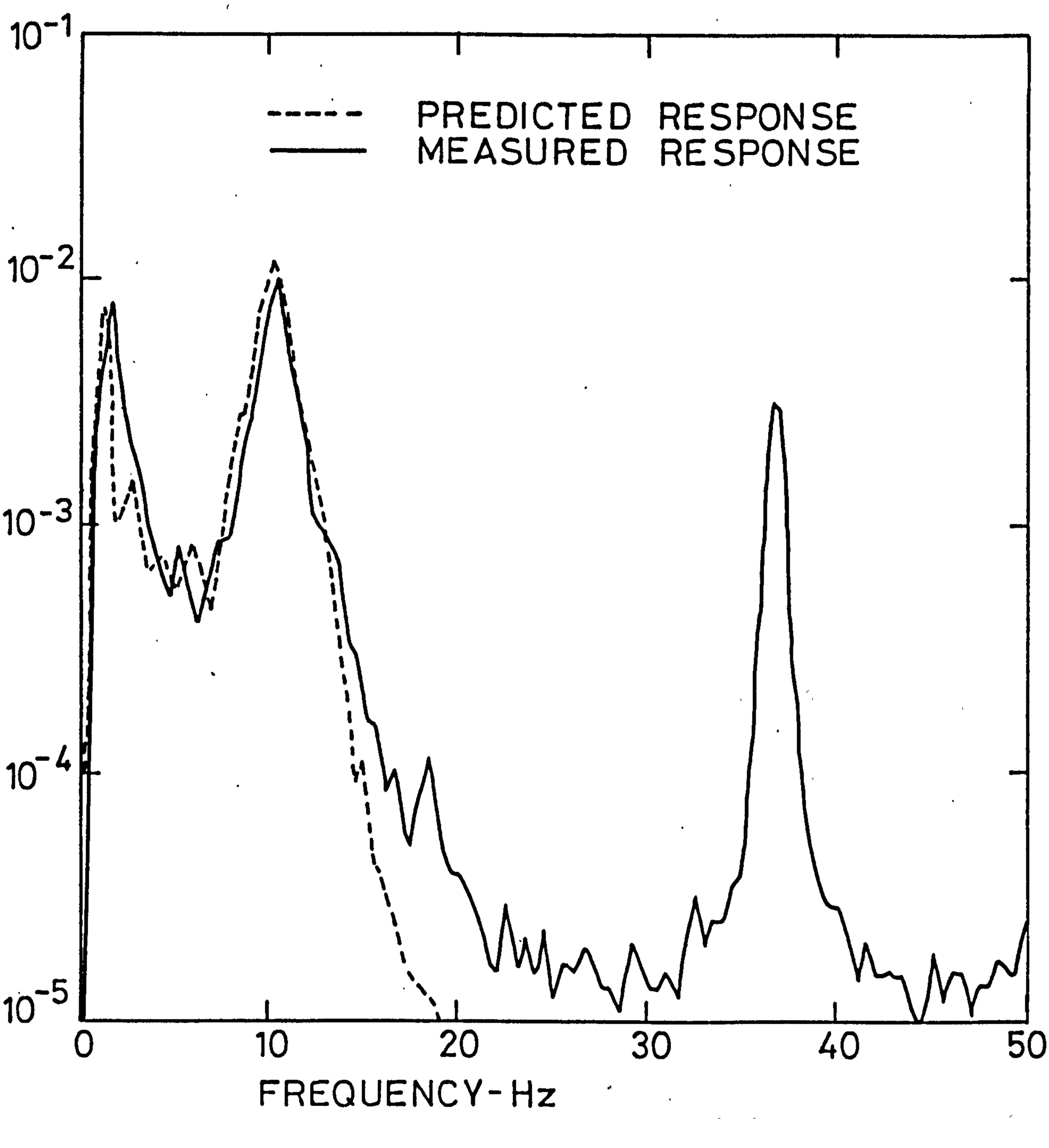

FIGURE 38. PREDICTED AND MEASURED RESPONSE SPECTRA OF RIGHT HAND ENGINE MOUNT.

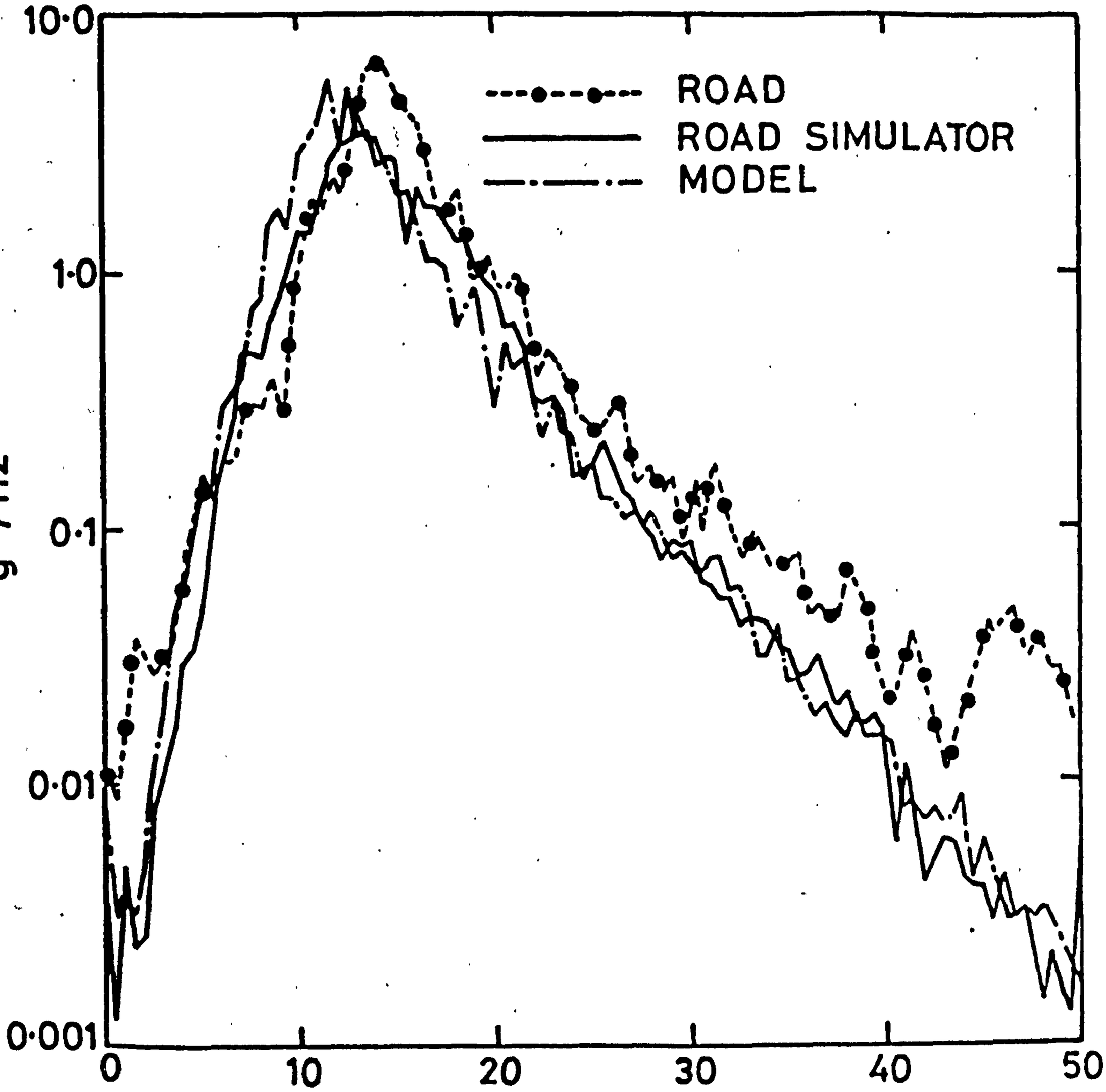

FIGURE 39. RELATIVE AXLE ACCELERATION SPECTRA FROM ROAD, ROAD SIMULATOR AND MATHEMATICAL MODEL.

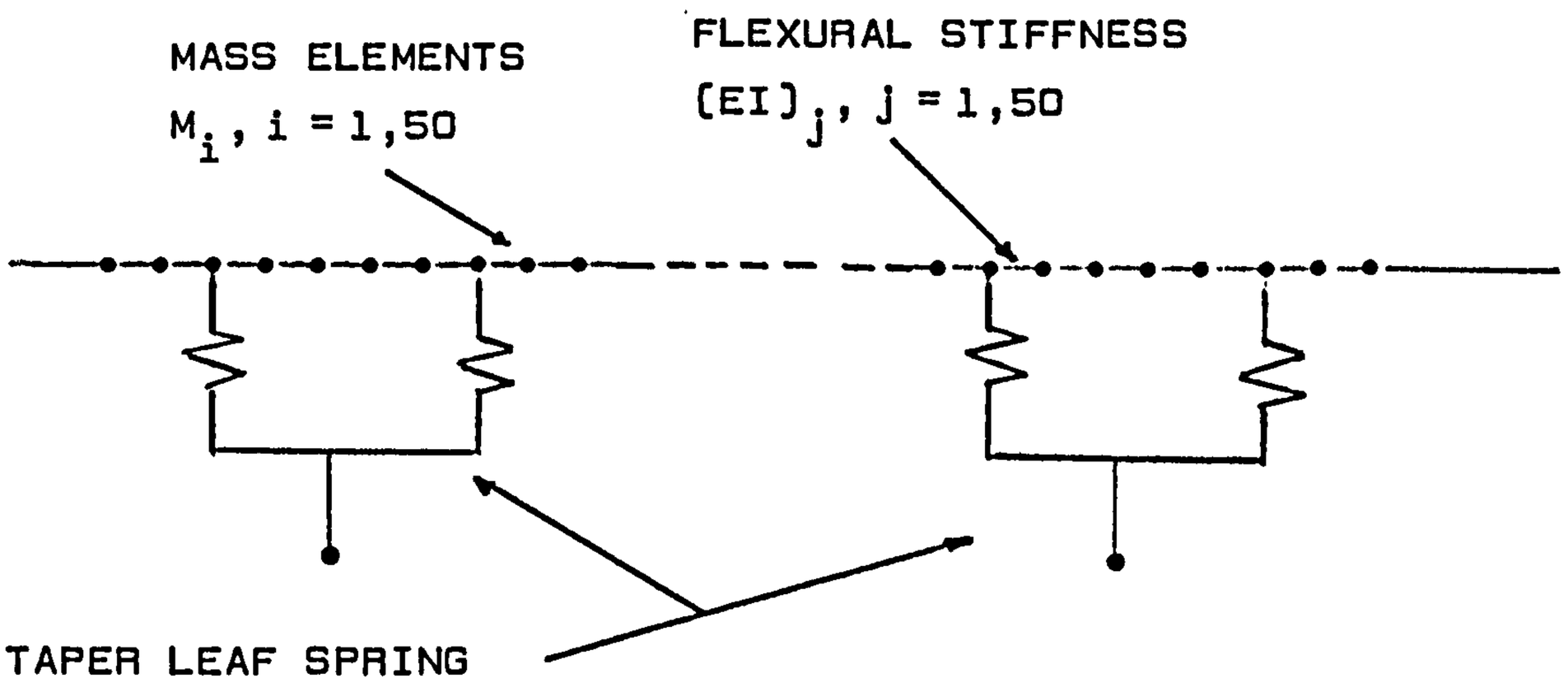

- FRAME IDEALISATION - 50 MASS/STIFFNESS ELEMENTS.
- NO TYRES/AXLES INCORPORATED.
- CAB/ENGINE MASS INCLUDED BUT NOT DYNAMICS.

FIGURE 40

MATHEMATICAL MODEL OF TRACTOR FRAME
(TRANSFER MATRIX APPROACH)

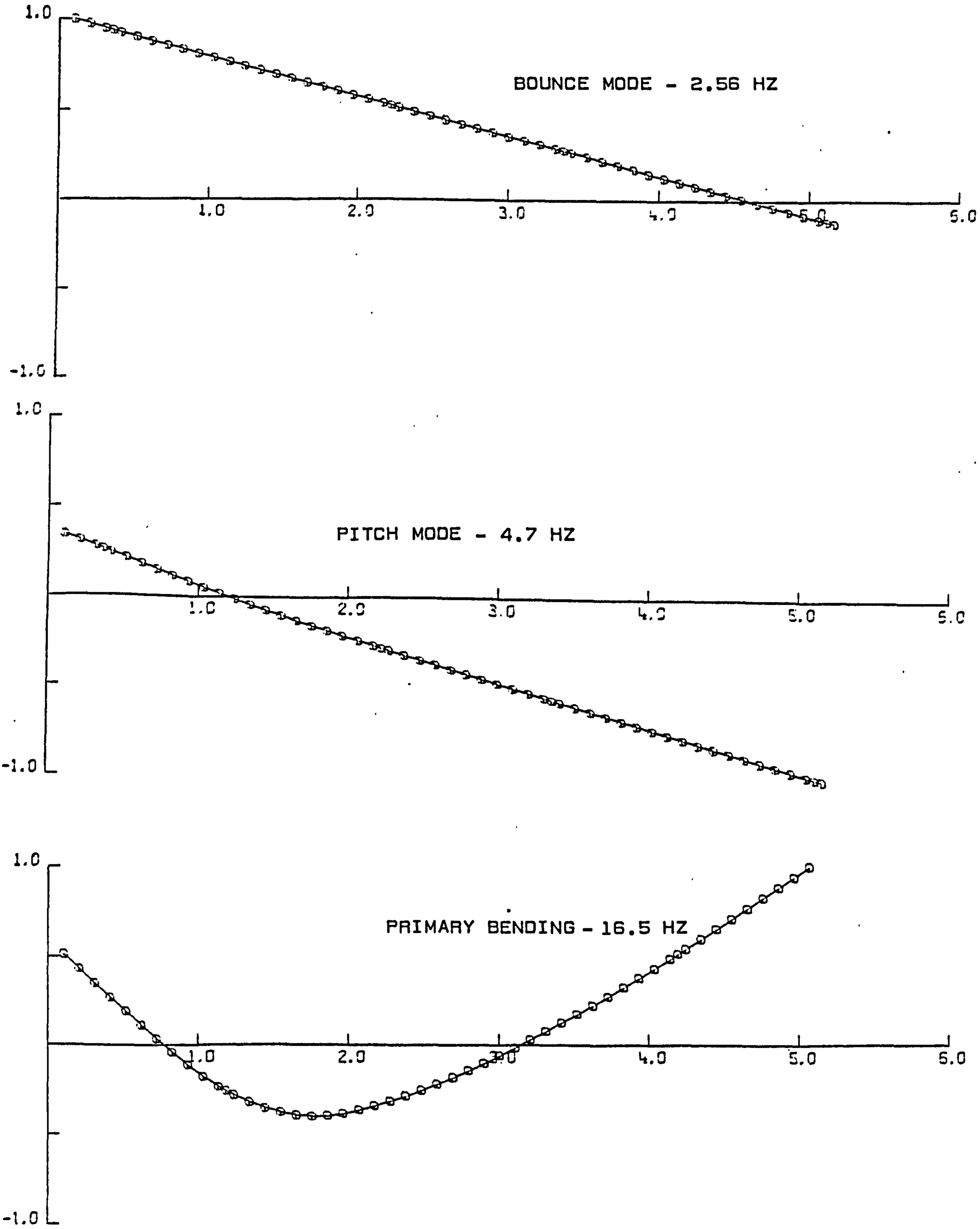

FIGURE 41

TRACTOR UNIT MODE SHAPES

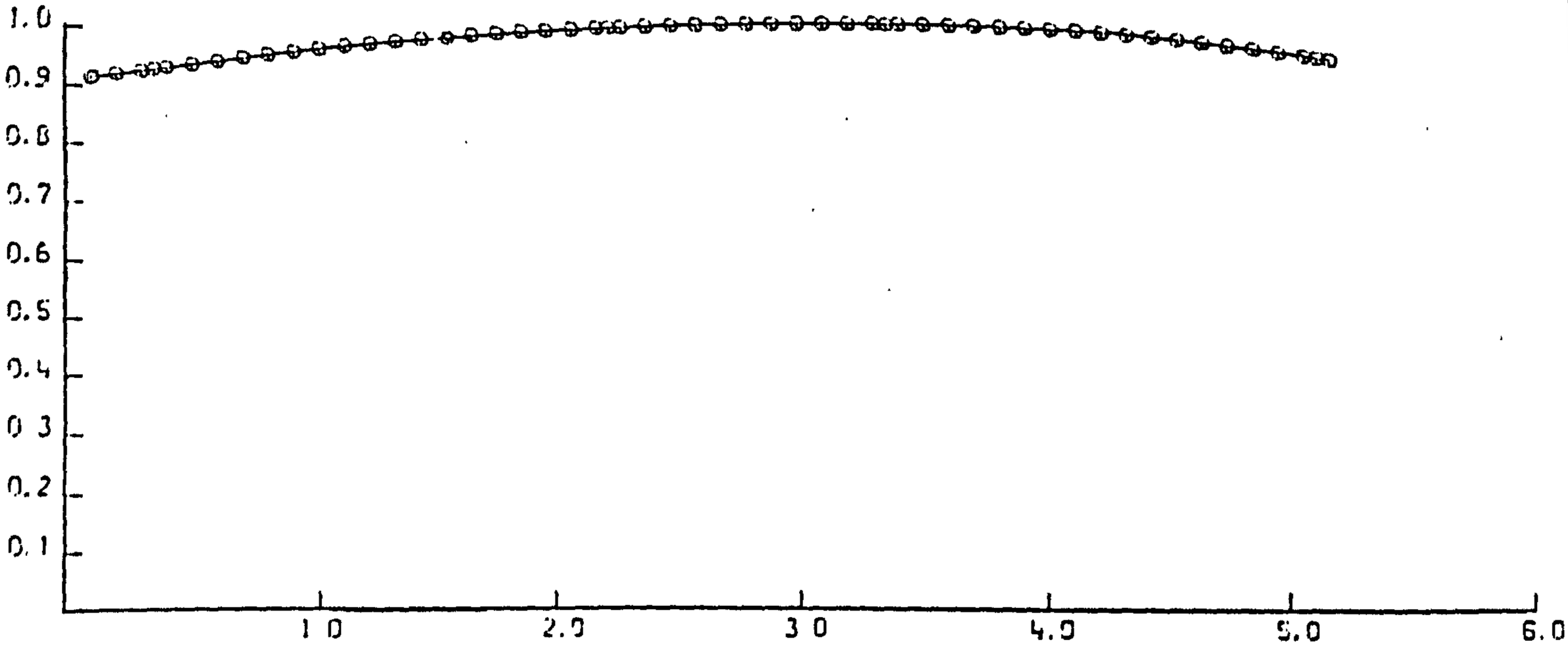

BOUNCE MODE AT 2.14 HZ

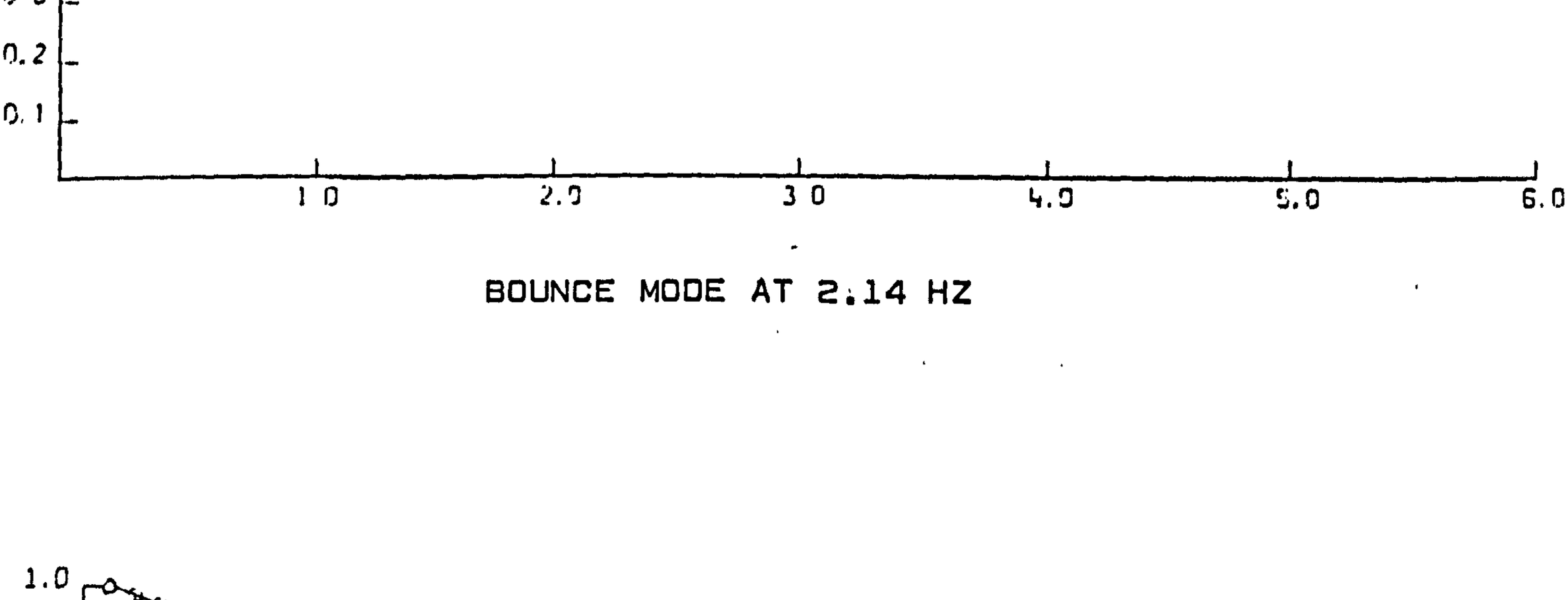

PITCH MODE AT 3.48 HZ

FIGURE 42

TRACTOR RIGID BODY MODES WITH
TRAILER REACTION MASS ADDED

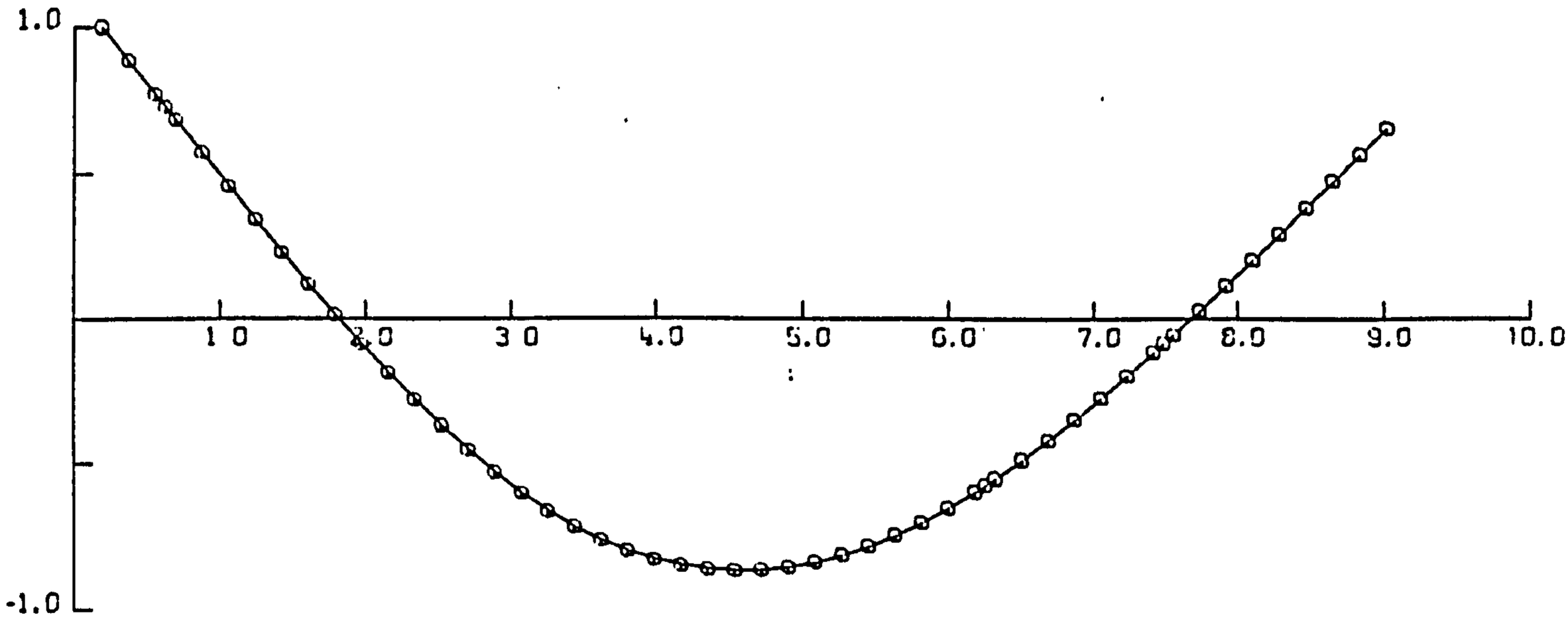

TRAILER BENDING FREQ -6.45HZ

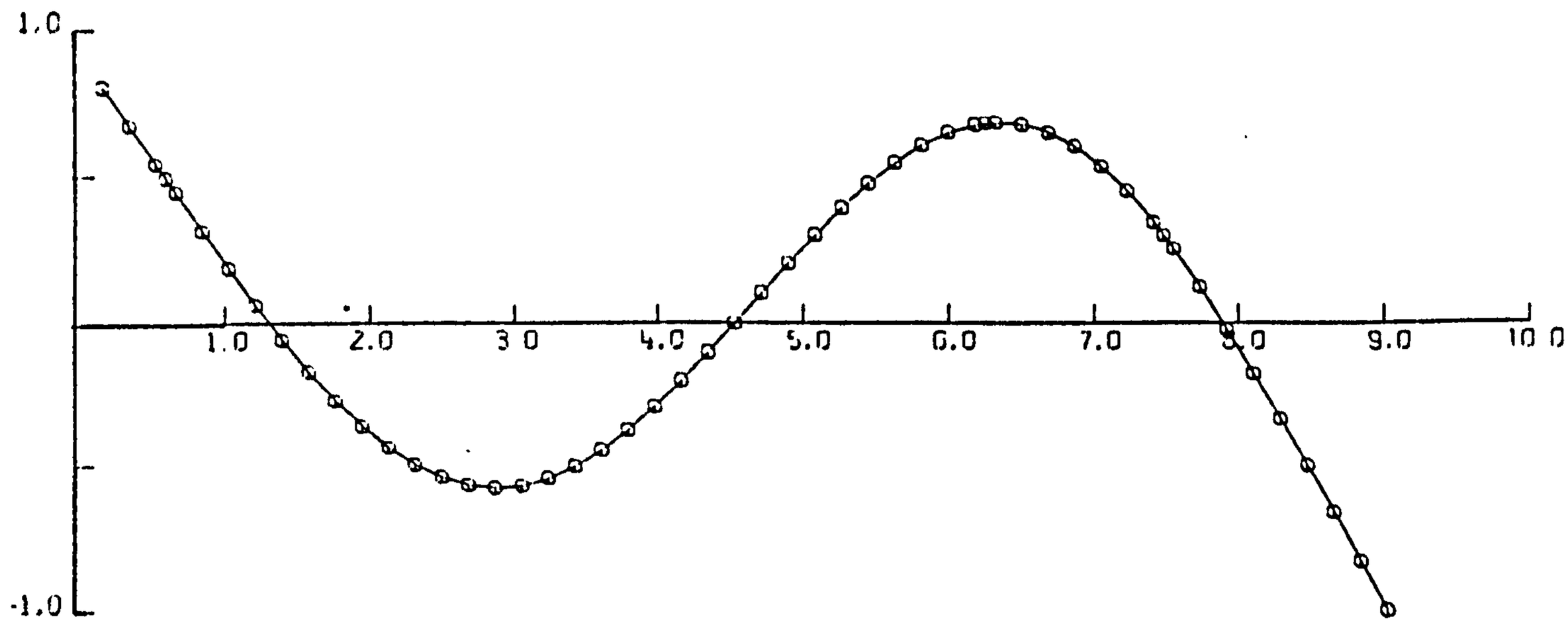

TRAILER 2ND BENDING 14.1HZ

FIGURE 43

TRAILER BENDING MODES

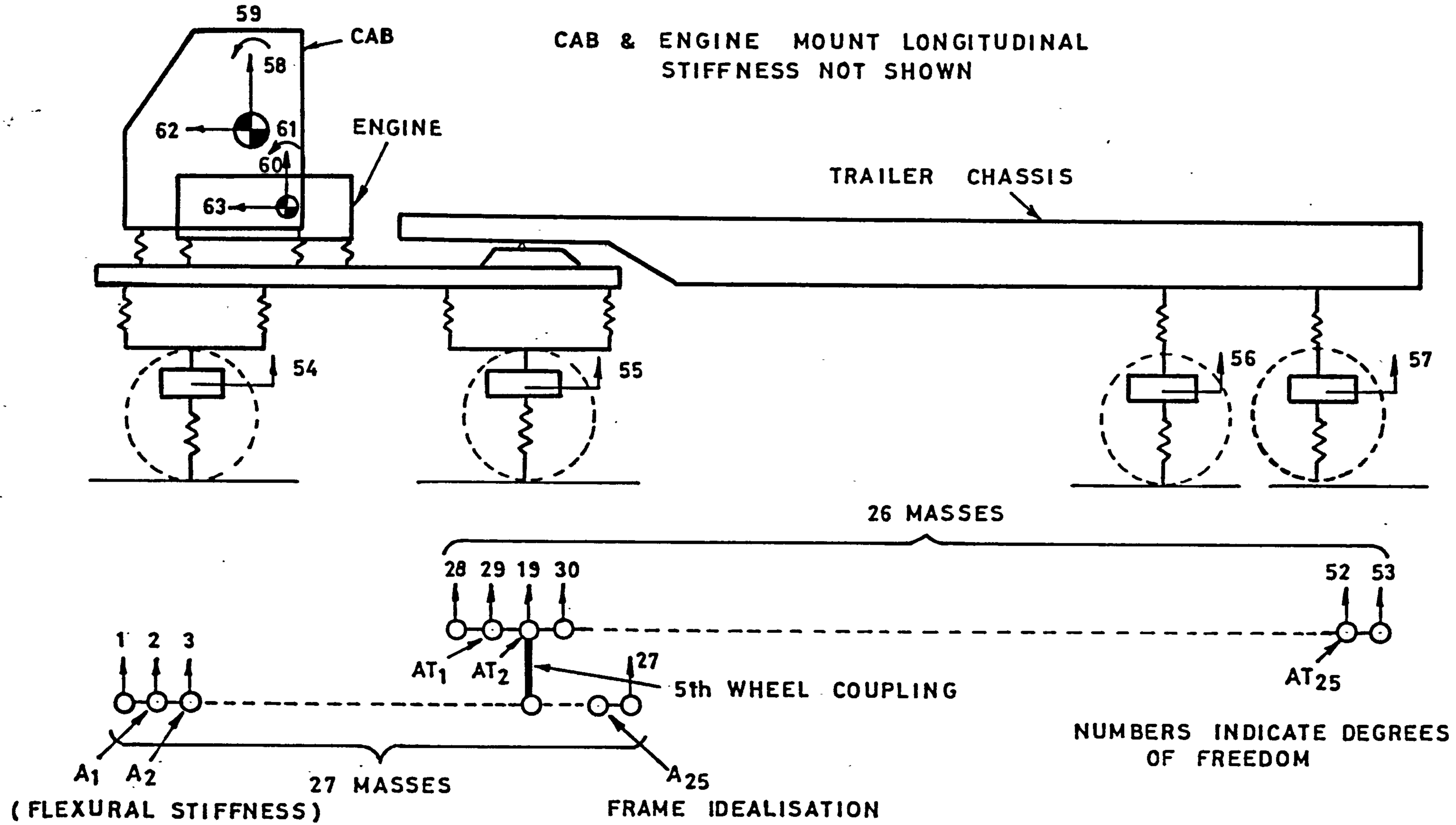

FIGURE 44. 2-D 63 DEGREE OF FREEDOM TRACTOR-TRAILER MODEL SCHEMATIC.

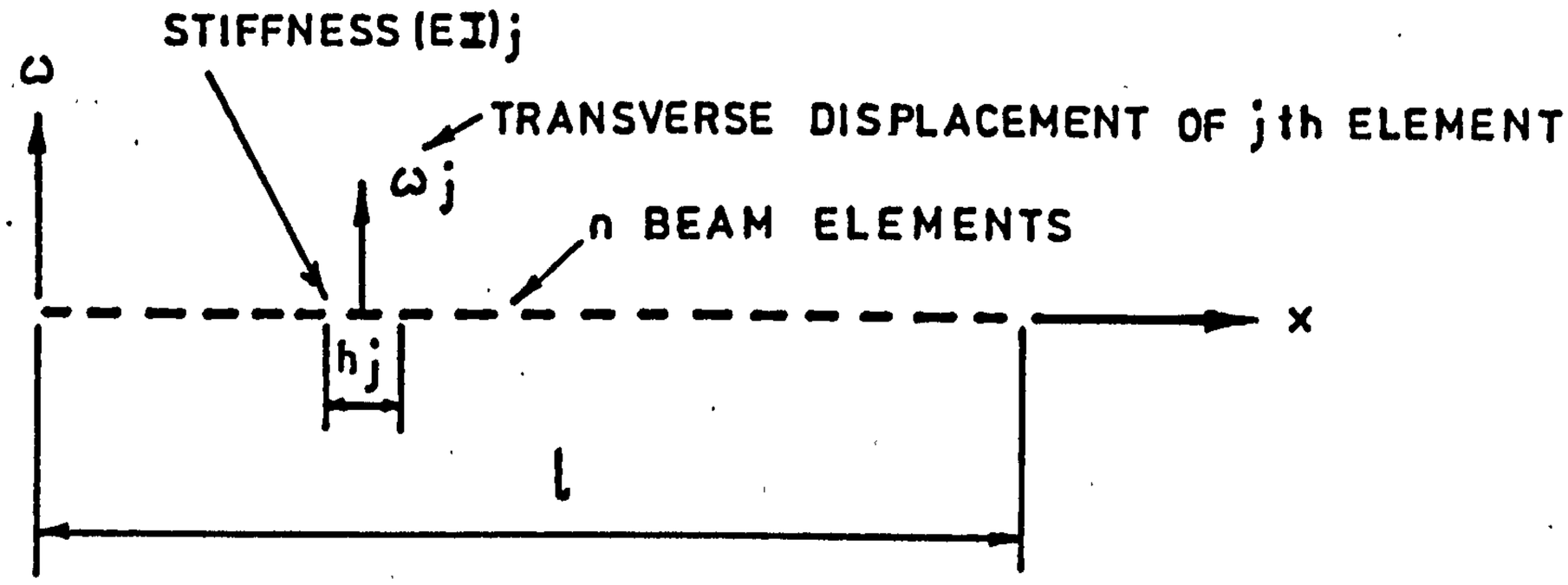

FIGURE 45(a). BEAM IDEALISATION.

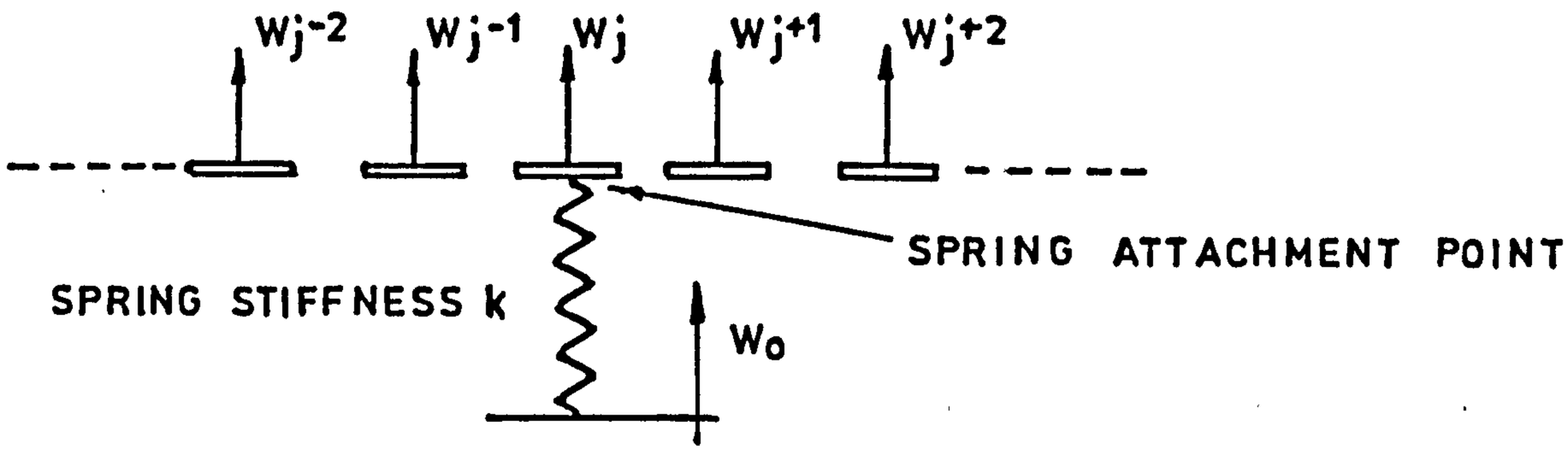

$$\ddot{W}_j = \left[2(A_{j-1}+A_j)W_{j-1} + 2(A_j + A_{j+1})W_{j+1} - A_{j-1}W_{j-2} - (A_{j-1}+4A_j+A_{j+1})W_j - A_{j+1}W_{j+2} - k(W_j - W_o)\right] / M_j$$

FIGURE 45 (b).
ADJUSTMENT TO DIFFERENTIAL EQUATION DUE TO SPRING ATTACHMENT.

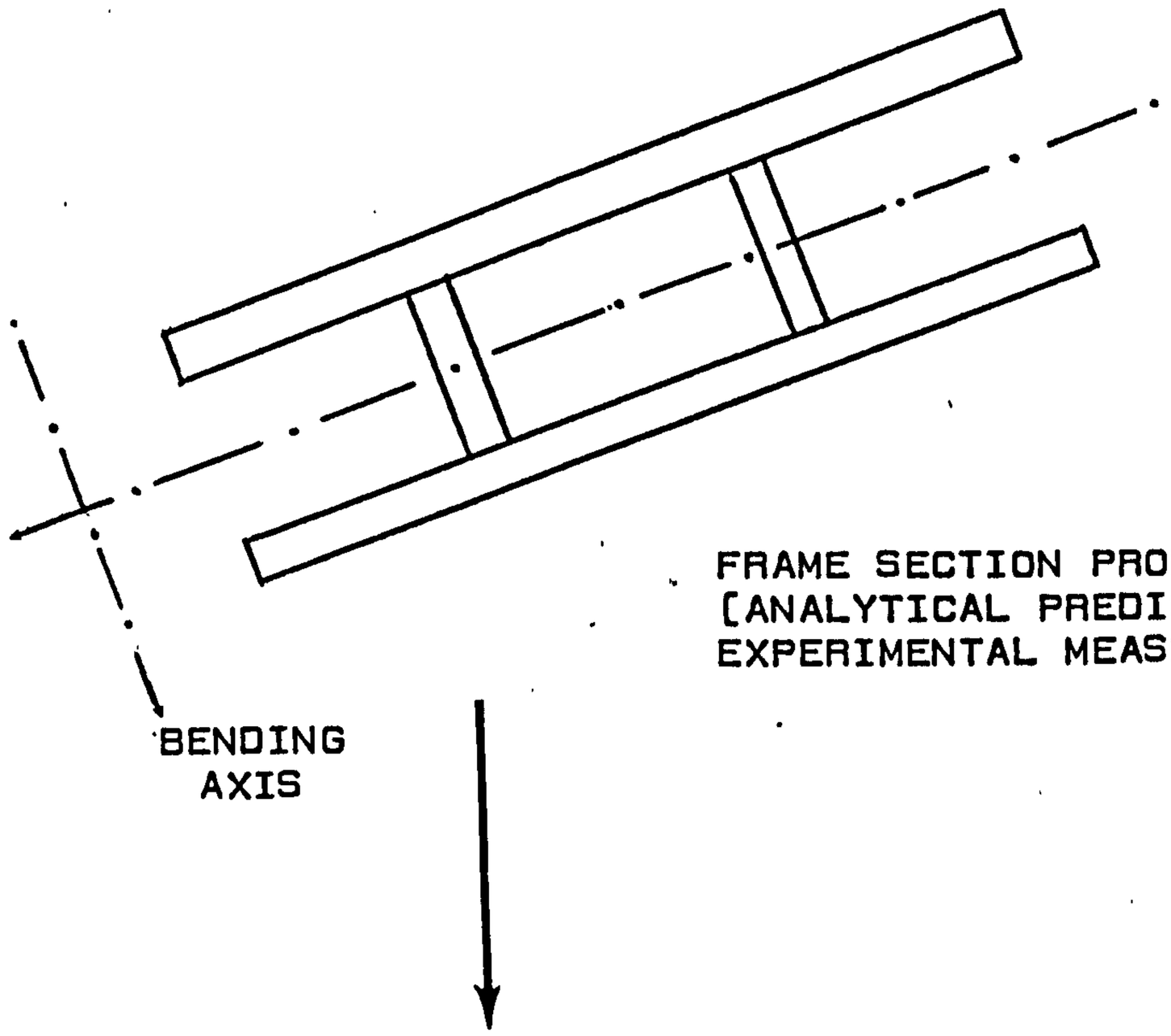

FRAME SECTION PROPERTIES
[ANALYTICAL PREDICTION OR
EXPERIMENTAL MEASUREMENT]

MATHEMATICAL
IDEALISATION:

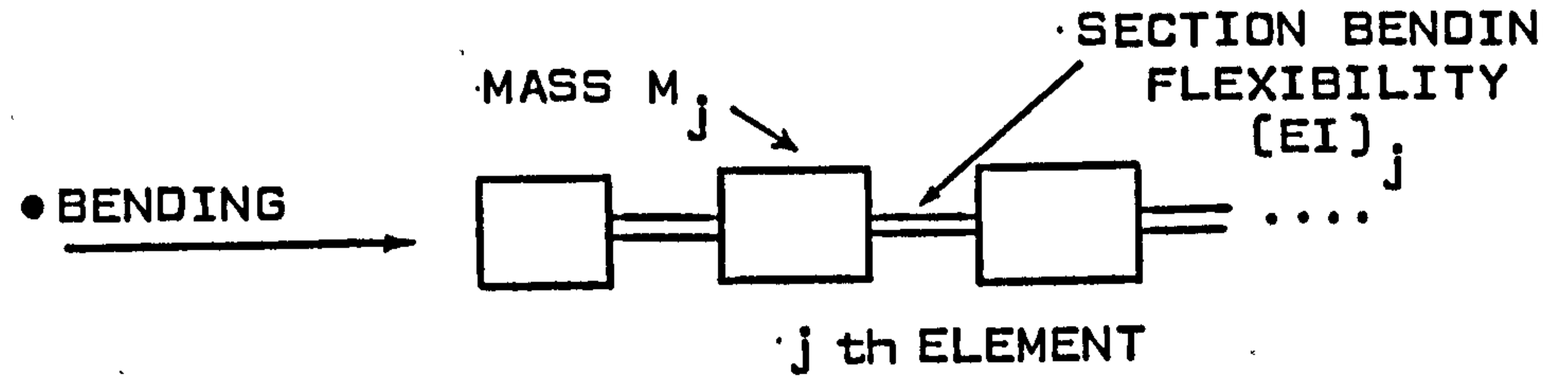

FIGURE 46 INCLUSION OF TORSIONAL FLEXIBILITY INTO FRAME MODEL

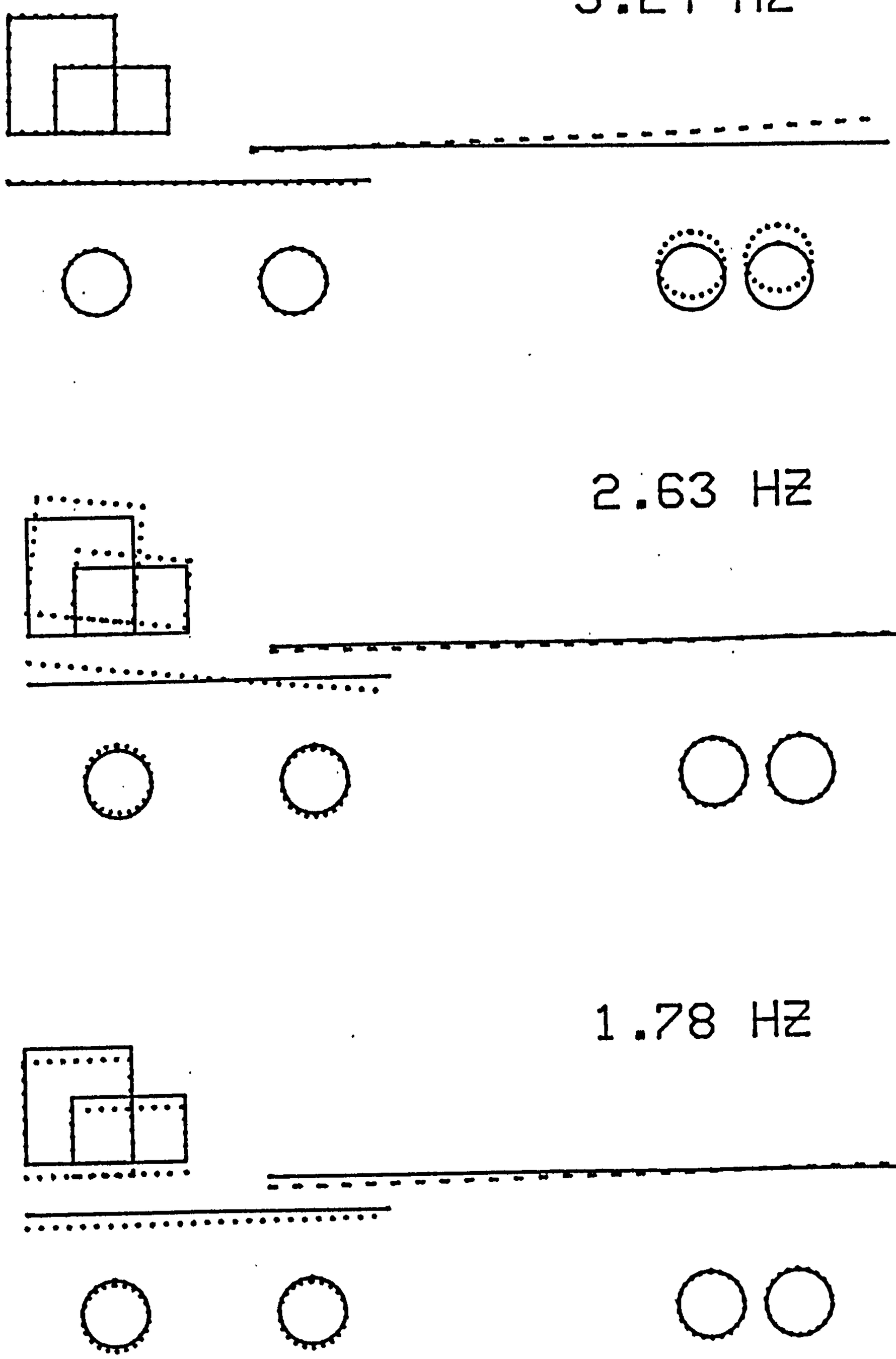

FIGURE 47 FULLY LADEN VEHICLE MODES

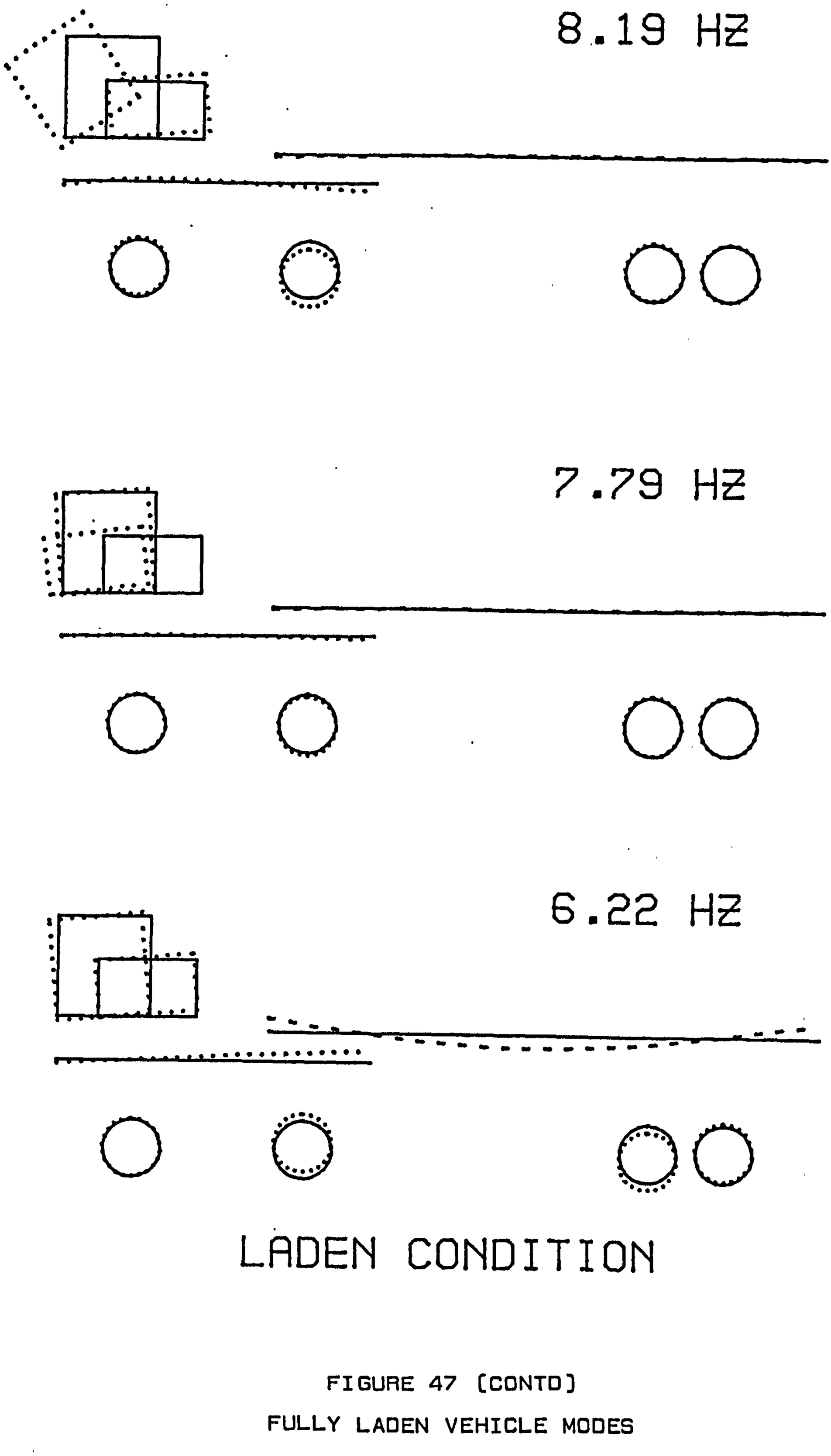

FIGURE 47 (CONTD)

FULLY LADEN VEHICLE MODES

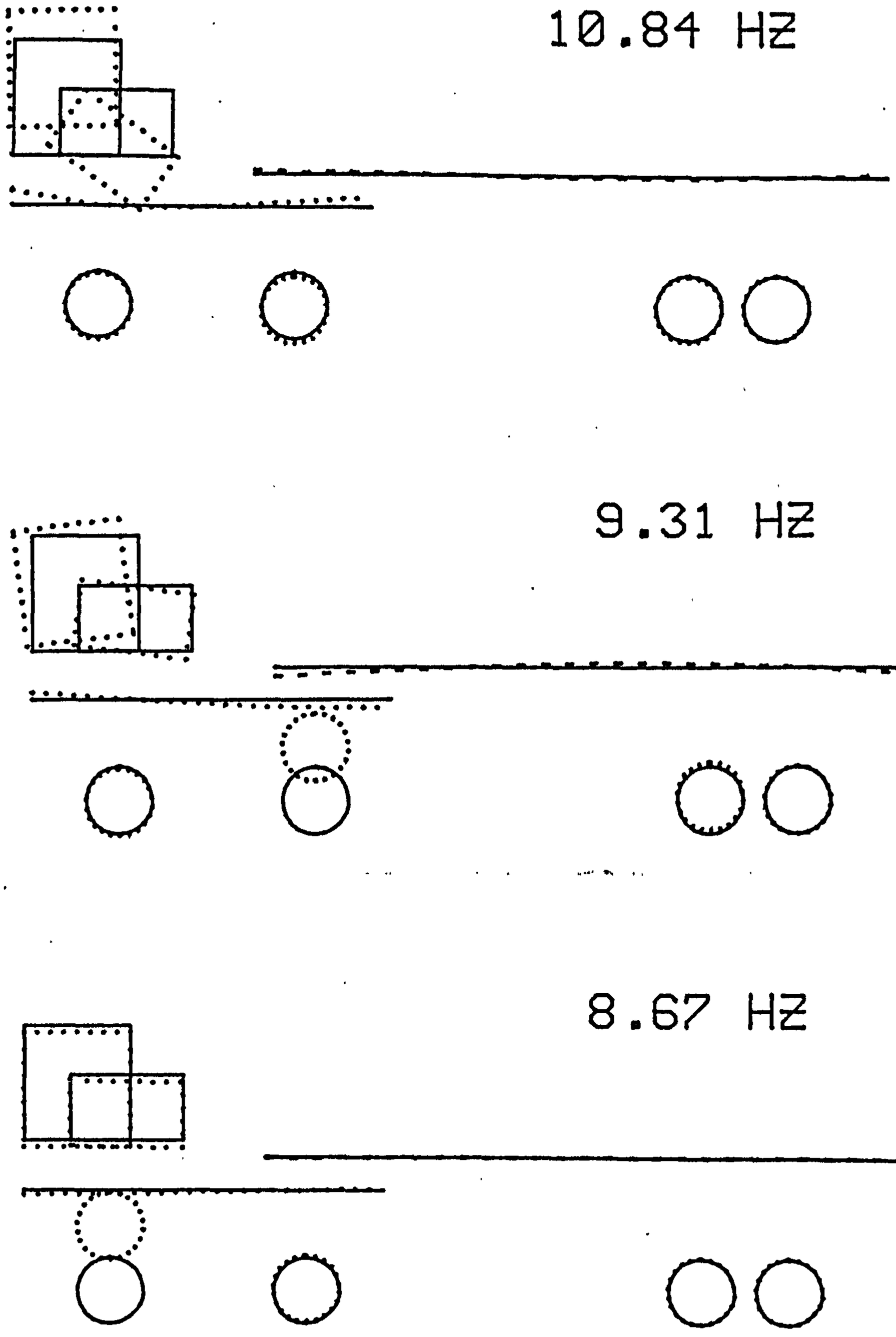

FIGURE 47 (CONTD)

FULLY LADEN VEHICLE MODES

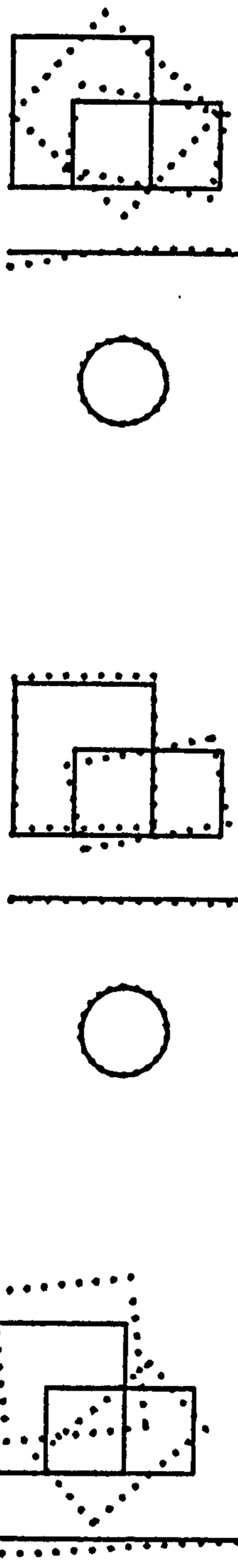

FIGURE 47 (CONTD)

FULLY LADEN VEHICLE MODES

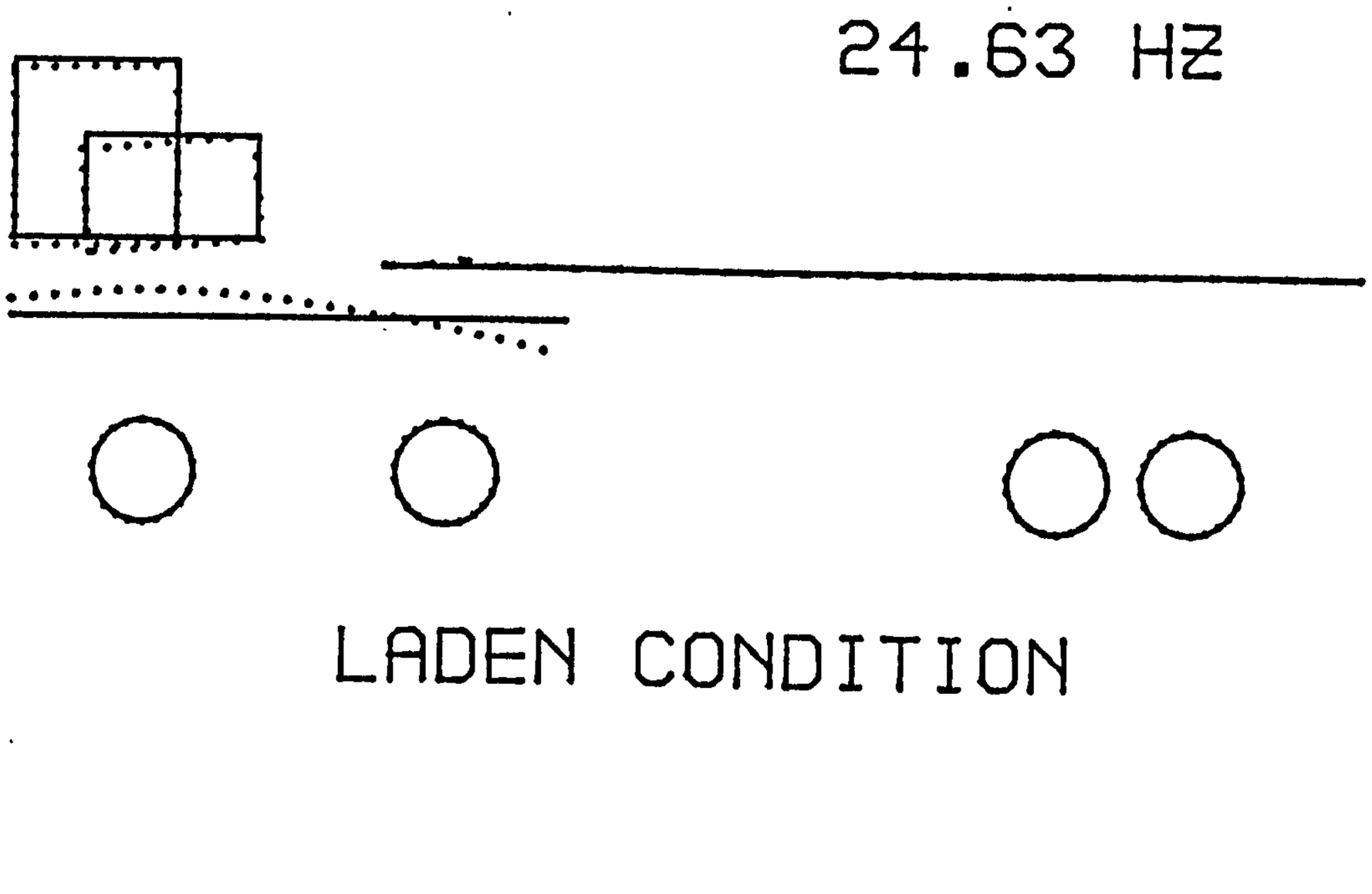

FIGURE 47 (CONTD)

FULLY LADEN VEHICLE MODES

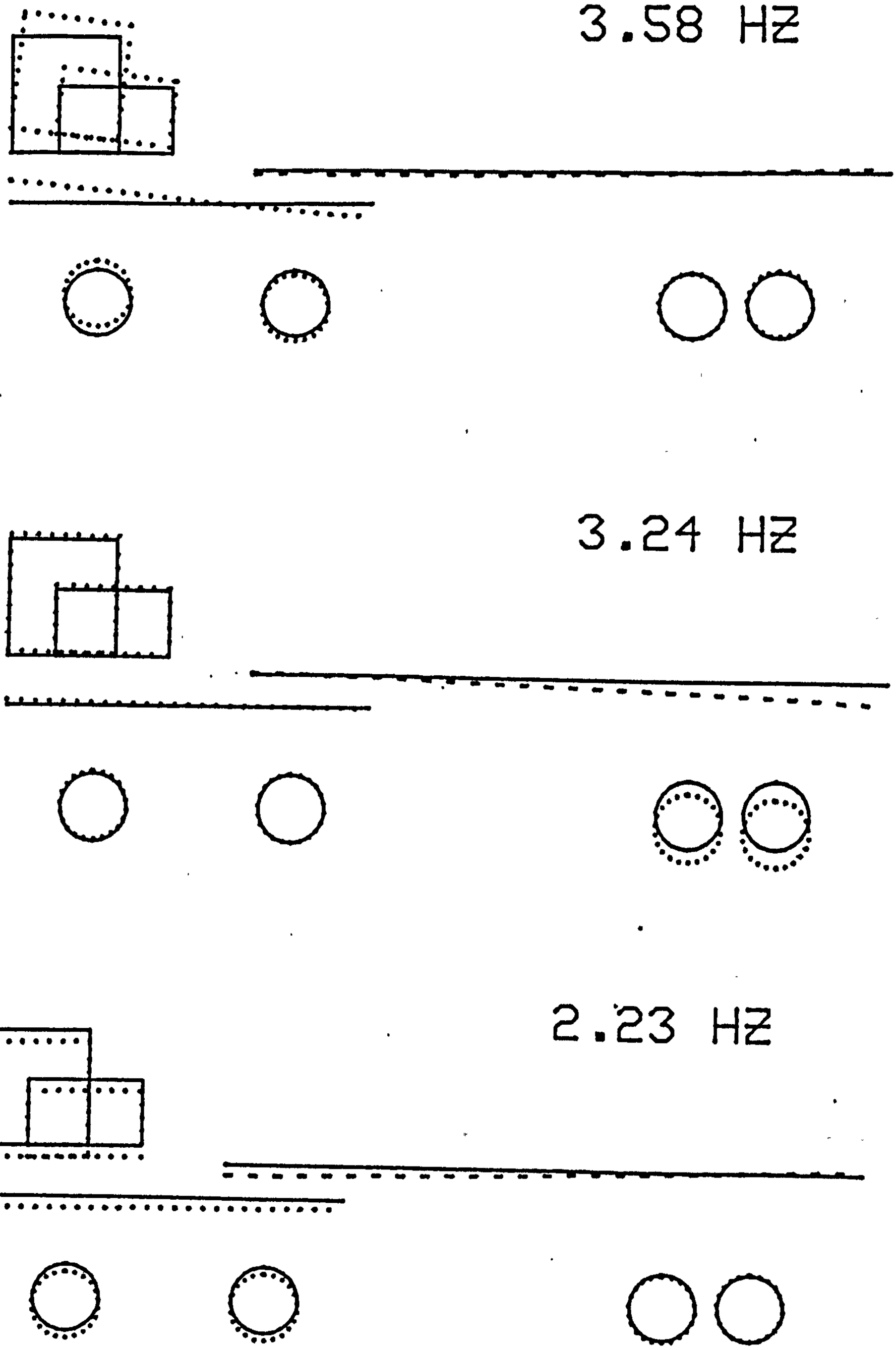

FIGURE 48

FULLY LADEN MODES (WITH SPRING FRICTION)

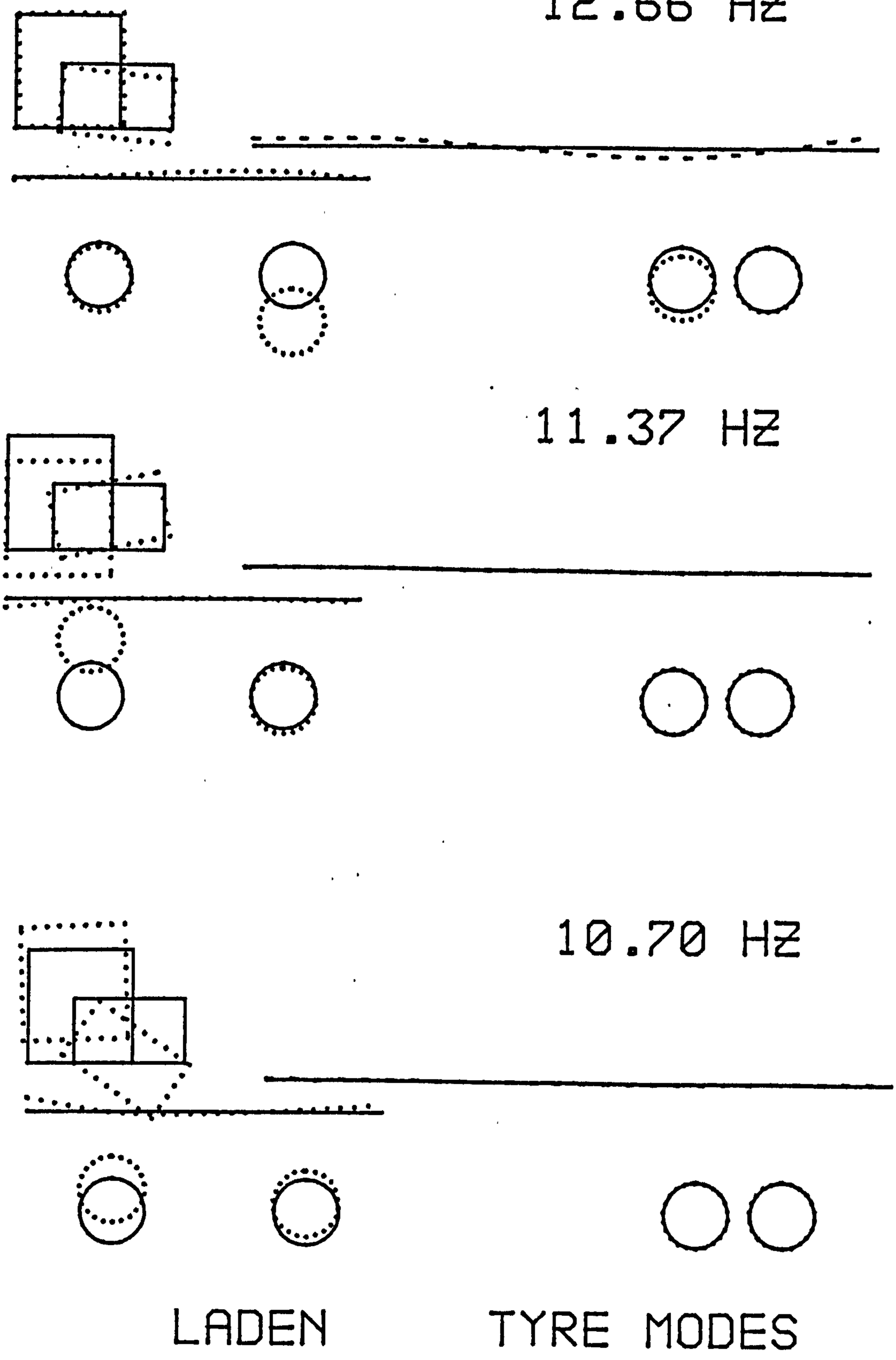

FIGURE 48 (CONTD)

FULLY LADEN MODES (WITH SPRING FRICTION)

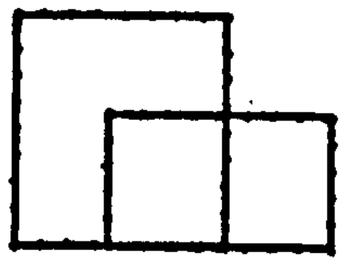

5.42 HZ

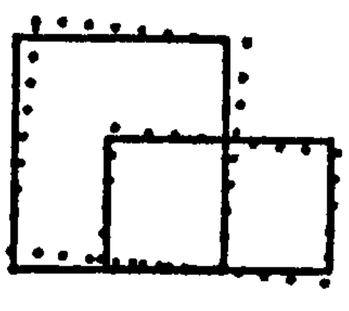

3.93 HZ

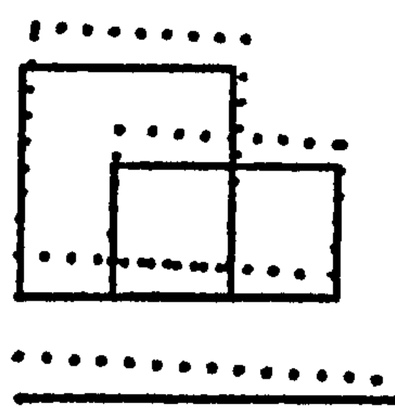

2.27 HZ

UNLADEN

FIGURE 49 UNLADEN MODES

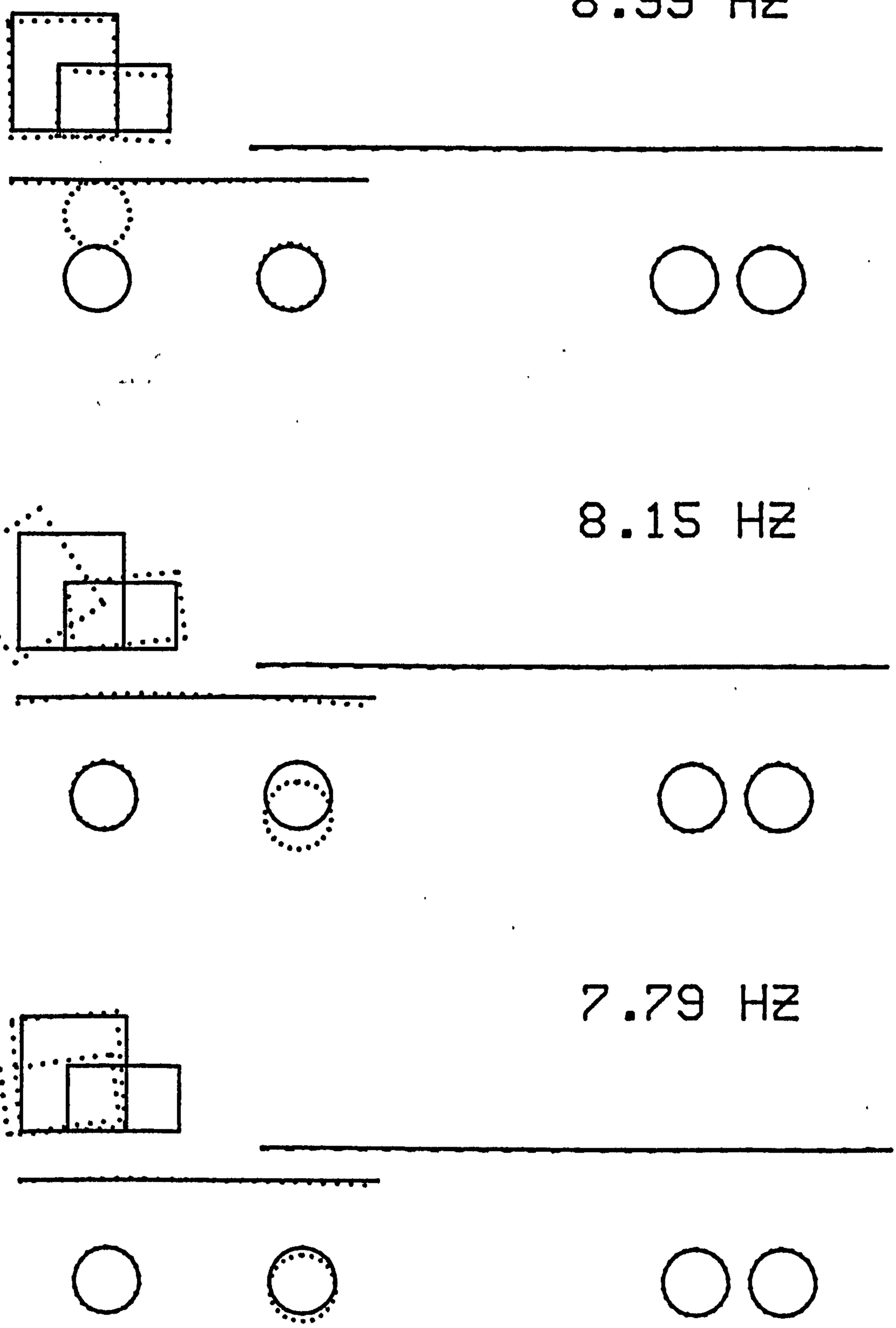

FIGURE 49 [CONTD] UNLADEN MODES

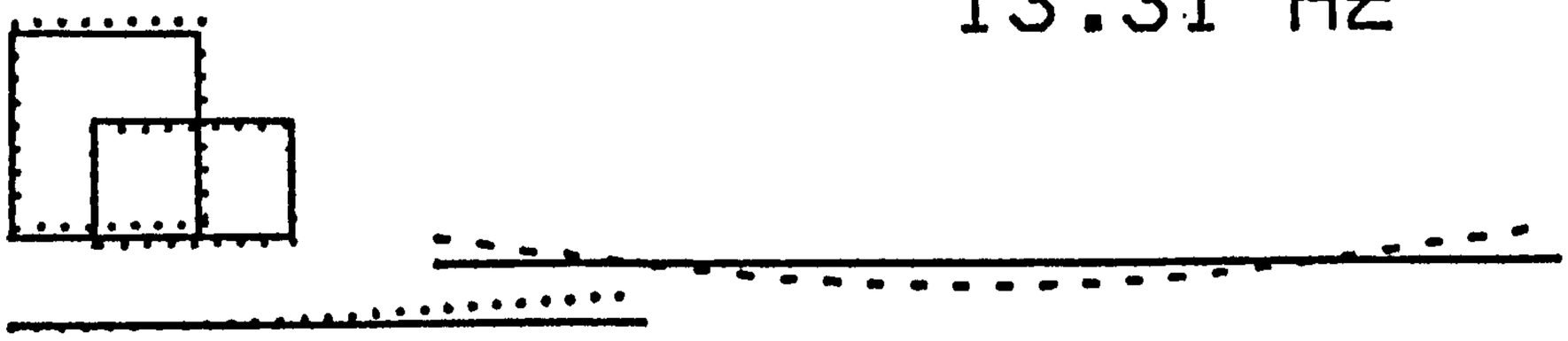

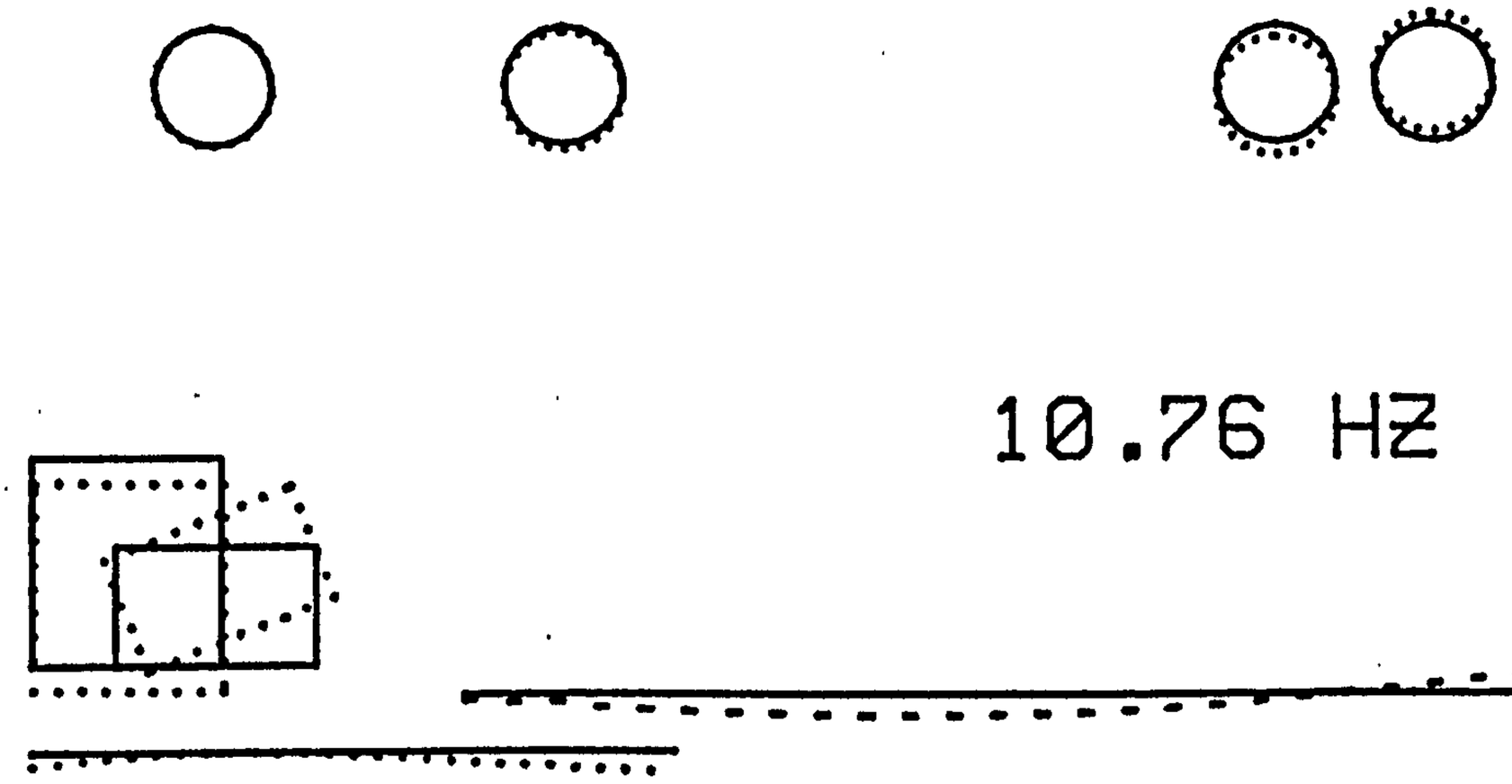

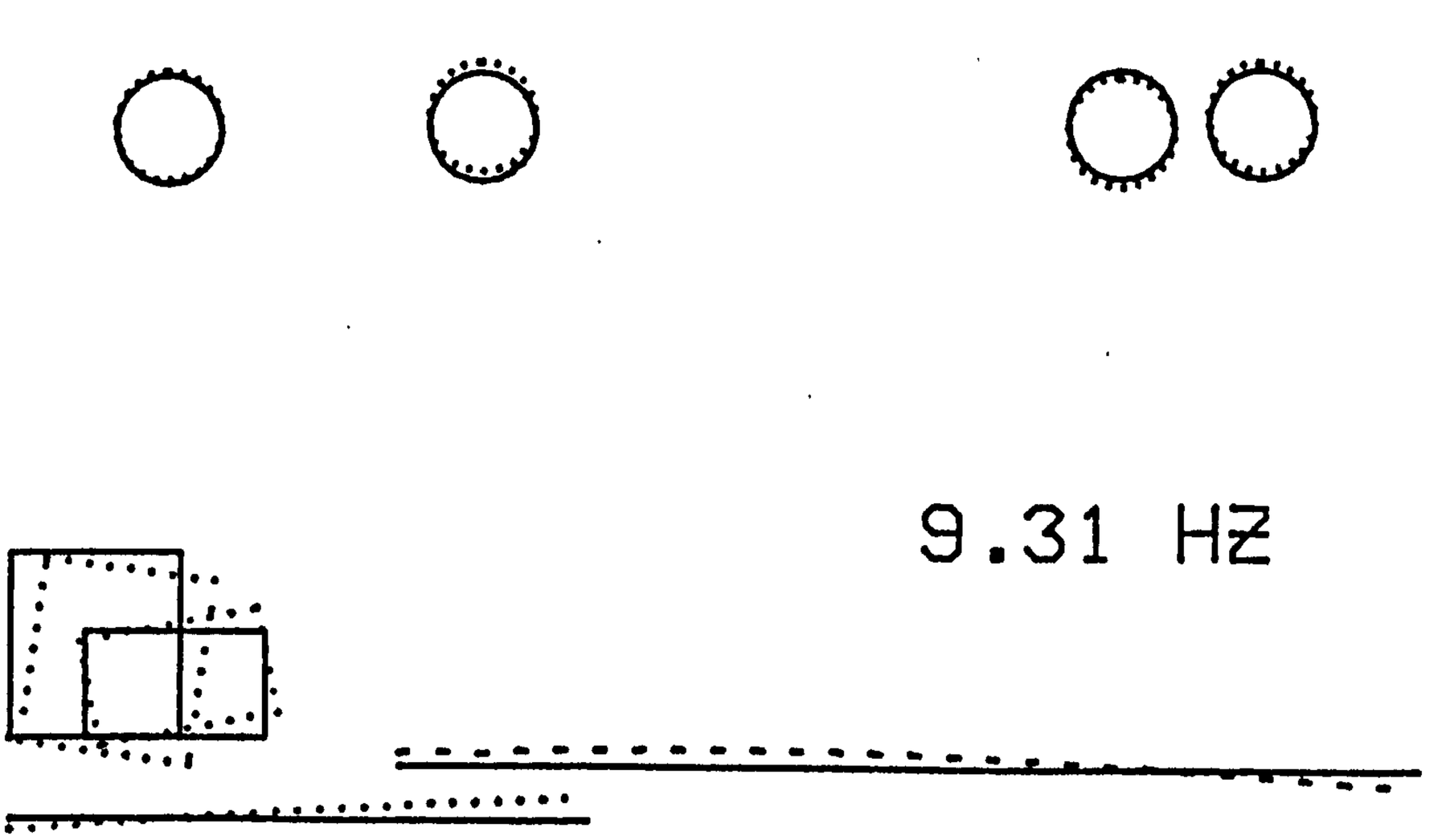

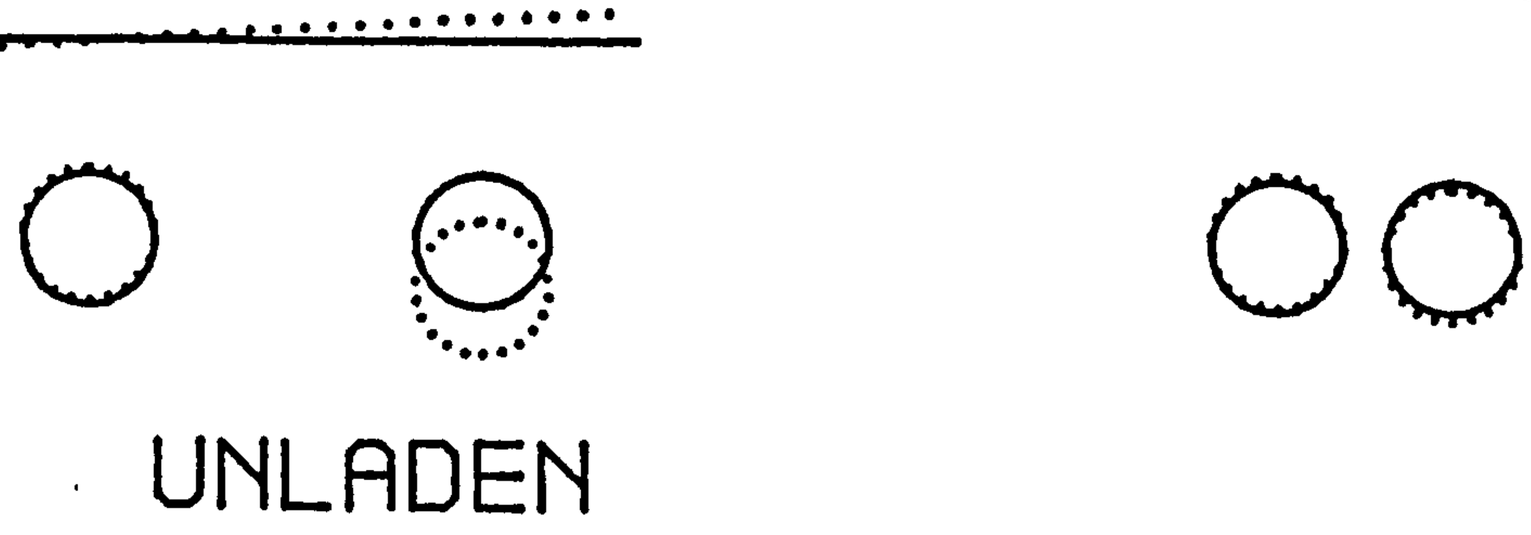

FIGURE 49 [CONTD] UNLADEN MODES

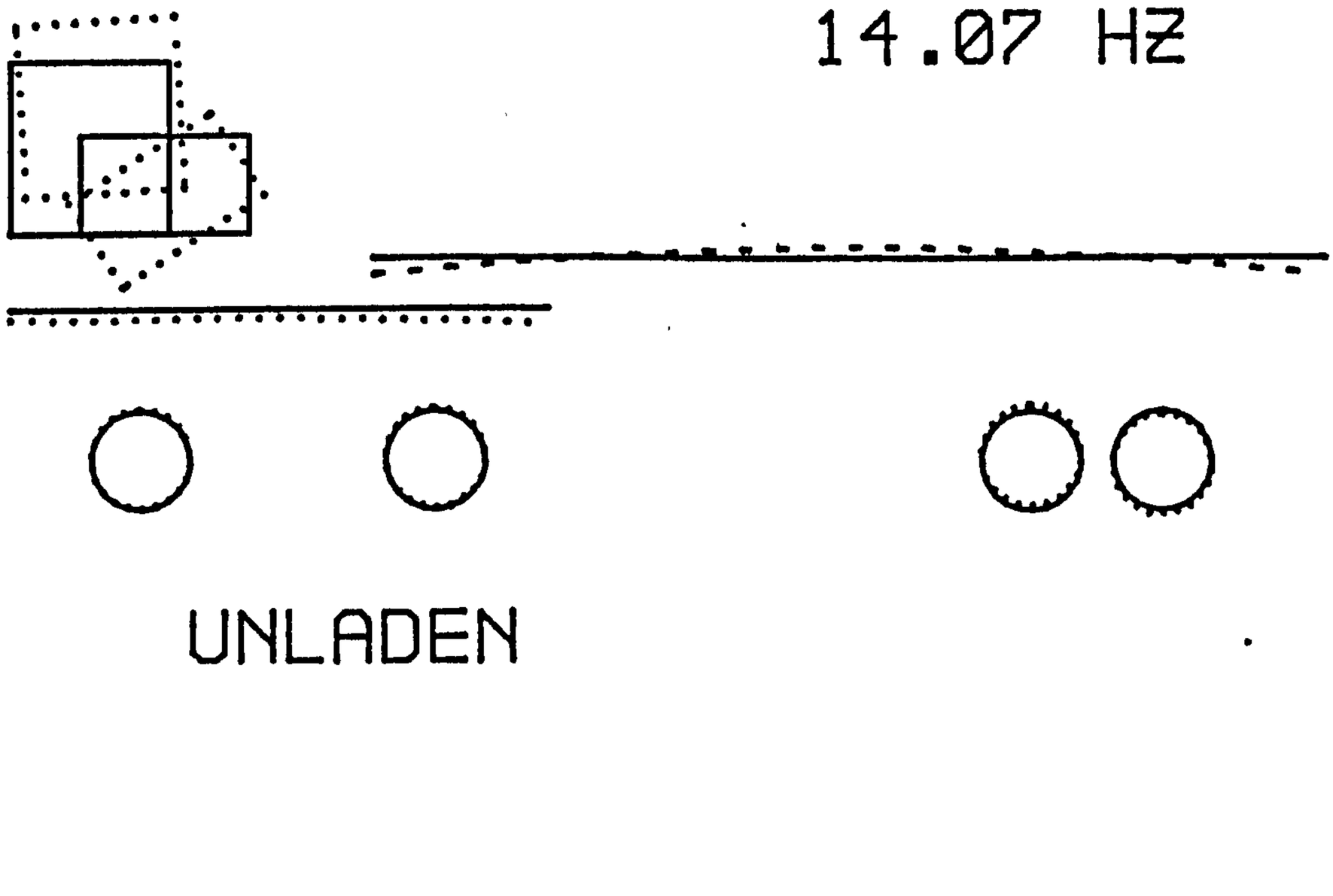

FIGURE 49 (CONTD) UNLADEN MODES

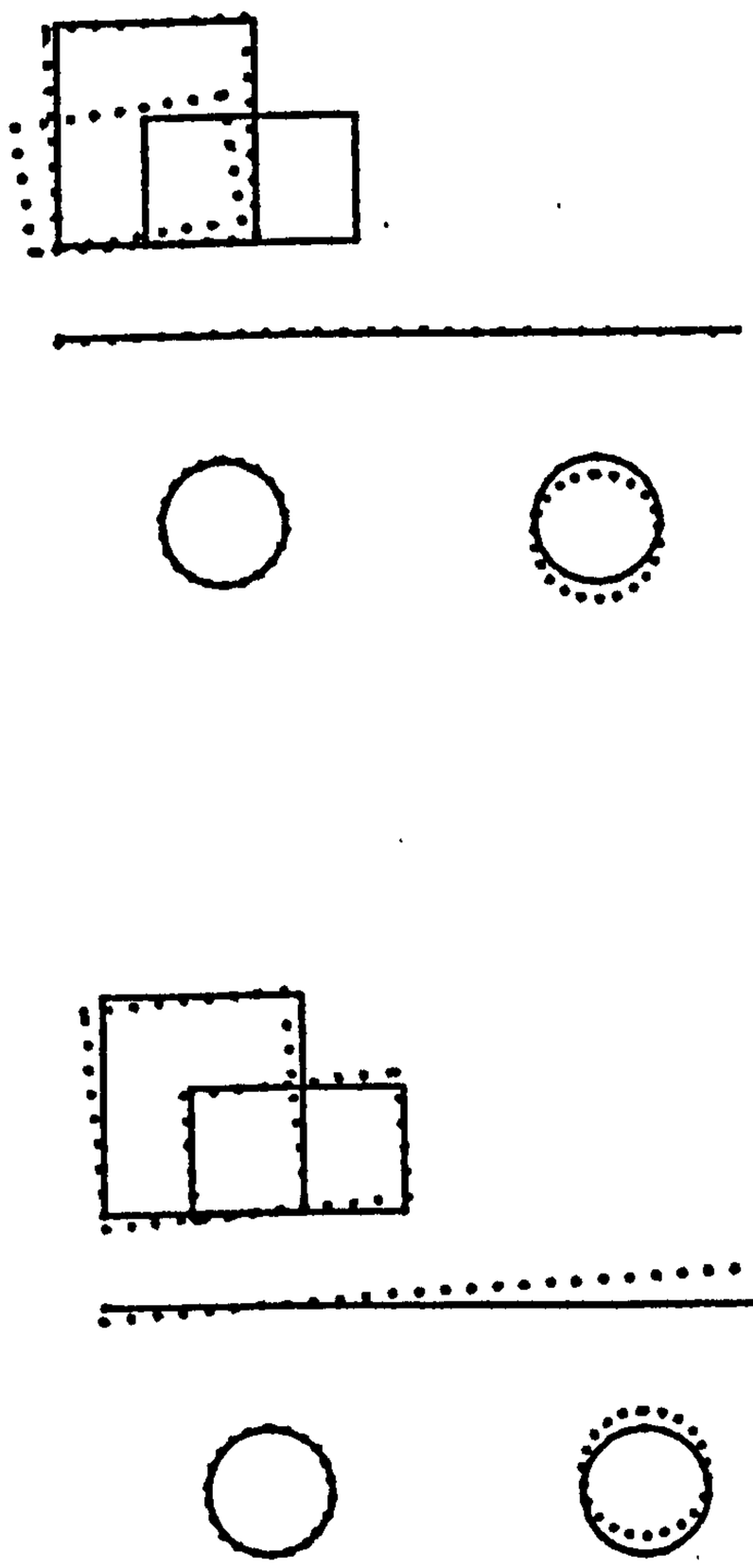

FIGURE 50 TRACTOR MODES

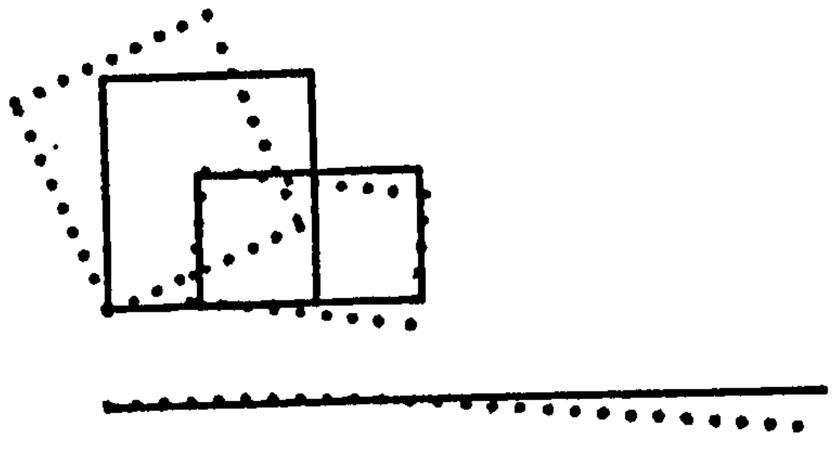

11.02 HZ

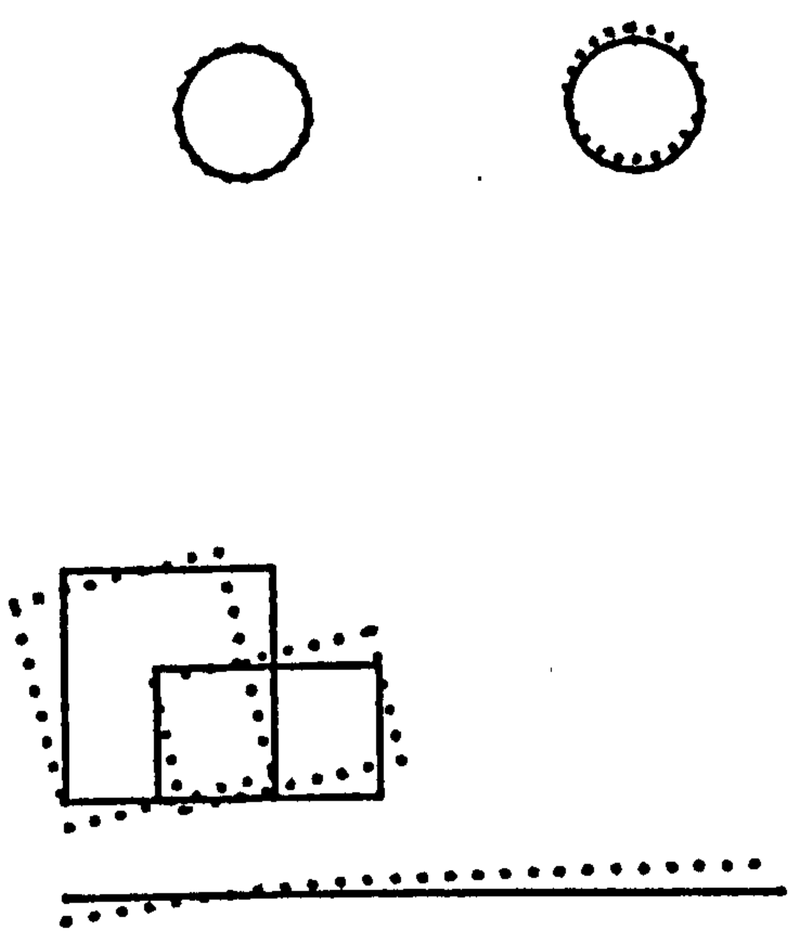

8.61 HZ

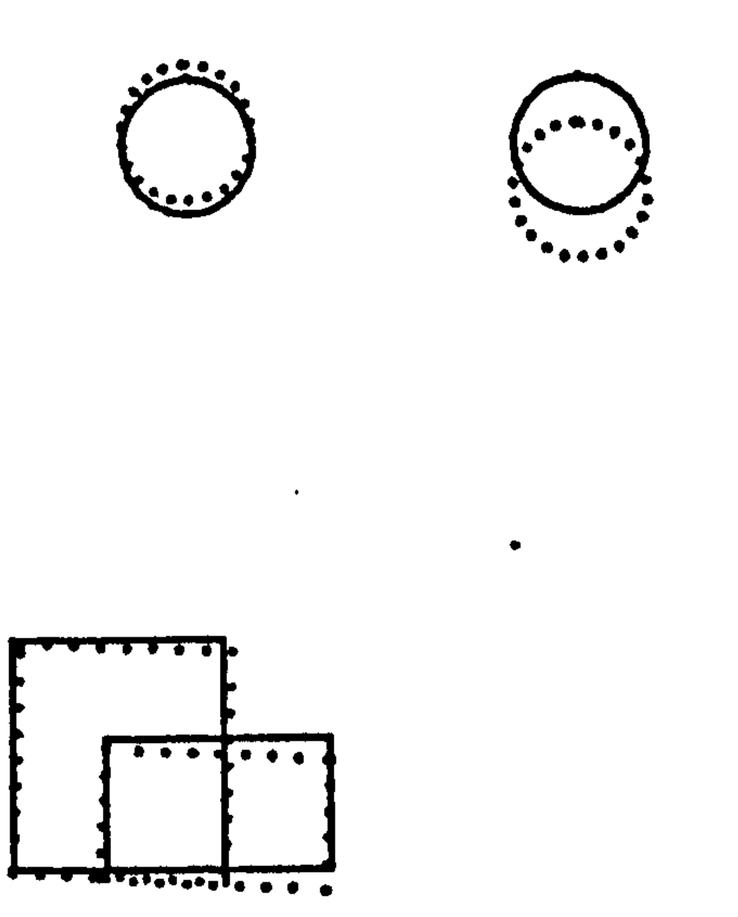

8.52 HZ

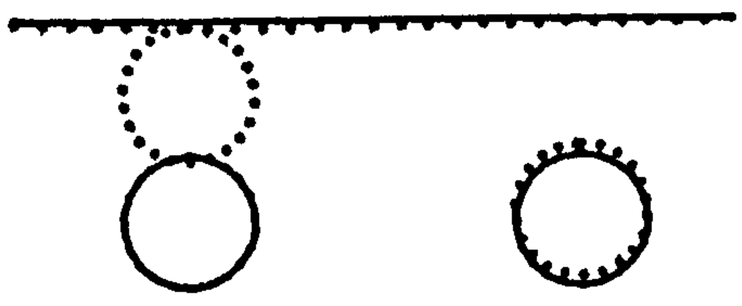

FIGURE 50 (CONTD) TRACTOR MODES

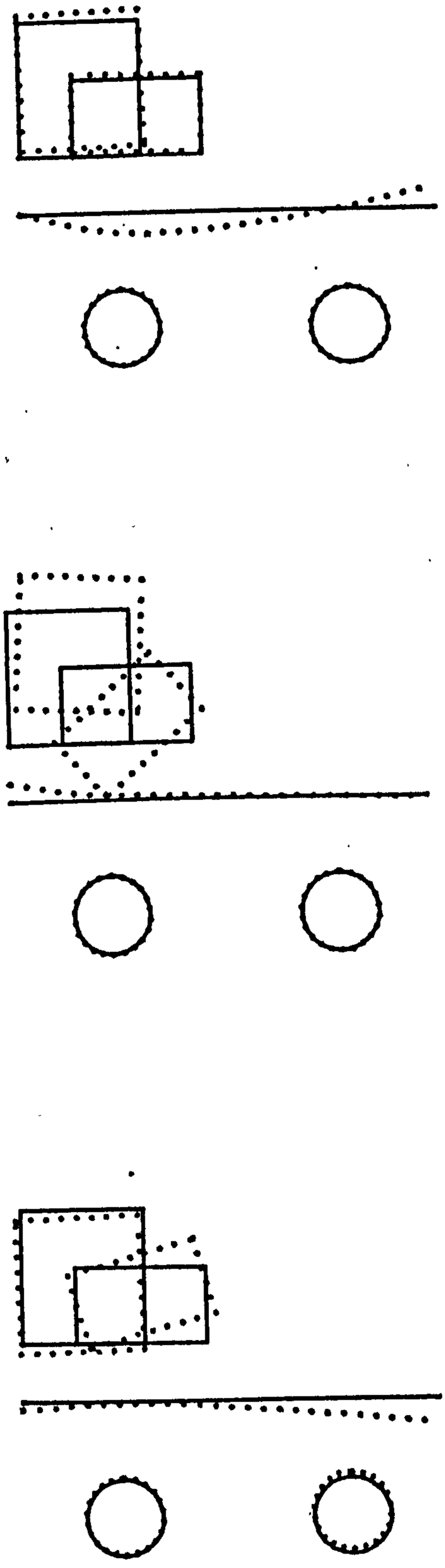

27.97 HZ

17.25 HZ

12.06 HZ

FIGURE 50 (CONTD) TRACTOR MODES

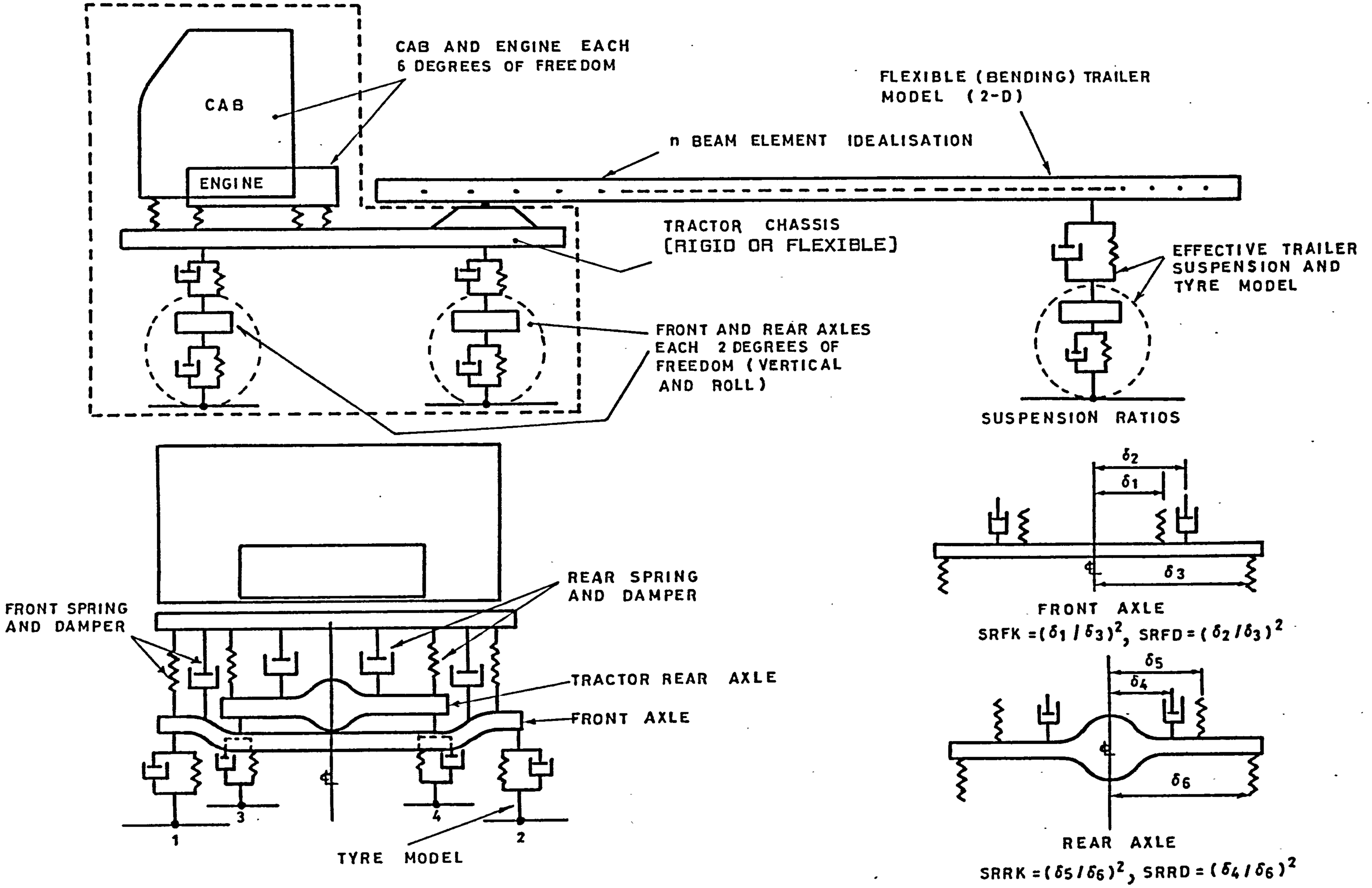

FIG 51 TRACTOR - TRAILER MODEL SCHEMATIC

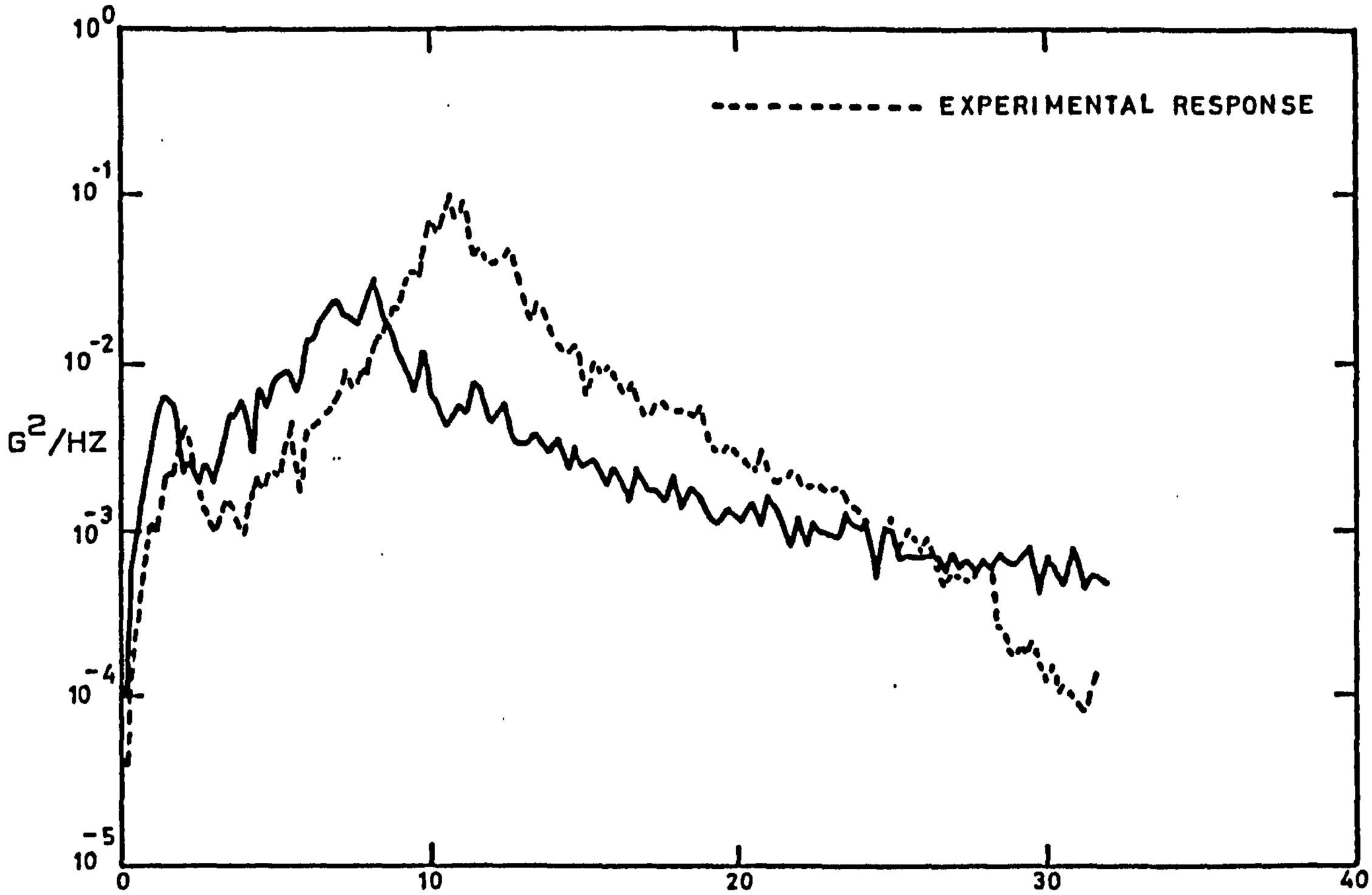

FIGURE 52

PREDICTED & EXPERIMENTAL TRACTOR RESPONSE
(RIGHT HAND FRONT AXLE)

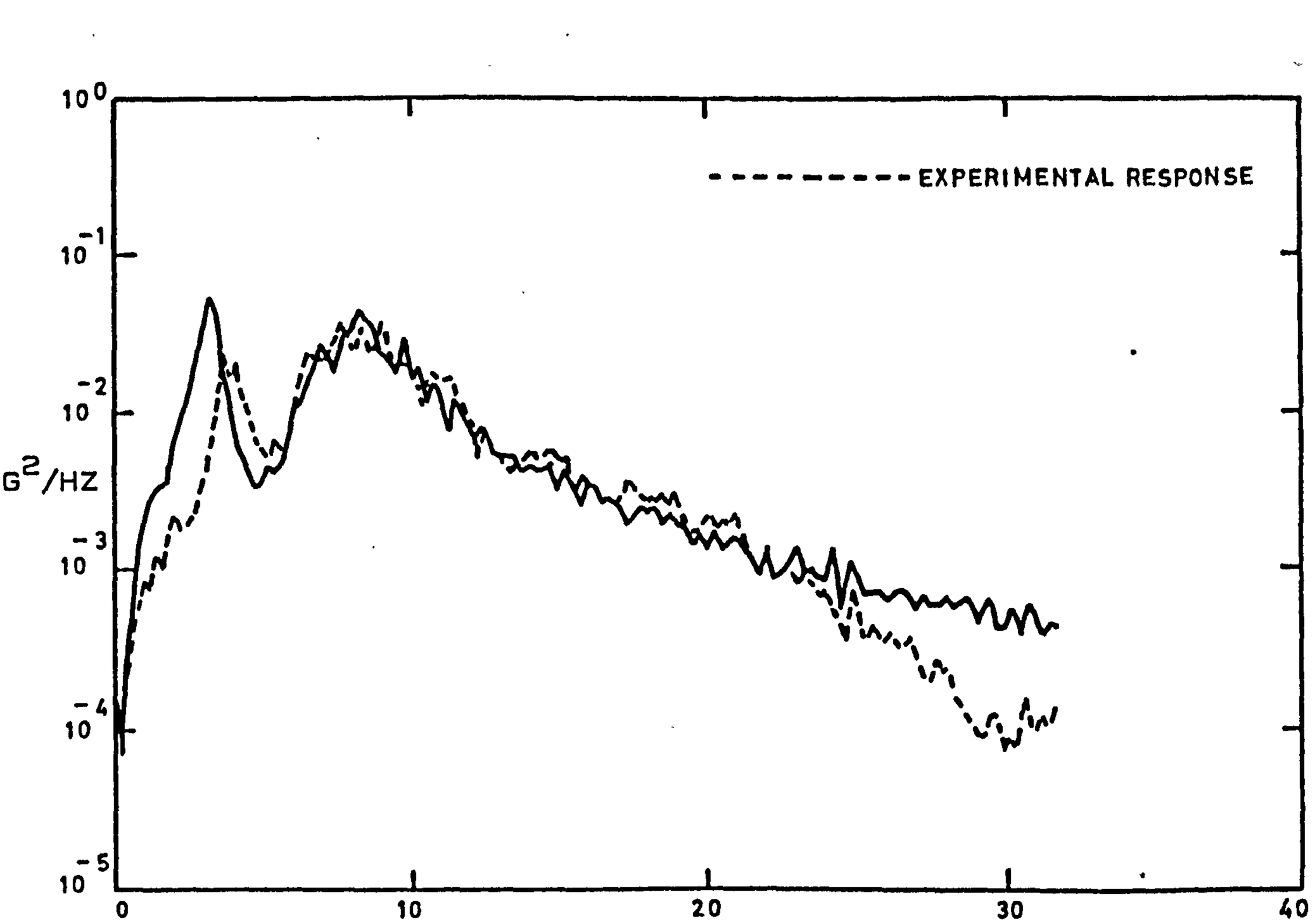

FIGURE 53

PREDICTED & EXPERIMENTAL TRACTOR RESPONSE
(RIGHT HAND REAR AXLE)

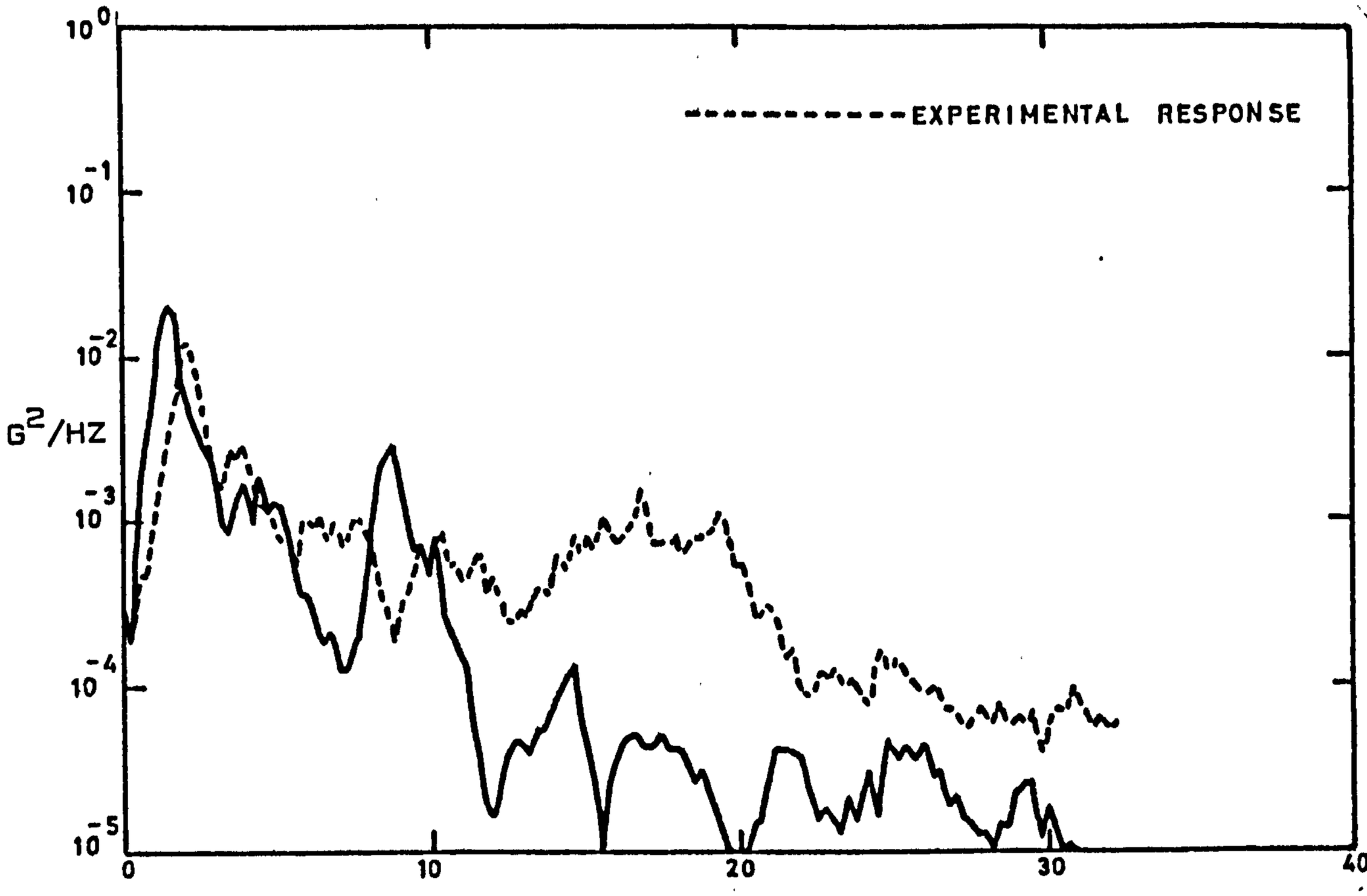

FIGURE 54

PREDICTED & EXPERIMENTAL TRACTOR RESPONSE
(RIGHT HAND FRONT FRAME)

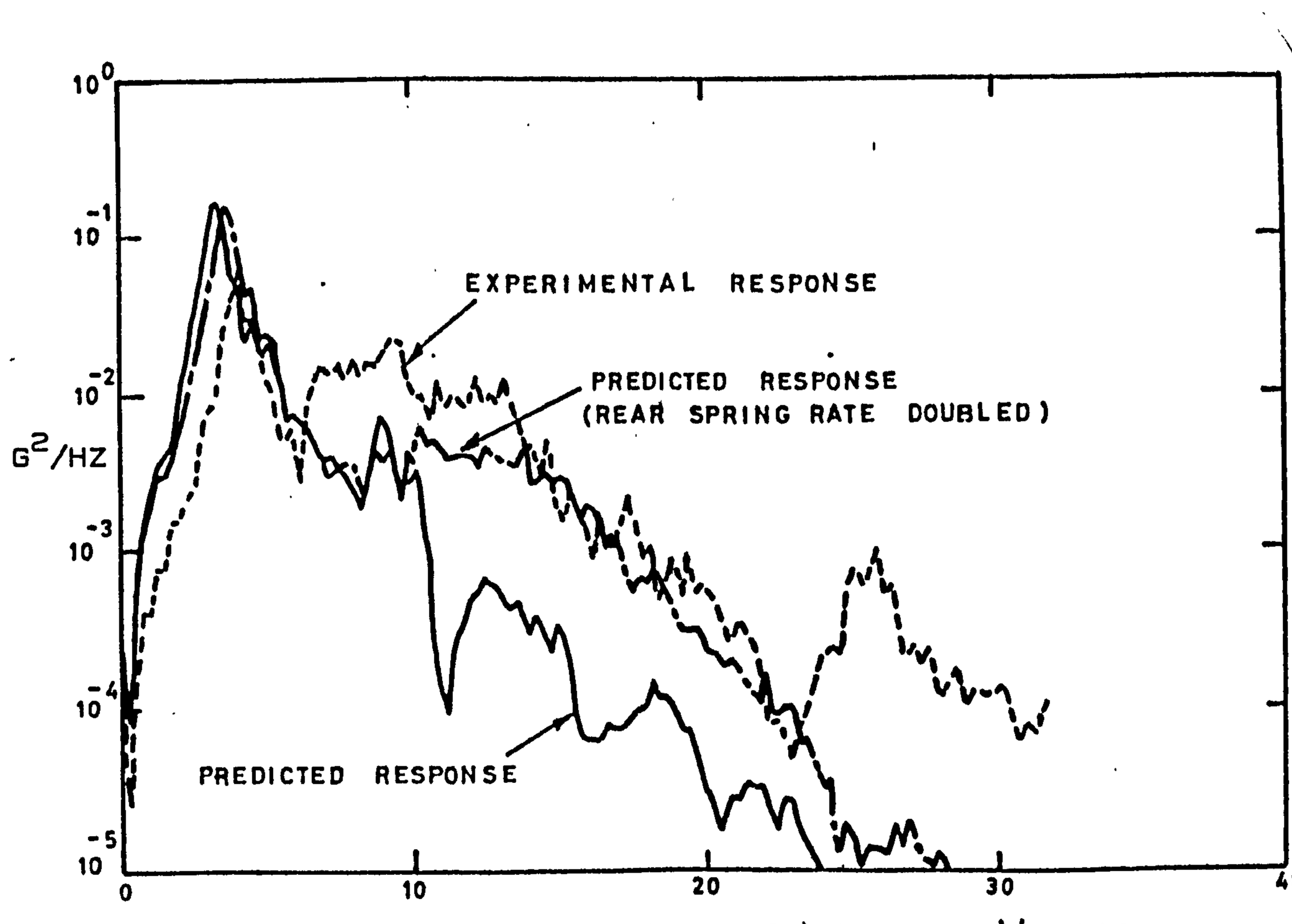

FIGURE 55

PREDICTED & EXPERIMENTAL TRACTOR RESPONSE
(RIGHT HAND REAR FRAME)

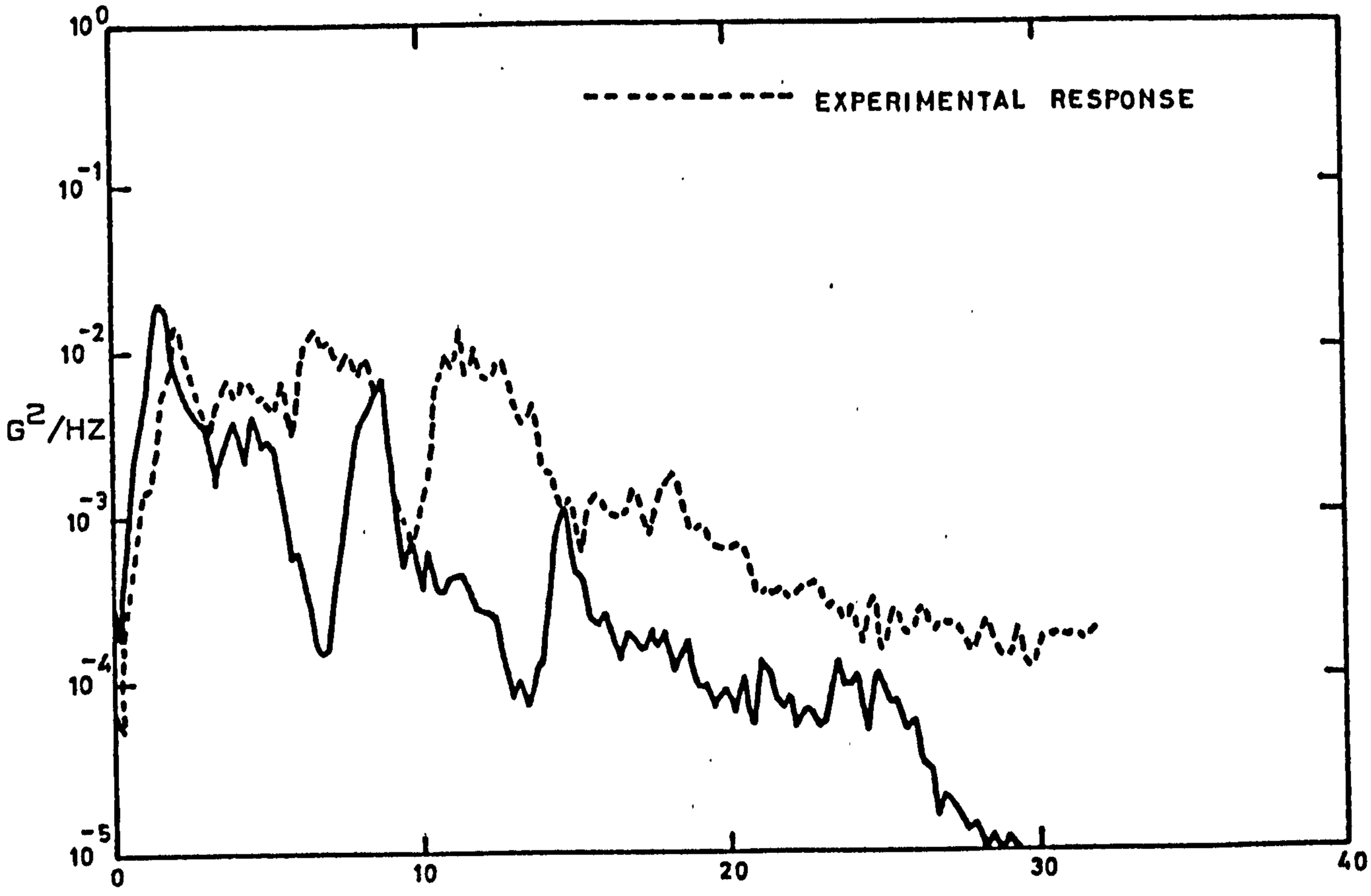

FIGURE 56

PREDICTED & EXPERIMENTAL TRACTOR RESPONSE
(DRIVER SEAT VERTICAL)

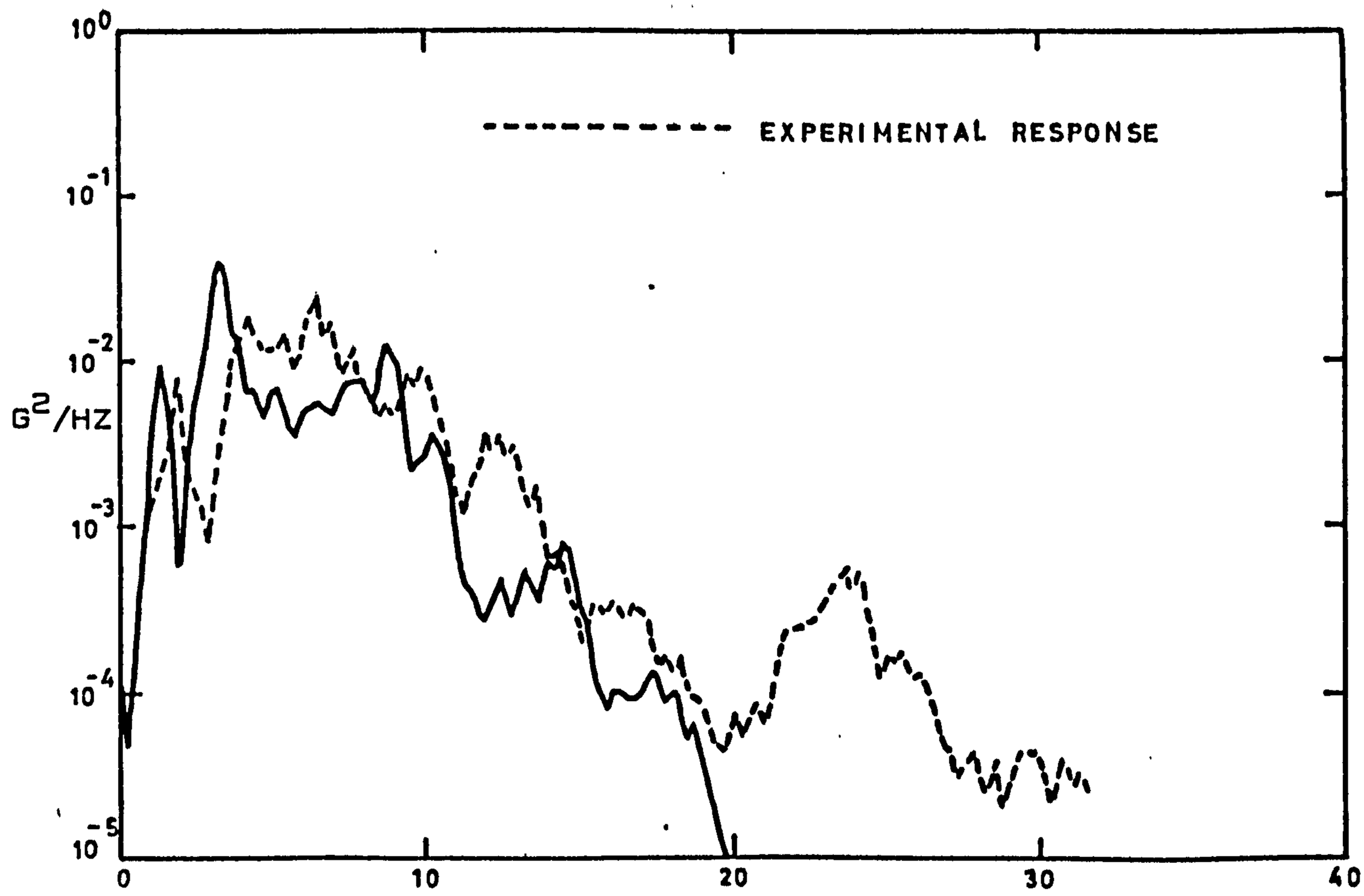

FIGURE 57

PREDICTED & EXPERIMENTAL TRACTOR RESPONSE
(DRIVER SEAT LONGITUDINAL)

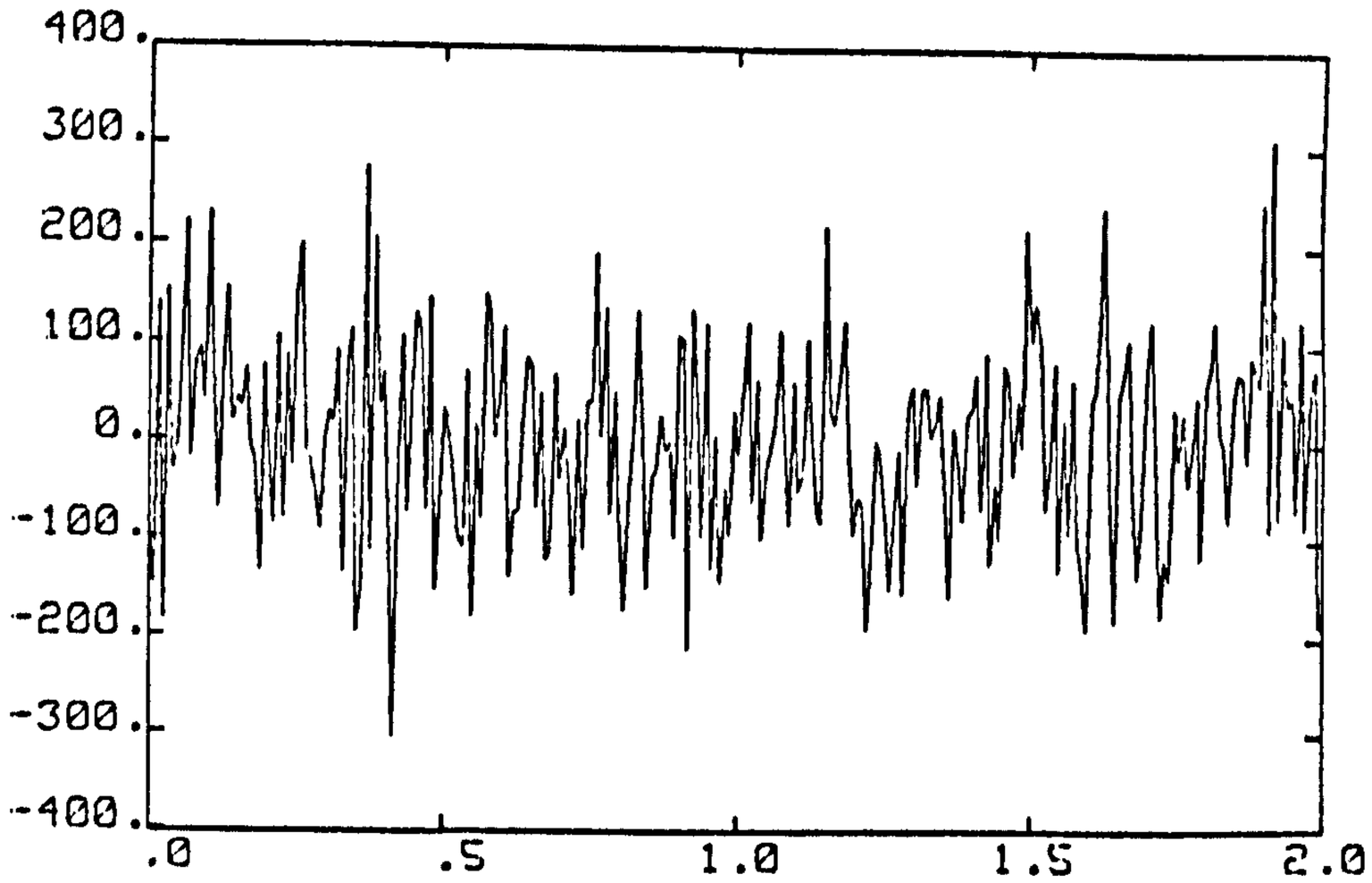

TIME (SECS) SAMPLING FREQ= 128. HZ

FIGURE 58[a] NEARSIDE FRONT WHEEL INPUT [DISPLACEMENT]

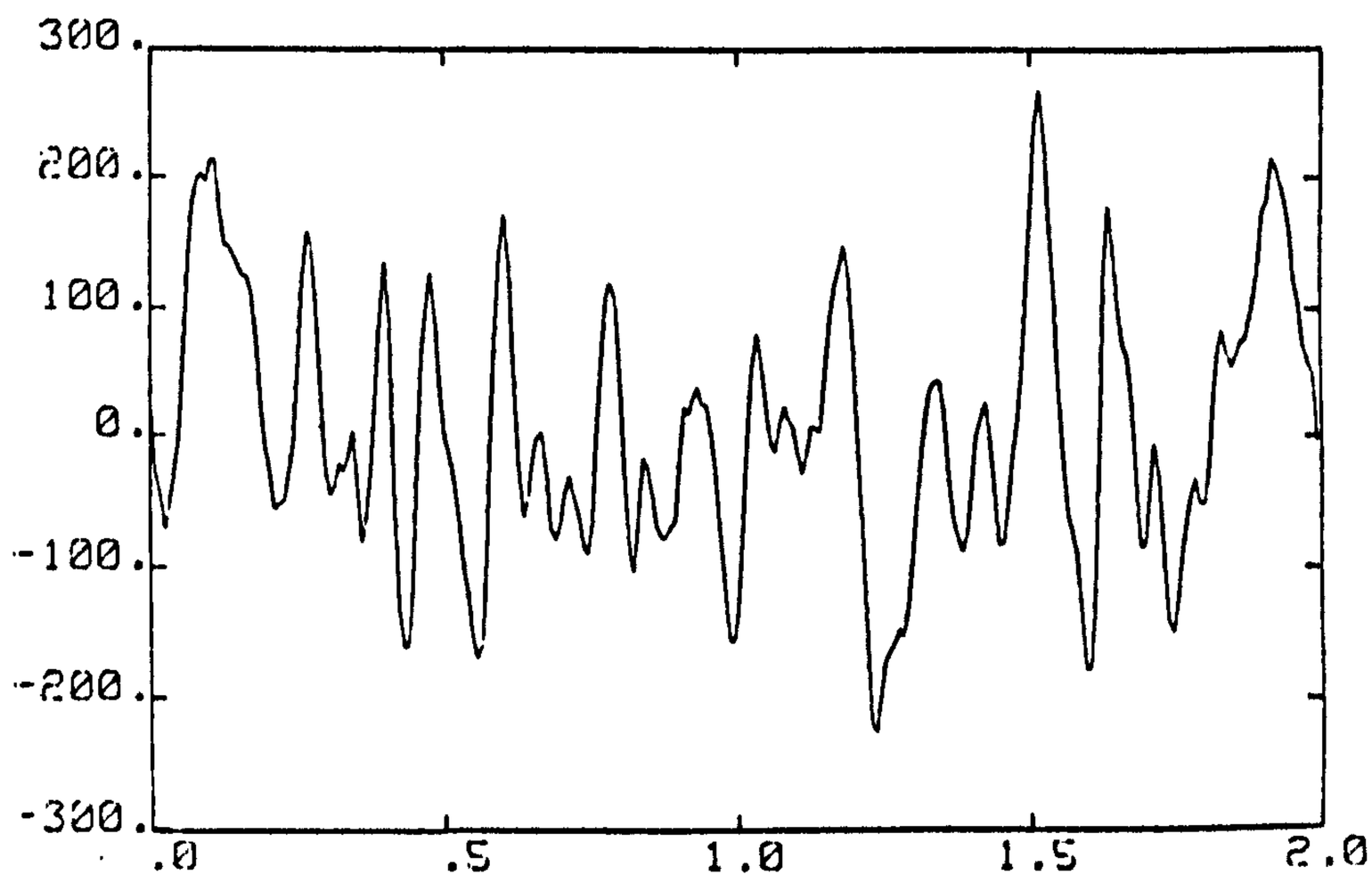

TIME (SECS) SAMPLING FREQ= 128. HZ

FIGURE 58[b] FRONT AXLE CENTRE VERTICAL [ACCELERATION]

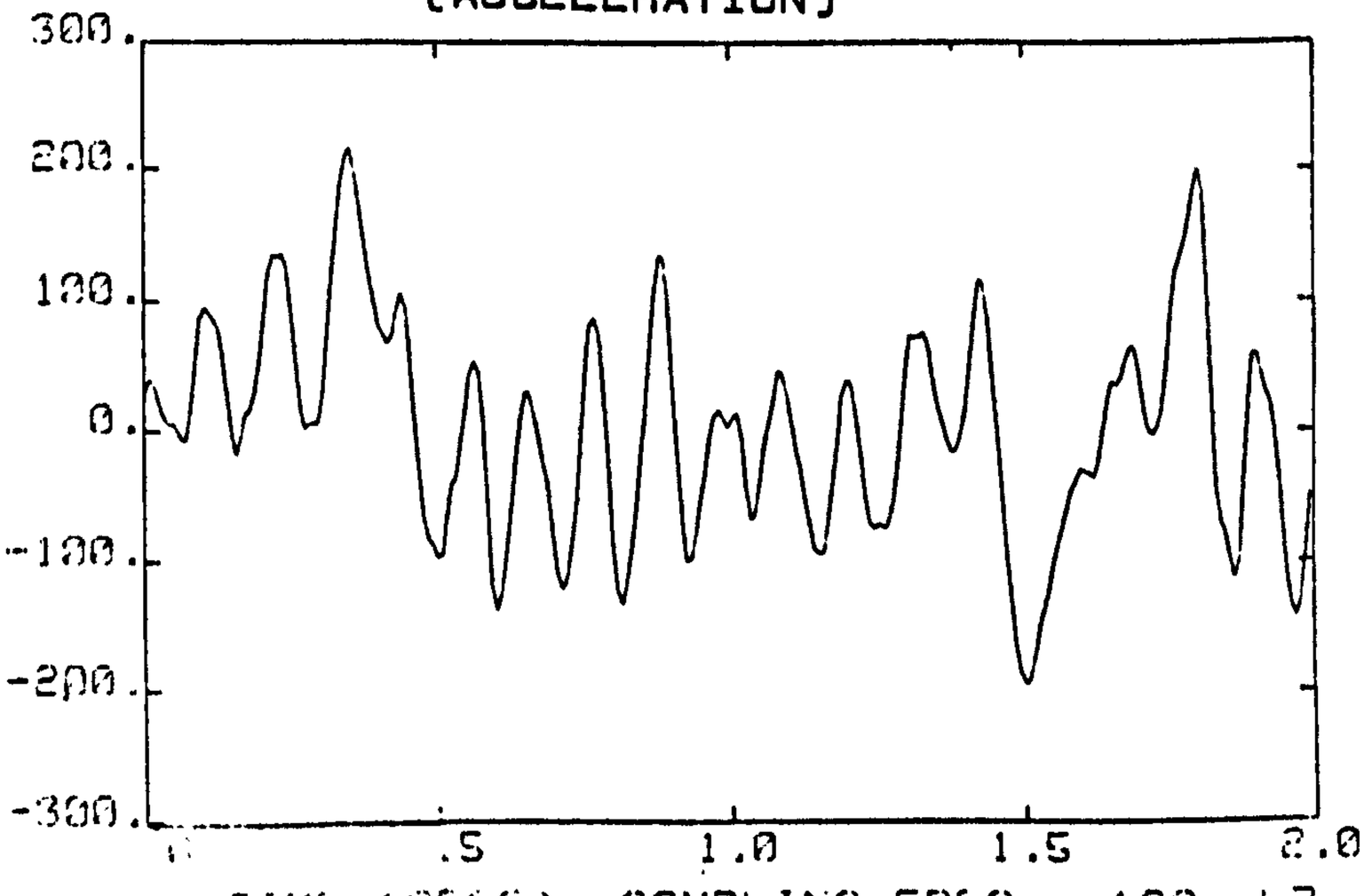

TIME (SECS) SAMPLING FREQ= 128. HZ

FIGURE 58[c] TRACTOR FRAME C OF G VERTICAL RESPONSE [ACCELERATION]

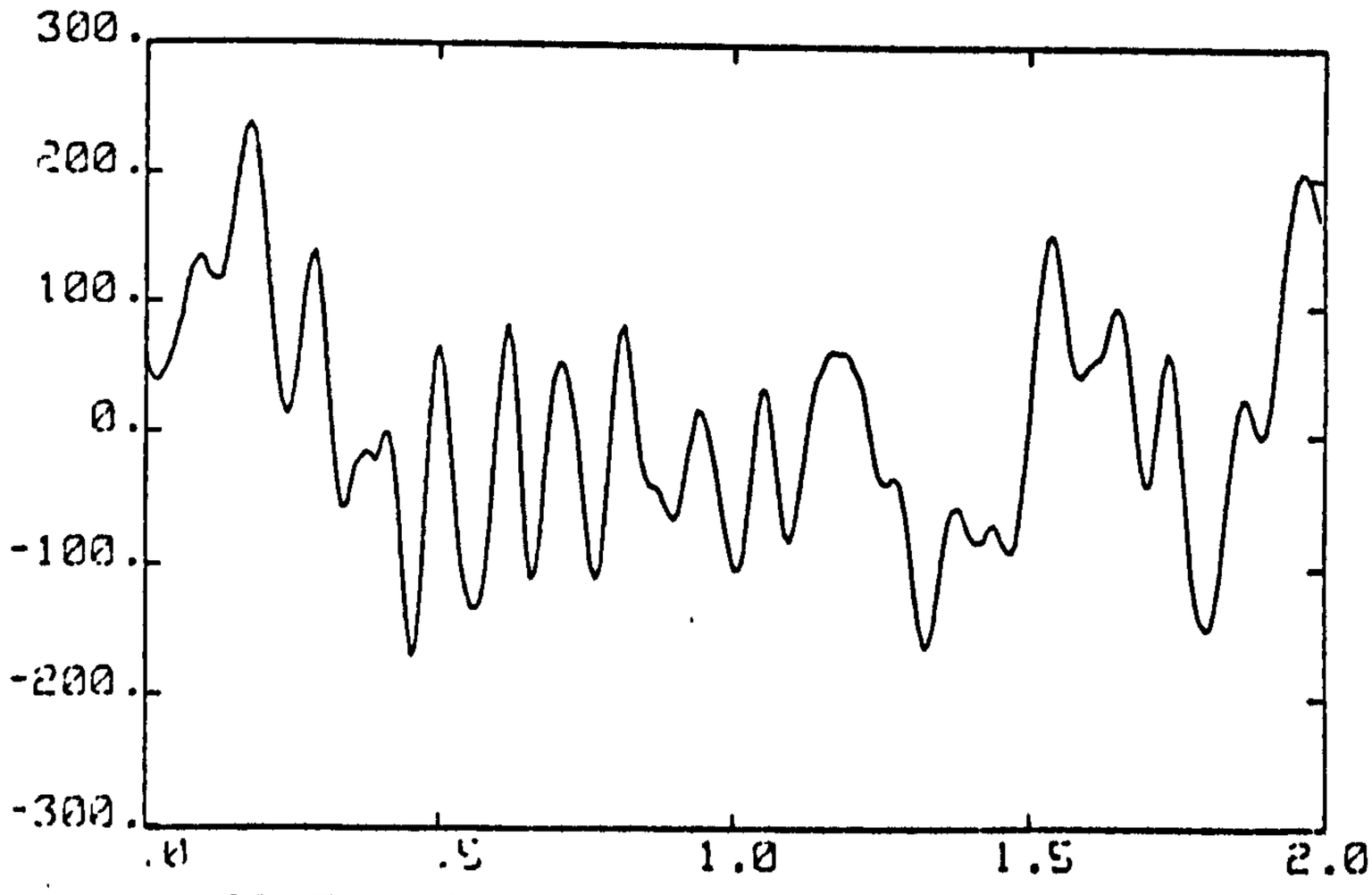

TIME (SECS) SAMPLING FREQ= 128. HZ

FIGURE 58[d] C OF G VERTICAL RESPONSE [ACCELERATION]

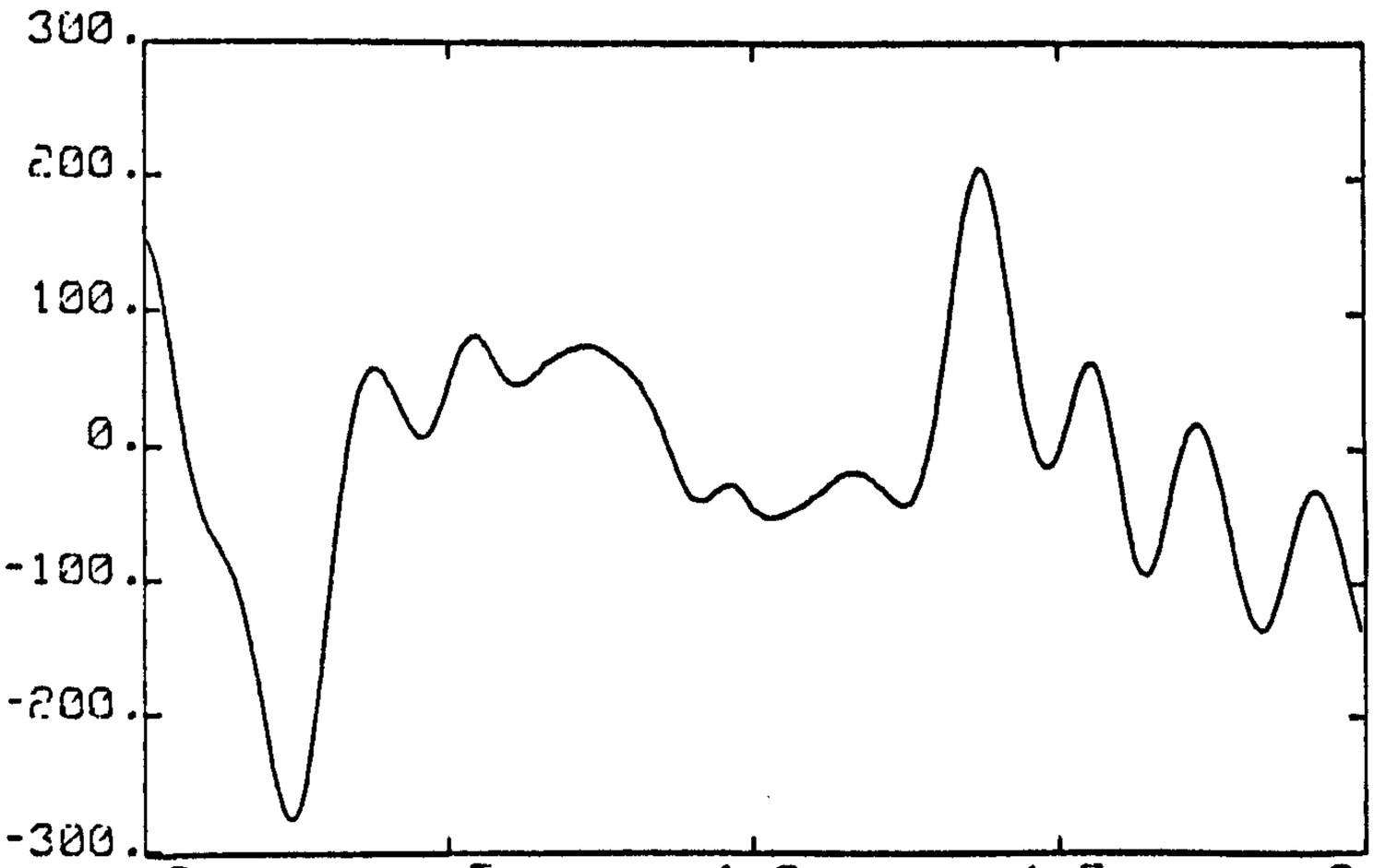

TIME (SECS) SAMPLING FREQ= 128. HZ

FIGURE 58[e] ROLL RESPONSE OF TRACTOR FRAME C OF G

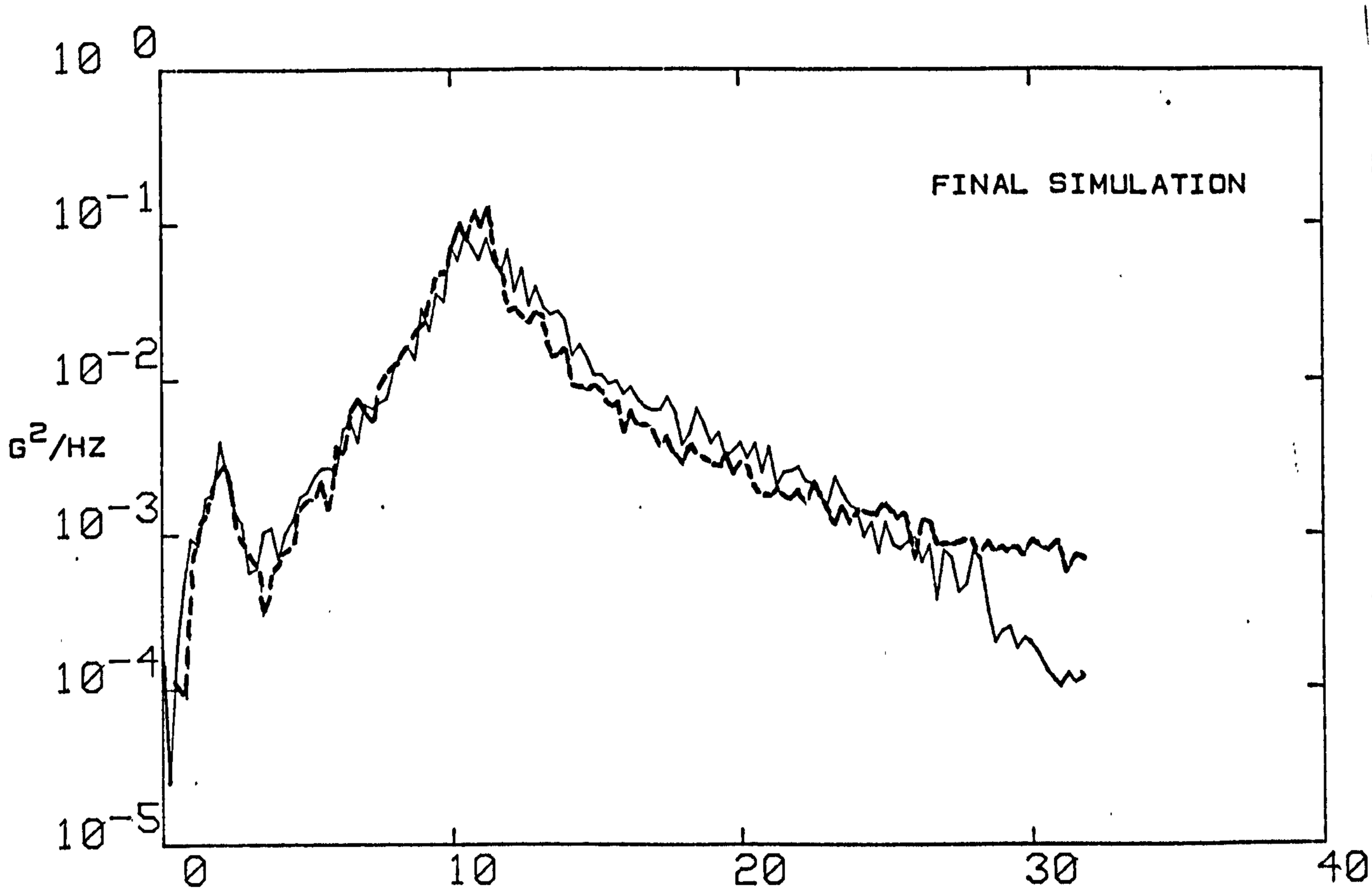

FIGURE 59

PREDICTED & EXPERIMENTAL TRACTOR RESPONSE (LEFT HAND FRONT AXLE)

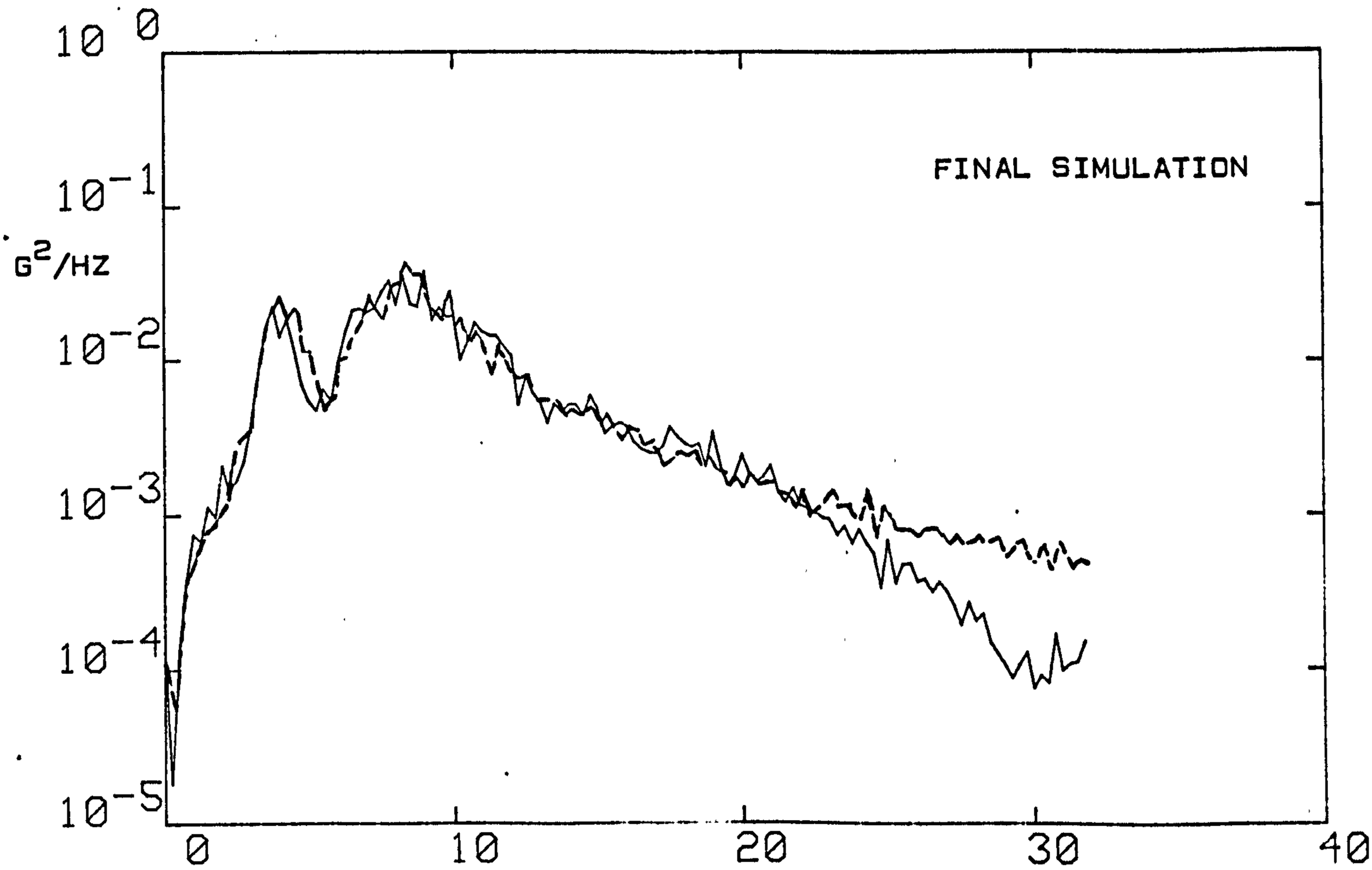

FIGURE 60

PREDICTED & EXPERIMENTAL TRACTOR RESPONSE (RIGHT HAND REAR AXLE)

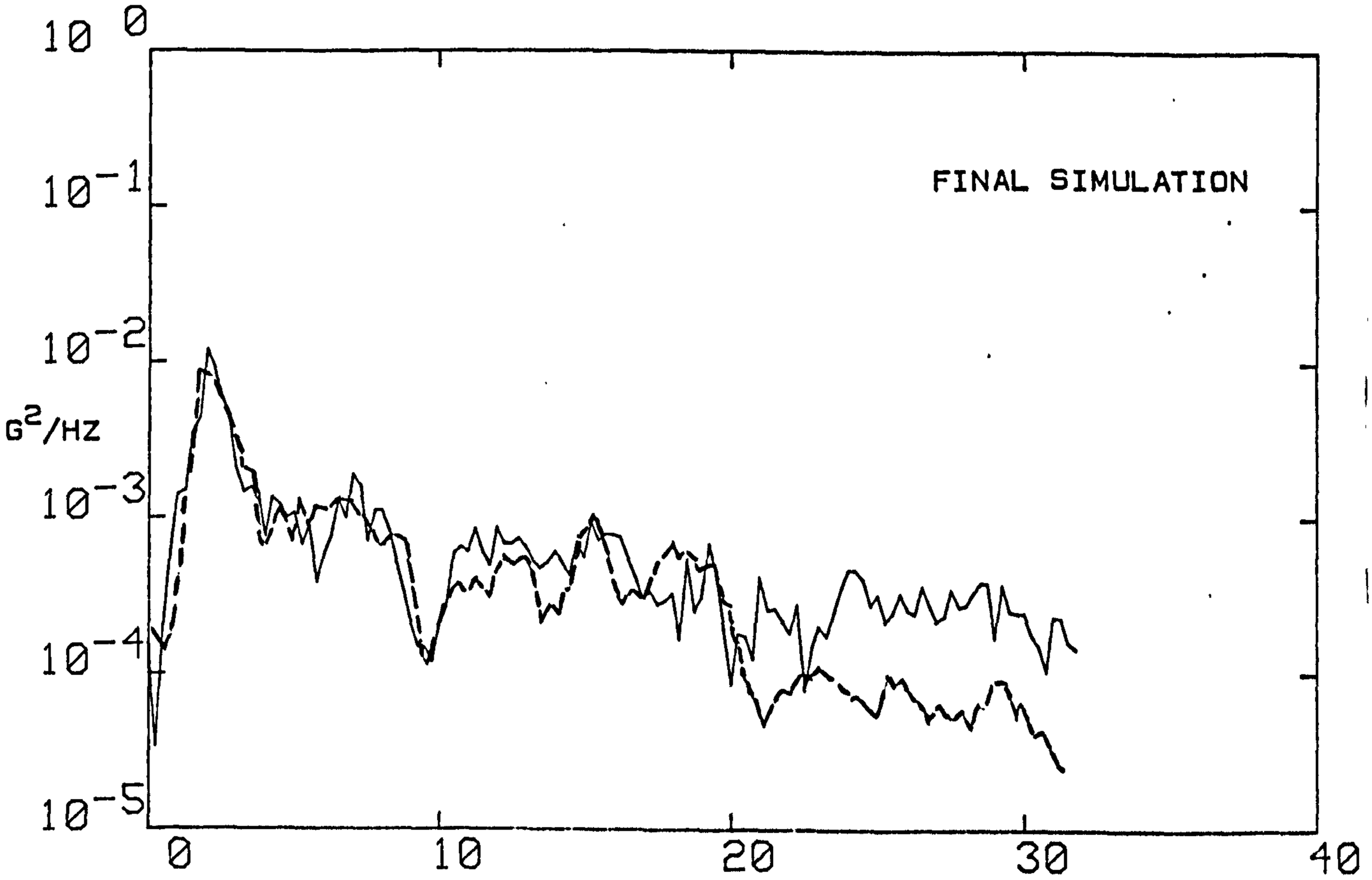

FIGURE 61

PREDICTED & EXPERIMENTAL TRACTOR RESPONSE (LEFT HAND FRONT FRAME)

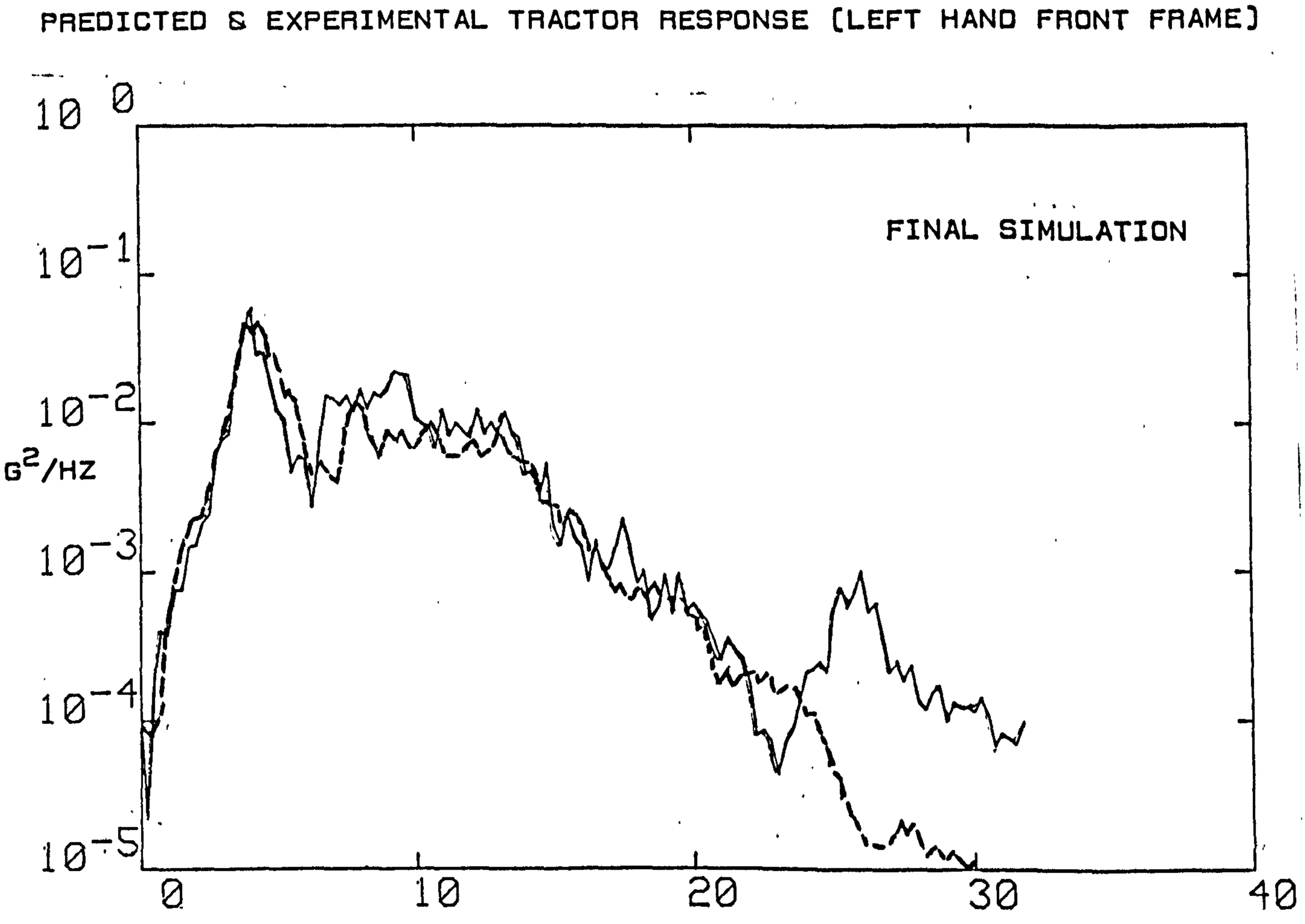

FIGURE 62

PREDICTED & EXPERIMENTAL TRACTOR RESPONSE (RIGHT HAND REAR FRAME)

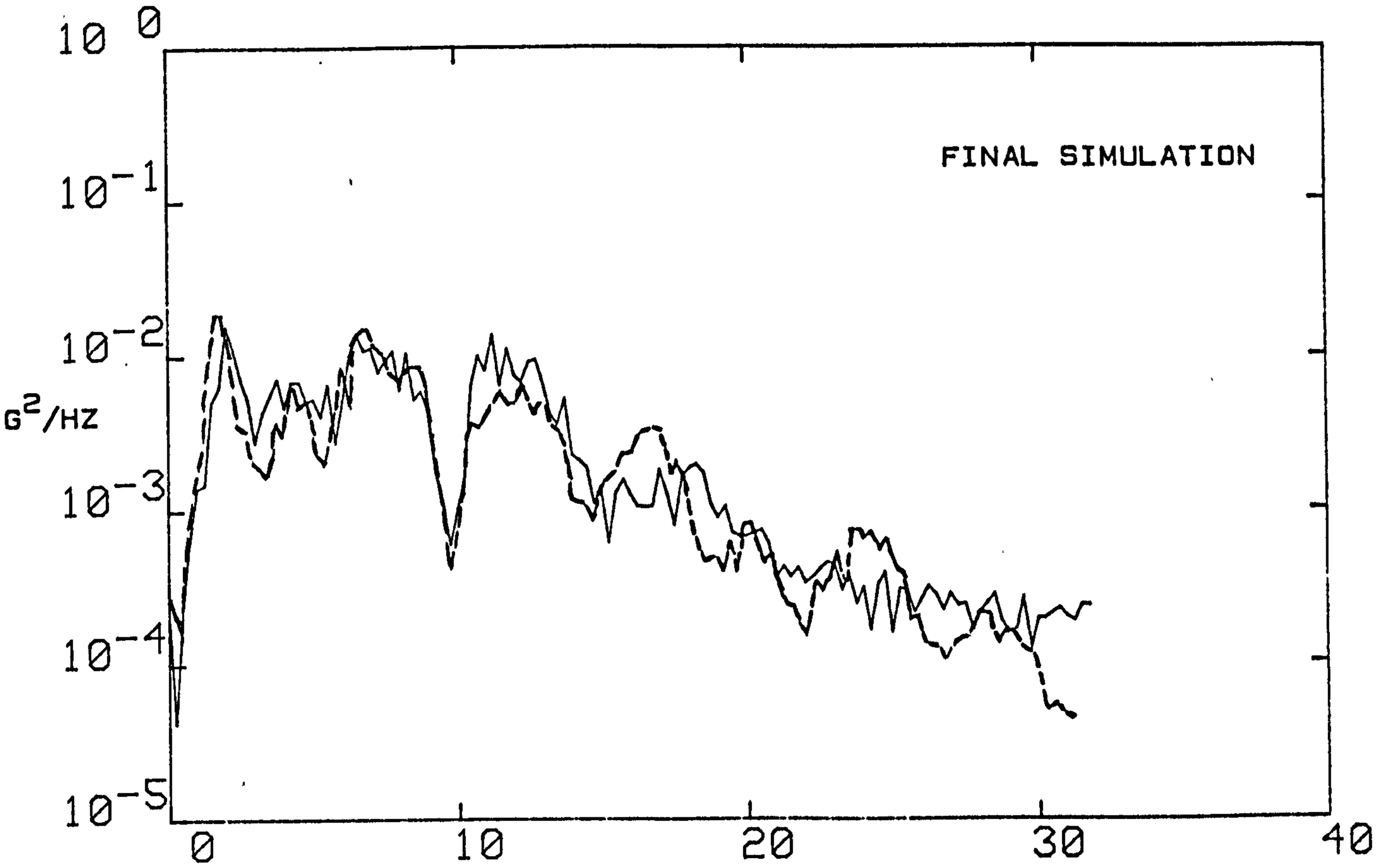

FIGURE 63

PREDICTED & EXPERIMENTAL TRACTOR RESPONSE (DRIVER SEAT VERTICAL)

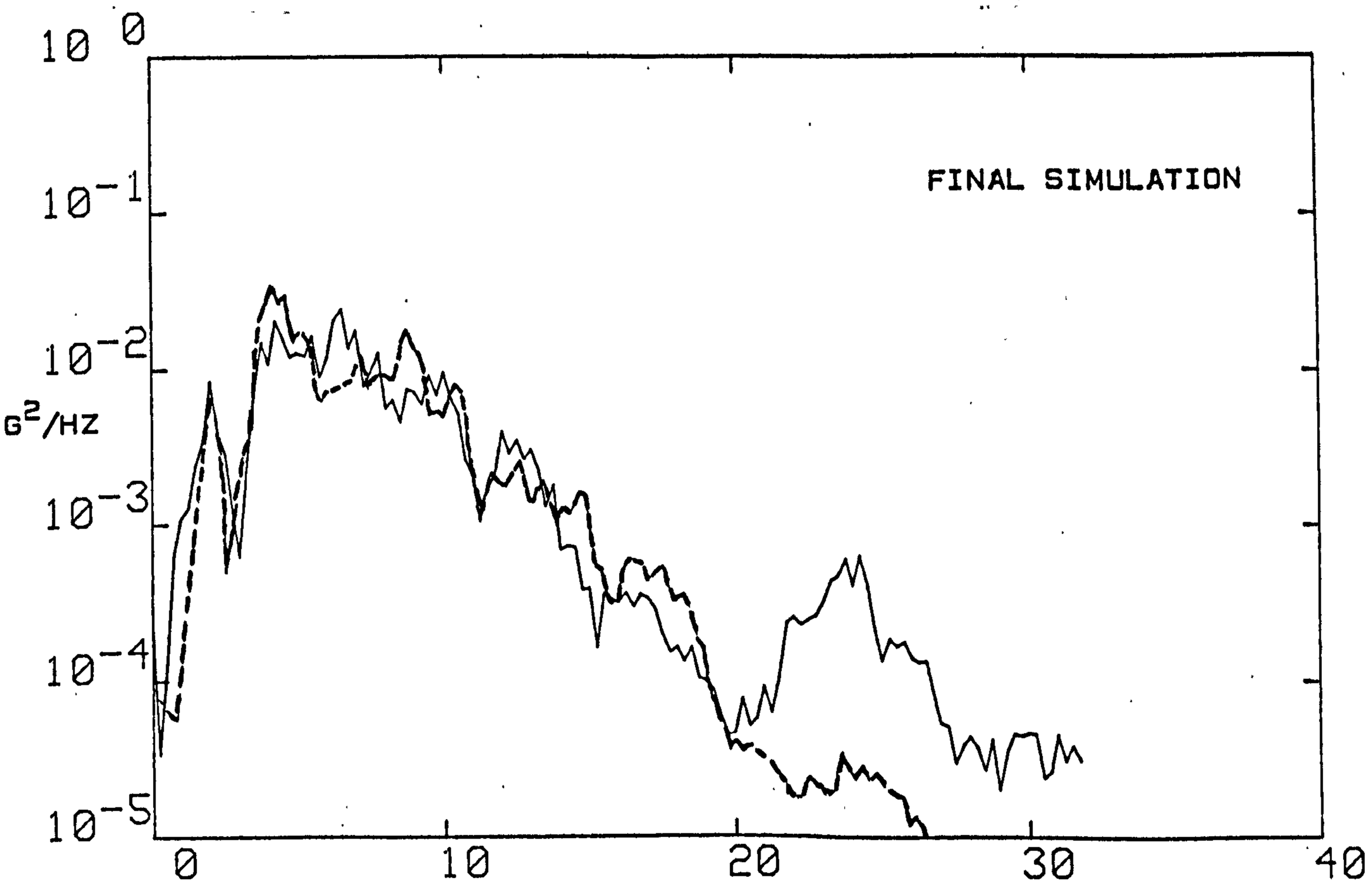

FIGURE 64

PREDICTED & EXPERIMENTAL TRACTOR RESPONSE (DRIVER SEAT LONGITUDINAL)

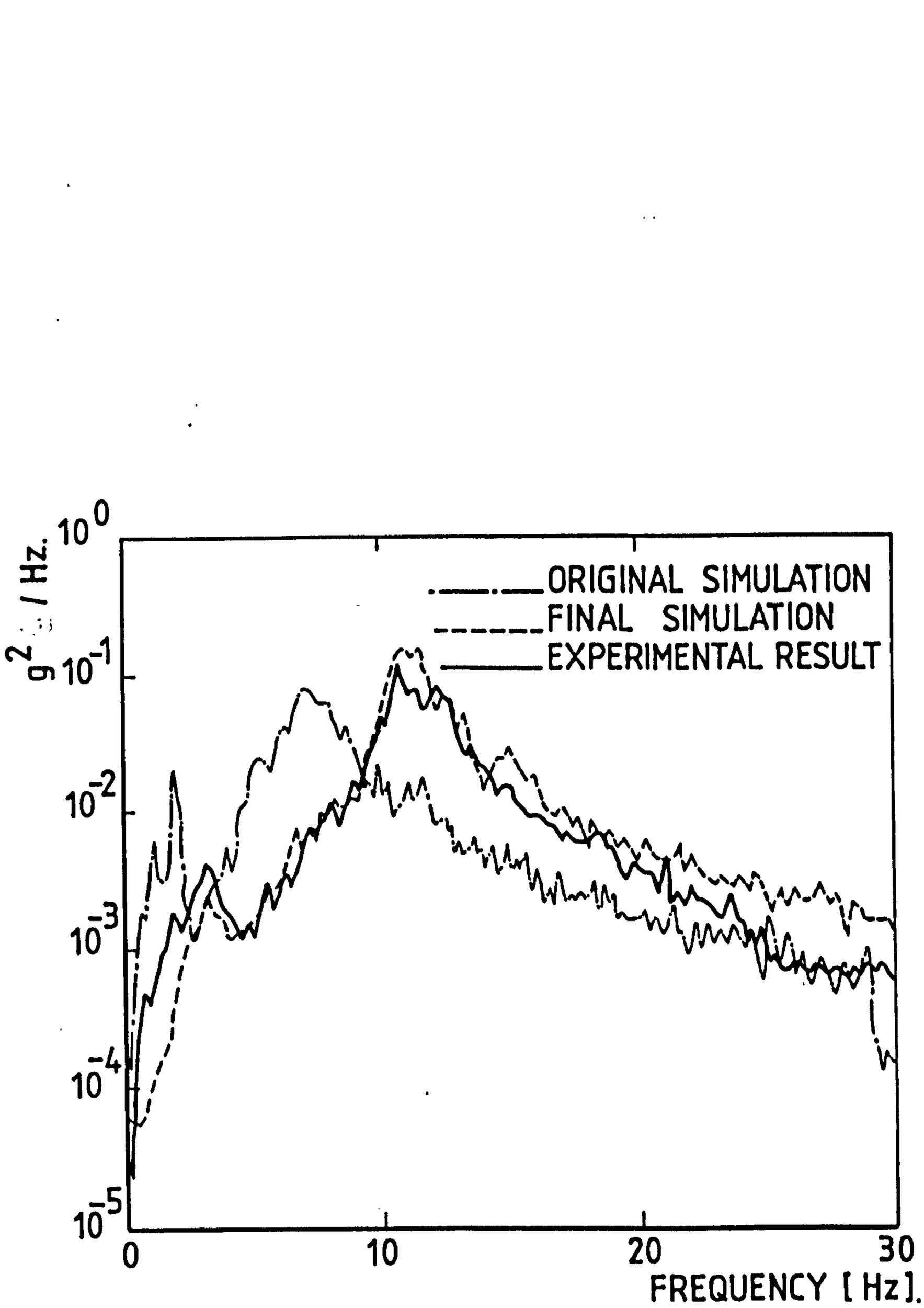

FIGURE 65. RESPONSE CORRELATION FRONT AXLE VERTICAL.

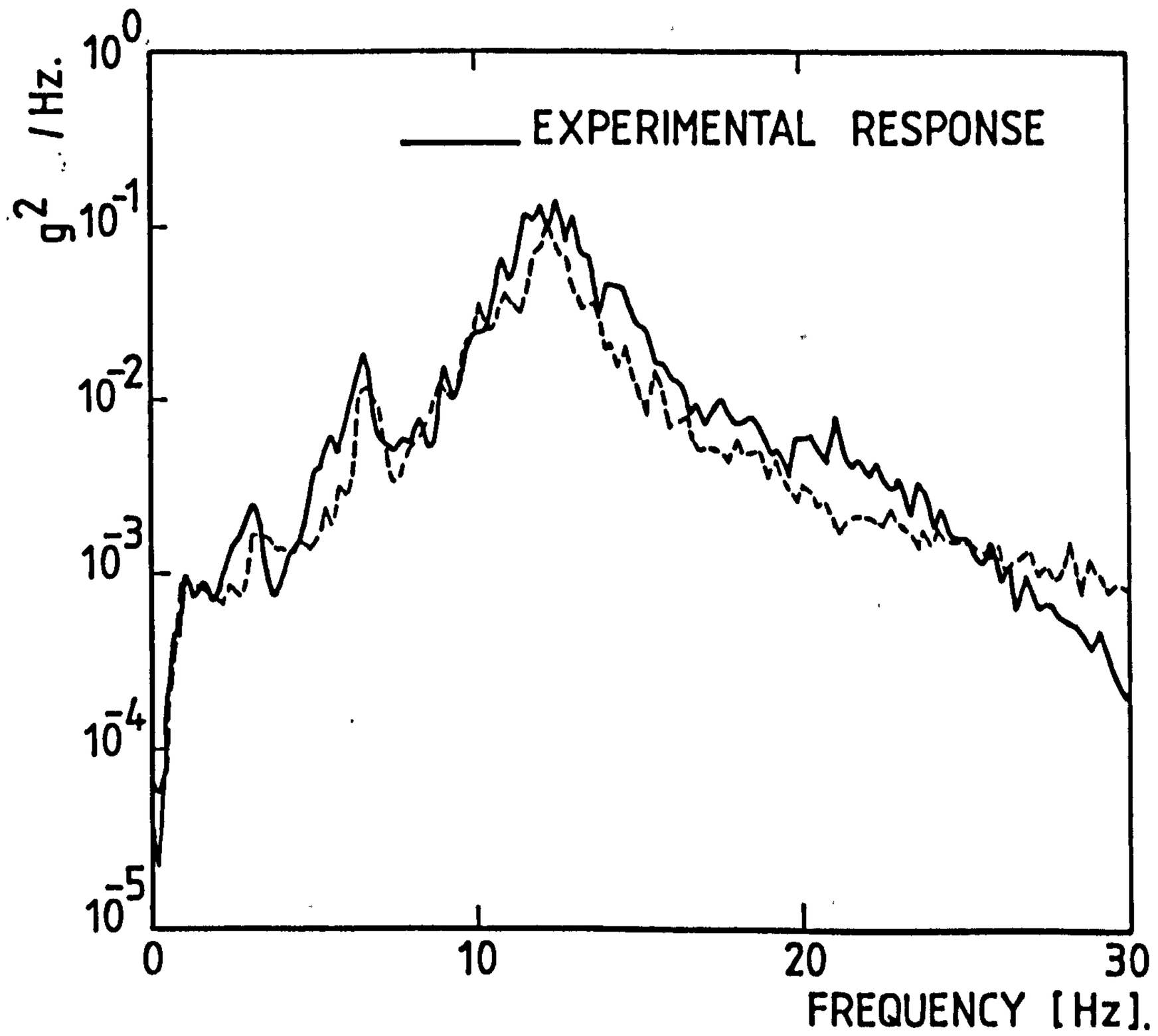

FIGURE 66. RESPONSE CORRELATION
R.H. REAR AXLE VERTICAL.

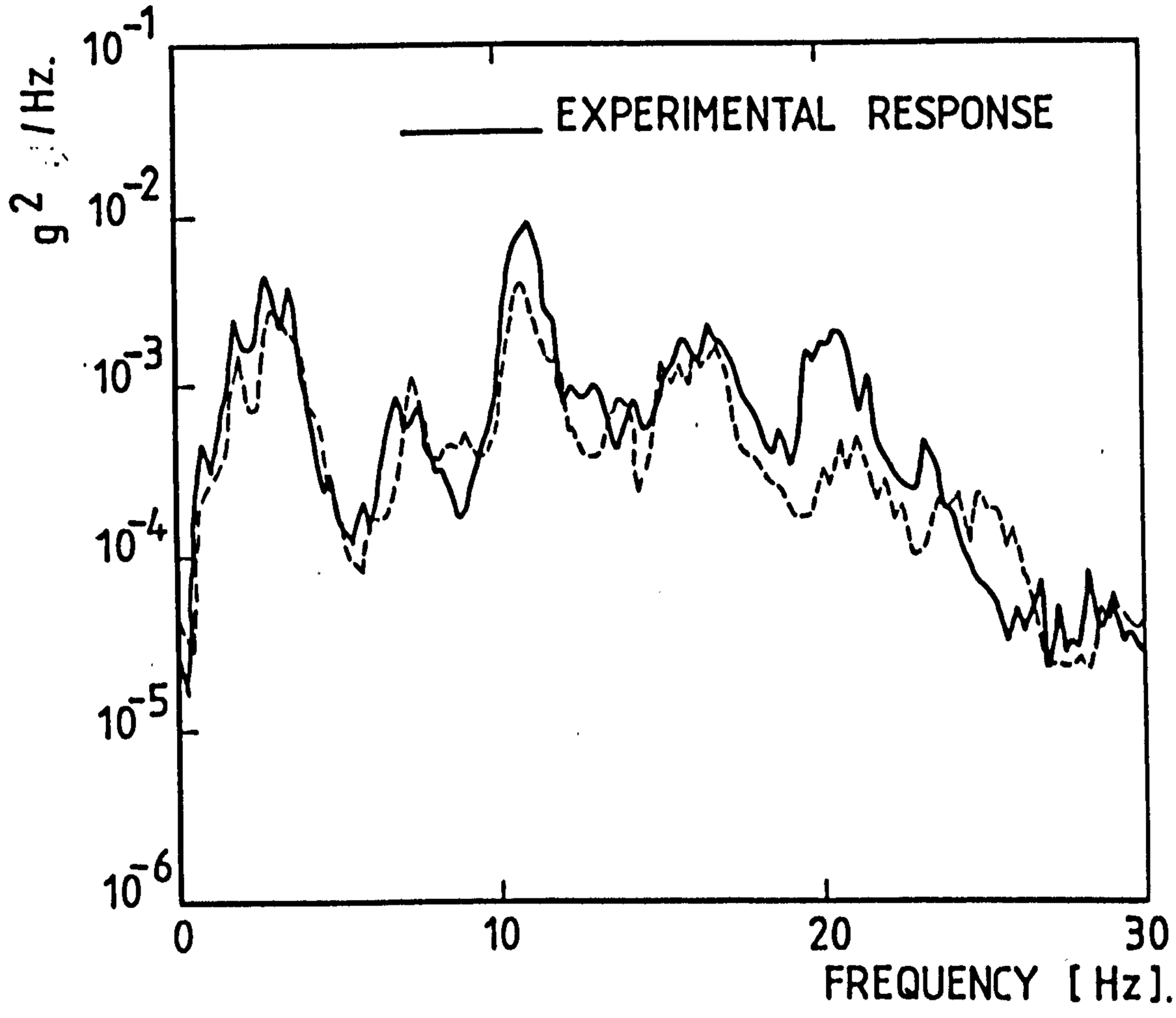

FIGURE 67. RESPONSE CORRELATION FRONT CHASSIS VERTICAL.

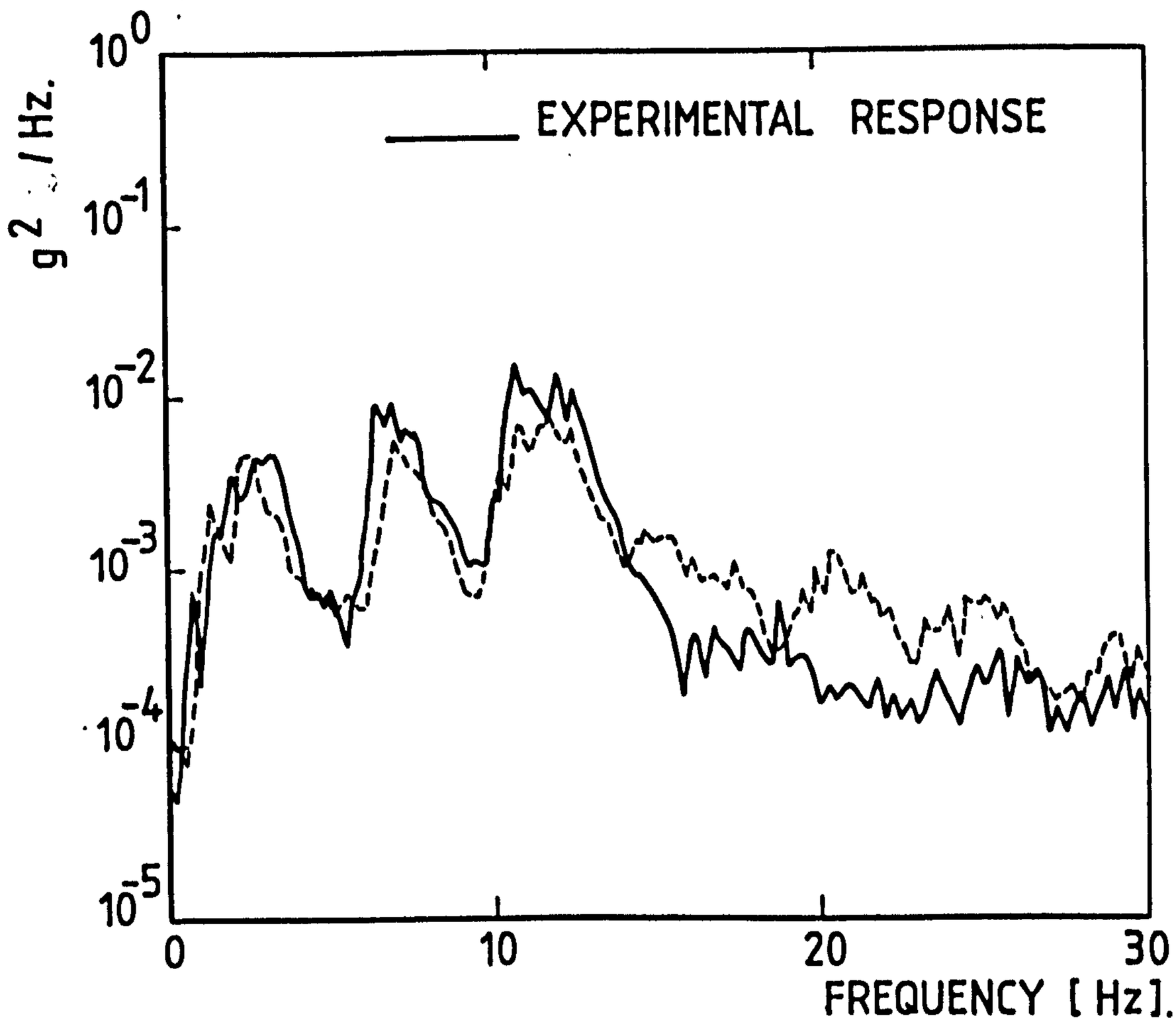

FIGURE 68. RESPONSE CORRELATION DRIVER SEAT VERTICAL.

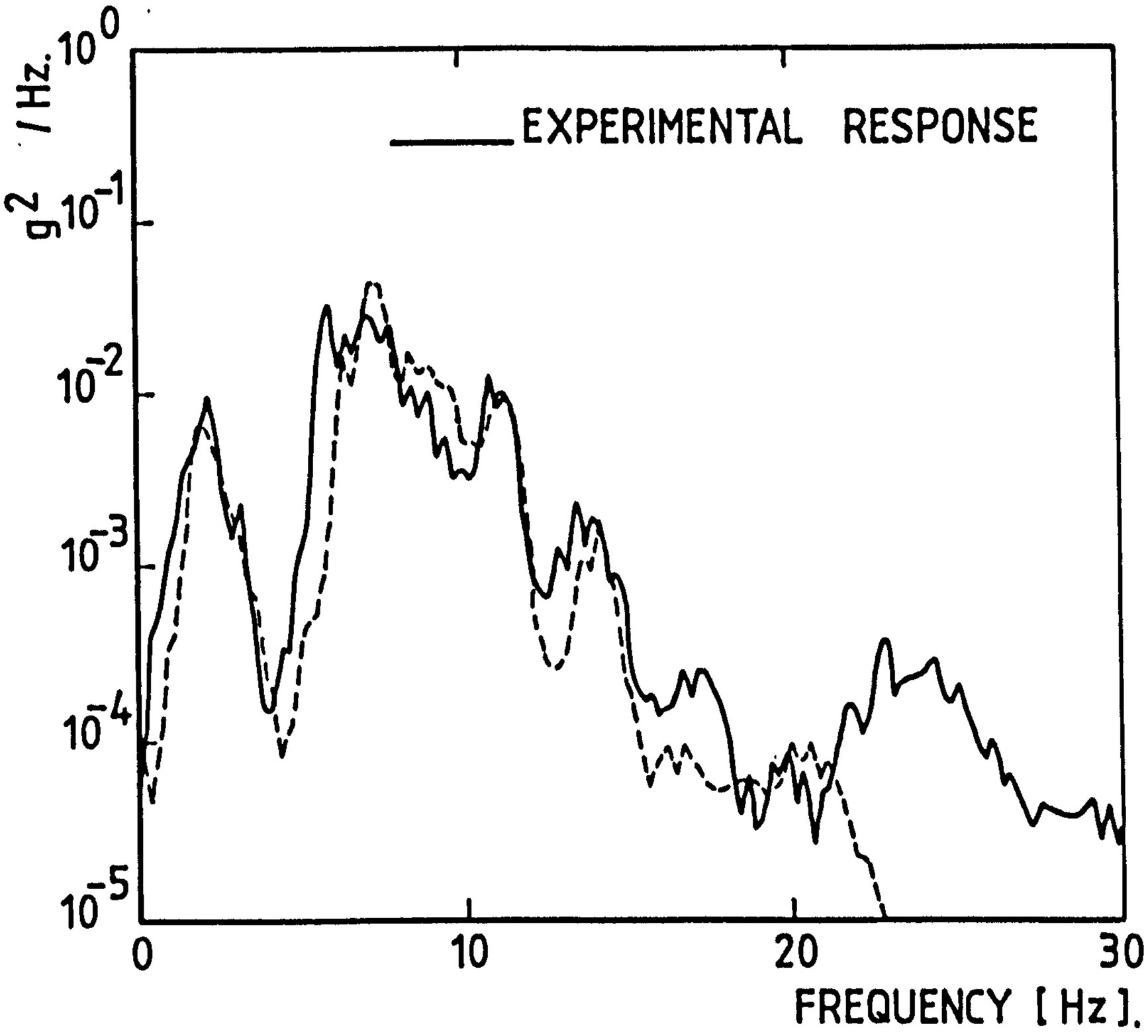

FIGURE 69. RESPONSE CORRELATION DRIVER SEAT LONGITUDINAL.

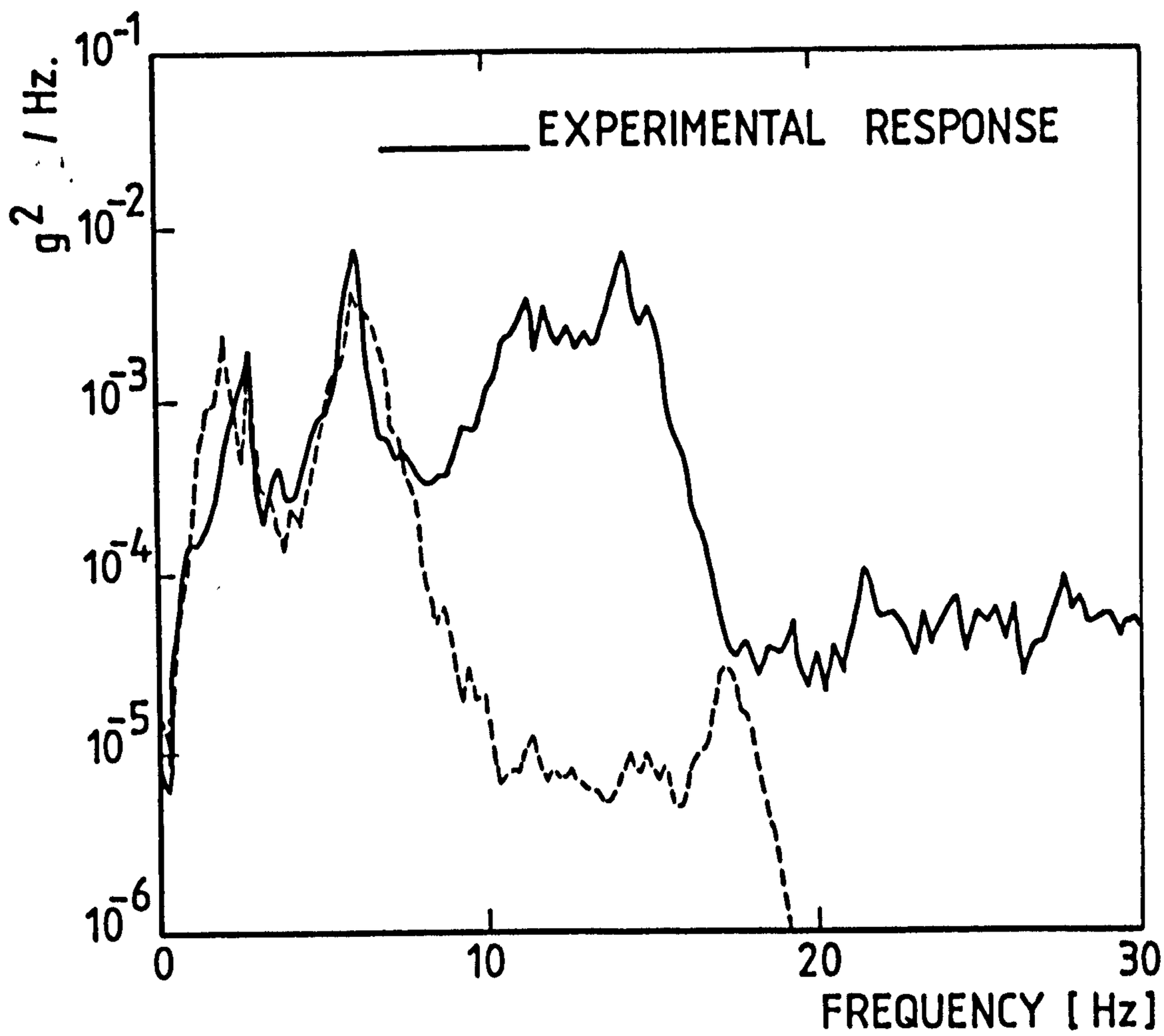

FIGURE 70. RESPONSE CORRELATION
TRAILER CENTRE VERTICAL.

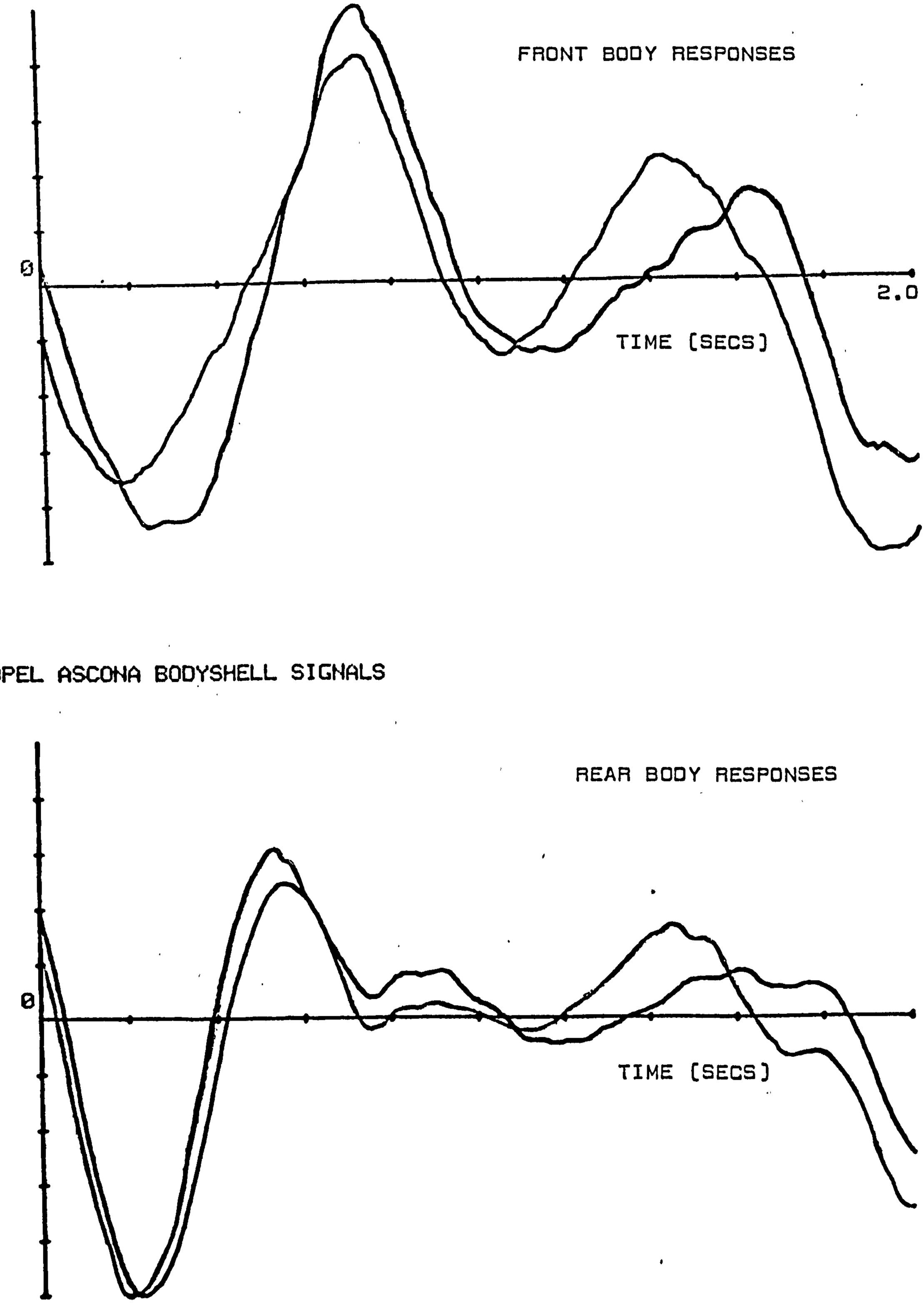

FIGURE 71

TWO SECOND TIME HISTORIES OF SIMULATED
BODY DISPLACEMENT RESPONSE

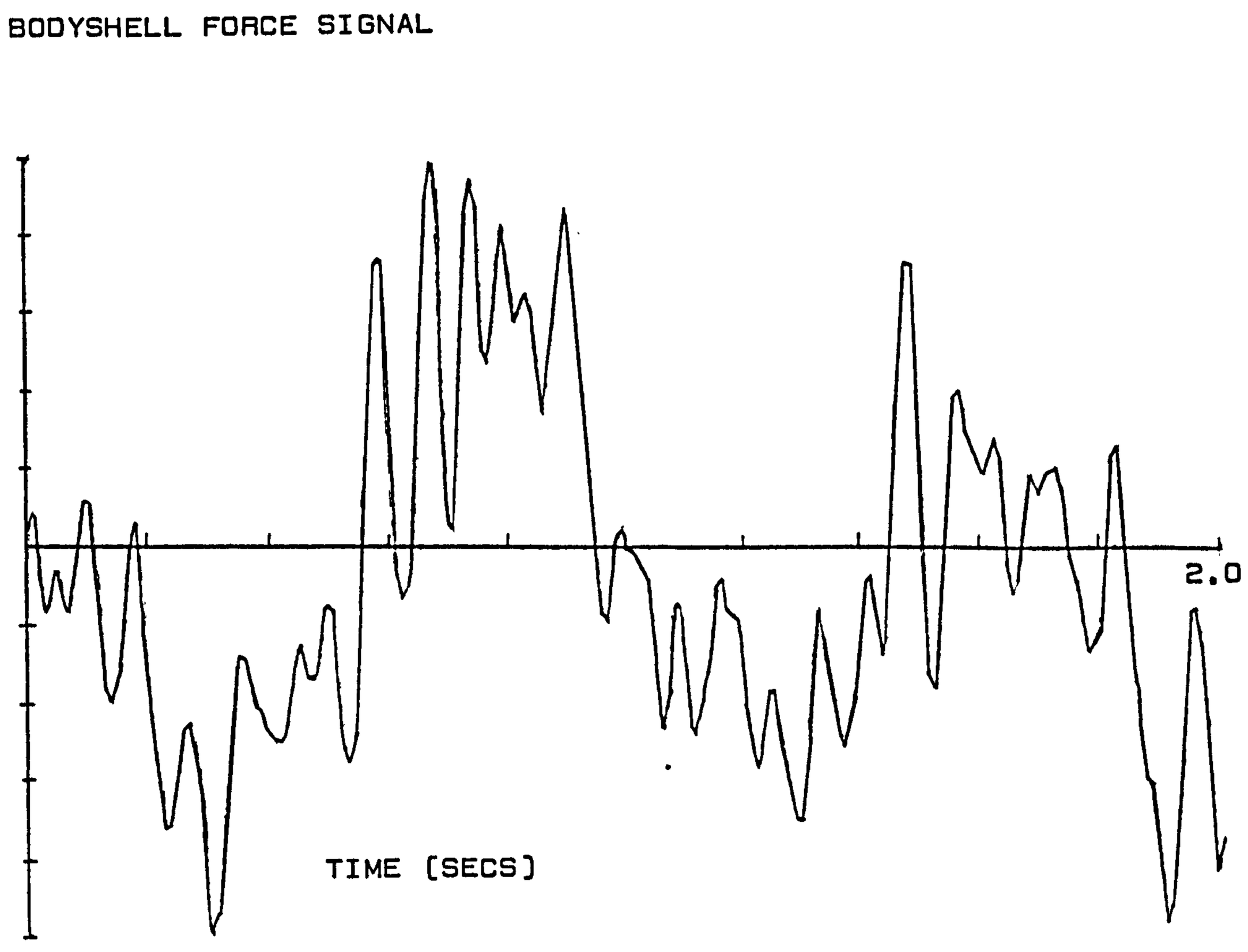

FIGURE 72

TWO SECOND TIME HISTORY OF BODYSHELL FORCE SIGNAL

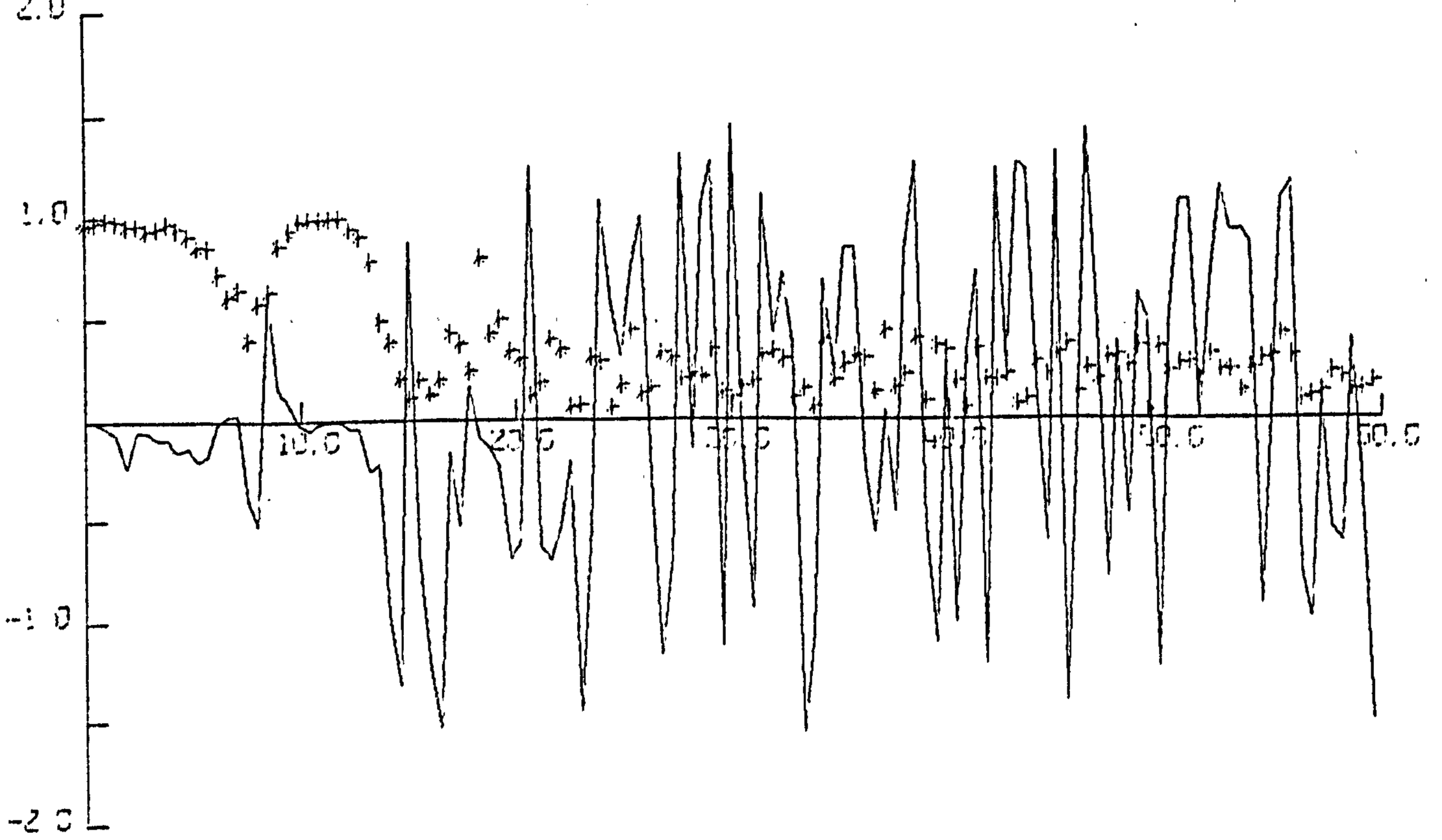

COHERENCY (*) AND PHASE OPEL DRIVE SIGNALS

RIGHT & LEFT HAND FRONT BODY RESPONSES

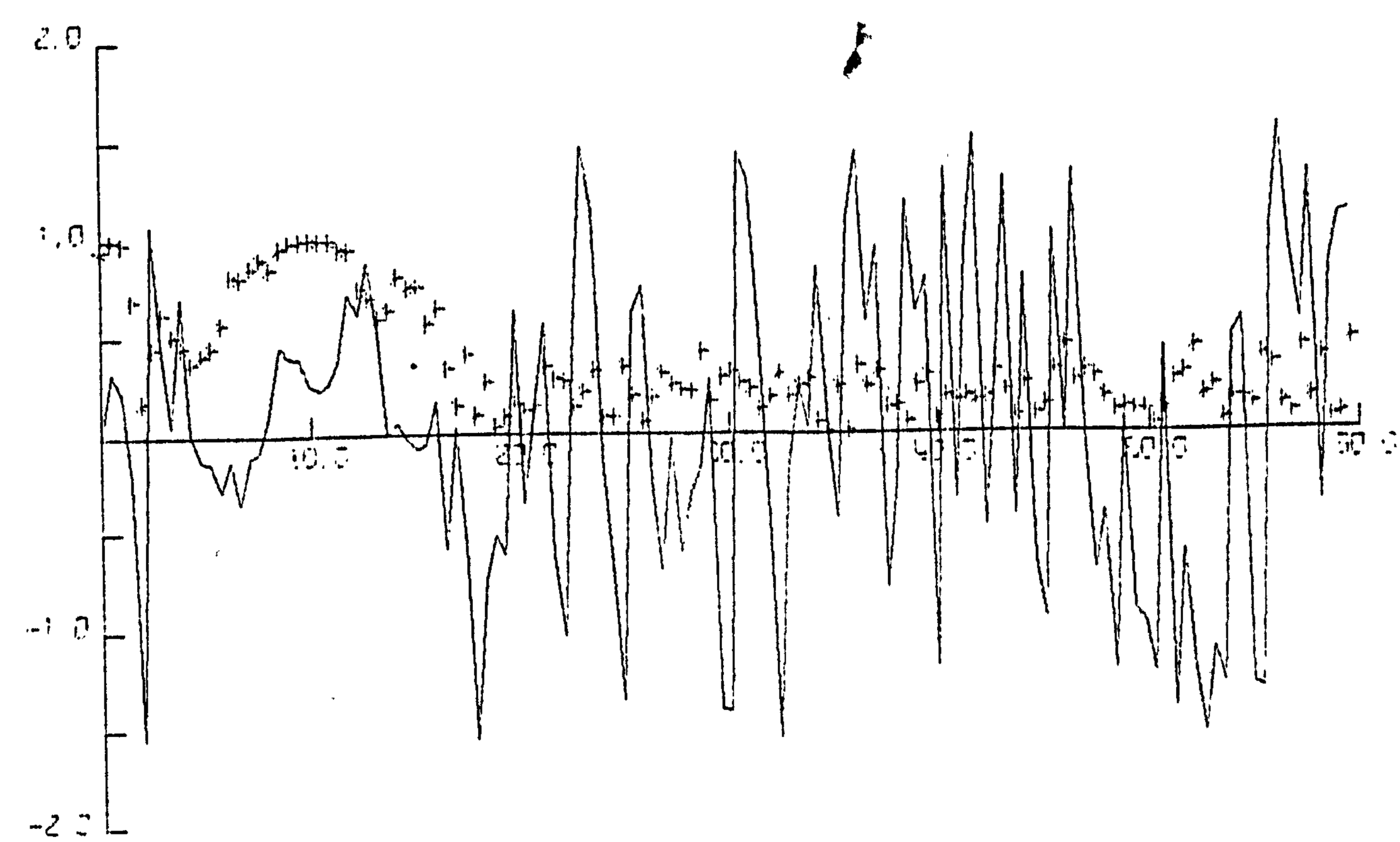

COHERENCY (*) AND PHASE OPEL DRIVE SIGNALS

RIGHT HAND FRONT & RIGHT HAND REAR BODY RESPONSES

FIGURE 73
COHERENCE & PHASE RELATIONSHIPS BETWEEN BODY RESPONSES

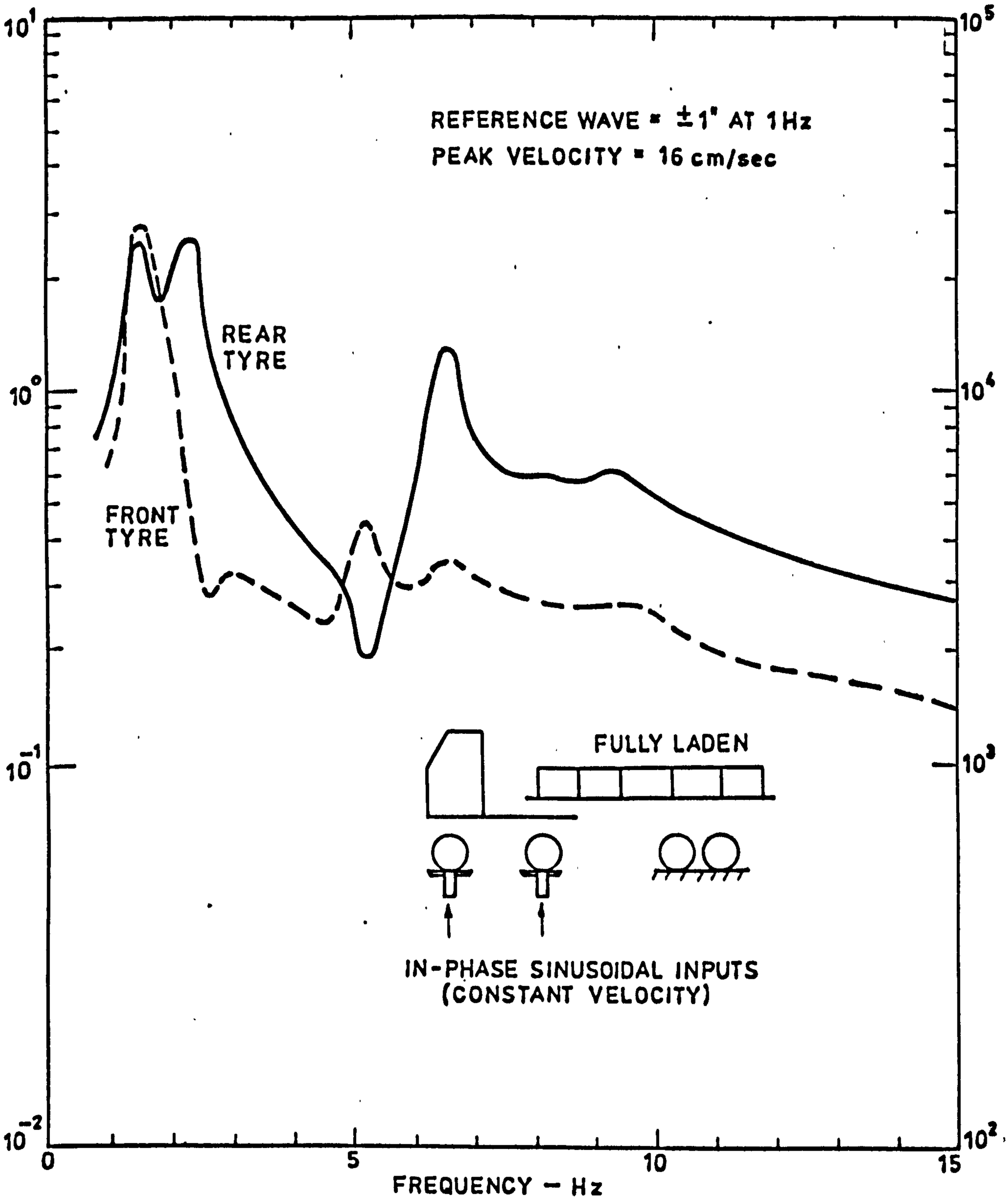

FIG 74 TYRE AND WHEELPAN INTERFACE FORCES
(CONSTANT VELOCITY SINUSOIDS)

COHERENCY BETWEEN LH & RH PROFILES

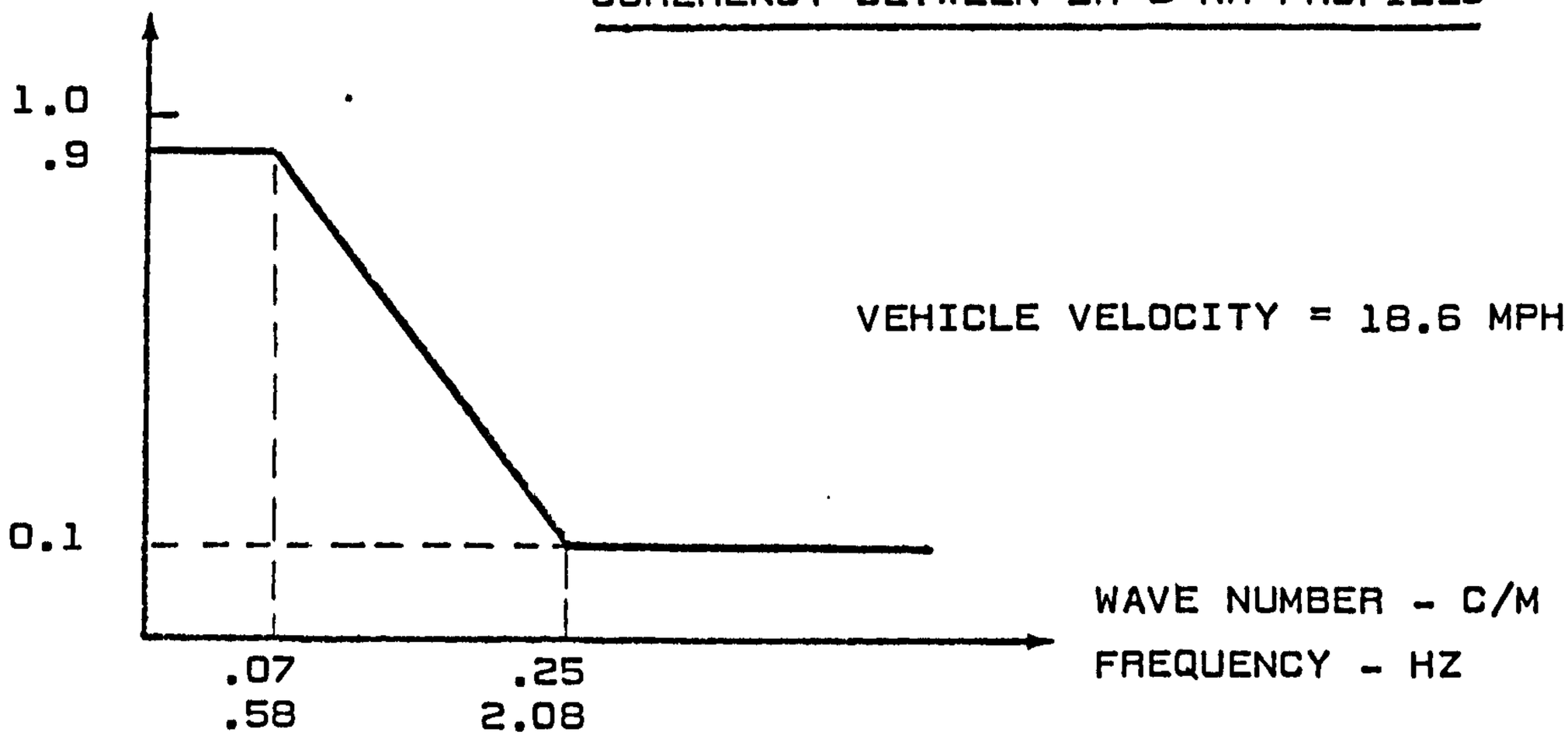

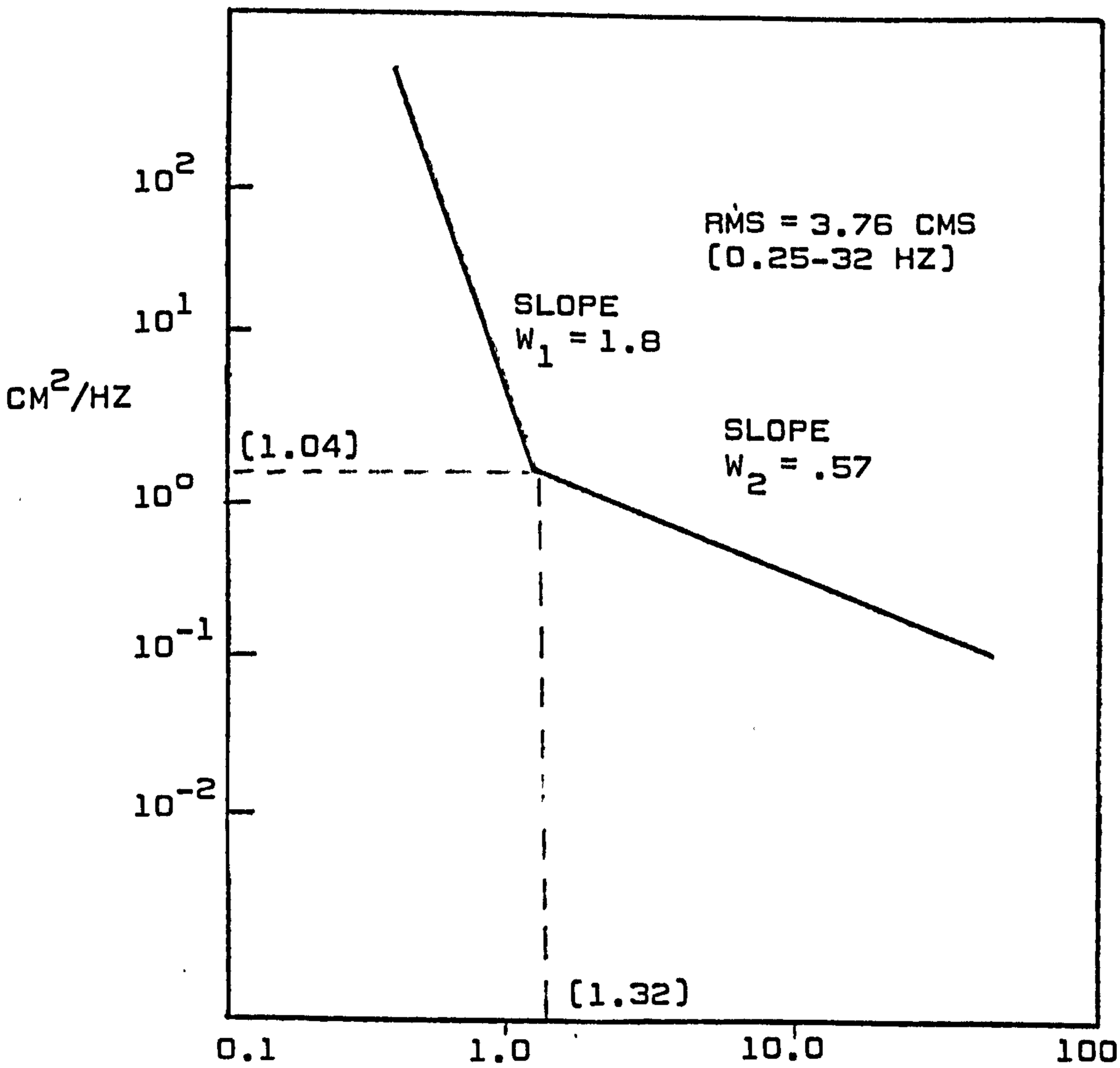

PSD OF SINGLE PROFILE

FIGURE 75

DETAILS OF PAVE INPUT FOR SEISMIC BLOCK EVALUATION

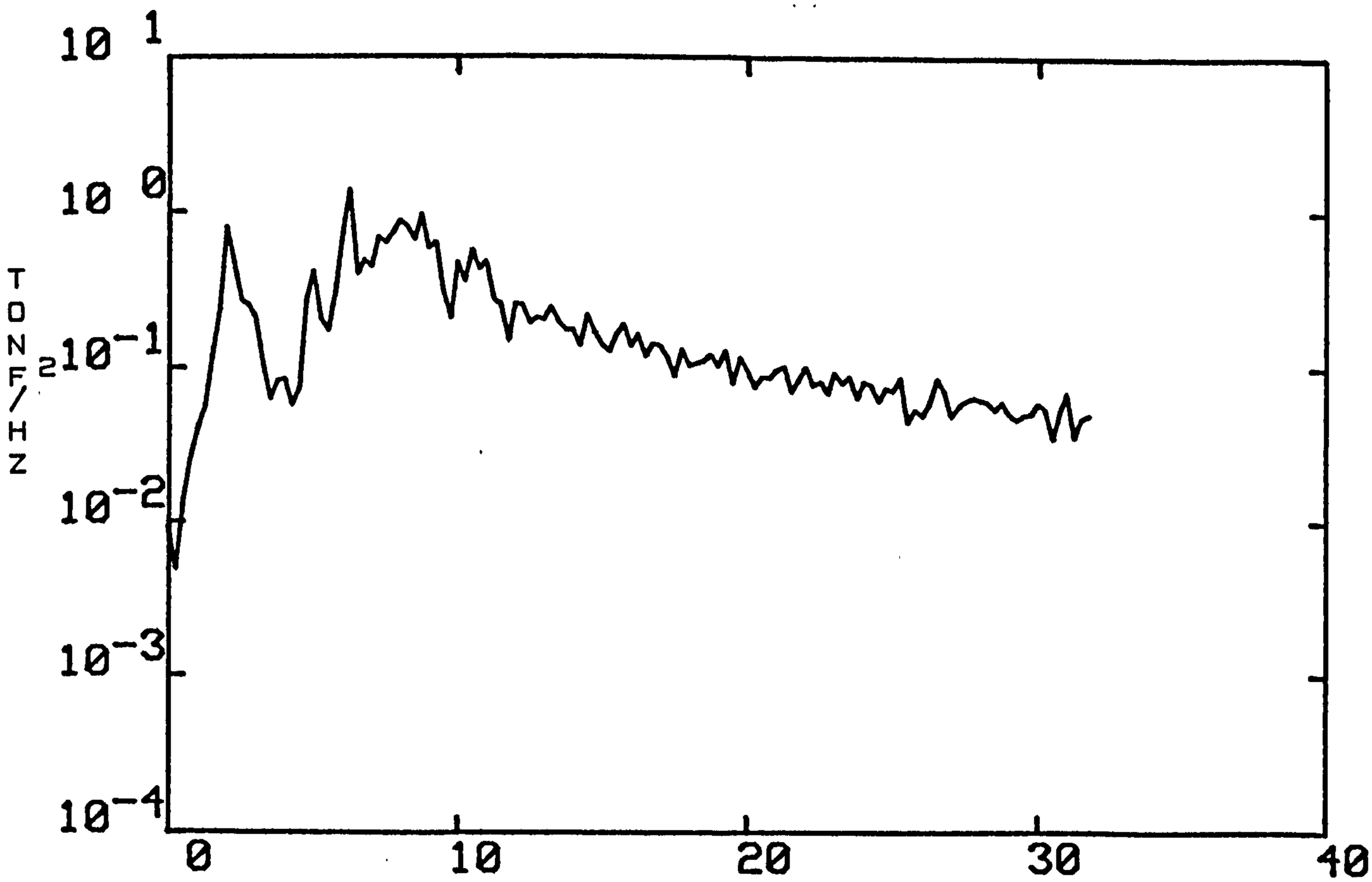

FIGURE 76

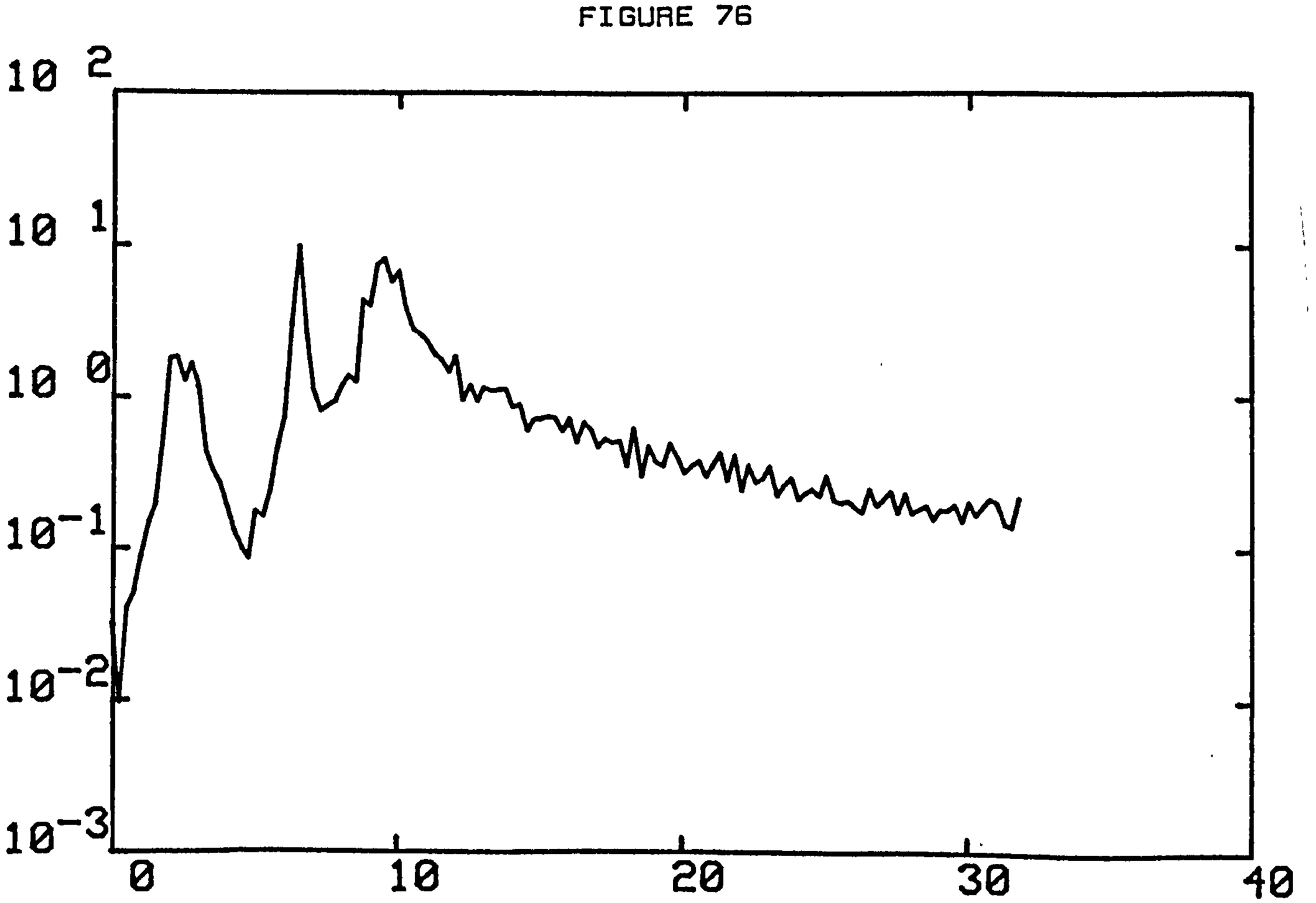

FIGURE 77